Use of a 3D Liver Microreactor as an *In Vitro* Model for the Study of Bile Acid Synthesis and Hepatobiliary Circulation

by

Jose Ricardo Llamas Vidales

Bachelor of Science in Engineering, Mechanical Engineering
University of Michigan, Ann Arbor, 2003

Submitted to the Department of Biological Engineering
in Partial Fulfillment of the Requirements for the Degree of

Doctor of Philosophy in Biological Engineering
at the
Massachusetts Institute of Technology

June, 2009

Signature of the Author:_____
Department of Biological Engineering
March 4th, 2009

Certified by:_____
Linda G. Griffith
S.E.T.I. Professor of Biological and Mechanical Engineering
Thesis Supervisor

Certified by:_____
Steven R. Tannenbaum
Underwood-Prescott Professor of Toxicology and Chemistry
Thesis Supervisor

Accepted by:_____
Alan J. Grodzinsky
Professor of Electrical, Mechanical, and Biological Engineering
Chairperson, Graduate Program Committee

This doctoral thesis has been examined by a committee of the Department of Biological Engineering as follows:

Peter T. So, Ph.D.
Professor of Mechanical and Biological Engineering
Chairperson, Graduate Thesis Committee

Linda G. Griffith, Ph.D.
S.E.T.I. Professor of Biological and Mechanical Engineering
Thesis Supervisor, Committee Member

Steven R. Tannenbaum, Ph.D.
Underwood-Prescott Professor of Toxicology and Chemistry
Thesis Supervisor, Committee Member

Keith A. Hoffmaster, Ph.D.
Research Investigator, Novartis Institute for BioMedical Research
Thesis Committee Member

Use of a 3D Liver Microreactor as an *In Vitro* Model for the Study of Bile Acid Synthesis and Hepatobiliary Circulation

by

Jose Ricardo Llamas Vidales

Submitted to the Department of Biological Engineering in partial fulfillment of the requirements for the Degree of Doctor of Philosophy in Biological Engineering

Abstract

The liver regulates a myriad of vital functions including bile acid synthesis, hepatobiliary circulation, cholesterol homeostasis, drug metabolism, etc. This thesis focuses on the use of a 3D *in vitro* model of liver to study the effects of compounds and culture conditions on hepatobiliary transport and bile acid synthesis. In order to achieve this goal, protocols were developed to perform hepatic transport studies of bile acids in perfused 3D primary rat hepatocyte cultures. An established 2D sandwich culture model was used as a foundation for evaluation of variations in protocol parameters including culture medium composition and assay incubation times. In 2D sandwich cultures, dexamethasone (DEX) was essential for the formation of canalicular networks, whereas epidermal growth factor (EGF) disrupted the formation of these networks. Strikingly, EGF promotes cellular re-polarization and canalicular network formation in perfused 3D cultures, in contrast to its effect on 2D cultures. Perfused 3D cultures were found to have greater bile acid transport capabilities and closer to *in vivo* expression of certain liver transporters than 2D sandwich cultures on day 7. Perfused 3D cultures also had greater bile acid synthesis on day 7 than 2D cultures, however this was inhibited by EGF in both cultures. A numerical model was also developed for the reduction of experimental measurements necessary to determine pharmacokinetic parameters of hepatic transport, thus allowing for quantitative comparison of the effects of different culture conditions and culture platforms on transporter activity. The result of this thesis is the adaptation of a system for the study of hepatic transport and bile acid synthesis to 3D cultures. This system has also been previously shown to maintain other liver functions such as drug metabolism, and the work of this thesis thus allows for the concerted study of all these functions and potentially others.

Advisors: Prof. Linda G. Griffith and Prof. Steven R. Tannenbaum

Acknowledgements

I would like to begin by thanking my advisors, Prof. Linda G. Griffith and Prof. Steven R. Tannenbaum, without whom I would not have been able to complete this research. Their intellectual guidance and support made it possible for me to continue these studies even at points where completion of this project seemed impossible to me. They also provided me with the opportunity to collaborate with private research laboratories, which gave me a great perspective of what research is like outside the academic arena. On a more personal note, their advice on the directions that I should take with my life have helped me look at my future not only in terms of my career but in terms of what will ultimately make me happiest. I would also like to take this opportunity to thank the other two members of my thesis committee, Prof. Peter T. C. So and Dr. Keith A. Hoffmaster. I thank Keith not only for his never ending knowledge of liver transporter literature, but for the great enthusiasm he showed for my project and his dedication to help me understand exactly what the avenues of greatest interest to take this research would be. I thank Peter for his unique and fresh perspective that he would bring to my research. He always gave me great advice that came from a big picture point of view, a point of view outside the world of liver research, which in turn allowed me to view my research in that same way and shape it to have greater impact.

During my time at MIT, I had many great colleagues and friends who turned into great mentors that helped shape my research and understand what science really is and how to actually conduct "good science". I would especially like to thank Anand Sivaraman, Nathan C. Tedford, Alexandria V. Sams and Corey J. Moore. They were all instrumental in helping me transition from an undergraduate into a true independent researcher capable of formulating a thesis project. They went out of their way to show me the consequences of every action I made while conducting research and how these can affect the reliability of those measurements. They also consistently asked me questions about my research to help me to always keep the big picture in mind. I would also like to thank all of the other graduate students and post-docs I have shared a lab with: Benjamin D. Cosgrove, Joseph Moritz, Ajit Dash, Tachun Hang, Lorenna Lee-Houghton, Sharon Karackattu, and Courtney Williams. Aside from all the help they provided me with by teaching me protocols, lending a hand during experiments and providing me with reagents, they also just made my time in the lab incredibly enjoyable and I relish all the great conversations I have had with all of them. Having them around made doing experiments fly by. I am also indebted to Karel Domansky and S. Walker Inman for their great work in the development of the culture system I used in most of my research and for all their help while I was conducting experiments with this system. I would also like to thank our laboratory technicians who performed the liver perfusions and cell isolations, without whom I would not have had any cells to conduct research: Emily Larson, Laura Vineyard, Ryan "Romie" Littrell, Rachel Pothier and Megan Whittemore. I would especially like to thank Laura for going above and beyond and learning how to do bile duct cannulations just because I needed that experiment to be conducted. I would also like to thank Michal R. Bokovza, a visiting undergraduate researcher who aided me in many of the transport studies I conducted and I thoroughly enjoyed being one of her mentors. I would also like to thank the great undergraduate student I mentored through the Research Experience for Undergraduates Program, Blair Brettmann and Mycael

McDowell. They helped me so much in conducting my research with greater expedience and gave me the opportunity to develop my skills as a mentor and as a supervising investigator.

I owe a great debt of gratitude to Jungnyun Kim, Ju Liu, and Yu Zeng from the Tannenbaum lab. They were great collaborators and conducted all of the LC/MS bile acid studies, which were instrumental in completion of my thesis project. I also owe great gratitude to all of my collaborators at Pfizer RTC in Cambridge and the Pfizer laboratories in Groton, CT. I would especially like to mention David B. Duignan, Yi-An Bi, Joan M. Kelly, and Vsevolod E. Kostrubsky. They provided great direction and help in adapting hepatic transport protocols to the multiwell reactor system and greatly expanded my knowledge of liver transporters in culture. I would also like to take this opportunity to thank my sponsor, Pfizer Inc., which through our collaboration with Pfizer RTC provided all the funding for my research.

My gratitude is also owed to Hyung-Do Kim, Craig Furman and Eliza Vasile who went out of their way to show me how to conduct spinning disc confocal microscopy and how to process the images collected. I would also like to thank Prof. Frank Gertler and the Cancer Research Center at MIT for allowing me access to this phenomenal instrument. I would also like to thank Judith M. Reilly from the MIT Radiation Protection Program who went out of her way to help me set up our laboratory for the tritiated species experiments I needed to conduct. I also owe a debt of gratitude to Dr. Bruno Stieger from University Hospital, Zurich, Switzerland, for his kind gift of primary antibodies for rat Ntcp, without which this thesis would be incomplete.

During my time at MIT, I have also made a great number of friends who have made my time here so joyous and always kept my spirits up. Rogelio, Gerardo, Pepe, Federico, Pamela, Rebecca, Aristos, Alberto, Antonios, Elizabeth, Leticia, Enrique, Josh, Courtney, Mac, Dave, Brian, Lauren, Megan, Nancy, Shan, Victor, Andrea, Sreeja, Julie, Karla, Bobby, Denise, Fausto, Iris, Ken, Charlotte, Catherine, Ara, Linda, Marie, Marisa, Seth, Ryan, Frank, and David, I owe you all for my sanity. Of special mention are the members of the Rock in Spanish band, La Cupula, I formed here at MIT. Pepe, Alberto, Rogelio, Aristos, Ryan, Antonios, Elizabeth, David, Frank and Leticia...thank you for making me feel like a rock star.

Finally, I would very much like to thank my in-laws, my family, and my wife. My in-laws, Bob and Roseann Gonzalez, for all the support they gave me during my thesis writing; providing me with a home, great meals, and invaluable advice and boosts to my morale. Thank you to Roberto, my brother-in-law, for being a great friend and a source of support. I would like to thank my parents, Dr. Ricardo Llamas Garcia and Maria Celida Vidales de Llamas, for all of their love and support and for shaping me into the man I am today. Without their guidance throughout my life, I would have never dreamt of coming to the U.S. to pursue a Bachelor's and even less a Ph.D. Their never-ending love and dedication for me have allowed me to look beyond the confines of a mid-sized Mexican city. I would also like to thank my sister, Paola M. Llamas Vidales, and her husband, Juan Carlos Rodriguez Bejarano, for their love and their unwavering positive outlook on everything. Last, but for most certain not least, I would like to thank my wife, Dr. Marisa C. Gonzalez, whose love, patience, and support have made me happier than I ever thought I could be. She gives me hope for the future and the drive to be the best man I can be. Thank you!

Table of Contents

List of Tables and Figures

Chapter 1

Chapter 2

Chapter 3

Chapter 4

Chapter 1
Introduction, Background and Motivation

The liver is one of the largest and most complicated organs in the human body. It regulates such crucial processes as blood glucose levels, xenobiotic and endogenous compound metabolism and excretion, and biliary production and transport[1]. Thus, the study of how the liver accomplishes these functions and how they can be altered is of great scientific importance. However, because of the complexity of the liver, its functions are not easily maintained in an *in vitro* environment[2-5]. The motivation of this project centers on the need for an *in vitro* system that recreates the liver microenvironment and is capable of long-term maintenance of bile acid synthesis and liver transporter function for appropriate hepatobiliary disposition, and the study of the different effects that signaling molecules and proteins can have on a system such as this and other widely-used *in vitro* systems. This chapter centers on a review of these important liver functions, how they are interrelated, and current *in vitro* systems for their study, is presented. Additionally, a description of the key features of a microreactor system that has been characterized for overall liver function[2] is provided with a brief discussion of modifications necessary to increase its throughput and reliability.

1.1 Liver Architecture and Hepatobiliary Circulation

The liver is organized into four lobules and each lobule receives blood from the portal triad, which transverses the liver sinusoid, and exits via the central, or hepatic, vein[6, 7]. Three separate vessels comprise the portal triad: the hepatic artery, which provides oxygenated blood from the heart to the liver; the portal vein, which provides blood rich with nutrients and other chemicals from the intestine for further metabolism and detoxification by the liver; the common bile duct, which drains bile from the liver

that will be deposited into the intestine during digestion[7-9]. Of course, each one of these large vessels divides into complicated branched networks of portal venules, hepatic arterioles, and bile ducts which supply or drain each sinusoid (Figure 1-1A & B). The bile ducts are further branched into bile canaliculi which are small structures formed between neighboring hepatocytes[7, 10].

To better understand how the liver achieves many of its functions, it is important to comprehend the complexity of the liver microarchitecture. The region stretching a single sinusoid from the portal triad to the hepatic venule composed mostly of a thin plate of hepatocytes is named an acinus, which has three distinct zones from the triad to the hepatic venule[10-12]. The acinus is composed of the parenchyma, which is a sponge-like capillary bed structure composed primarily of thin plates of hepatocytes (or parenchymal cells)[7]. The hepatocytes are the main cells of the liver, comprising 60-65% of all cells in the liver and are responsible for most of the functions the liver accomplishes[7]. Hepatocytes are known to have different phenotypes depending on which of the three zones of the acinus they are located in because of the relative depletion of oxygen in the red blood cells (RBCs) and exposure to other metabolites as blood travels down the sinusoid from the triad to the hepatic vein (Figure 1-1C) [6, 10-12].

Hepatocytes themselves have two different membrane domains to achieve their various functions, which confer a high degree of polarization within the hepatocyte with proteins being specifically expressed in only one domain[4, 6, 7]. The two main domains are the apical, or canalicular, surface which form canalicular networks in which bile components (bile acids, cholesterol, and other lipids) are deposited along with hydrophobic xenobiotic metabolites and the basolateral, or basal, surface which interacts

with the extracellular matrix (ECM) and participates in cell signaling; this surface also participates in the absorption of nutrients and xenobiotics from the blood[7]. The basal surface is separated from direct contact with the blood coursing through the sinusoid by a layer of ECM known as the Space of Disse, which is traversed by liver fibroblasts called Stellate cells[7].

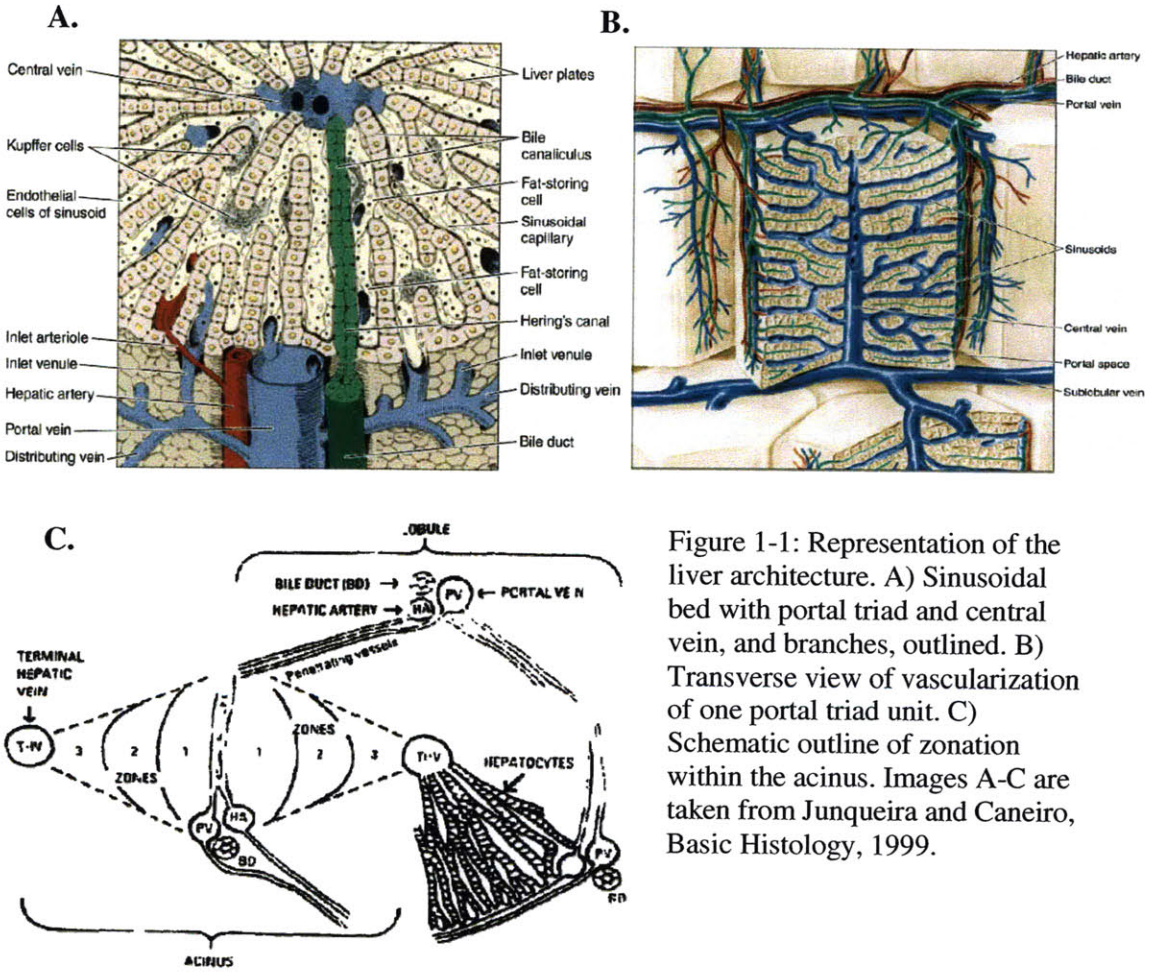

Figure 1-1: Representation of the liver architecture. A) Sinusoidal bed with portal triad and central vein, and branches, outlined. B) Transverse view of vascularization of one portal triad unit. C) Schematic outline of zonation within the acinus. Images A-C are taken from Junqueira and Caneiro, Basic Histology, 1999.

The apical surface of the hepatocytes is separated from the basal surface by a series of tight junctions (TJs) between neighboring hepatocytes. These TJs are comprised primarily of transmembrane proteins, such as E-cadherin, occludin and claudins[5]. The TJs help contain bile components within the bile canalicular space they create, and these

components drain to bile ducts which themselves drain into the common bile duct, which constitutes part of a process known as hepatobiliary circulation.

Hepatobiliary circulation is a process by which bile is collected from the liver into the common bile duct, the bile is then deposited into the intestine to aid in solubilizing fats and other lipophilic compounds, and some of the bile components are then absorbed into the portal blood flow which is then circulated back to the liver (Figure 1-2) [13].

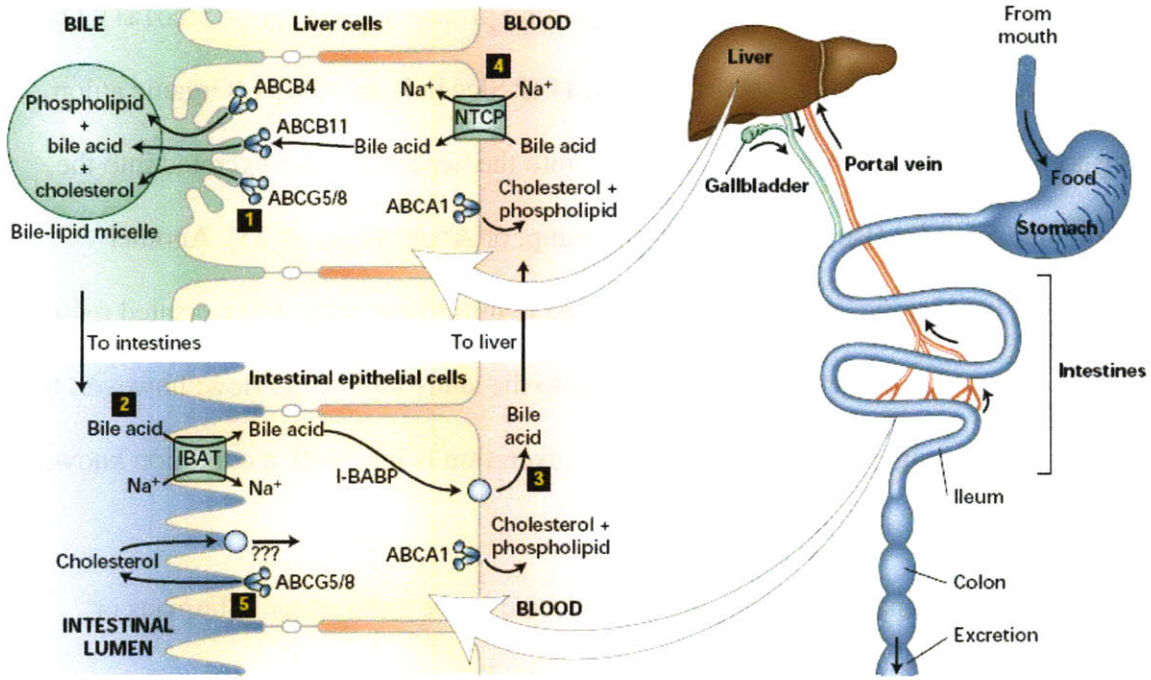

Figure 1-2: Visual representation of hepatobiliary circulation. Direction of flow is represented by arrows, with bile flowing from the liver to the intestine and blood flowing from the intestine to the liver. Processes within the liver and small intestine are expanded to the cellular level on the left. In the liver, bile acids are mainly transported into hepatocytes by the sodium-taurocholate co-transporting polypeptide (NTCP), and excreted into the bile canaliculus by the bile salt export pump (ABCB11 or BSEP). In the intestine, bile acids are absorbed from the intestinal lumen by the ileal bile acid transporter (IBAT) into intestinal epithelial cells and excreted into the portal blood flow with the aid of the ileal bile acid binding protein (I-BABP). Other bile components are also shown and their respective transporters outlined. Image taken from Lodish, H. et al., Molecular Cell Biology, 2004.

1.2 Bile Acid Synthesis Pathways

Bile acids are essential for the appropriate digestion and solubilization of fatty acids, cholesterol, steroids, lipid-soluble vitamins, bilirubin and other lipophilic

compounds[9, 13]. Bile acids are synthesized in hepatocytes, and secreted into bile canaliculi, and ultimately into the intestine. Approximately 95% of secreted bile acids are reabsorbed from the intestine where they enter the portal blood, and are subsequently taken up by hepatocytes to be transported back into bile[9]. This process is called enterohepatic bile acid circulation. Most bile acids are taken up from the portal blood flow by Ntcp (Sodium taurocholate co-transporting polypeptide, or Slc10a1), and to a lesser extent by Oatp1 (Organic anion transporting protein 1, Oatp1a1 or Slco1a1), Oatp2 (Organic anion transporting protein 2, Oatp1a4 or Slco1a4) and Oatp4 (Organic anion transporting protein 2, Oatp1b2 or Slco1b2), into the hepatocyte and excreted into the canalicular space by Bsep (Bile salt export pump, or Abcb11) [3, 14-25]. Another component in enterohepatic circulation is Mrp3 (Multidrug-resistance associated proteins 3, or Abcc3) which excretes bile acids back into the sinusoidal blood flow; however, this excretion is only significant when canalicular excretion is inhibited, a condition known as cholestasis[26-28].

From the canaliculi, bile acids are collected in the gallbladder in humans or transported directly into the intestine in rats. In the intestine, the bile acids serve as detergents to break down, collect, and transport lipophilic substances[9]. From the intestine, ~95% of bile acids are directed back into blood circulation where it will be taken up by hepatocytes again[9]. Only about 5% of bile acids are synthesized *de novo* by hepatocytes in the liver at a rate of 2 nmol/mgprotein/day[29]. However, *de novo* synthesis can be upregulated up to 6-10 fold if bile acid circulation is inhibited[30].

The synthesis of bile acids is a complicated process that begins with the oxidation of cholesterol, and requires many of the cytochrome p450s (cyp450s), a superfamily of

enzymes among which are enzymes responsible for most phase I metabolism of drugs and other xenobiotics (Figure 1-3) [4, 9, 31, 32]. The importance of this process is underscored by the fact that 90% of actively metabolized cholesterol is converted to bile acids[9]. The classic pathway of bile acid synthesis involves the hydroxylation of cholesterol by cholesterol 7alpha-hydroxylase (cyp7a1) at C_7. However, in the absence of cyp7a1, C_{27} hydroxylation by sterol 27-hydroxylase (cyp27a1) initiates the "acidic" pathway of bile acid synthesis and makes cholesterol a substrate for oxysterol 7alpha-hydroxylase (cyp7b1) mediated C_7 hydroxylation, leading exclusively to the formation of chenodeoxycholic acid and its derivatives[9, 31, 33]. Although there is low baseline activity of this pathway, it can account for 25% of baseline bile acid production when cyp7a1 pathway is inhibited, such as in Cyp7a1$^{-/-}$ knockout mice, though this might not be as important a pathway in rat[9, 31, 33, 34]. Subsequent hydroxylations and ring structure modifications involve sterol 12alpha-hydroxylase (cyp8b1, formerly cyp12), cyp27a1, and enzymes involved in fatty acid beta-oxidation[9, 31]. Cyp8b1 performs a very important function as it is the enzyme that catalyses the hydroxylation at the C12 position in the ring structure, which subsequently leads to the formation of cholic acid (CA), the major primary bile acid found in both humans and rats[9, 31]. Decrease in cyp8b1 activity, or increase of the relative synthesis of bile acids by the "acidic" pathway, leads to an increase in chenodeoxycholic acid (CDCA), which is a more hydrophobic bile acid than CA and a more potent repressor of cyp7a1 and cyp27a1 activity and expression in rats[31, 35-38]. It has even been proposed that one of the functions of the "acidic" pathway serves is to increase the relative amount of

hydrophobicity in the bile acid pool, in effect leading to a higher suppression of bile acid synthesis[29].

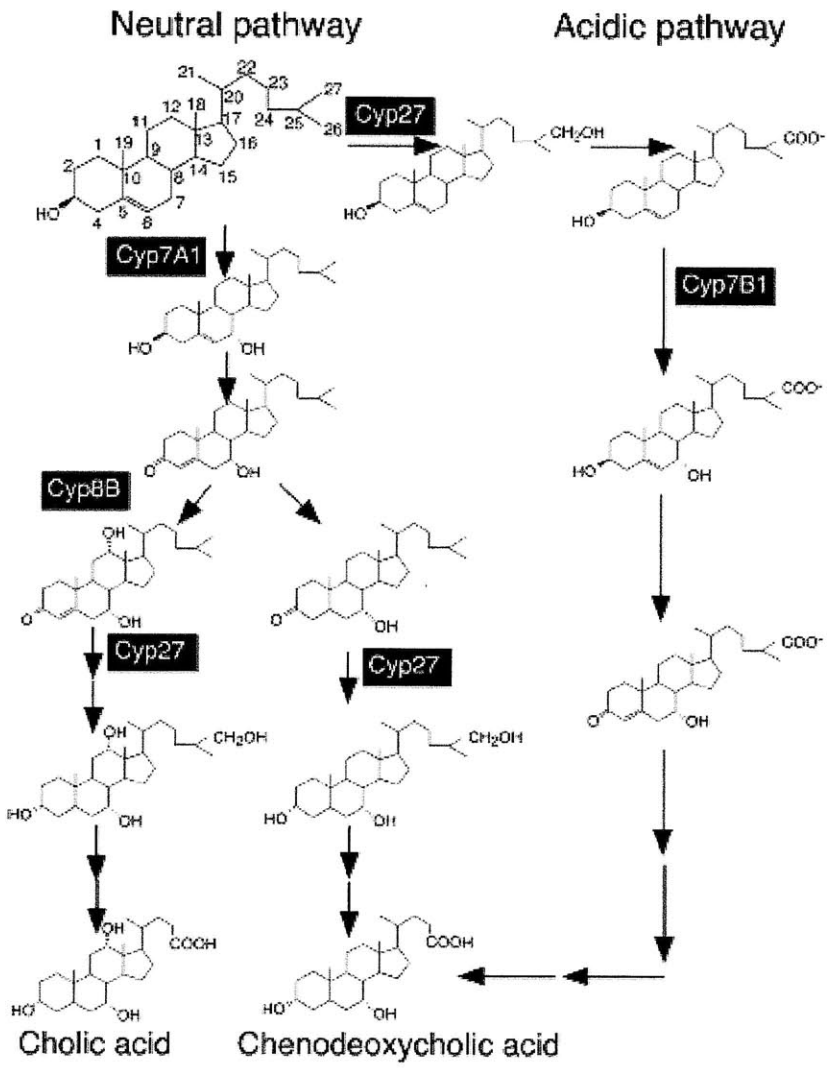

Figure 1-3: Major bile acid biosynthesis pathways. This simplified schematic of the two major pathways outlines the most important enzymes in the biotransformation of cholesterol (top left molecular structure, shown with detailed carbon positions) to bile acids. Important structural modifications shown for each metabolite. Image taken from Repa, JJ & Mangelsdorf, MJ, 2000.

Over 98% of primary bile acids are conjugated to either taurine or glycine in the rat and human, catalyzed by bile acid coenzyme A: amino acid N-acyltransferase enzyme[39-42]. This enzyme seems to have no preference for conjugation with either taurine or glycine, but seems to have a higher specificity for taurine in the rat. The relative amount of taurine or glycine conjugated bile acids in the rat and human seems to

be completely dependent on the size of the hepatic taurine pool[41, 42]. Many other species cannot conjugate bile acids to glycine, including mice, and this seems to be a rather recent evolutionary adaptation[39, 40].

1.3 Liver Transporters Involved in Enterohepatic Circulation of Bile Components

Liver transporter proteins are essential in the appropriate uptake and excretion of all bile components including bile acids, cholesterol, other lipids, conjugated and non-conjugated xenobiotics, and bilirubin diglucoronoides (Figure 1-4) [16]. These proteins can be divided into basolateral, or basal, and canalicular transporters.

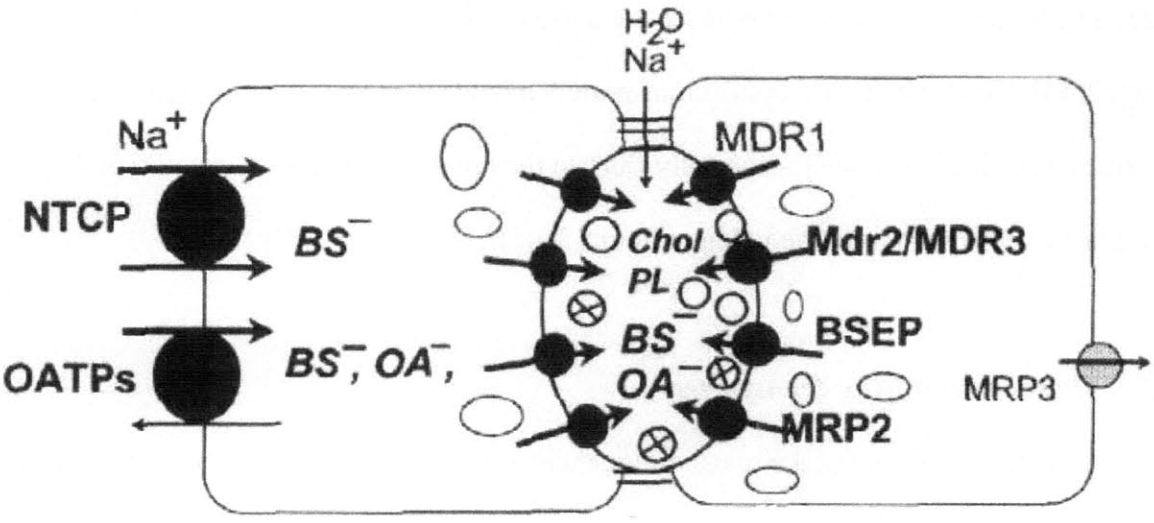

Figure 1-4. Major liver transporters of bile components. Depiction shows two neighboring hepatocytes forming a bile canaliculus between them. Transporters depicted with the direction in which they transport compounds and major compounds outlined. NTCP, sodium taurocholate co-transporting polypeptide, transports bile acids (bile salts ions, BS^-) into hepatocytes; OATPs, organic anion transporting polypeptides, transport bile acids and organic anions into hepatocytes; MDR1, multidrug resistance P-glycoprotein 1, transports cytotoxic cations into bile while Mdr2 (MDR3 in human) transports phospholipids (PL); BSEP, bile salt export pump, is believed to be the only transporter of monoconjugated and unconjugated BS^- into bile; MRP2, multidrug resistance protein 2 mediates efflux of most organic anions into bile including diconjugated BS^- and bilirubin glucoronoides, while MRP3, and other members of the MRP family, not depicted, facilitates basolateral efflux of OA^- and BS^-; Cholesterol (Chol) is thought to be transported into bile by Abcg5/Abcg8 heterodimer (not depicted).

1.3.1 Basolateral Uptake Transporters

As mentioned previously, the main basolateral bile acid transporter is Ntcp (Slc10a1), which preferentially transports conjugated bile acids, and unconjugated bile acids to a lesser extent, from the lumen into the cytosol[3, 17, 43]. The Oatp (Slco1) superfamily transports a wide array of different organic compounds, including bile acids, organic anions, various glucoronide, sulfate and glutathione conjugates, and some neutral and type II cationic compounds. Oatp1, 2 and 4 (Slco1a1, Slco1a4, and Slco1b2) are the Oatps most generally expressed in liver[15, 19-23]. Specific substrates for some Oatps have been discovered, making the study of their specific activity in culture possible[19, 23, 44]. Notably, the cardiac pharmaceutical digoxin is specifically transported by oatp2[44]. Other basolateral uptake transporters include the Oct (Organic cation transporters, Slc22a) family, especially Oct1 in the rat, which transports small type I organic cations such as tetraethylammonium[3, 45].

1.3.2 Basolateral Efflux Transporters

Along with basolateral uptake transporters, there are also efflux transporters on the basal membrane. One major class of efflux transporter are the multidrug resistance proteins (MRPs), which are part of the ATP-binding cassette (ABC) superfamily of transporters[3]. Of most importance for bile transport in the rat hepatocyte are Mrp1 and Mrp3, which can both transport bile acids out of hepatocytes, however their function seems to only be significant during cholestasis[16, 27, 28]. Other members of the Mrp family are also found on the basolateral membrane, such as Mrp4 and Mrp6, which excrete organic anions primarily[3, 16, 46]. Finally, the Oat (Organic anion transporter,

Slc22a) family of transporters, with Oat2 and Oat3 being expressed in the rat liver, perform basolateral excretion of many small organic anionic molecules[3, 16]. The effects of these transporters in bile transport are not yet understood.

1.3.3 Canalicular Transporters

All known canalicular transporters are part of the ABC superfamily of proteins. The most important in bile acid secretion is Bsep (Bile salt export pump, Abcb11), which appears to be the only canalicular transporter of monoconjugated and unconjugated bile acids[3, 14, 25]. Mrp2 (Abcc2) is the only known member of the MRP family to be expressed on the canalicular membrane and it is the predominant transporter of organic anions such as diconjugated bile acids, bilirubin metabolites, glucoronoids, sulfate conjugates, and glutathione[16, 47]. Absence of Mrp2, as in Dubin-Johnson disease, causes upregulation of Mrp1 & 3 as they are specific for many of the same substrates and thus when biliary excretion is not possible, urinary excretion is upregulated[3, 16]. Multidrug resistance P-glycoprotein (Mdr1, or Abcb1) preferentially transports hydrophobic cations with planar aromatic rings[3]. This transporter has been very well studied for its involvement in resistance of cancer cells to a wide array of chemotherapeutic agents[48]. Mdr2 (Abcb4) has the primary function of excreting phosphotidylcholine into bile which allows for the formation of large micelles in bile to suppress its detergent action during canalicular transport[49, 50]. Finally, cholesterol and other neutral sterols are transported into the bile canaliculus by a heterodimer of the Abcg5 and Abcg8 transporters, which are part of a subfamily of the Abc transporters mostly constituted of half-transporters; this mechanism has only relatively recently been established in mice and humans[51]. Other

members of the Abcg subfamily have also been detected on the canalicular membrane, such as the breast cancer resistance protein (BCRP, or Abcg2), which homodimerizes and transports sulfated conjugates of steroids and xenobiotics [3, 52].

The regulation of most of these transporters and bile acid synthesis enzymes is very much interrelated, and it is dependent on the activity of many intracellular signaling networks, which in turn are regulated by growth factors, such as epidermal growth factor (EGF).

1.4 Regulation of Bile Acid Synthesis and Liver Transporter: A Role for Epidermal Growth Factor

The processes of bile acid synthesis and hepatobiliary transport are very interrelated and share many common transcription factors as regulators. Activation and inhibition of these transcription factors can be affected by the activity of kinases involved in the epidermal growth factor (EGF) signaling pathway[3, 9, 16, 31, 53, 54].

One of the most important factors in regulation of bile acid synthesis is farnesoid X receptor (FXR) [3, 54]. FXR is activated by bile acids, especially non-conjugated hydrophobic bile acids like CDCA and deoxycholic acid (DCA), a CDCA derivative synthesized by intestinal flora[54-56]. When activated, FXR heterodimerizes with retinoic acid X receptor (RXR) in order to bind to the FXR response element (FXRE) of genes; this heterodimerization is common for other X receptors as well. The FXR/RXR heterodimer upregulates the transcription of small heterodimer partner (SHP), which binds to the liver receptor homologue-1 (LRH-1) and suppresses its activity but not its binding to the LRH response element (LRHRE) in the promoter region of the cyp7a1

gene and the SHP gene promoter region, which shows the potential for SHP-mediated feedback inhibition of its own expression (Figure 1-5) [57-59]. LRH-1 is necessary but not sufficient for the transcription of cyp7a1 mRNA[9]. Another transcription factor which is necessary to promote cyp7a1 transcription is liver X receptor (LXR), which also binds to RXR in order to bind to its response element (LXRE)[59]. LXR is activated when cholesterol or some oxysterols bind to it and seems to serve the purpose of increasing bile acid production in order to regulate cholesterol homeostasis[32, 59, 60]. The basal level of cyp7a1 expression, and of cyp8b1 expression as well, seems to be regulated by the hepatocyte nuclear factors (HNFs), particularly HNF4-alpha[61-63]. The regulation of cyp8b1 by SHP is different than cyp7a1, SHP interacts with the binding of HNF4-alpha to LRH-1 and thus inhibiting the activity of these transcription factors[9, 62, 64, 65]. However, there is evidence of a bile acid binding site in HNF4-alpha within two overlapping LRH-1 binding sites, providing a SHP-independent pathway for cyp8b1 regulation[62]. Cyp27a1 is also regulated by similarly by HNF4-alpha and LRH-1, and is repressed by FXR-dependent and SHP-dependent pathways, as well its expression being repressed by bile acids similarly to cyp7a1[35, 66]. However, the turnover rate of cyp27a1 mRNA and protein is approximate 10 times slower than cyp7a1 and its expression is very well maintained in cultured rat hepatocytes[67].

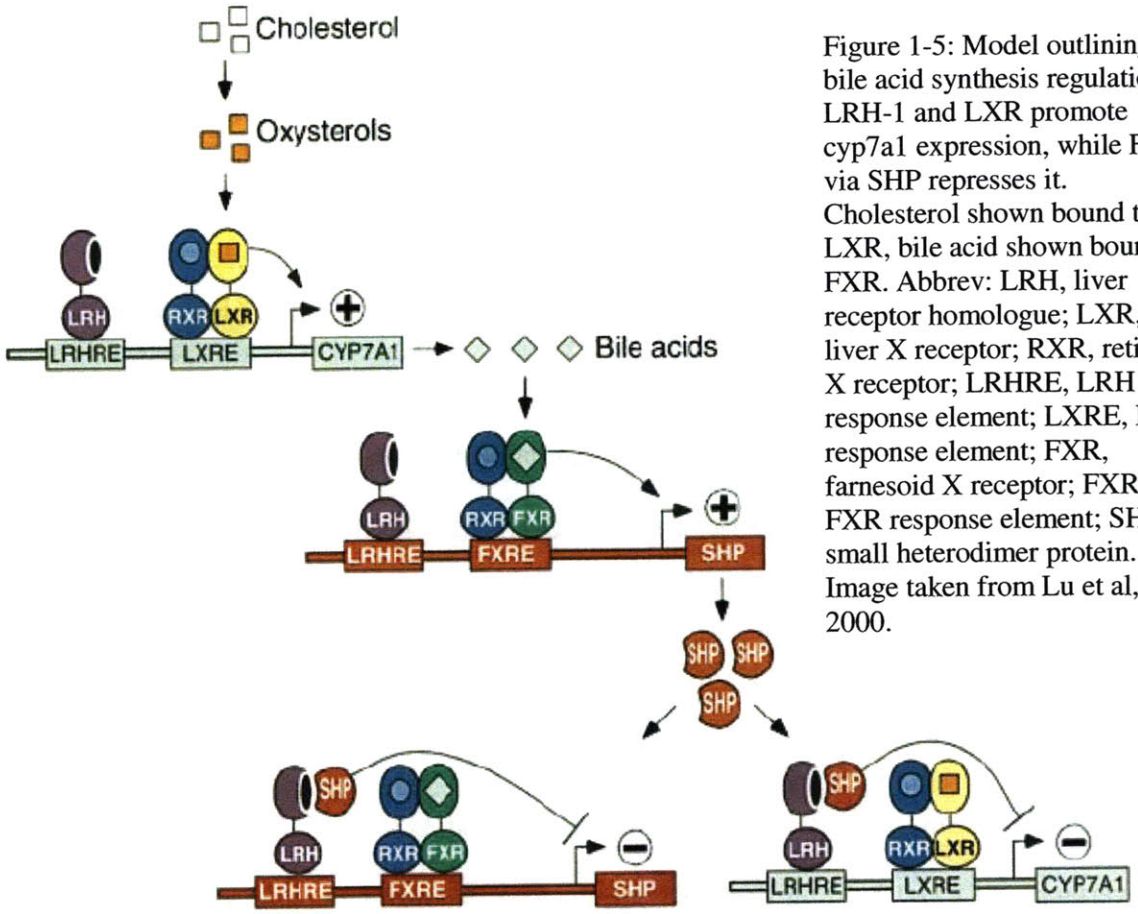

Figure 1-5: Model outlining bile acid synthesis regulation. LRH-1 and LXR promote cyp7a1 expression, while FXR via SHP represses it. Cholesterol shown bound to LXR, bile acid shown bound to FXR. Abbrev: LRH, liver receptor homologue; LXR, liver X receptor; RXR, retinoid X receptor; LRHRE, LRH response element; LXRE, LXR response element; FXR, farnesoid X receptor; FXRE, FXR response element; SHP, small heterodimer protein. Image taken from Lu et al, 2000.

The regulation of liver transporters involved in the direct transport of bile acids is also regulated by FXR and SHP[3]. Of note, is the direct involvement of FXR/RXR heterodimer in promoting the transcription of Bsep mRNA, with LRH-1 modulating this activity[68, 69]. FXR also suppresses the expression of Ntcp through the action of SHP binding to retinoic acid receptor-alpha (RAR-alpha)/RXR heterodimer[70]. RAR-alpha seems to be the main transcription factor involved in Ntcp transcription regulation, which may be because of the high amount of retinoids in the liver conferring liver-specific expression of Ntcp[7, 71]. Mrp2 also seems to be upregulated by activated FXR, though Mrp2 is also upregulated by activation of RAR-alpha, pregnane X receptor (PXR), and

constitutive androstane receptor (CAR)[46, 71, 72]. In fact, Mrp2 expression can be upregulated by bile acids and phenobarbital in both $FXR^{-/-}$ and $PXR^{-/-}$ mice[73]. Interestingly, expression of Mrp3, which transports bile acids and organic anions out of the hepatocyte on the basolateral membrane, is similarly regulated, except for lacking regulation by FXR or RAR-alpha[27, 28, 74-76]. PXR is activated by many compounds, including many xenobiotics, but can also be activated by many bile acid, especially highly hydrophobic ones like lithocholic acid (LCA)[73, 77]. PXR or CAR activation also increases the expression of Oatp2. Though the factors regulating the other two main Oatps in the rat liver are still not well known; their expression is affected by tumor necrosis factor-alpha (TNF-alpha) and interleukin-1 beta (IL-1beta) [24, 74, 78, 79]. Interestingly, Oatp1 seems to be expressed uniformly in the rat liver, while Oatp2 & 4 seem to be expressed more in the pericentral region, a distribution hypothesized to facilitate complete removal of important compounds from blood before it leaves through the central vein[20, 79].

Along with regulation of the Oatps and Mrps, PXR also seems to regulate the expression of Mdr1, a canalicular organic cation efflux transporter[80, 81]. However, the most important consequence of PXR activation is that it also upregulates expression of cyp450s involved in drug metabolism, most importantly cyp3A[3]. Therefore, this is a mechanism for drug metabolism to also be upregulated during cholestasis by bile acids[77].

Other transporters of bile components are also regulated by receptors involved in the regulation of bile acid synthesis. Notably, the canalicular cholesterol efflux transporter heterodimer Abcg5/Abcg8 is upregulated by LXR, which itself is activated by

cholesterol[82]. This is probably another mechanism of maintenance of cholesterol homeostasis in hepatocytes. Finally, the regulation of Mdr2, which exports phospholipids into bile, is not regulated by any of these transcription factors but by the peroxisome proliferator activated receptor-alpha (PPAR-alpha) as shown by stimulation of fibrates and other peroxisome proliferators[83, 84].

Though these are the direct regulatory mechanisms of bile synthesis enzymes and liver transporter proteins, their regulation is also intrinsically affected by the activity of several kinase signaling pathways, which are also activated or affected by the EGF signaling pathway.

1.4.1 EGF Regulation of Bile Acid Synthesis Enzymes and Liver Transporter Proteins

EGF has many effects on different liver functions and these have been researched extensively *in vivo* and *in vitro*. Its relationship to bile acid synthesis and transport is complicated and acts through many different pathways.

EGF binds to and activates the EGF receptor (EGFR), a receptor tyrosine kinase (RTK). This initiates a cascade of downstream signaling events through activation of mitogen-activated protein kinases (MAPKs), such as $p38^{MAPK}$, protein kinase C (PKC), extracellular signal-regulated kinase 1/2 (ERK1/2, also known as $p44/p42^{MAPK}$), phosphotidylinositol 3-kinase (PI3K), and Akt (also known as protein kinase B, PKB) (Figure 1-6, Figure 1-7) [13, 85-92]. In the presence of EGF, EGFR is rapidly endocytosed[85, 91, 92]. EGFR endocytosis can lead to its ubiquitination and degradation but signaling can also continue while the receptor-ligand complex traffics through the

endosomal pathway[85, 89]. The feedback mechanism in the activation of kinases involves several interlinked signaling and transcriptional networks[86, 88, 93].

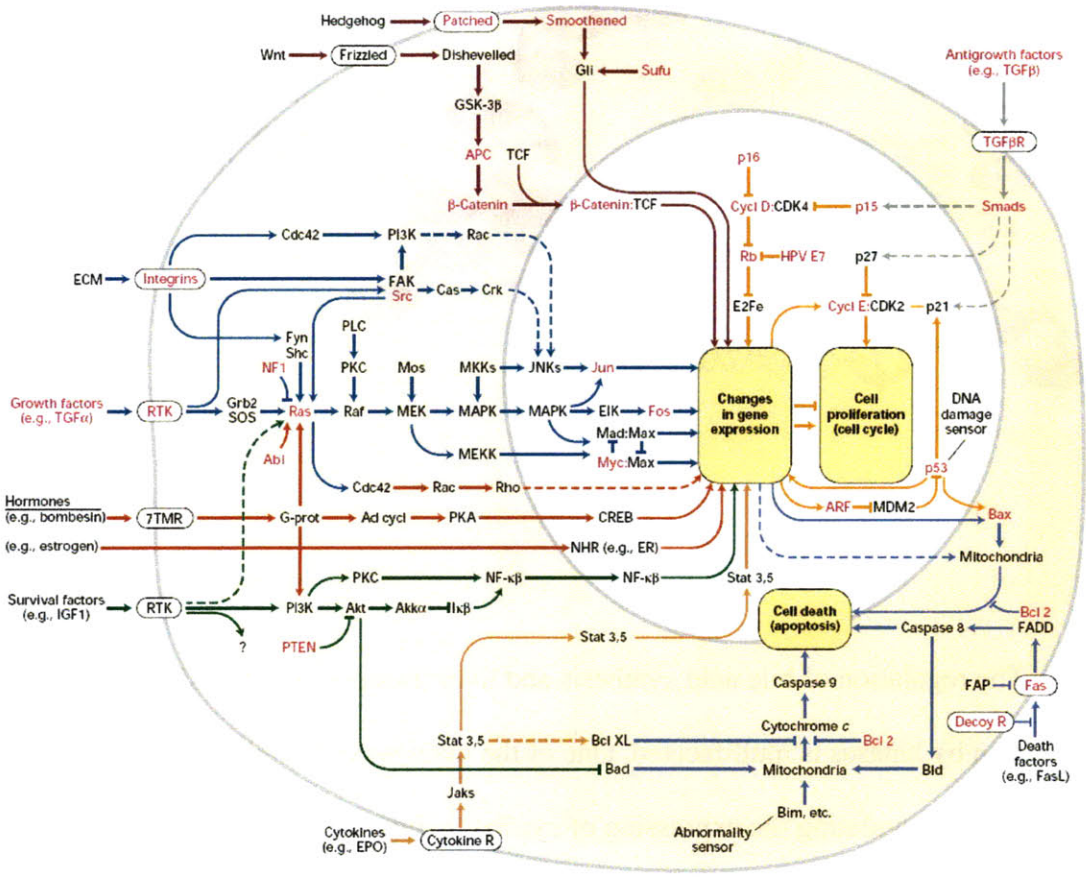

Figure 1-6: Cell signaling pathways. Simplified diagram of the most important survival, replication, and death signaling pathways. Of most importance, growth and survival factor mediated activation of PI3K, Akt, PKC, JNK, cJun, and MAPKs. Image taken from Lodish et al, 2004, Figure 23-12, p. 949.

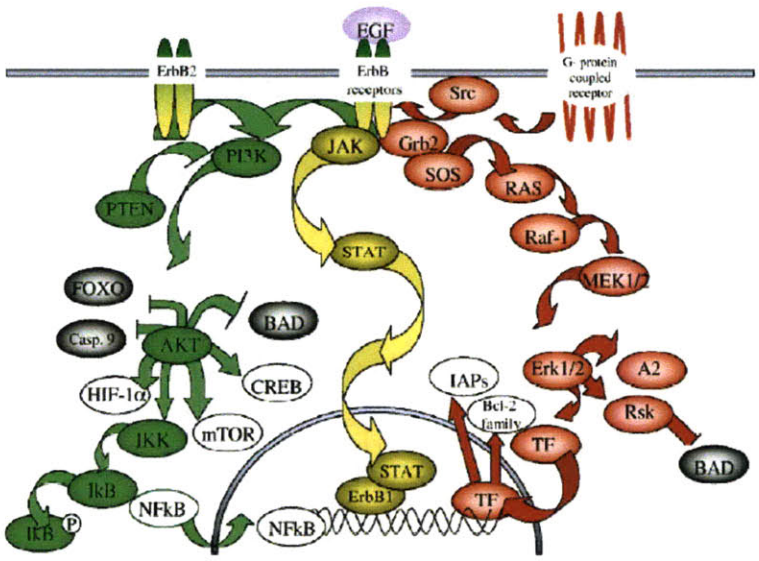

Figure 1-7: EGF stimulated pathways. EGF activates many pro-survival and pro-proliferation signaling pathways. Key nodes include the activation of Erk1/2, PI3K and Akt. Image (A) taken from Henson et al, 2006.

The regulation of bile acid synthesis and liver transporter expression and localization by kinases is multifaceted. One of the main ways that kinases affect bile acid synthesis is by regulating the expression of cyp7a1. c-Jun NH12-terminal kinase (JNK) and cJun, JNK/cJun have been reported to be activated by bile acids in an FXR-independent manner and causing the downregulation of cyp7a1 expression[94, 95]. JNK/cJun may achieve this downregulation after activation by bile acids of Fas receptor (FasR, also called CD95) signaling in a Fas ligand (FasL)-independent manner, and this activation can cause the binding of EGFR to FasR inducing a pro-apoptotic response in the rat liver by hydrophobic bile acids[94, 96].

EGF and EGFR can have a more direct effect on bile acid biosynthesis. EGF can upregulate the expression of cyp7a1 through the signaling for the phosphorylation of the hinge domain on LRH-1 through activation of ERK1/2 within the first 24 hours of

exposure to this growth factor[97]. Phorbol 12-myristate 13-aldehyde (PMA), a potent PKC activator, was also reported to increase the expression of cyp7a1 through phosphorylation of LRH-1; however, Crestani et al showed that while there is an increase of Cyp7a1 expression within the first 24hrs of incubation with PMA, PMA actually inhibits the expression of Cyp7a1 after prolonged exposure[97, 98]. Cyp7a1 can also be upregulated by the activation of $p38^{MAPK}$, which then promotes the phosphorylation and increased DNA binding of HNF4-alpha. This activation of HNF4-alpha leads to greater transcription of cyp7a1, but the phosphorylation of HNF4-alpha also leads to its degradation[53]. Insulin, which activates $p38^{MAPK}$, promotes HNF4-alpha phosphorylation and cyp7a1 upregulation after initial exposure but the effect is negligible after ~20hrs of exposure[61]. This time-dependent deactivation of $p38^{MAPK}$ activity is consistent with prolonged EGF exposure[99]. However, hepatocytes cultured for very long periods with EGF and hepatocyte growth factor (HGF) have been shown to have similar to, or higher than, *in vivo* levels of HNF4-alpha gene and protein expression and other liver-specific transcription factors[2, 100].

Activation of $p38^{MAPK}$ and PKC can also influence the localization and expression on liver bile acid transporters. $p38^{MAPK}$ has been shown to increase the localization of BSEP to the canalicular membrane, increasing canalicular excretion of bile acids, through a PKC-dependent pathway, especially through Ca^{2+}-independent PKC isoforms[101]. However, PKC-zeta, part of the atypical PKCs and Ca^{2+}-independent as well, seems to increase the translocation of Ntcp to the plasma membrane, increasing bile acid uptake, through a pathway activated by cyclic-AMP (cAMP) which is PI3K/Akt dependent[102]. This indicates that $p38^{MAPK}$ and PI3K pathways induce the translocation of both the

uptake and excretion of transporters, therefore overall increasing the cycling of bile acids through the hepatocyte. Interestingly cAMP does not have an effect on cyp27a1 expression, and therefore seems not to have an effect on the "acidic" pathway of bile acid synthesis[67].

Activation of Ca^{2+}-dependent PKC isoforms (cPKCs) stimulate internalization of Bsep contributing to cholestasis in the rat liver, and has similarly been associated with internalization of Ntcp in hamster hepatocytes[103, 104]. This indicates that cPKC activation contributes to severe cholestasis in the liver. One more piece of evidence is that cPKC activation leads to the migration of Mrp2 from the apical membrane to the basolateral membrane, possibly causing depolarization of the rat hepatocyte *in vivo*[105]. The effects of cPKCs on bile secretion seem to be antagonized by the activation of ERK1/2 and $p38^{MAPK}$, therefore the effects of EGF may be to increase flow of bile acids to combat non-obstructive cholestasis[106, 107].

The complicated role of EGF and kinases in the regulation of bile acid synthesis and transport is compounded by the fact that bile acids themselves can serve as signaling molecules. Their effect is not only limited to feedback signaling of their own homeostasis, but they can activate signaling pathways that influence seemingly unrelated behaviors as will be discussed in the following subsection.

1.4.2 Bile Acid Signaling Within the EGF Signaling Pathway

As discussed before, bile acids have a very potent effect in regulating their own biosynthesis and transport through many transcription factors, including FXR, SHP, PXR, and LRH-1[9, 31, 108]. It has been well documented that bile acids can modulate

the levels of both the classic and alternative pathway of bile acid synthesis in the rat and human, though there might not be as much regulation of the acidic pathway in the mouse[35-37, 109, 110]. More recently, the ability of bile acids to activate EGFR and other kinase signaling pathways has been described. Bile acids can have many effects, such as stimulation of cAMP synthesis and promoting apoptosis, on cells other than hepatocytes, including liver endothelial cells through binding and activation of TGR5, a bile acid responsive G-protein coupled receptor (GPCR) which stimulates cAMP synthesis, gastric carcinoma cells through TGR5-induced EGFR phosphorylation, Kupffer cells through TGR5 activation, intestinal cell derived cell lines like Caco2 cells through the activation of EGFR and the MEK/ERK cascade, pancreatic acinar cells through PI3K-mediated depolarization and eventual apoptosis and pathogenesis[111-119]. Bile acids have been implicated in carcinogenesis in the gastrointestinal tract, including the upper intestinal tract in humans with longer lifespan and therefore longer exposure than rodent models[117, 120]. Even though bile acids can have this myriad of effects on cell types other than hepatocytes, the rest of this section will focus on hepatocytes, since they are of most importance to the work of this thesis.

Much evidence is accumulating that bile acids activate signaling kinases in hepatocytes. One of the pathways by which bile acids can cause these activations is the activation of EGFR which can then activate many other kinases, but they can also activate PKCs and JNK in an EGFR-independent manner (Figure 1-8) [94, 96, 104, 112, 121-125]. Phosphorylation of EGFR by bile acids seems to be mediated by a G protein-coupled receptor (GPCR)-dependent pathway, in particular involving $G_{i\alpha}$[121]. Activation of EGFR seems to have the downstream effect of activating ERK1/2, PI3K

and Akt, and $p38^{MAPK}$ [91, 123, 124, 126]. As discussed previously, activation of these kinases can then exert effects on bile acid synthesis and bile acid transport. Bile acids can also activate JNK/cJun in a Fas receptor-dependent, ligand-independent manner[94-96]. This activation can then also cause EGFR binding to FasR (CD95) and subsequent formation of death-inducing signal complex (DISC) in a pro-apoptotic response. However, the formation of these complexes can be inhibited by PI3K, which can be activated by EGFR[96, 124]. Bile acids have also elicited a proliferative response in hepatocytes in *in vitro* culture and after partial hepatectomy, possibly through the EGFR signaling pathway[127].

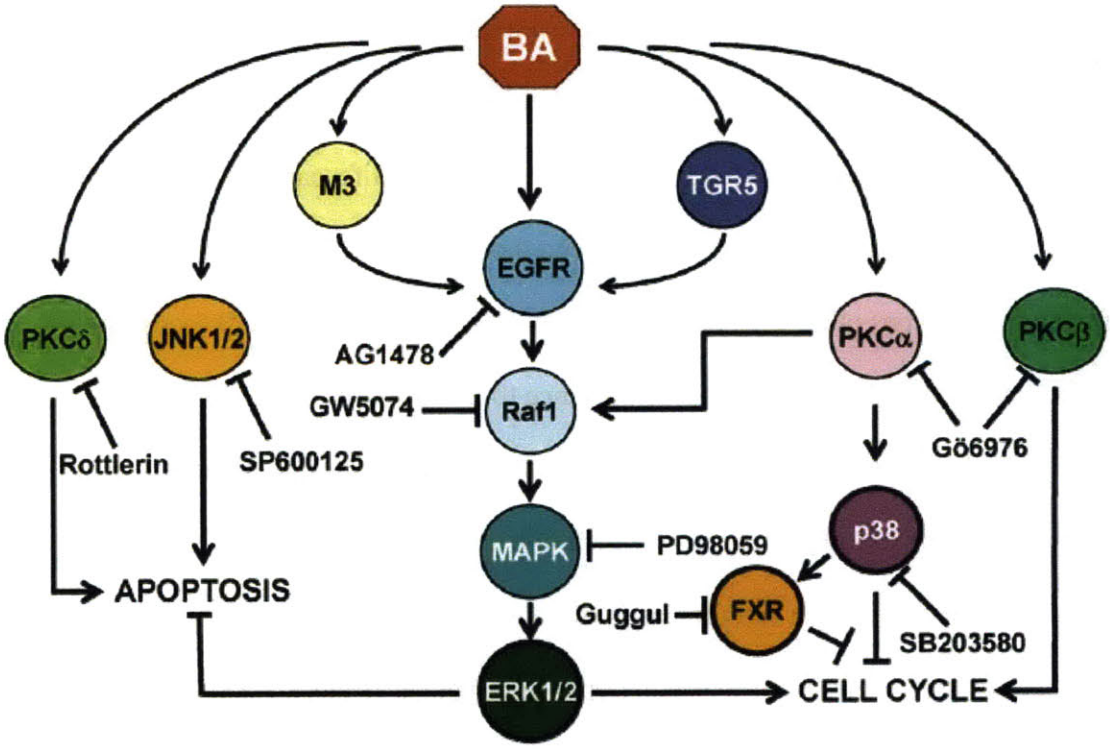

Figure 1-8: Activation of EGFR and other kinases by bile acids. Bile acids can activate many kinases including EGFR which leads to a MAPK cascade and ERK1/2 activation leading to a proliferative response. Jnk activation can lead to a pro-apoptotic response. Figure taken from Nguyen et al, 2008.

Bile acids are also important players in the regulation of glucose homeostasis through many signaling pathways including EGFR (Figure 1-9) [122]. Bile acids can stimulate the intracellular concentration of Ca^{2+}, which can increase glycogen breakdown, but can also activate cPKC-mediated decrease in bile acid uptake[128, 129]. Activation of PKC-alpha and -delta by bile acids has also been linked to decreased synthesis of cAMP, which can decrease glucagon sensitivity, but also has the effect of decreasing activation of PKC-zeta which increases localization of Ntcp to the basolateral membrane[102, 104, 125, 128, 130].

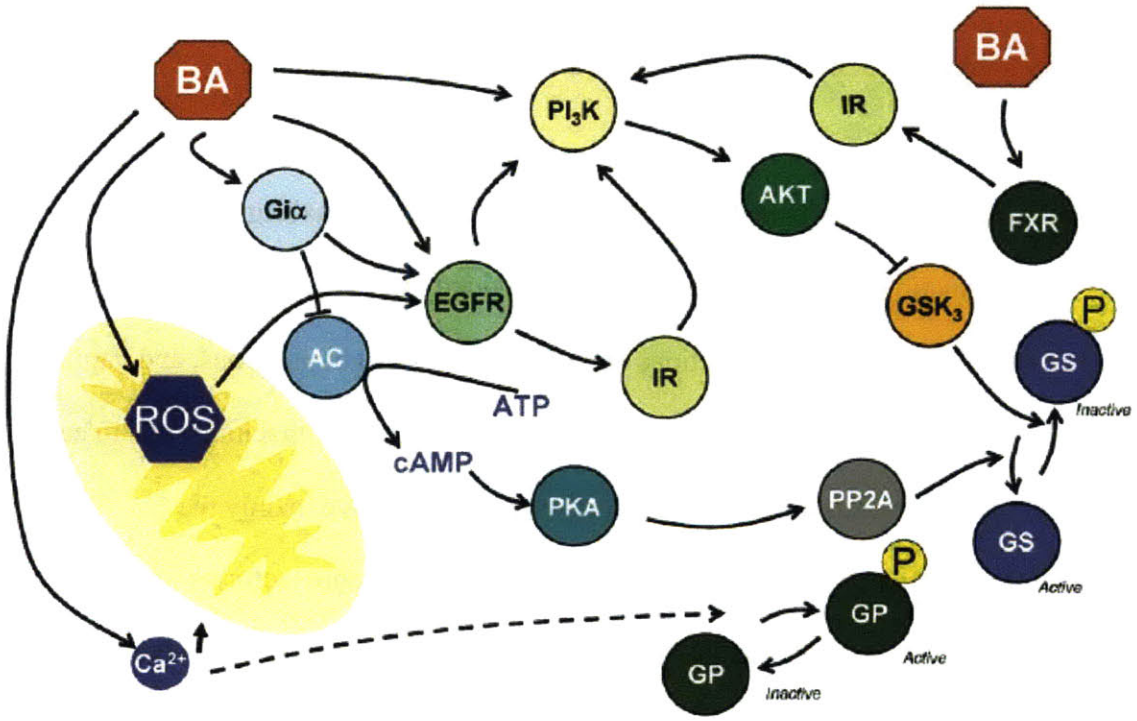

Figure 1-9: Signaling pathways activated by bile acids. Bile acids activates EGFR which can activate the insulin receptor (IR) and PI3K. Bile acids can also inhibit the formation of cAMP by activation of G protein-coupled receptor $G_{i\alpha}$. Intracellular Ca^{2+} concentration and reactive oxygen species formation (ROS) in the mitochondria is also affected by bile acids. These signals can ultimately affect glucose homeostasis by modulation of glycogen phosphorylase (GP) and glycogen synthase (GS) activity, but can also have many other cell signaling effects. Image taken from Nguyen et al, 2008.

In summary, bile acids seem to activate two pathways which have opposite effects on cell survival and cell proliferation. By activating EGFR, bile acids increase bile acid transport and, initially, bile acid synthesis[61, 97, 101, 106]. However, hydrophobic bile acids or high concentrations of bile acids (cholestasic conditions) activate Fas-receptor/JNK-dependent pro-apoptotic responses, and decrease in bile acid synthesis and bile acid uptake[94-96]. Moreover, this JNK-mediated response can be inhibited by PI3K, which is also activated by bile acids by an EGFR-dependent pathway[96]. This outlines a complex interwoven feedback process of bile acid homeostasis through kinase-dependent pathways, which can have many effects on cell survival, proliferation and cell death. EGF signaling, kinase activation, and bile acid concentration and composition can also have a great influence on cell-cell interactions and tissue structure.

1.5 Cell Junctions: Effects of Epidermal Growth Factor Signaling

Cell junctions in hepatocytes can be subdivided into three categories: anchoring junctions (including adherens junctions and desmosomes), tight junctions, and gap junctions (Figure 1-10) [5]. Anchoring junctions are involved in attaching cells to each other and can be divided into adherens junctions, which involve mainly the transmembrane proteins E- and N-cadherin and cytosolic catenin isoforms (alpha, beta, and gamma) in hepatocytes, and desmosomes, which involve the transmembrane proteins desmogleins and cytosolic plakophilins and desmoplakins in hepatocytes[131-145]. Adherens junctions are formed primarily of homodimers of cadherins extending from neighboring cells with the intracellular members anchoring the cadherins to microfilaments[133, 145, 146]. These junctions are highly Ca^{2+}-dependent and can be

modulated by extracellular Ca^{2+} concentration[145, 147]. Desmosomes, which are also Ca^{2+}-dependent, form primarily heterodimers of transmembrane components of neighboring cells and their intracellular components bind primarily to intermediate filaments[136, 148].

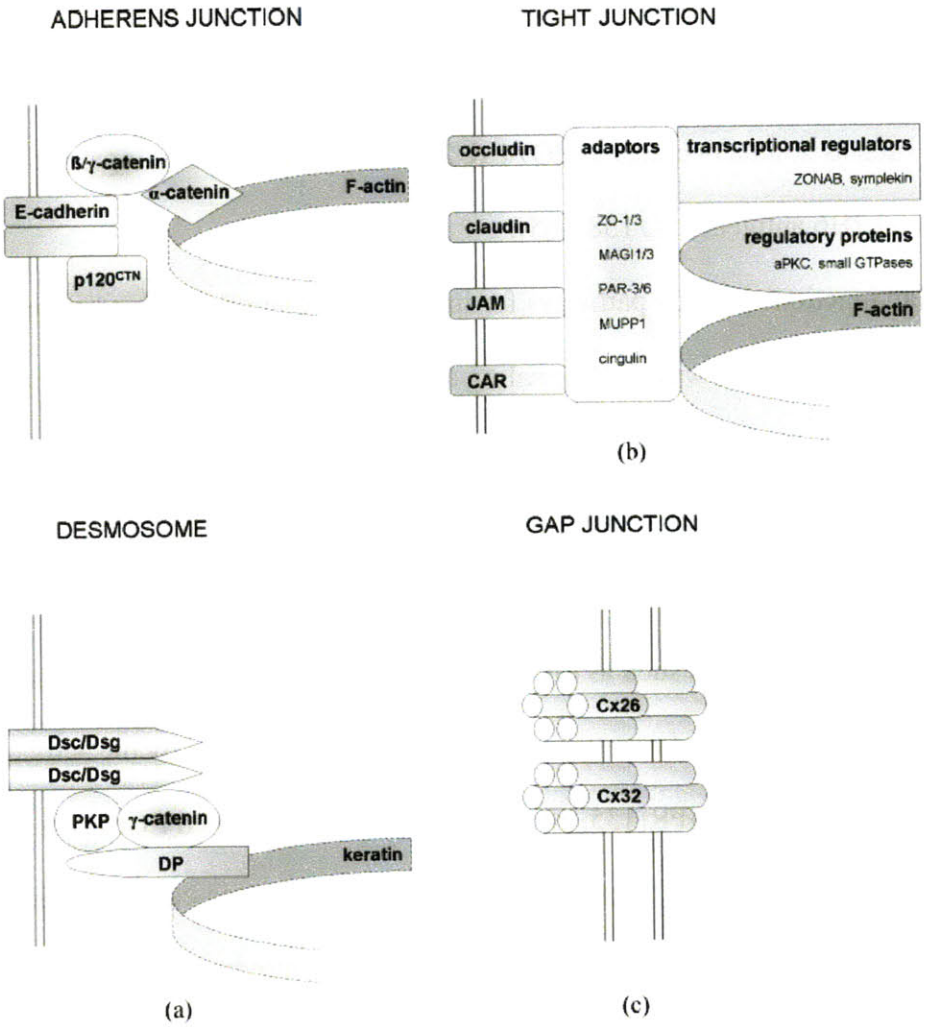

Figure 1-10: Major types of cell junctions. (a) Anchoring junctions include adherens junctions and desmosomes, which are cell junctions that attach one cell to another. (b) Tight junctions which are specialized in sealing cells together, especially in sealing off the apical reagion from the lumen. (c) Gap junctions provide a pathway for intracellular communication. Major transmembrane and cytosolic proteins involved in each type of junction are outlined. Image taken from Vinken et al, 2006.

Tight junctions in hepatocytes seal off the apical region of the cell membrane from the basolateral membrane region. These junctions ensure that components in the bile canaliculi do not diffuse out into the lumen[5]. The primary transmembrane components of tight junctions in hepatocytes are occludin, claudins (1, 2 and 3), junctional adhesion molecule 1 (JAM1) and the coxsackieadenovirus receptor[149-157]. The primary cytosolic components of tight junction in hepatocytes include postsynaptic density protein-95/disc large protein/zonula occludens-1 (PDZ) domain-containing proteins, such as zonula occludens (ZO) 1 & 2, and non-PDZ-containing proteins, such as cingulin and 7H6 antigen[151, 158-165].

Gap junctions provide pathways for intercellular communication between neighboring cells and for waves of signaling along a sinusoid[5, 6]. Gap junctions are primarily made up of connexon channels developed between adjacent cells that are made up of bundles of six connexin proteins (Cx) with Cx32 and Cx26 being the main Cx proteins in hepatocytes[166-172]. Gap junctions allow for the passive diffusion of many small messenger molecules such as cAMP, inositol triphosphate (IP3) and ions[173].

Cell-cell interaction formation and stability can be affected by the activation of many kinases including EGFR[135, 146, 174-176]. Phosphorylated EGFR has been associated with the tyrosine phosphorylation of beta- and gamma-catenin, which disrupts the interaction of catenins with cadherins and reduces the number of adherens junctions[174, 176]. EGF stimulation has also been associated with higher rates of E-cadherin internalization and recycling in epithelial cell lines[177]. The expression of E-cadherin on cell membranes and their dimerization between cells is not only necessary for the formation of adherens junctions, it is also necessary for the subsequent formation

of tight junctions[175, 178-180]. PKA is associated with the prevention of the disassembly of tight junctions after the disruption of E-cadherin dimers, however it is also associated with the disruption of *de novo* formation of tight junctions[175, 181]. Inhibitory G-proteins, especially G-alpha-i proteins, have been associated with increased paracellular permeability involving colocalization with ZO-1[182-185]. One of the main kinases associated with tight junction regulation are PKCs, especially atypical PKCs (aPKCs, including zeta and lambda isoforms). aPKCs are associated with the recruitment of ZO-1 and alpha-catenin to the cell membrane and an increase in the formation of tight junctions[175].

EGF exerts pleiotropic effects on cell-cell interactions. As discussed before, activated EGFR can phosphorylate beta-catenin and disrupts the formation of cadherin-catenin complexes, and stimulation of cells with EGF increase E-cadherin internalization[174, 176, 177, 186]. However, EGF is also associated in the stimulation in hepatocytes of cell membrane ruffling and spheroid formation in a PI3K-dependent pathway[187-189]. EGF activation of the PI3K pathway also seems to decrease expression of Cx32 and claudin-1 in cultured proliferative rat hepatocytes, which may also involve a $p38^{MAPK}$-dependent pathway[190-193]. Proliferative hepatocytes *in vivo*, after partial hepatectomy, demonstrate a transient increase in ZO-1, E-cadherin, claudin-1, and claudin-3, with a decrease in the expression of Cx32[191, 192, 194]. The effects of partial hepatectomy on claudin-1 and Cx32 have been shown to be mediated by $p38^{MAPK}$ activation[192]. Hepatocytes after partial hepatectomy have also been seen to have transient activation of $p38^{MAPK}$, Akt, and MAPK, and higher activation and internalization of EGFR[191, 192, 195]. These effects are similar to those observed by

EGF exposure[92]. There is some evidence that the EGF mediated decrease in Cx32 expression is related to phosphorylation of Cx32 by activated EGFR[196]. Upregulation of claudin-2 has been associated with $p38^{MAPK}$-dependent and PI3K-dependent pathways[155, 197]. Occludin upregulation is also mediated by a PI3K-dependent pathway[155]. The EGF mediated decrease in apical localization of tight junction components may be reduced by activation of PKA and PKA activation is greater in hepatocytes with greater ECM and cell-cell junctions[198, 199].

Interestingly, EGF has been shown to protect tight junctions in endothelial cells from the intestinal and colonic mucosa and in kidney cells after chemical stress by acetaldehyde and bile acids. These cell types all express similar tight junction components as hepatocytes[200-203]. This indicates that EGF may have a paradoxical effect on tight junction formation where it may protect tight junctions when cells are under stress while it may disrupt tight junction formation in quiescent cells. This is similar to the paradoxical effects of PKA and G-proteins which inhibit the dissociation of tight junctions but also inhibit the *de novo* formation of these structures[175].

Understanding of the many components and regulatory pathways involved in the formation and modulation of tight junctions in cultured hepatocytes, including the effects of media components on these structures, is of great scientific interest as it can provide a tool for the study of canalicular transport of chemical compounds including bile acids.

1.6 Formation and Modulation of Tight Junctions and Canalicular Networks in Cultured Primary Hepatocytes

The *de novo* formation of tight junctions in cultured hepatocytes and the effects of media components on these structures and the polarization of these cells have been extensively studied. The formation of canalicular networks in hepatocytes cultured under certain conditions and the ability to modulate these networks have been used to study canalicular transport of many chemical compounds including bile acids[147, 204-220]. One of the most widely-used system for this purpose is the collagen gel sandwich culture system in which hepatocytes are seeded on a layer of gelled collagen type I and after enough time for cell attachment a second layer of gelled collagen type I is laid on top of the cell cultures[206, 221]. However, other sandwich culture systems, such as hepatocytes cultured on absorbed collagen type I overlayed with Matrigel® matrix, have also been used to study biliary transport of bile acids and other chemical compounds[204, 214].

Canalicular networks in these hepatocyte cultures can be disrupted by removal of Ca^{2+} ions, which causes disruption of the tight junctions between the cells[147]. The disrupted canaliculi have been shown to remain open ~60 min after Ca^{2+} is replenished in these cultures, which allows for differences in transport of compounds within hepatocytes and into canalicular networks to be measured[147]. Studies have observed that formation of canalicular networks and re-polarization of transporters occurs over ~4 days in culture, however other studies have shown that there is a significant decrease of liver specific functions and transcription in these cultures over ~7 days in culture[2, 209, 210].

Interestingly, transmission electron microscopy studies of similarly cultured hepatocytes have provided some evidence that EGF can decrease the formation of canalicular networks in these cultures[207].

Other hepatocyte culture systems have also been shown to develop extensive canalicular networks, including systems which allow for hepatocytes to have a three-dimensional configuration. These systems include spheroidal cell aggregates and roller bottle organoid cultures[100, 222-224]. EGF was seen to increase tissue and ECM formation in all of these studies and it was observed that these effects were concentration dependent in some of these studies[100, 188, 189, 223, 224]. This effect could be attributed not only to the effect of EGF on hepatocytes but also to its effect on non-parenchymal cells in these 3D cultures. Even though polarized canalicular networks have been observed in several of these cultures, hepatobiliary transport rate studies have not been conducted in 3D systems. Hepatocyte cultures in a single-unit *in vitro* 3D physiological perfused model in an environment that mimics many aspects of *in vivo* liver have been shown to have closer to *in vivo* expression of liver-specific genes, drug metabolism activity and other liver-specific functions than 2D sandwich cultured hepatocytes, and these functions were maintained for longer than 7 days in culture[2]. However, formation of canalicular networks and hepatobiliary transport studies had not been conducted in these cultures. Adaptation of transport study protocols developed for 2D sandwich cultures is necessary to conduct long term studies of the effects of different culture conditions and chemical compounds on hepatobiliary transport in *in vitro* hepatocyte cultures.

1.7 Single-Unit *In Vitro* 3D Physiological Perfused Model

A single-unit *in vitro* 3D physiological perfused model of the liver has been previously described and liver specific functions in primary rat hepatocyte cultures in this system have been extensively studied (Figure 1-11) [2, 225]. This system was designed to mimic many aspects of the *in vivo* liver microenvironment, including the length scales of the acinar and sinusoidal unit. It also allowed for media flow through the hepatocyte culture tissues at rates which allowed the system to mimic *in vivo* oxygen concentrations, allowing for possible zonation of hepatocytes. Primary rat hepatocyte cultures in this perfused 3D system were observed to maintain closer to *in vivo* rates of albumin and urea secretion, drug metabolism, and liver specific gene transcription than 2D collagen type I sandwich cultures over 7 days in culture[2, 225]. It should be noted that description of the development and design of this system, as well as all the findings in this system previously described, is detailed in the thesis of Anand Sivaraman and in Sivaraman et al, 2005, and the reader is referred to these documents for further detail on this subject[2, 225]. Although this system has been shown to maintain liver specific functions over time in culture, it is cumbersome to set up and maintain each single-unit system. Therefore a multi-unit version of this system is desirable to conduct studies comparing the effects of different conditions on hepatocyte cultures.

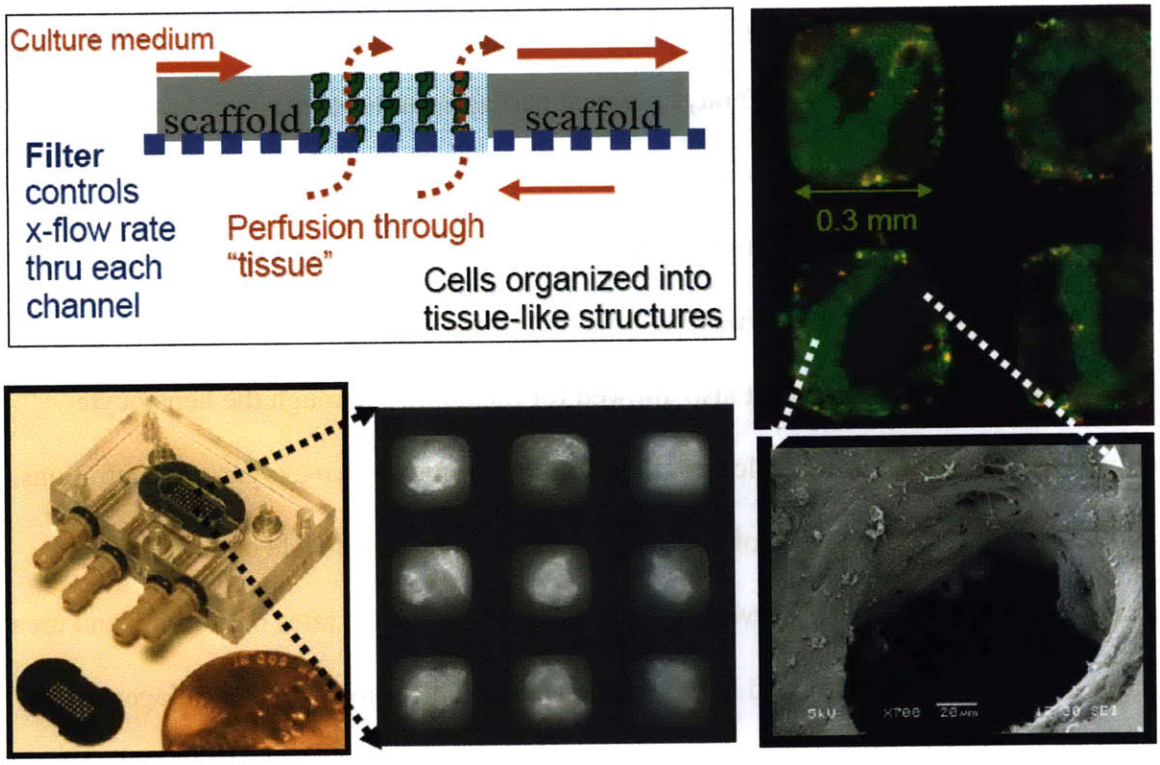

Figure 1-11: Single-unit *in vitro* 3D physiological perfused model. Hepatocytes in reactor channels as perfused with culture medium and form tissue-like structures which remain viable over long term culture and maintain liver phenotype as compared to other *in vitro* culture systems. Image taken from Sivaraman et al, 2005.

1.8 Multi-Unit *In Vitro* 3D Physiological Perfused Model

A multi-unit version of the single unit reactor was developed to increase the number of conditions and replicates that can be analyzed in a single experiment involving 3D perfused cultures of hepatocytes. The multi-unit 3D model was designed to allow facile adaptation of functional assay protocols developed for 2D hepatocyte cultures to perfused 3D cultures. In designing this new device, it was desirable for the format to be similar to multiwell culture plates to allow for the used of multichannel pipettors and other standard laboratory supplies and devices.

The multi-unit device was designed and developed by Dr. Karel Domansky and Walker Inman, under the supervision of Prof. Linda G. Griffith. The multi-unit device

consists of 12 reactor/media reservoir pairs in a culture plate-like format (Figure 1-12). Each reactor/reservoir pair consist of an upper open chamber and lower closed chamber which are separated by two 5μm filters. The lower chamber contains a set of microfabricated, pneumatically-actuated, pumping chambers to produce culture media flow. The pumping chambers are actuated by a programmed controller which regulates positive and negative air pressure below the membrane sealing off each pumping chamber. The positive and negative pressure regulates whether each chamber is open or closed. The chambers are opened and closed by the controller resulting in a peristaltic motion producing culture media flow through the hepatocyte cultures. The closed chamber below the hepatocyte cultures contains a flexible membrane which acts as a flow capacitor that reduces flow pulsatility through the cultures.

a)

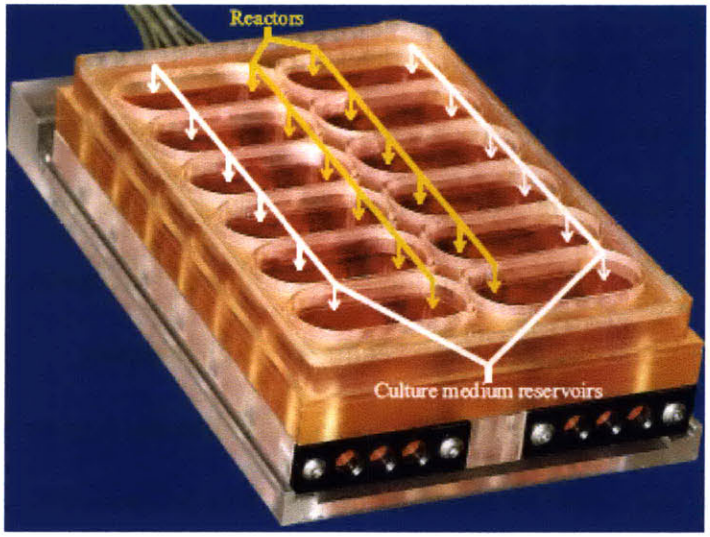

b)

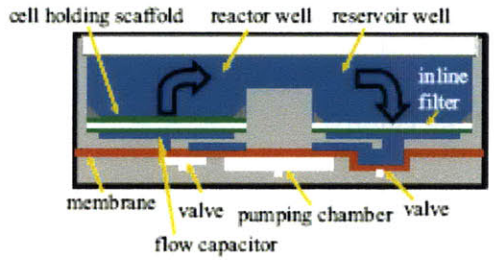

c)

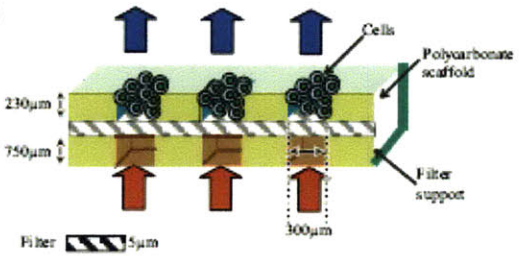

d)

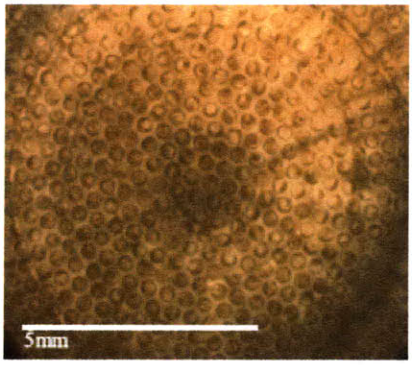

Figure 1-12: Multi-unit *in vitro* 3D physiological perfused model of liver in multiwell plate format. (a) Photograph of device showing 12 culture medium reservoir/reactor pairs. (b) Cross-sectional view of one reservoir/reactor pair showing upper and lower chambers, pneumatically-actuated microfabricated valves and pumping chamber, and flow capacitor to attenuate flow pulsatility. (c) Polycarbonate scaffold, filter and support scaffold assembly. Hepatocytes are seeded into channels in polycarbonate scaffolds. (d) Phase contrast image of perfused 3D cultures.

Hepatocytes are seeded and maintained in an array of 300μmX230μm (DIA X D) channels fabricated on a polycarbonate scaffold. Similar to the single-unit system, the dimensions of the channels were designed to mimic the length-scale of the liver acinus, and flow rates were optimized to modify inlet and outlet oxygen media concentrations to mimic periportal and pericentral concentrations as well as to mimic sinusoidal blood flow rate in the liver. A 5μm filter is located below the polycarbonate scaffold which produces uniform culture media flow through each channel. A plastic support is placed below each filter to provide mechanical support for the filter and scaffold setup. A description of the development and design of this system is detailed in the thesis of Walker Inman, and the reader is referred to this document for further detail[226].

This multi-unit device allows for easier adaptation of functional assay protocols developed for 2D sandwich cultures to perfused 3D primary rat hepatocyte cultures. Of specific interest for the work presented in this thesis is the adaptation of hepatobiliary transport protocols, which have been widely used to study *in vitro* bile acid transport as detailed in previous sections of this chapter[147, 208-210, 212-215].

1.9 Overall Thesis Objective and Specific Aims

The overall objective of this thesis is to use perfused 3D hepatocyte cultures which have been shown to maintain liver specific functions in long-term culture to study the effects of culture conditions and media components on hepatobiliary transport and bile acid synthesis. Successful completion of this goal would provide an *in vitro* system for the concerted study of several liver-specific functions in long-term culture, including drug metabolism, transcription of liver-specific transcripts, and albumin secretion, with

hepatobiliary circulation and bile acid homeostasis. To achieve this overall objective, the specific aims of this thesis are as follows:

1. Development and adaptation of bile acid transport functional assays for perfused 3D hepatocyte cultures.
    a. This will require determination of the effect of varying media component concentrations and cholestatic agents on bile acid transport in 2D sandwich cultures. This will provide information about the appropriate media component concentrations to be used for perfused 3D hepatocyte cultures, and the expected effects of these components and cholestatic agents on these cultures.
    b. This will also require the determination of the effect of modification of different protocol parameters on bile acid accumulation in perfused 3D hepatocyte cultures.
    c. The protocol parameters should be determined so that studies of the effects of culture condition, media components or chemical agents on bile acid transport in perfused 3D hepatocyte cultures can be conducted robustly. Of special interest is that differences in bile acid accumulation measured can be attributable to the conditions being studied and not to idiosyncratic variations from experiment to experiment.

2. Determination of the effects of media components on hepatobiliary transport and bile acid synthesis in long-term perfused 3D hepatocyte cultures.

a. Of specific interest will be the effect of EGF on perfused 3D cultures. Characterization of the effects of EGF on tissue morphology and polarization, bile acid transport, and bile acid synthesis will be performed. Measurement of protein and gene expression of specific transporters, bile acid synthesis enzymes and transcription factors will also be conducted both in perfused 3D cultures and 2D sandwich cultures.
b. EGF is of specific interest because of the potentially paradoxical effects that have been observed on tissue morphology and canalicular networks formation in 3D and 2D cultures.

3. Develop a numerical modeling approach to minimize bile acid transport measurements necessary to quantitatively assess the effects of experimental conditions on bile acid transport in perfused 3D hepatocyte cultures.
    a. A stochastic numerical model will be constructed to predict the reliability and robustness of quantitative measurements of bile acid transport kinetic parameters under varying experimental conditions. Assessment of the effects of reducing the number of measurements conducted on the reliability and robustness of determined kinetic parameters will be measured using this numerical model.
    b. Sensitivity analysis of this predictive model will be conducted to assess the applicability of the model predictions to expected experimental results, and the limitations of this model will also be explored through this analysis.

Chapter 2

Effects of Epidermal Growth Factor and Dexamethasone Media Concentrations on Bile Acid Transport

2.1 Introduction

The development of an *in vitro* system for the concerted study of the effects of liver specific functions on hepatobiliary transport is of great interest. In order to establish a system such as this, it is first important to determine the effects of different media components on canalicular network formation and bile acid transport in 2D primary rat hepatocyte sandwich cultures, an *in vitro* system widely used in hepatobiliary transport studies[147, 208-216]. Of particular interest are the effects of dexamethasone (DEX), a glucocorticoid steroid widely used in hepatocyte cultures, and epidermal growth factor (EGF), which has also been used widely for the establishment and maintenance of hepatocyte cultures[4, 67, 92, 187, 199, 207, 213, 216, 218, 221, 227-229].

As described in the previous chapter, EGF has been shown to promote the attachment of hepatocytes to layers of ECM proteins (e.g. collagen type I) and the development of tissue-like structures in *in vitro* hepatocyte cultures[100, 187-189, 207, 221, 227]. However, EGF has also been observed to decrease canalicular network formation in 2D hepatocyte sandwich cultures[207]. EGF has also been shown to elicit a proliferative response in monolayer hepatocyte cultures on collagen type I, although this response seems to be arrested by the addition of a second layer of matrix[4, 227]. EGF also activates a variety of signaling pathways, including the PI3K/Akt pathway and the

$p38^{MAPK}$ pathway, which can affect a myriad of liver specific functions including bile acid synthesis and hepatobiliary transport[53, 61, 92, 101].

DEX is a glucocorticoid steroid that has been widely used as a media component for *in vitro* hepatocyte cultures because it has been shown to retard hepatocyte dedifferentiation and increase cell-cell interactions and cell attachment[5]. It is commonly used as a way to maintain drug metabolism activity in hepatocyte cultures as it is a powerful inducer of cyp3a, one of the main phase I drug metabolism enzymes in the liver[4]. It has also been shown to increase canalicular network formation and alter mRNA expression of hepatic transporter proteins in 2D sandwich cultured hepatocytes[213, 229]. However, it has been observed that high doses of DEX (100μM) can decrease hepatic transport of bile acids in 2D sandwich cultures by decreasing the expression of Ntcp, the main bile acid uptake transporter of the liver[213]. Nonetheless, studies on the effects of low doses (<0.1μM) of DEX on bile acid transport in 2D sandwich cultures have not been published. It is important to determine how sensitive measurable bile acid transport capability is to changes in DEX concentration in the culture media. Conducting these experiments in 2D sandwich cultures may provide insight to appropriate culture media conditions for perfused 3D culture studies.

The effects of these media components on canalicular network formation and bile acid transport requires experimental measurement of transport using a set of compounds that are transported by transporters other than bile acid transporter proteins. Of special interest are transport studies with 5(and 6)-carboxy-2',7'-dicholorofluorescein diacetate (CDF-diacetate) and digoxin, which have both been shown to be transported and accumulated in canalicular networks in 2D sandwich cultures[212, 215]. CDF is

transported into canalicular networks by Mrp2 and digoxin is transported by Mdr1a/b, as opposed to bile acids which are transported into canalicular networks by Bsep[210, 212, 214, 215].

One of the main objectives of this thesis overall is to provide an *in vitro* system for hepatocyte culture in which long-term effects of culture conditions on hepatobiliary transport and bile acid synthesis can be determined. It is thus desirable to establish that bile acid transport in this system can be affected by cholestatic agents. A broad spectrum inhibitor of hepatobiliary transport is cyclosporin A (CyA), which has been used to inhibit bile acid transport in 2D sandwich cultures[219]. Supraphysiological levels of bile acids (>10μM) can also affect hepatobiliary transport significantly[16, 46]. However, the effects of prolonged exposure to these compounds on bile acid transport have not been determined in hepatocyte cultures.

In this chapter, the effects of varying DEX and EGF concentrations on bile acid transport and canalicular network formation were determined. [^{3}H]-TCA, digoxin, and CDF transport studies were conducted to differentiate effects on transporter expression and canalicular network formation. Finally, the effects of 24hr exposure to CyA and supraphysiological bile acid concentrations on [^{3}H]-TCA transport were determined as well. These studies provide a foundation for defining the medium composition for use with perfused 3D cultures.

2.2 Materials and Methods

2.2.1 Chemicals

[^{3}H] Taurocholic acid ([^{3}H]-TCA; 5 Ci/mmol, >95% purity), [^{3}H]digoxin (40 Ci/mmol, >97% purity) and UltimaGoldXR scintillation fluid (Perkin Elmer Life Sciences, Boston, MA, USA); Blendzyme® III and Complete® protease inhibitor cocktail (Roche Applied Science, Indianapolis, IN, USA); Dulbecco's modified Eagle's media (DMEM, w/sodium pyruvate, low glucose, pyridoxine HCl, w/o phenol red, glutamine), phosphate buffered saline (PBS), fetal bovine serum (FBS), insulin, epidermal growth factor (EGF), Trizol® LS reagent and 5(and 6)-carboxy-2',7'-dicholorofluorescein (CDF) diacetate (Invitrogen/Gibco, Carlsbad, CA, USA); anti-human/rat actin and anti-rat Oatp1a4 (rat Oatp2) antibodies (Chemicon, San Diego, CA, USA); anti-human/rat MRP2 (M_2III-6) antibody was obtained from Alexis Biochemical (San Diego, CA, USA); RIPA buffer (Teknova, Hollister, CA, USA); HRP-conjugated anti-rabbit and anti-mouse secondary antibodies (Amersham, Piscataway, NJ, USA); EGTA, dexamethasone (DEX), gentamicin, essentially-fatty-acid-free bovine serum albumin (faf-BSA), bovine serum albumin (BSA), TCA, cyclosporin A (CyA), Hanks balanced salt solution (HBSS, w/$NaHCO_3$, w/o phenol red) (Sigma Chemical Co, Saint Louis, MO, USA); ITS®, Matrigel® (w/o phenol red) and rat tail collagen type I (BD Biosciences, San Jose, CA, USA); all other chemicals and reagents were purchased at analytical grade from commercial sources.

2.2.2 Primary Liver Cell Isolation

Primary cells were isolated from male Fisher rats weighing 150-180 gm using a modification of the Seglen 2-step collagenase procedure as described previously [2, 230, 231]. Blendzyme III was used as the digestion enzyme instead of collagenase. Following isolation, the cell suspension DAG (DMEM w/2g/ml BSA, and 50mg/l gentamicin) was centrifuged two consecutive times at 50g (3min each) to obtain a hepatocyte rich fraction, and each time the supernatant was discarded, the cells were resuspended in 50ml of DAG. The final cell viability, as determined by trypan blue exclusion using a ViCell counter, was in the 90-95% range with cell density in the 8-13X10^6 cells/ml range.

2.2.3 Preparation of 2D Sandwich Cultures

Biocoat® Collagen Type I 24-well plates (BD Biosciences) were incubated with 350μL per well of plating hepatocyte growth media (pHGM; DMEM supplemented with 5% FBS, 4 mg/l insulin, 0.1 μM DEX, 0.03 g/l L-proline, 0.1 g/l L-ornithine, 0.305 g/l niacinamide, 2 g/l D-(+)-galactose, 1 mM L-glutamine, 50 mg/l gentamicin, 54.4 μg/l $ZnCl_2$, 75 μg/l $ZnSO_4 \cdot 7H_2O$, 20 μg/l $CuSO_4 \cdot 5H_2O$, 25 μg/L $MnSO_4$) overnight. Medium was aspirated off plates immediately before seeding. Primary hepatocytes from isolation were diluted in ice-cold seeding HGM (sHGM; pHGM w/1μM DEX) to a concentration of 10^6cells/mL, and 350μL of this dilution were added to each well. 2-3 hours post-seeding, plates were gently shaken and wells were washed with 350μL of warm pHGM twice to remove non-adherent cells. 24 hours post-seeding, Matrigel® aliquots were thawed on ice and diluted to a protein concentration of 0.25 mg/mL in ice-cold modified hepatocyte growth medium (mHGM; pHGM supplemented w/ITS and 2g/l faf-BSA, w/o

insulin and FBS). Cold pipette tips were always used when pipetting any Matrigel® dilution. Plates were very lightly shaken to remove any non-adherent cells, and 350μL of ice-cold Matrigel® dilution were added to each well. Plates were incubated at 37°C immediately. Medium was replaced with 350μL of warm mHGM every 24 hours for the duration of culture. Unless otherwise noted, all cultures were incubated in an environment at 37°C, 5% CO_2, and 95% humidity. Where noted, EGF at concentrations noted was added to all seeding and maintenance culture media. Where noted, DEX concentrations were modified in all seeding and maintenance culture media. For some studies, cyclosporin A (CyA) or TCA at concentrations noted were added to culture medium on day 3 post-seeding for 24hr, on day 4 cells were washed 3X with warm mHGM without CyA or TCA and either harvested or incubated at 37°C for 30min before transport studies were conducted.

2.2.4 Analysis of Hepatobiliary Transport in 2D Sandwich Cultures

Cultures were washed 3X with 500μl of either standard HBSS or Ca^{2+}-free HBSS (modified HBSS w/o Ca^{2+} or Mg^{2+}, w/1μM EGTA) and incubated for 10min in either buffer. Cultures were then incubated in standard HBSS with either 2μM CDF-diacetate w/1:1000 Hoechst stain, 1μM [^{3}H]digoxin, or 10μM [^{3}H]-TCA for 15min unless otherwise noted. Cultures were then either imaged (CDF) or rinsed vigorously 3X with ice-cold standard HBSS, 200μl of RIPA buffer was added to each well for cell lyses, and plate was put on a shaker for >20 min. 150μl of the cell lysate from [^{3}H]-TCA or [^{3}H]digoxin accumulation studies were then analyzed using liquid scintillation spectroscopy (LS 6500 scintillation counter, Beckman Coulter, Inc., Fullerton, CA,

USA). Total protein concentration was determined using microplate method of the MicroBCA kit[232] (Pierce Biotechnology, Rockford, IL, USA) as described by the manufacturer. The bile excretion index (BEI) was calculated as the difference in accumulation in cultures with intact bile canaliculi-like structures and those with disrupted bile canaliculi-like normalized by the accumulation in cultures with intact canaliculi to give the percentage canalicular accumulation of the substrate[147].

$$BEI = \frac{[TCA]_{CELLS+BC} - [TCA]_{CELLS-BC}}{[TCA]_{CELLS+BC}} * 100\%$$

where: BEI = Bile Excretion Index

$[TCA]_{CELLS+BC}$= the accumulation of TCA in the cells and canaliculi as measured by incubation of cultures in TCA after pre-incubation in a Ca^{2+}-rich environment

$[TCA]_{CELLS-BC}$= the accumulation of TCA in the cells with disrupted canaliculi as measured by incubation of cultures in TCA after pre-incubation in a Ca^{2+}-free environment

BEI for [^{3}H]digoxin were calculated similarly. The differences in accumulation between groups were analyzed with Student's t test and a p-value < 0.05 was considered statistically significant.

2.2.5 Light and Fluorescence Microscopy

Daily phase contrast images and fluorescent CDF and Hoescht stain images of 2D cultures were visualized on a Zeiss Axiovert 100TV inverted fluorescent microscope (Carl Zeiss Inc, Thornwood, NJ, USA) and acquired with a QImaging Retiga camera (QImaging, Surrey, BC, Canada). The microscope was fitted with a mercury lamp and filters for fluorescence microscopy.

2.3 Results

2.3.1 Imaging of Effects of EGF and DEX on Canalicular Network Integrity

Phase contrast imaging of 2D sandwich cultures was used to observe dose-dependent effects of EGF on the integrity and morphology of canalicular networks (Figure 2-1). Dose-dependent effects of DEX were also studied as this substrate is known to also have an effect on the attachment of hepatocyte to ECM and promotes development of tight junctions [5, 233, 234]. As the concentration of DEX increases the presence of canalicular networks seems to increase along with a prominent cuboidal shape and punctate nuclei in the cells, indicative of nucleus integrity, while lack of DEX resulted in a flattened cell shape, hollow nuclei, and greater cell detachment (Figure 2-1 a, b & c). The presence of EGF seems to have a deleterious effect on the integrity of the structures independent of dosage along with a flattened cell shape and a greater number of hollow nuclei (Figure 2-1 d & e). These findings are consistent with EGF's effect of reducing the number of cell junctions in primary rat hepatocyte cultures[207].

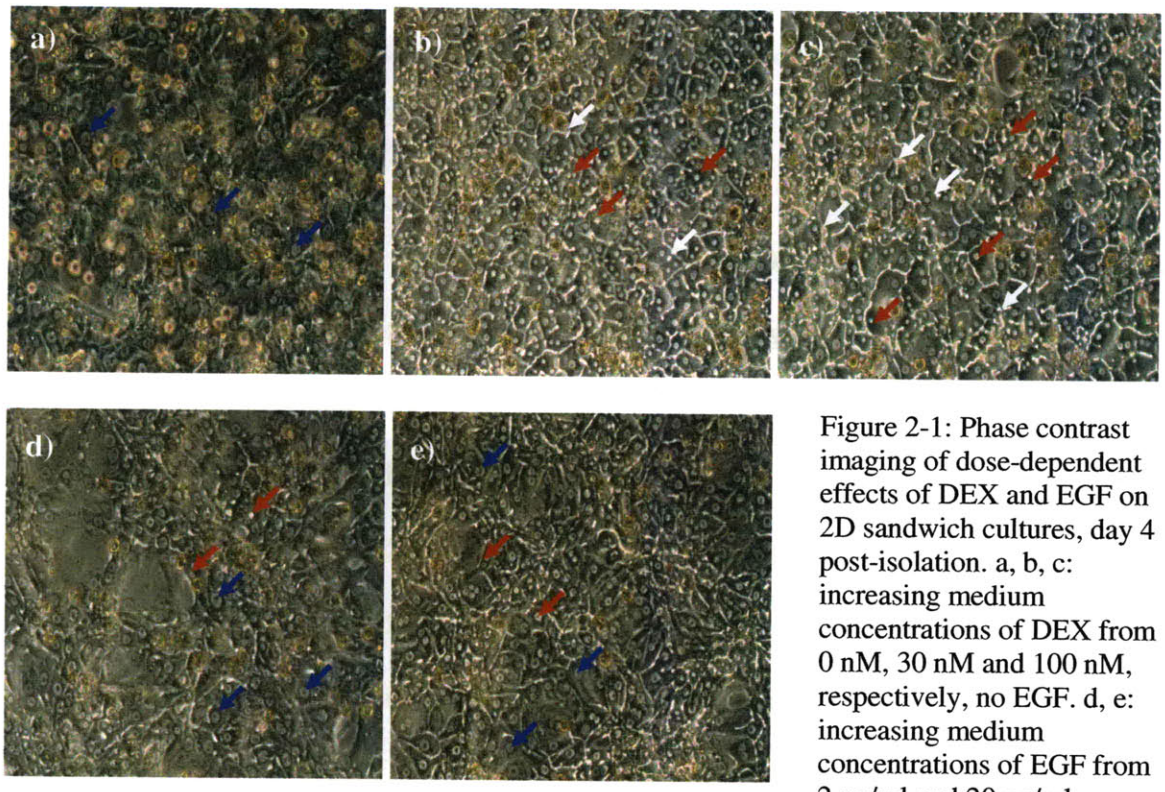

Figure 2-1: Phase contrast imaging of dose-dependent effects of DEX and EGF on 2D sandwich cultures, day 4 post-isolation. a, b, c: increasing medium concentrations of DEX from 0 nM, 30 nM and 100 nM, respectively, no EGF. d, e: increasing medium concentrations of EGF from 2 ng/ml and 20 ng/ml, respectively, 100nM DEX. White arrows, canalicular networks; red arrows, punctate nuclei; blue arrows, hollow nuclei

To assess the functionality and integrity of these structures, retention of CDF-diacetate (not fluorescent), which is hydrolyzed to CDF (green fluorescent) and quickly transported into canalicular networks was imaged[210, 215]. Congruent with phase contrast imaging, the network of canaliculi-like structures is more prominent, regular, and consistent when EGF is not present in the medium (Figure 2-2a) then when it is (Figure 2-2c). However, in the presence of EGF, CDF appears to be concentrated in punctate structures within the cell. These structures could indicate the presence of intracellular vesicles containing canalicular transporters, which have been observed in hepatocytes lacking tight junction proteins[235]. This method also demonstrates that a Ca^{2+}-free

environment completely disrupts the tight junctions and leaves the structures completely disrupted (Figure 2-2 b & d).

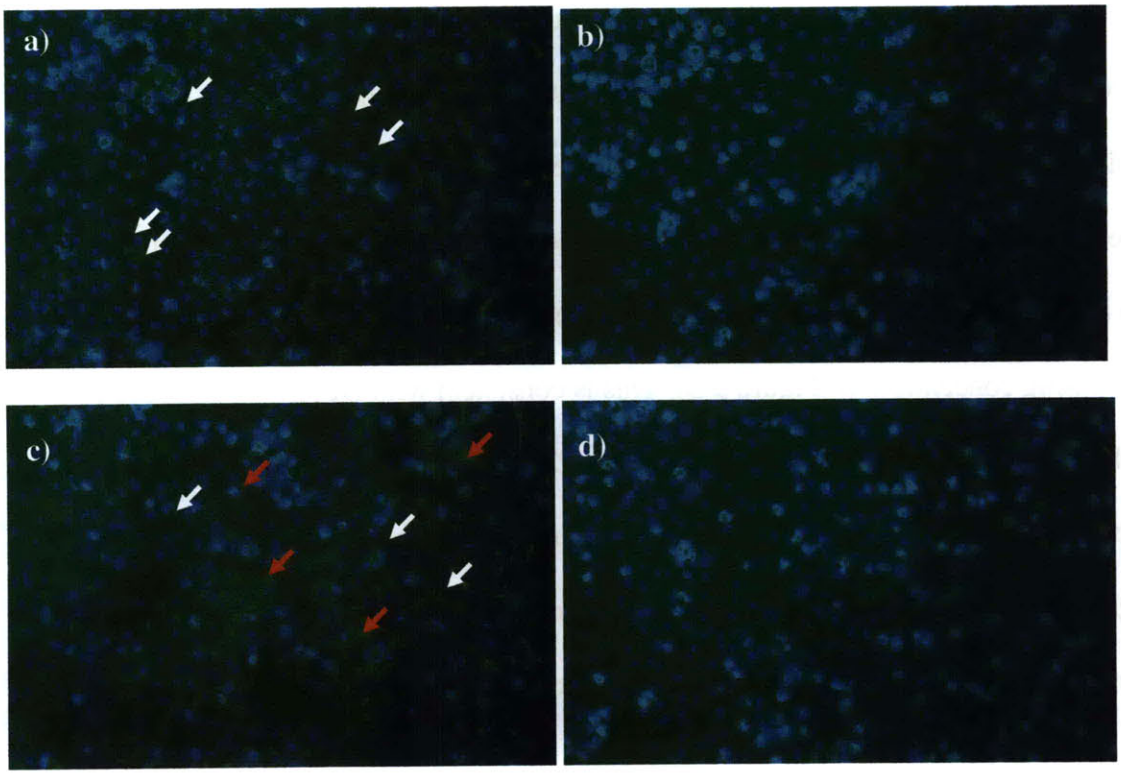

Figure 2-2: Cultures incubated with CDF-diacetate which is cleaved to CDF (green) and shuttled to canaliculi-like structures. Nuclear staining with Hoechst stain (blue). Images a & c pre-incubated in a Ca^{2+}-rich environment. Images b & d pre-incubated in Ca^{2+}-free environment. Images from: a and b, 2D sandwich cultures (day 4), no EGF; c and d, 2D sandwich cultures (day 4), 20ng/mL EGF. White arrows, canalicular accumulation of CDF; red arrows, intracellular CDF accumulation.

2.3.2 Effects of DEX and EGF Concentration on [^{3}H]-TCA transport

In order to assess the effects of DEX and EGF on canalicular network formation and transporter activity, [^{3}H]-TCA transport was measured in 2D sandwich cultures in the presence of increasing doses of EGF and DEX [213]. Transport was assessed by adding 10μM [^{3}H]-TCA to the culture buffer and assessing total accumulation after 15min incubation in matched pairs of cultures that had been pre-treated to exhibit either intact

(Cells+BC) or disrupted (Cells-BC) bile canalicular networks during the 15 min accumulation period. The accumulation levels are affected by the uptake and efflux rates of [^{3}H]-TCA while the difference in accumulation between culture with intact and disrupted canalicular networks is affected mostly by the baseline integrity and development of these canalicular networks. The bile excretion index (BEI) was calculated as described in the previous section to compare the transport capabilities of each culture. The BEI and canalicular [^{3}H]-TCA accumulation of 2D sandwich cultures increases as the concentration of DEX increases while the effect of EGF was not ameliorated by decreasing concentration (Figure 2-3). This is consistent with DEX's effect at promoting cell-cell junctions while EGF inhibits these[5, 207, 217, 233, 234]. However, the dose-dependent effect of DEX on [^{3}H]-TCA accumulation and transport may be biphasic as higher doses of DEX have been shown to reduce the expression of Ntcp, the main uptake transporter of TCA, and [^{3}H]-TCA accumulation in sandwich cultured hepatocytes[213].

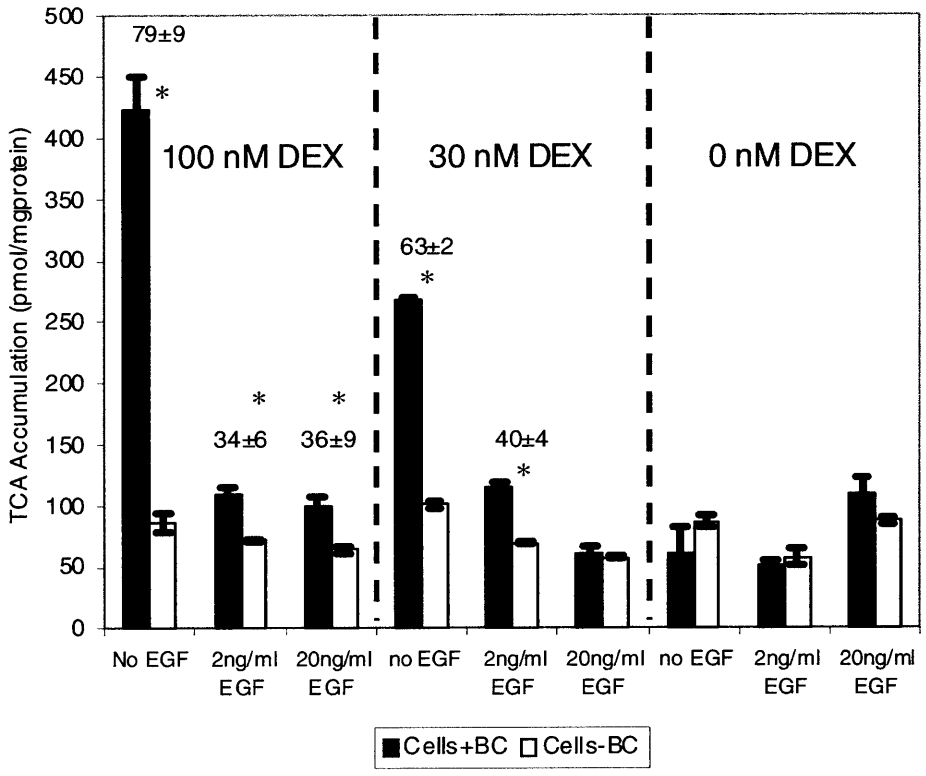

Figure 2-3: Influence of EGF and DEX medium concentration on 2D sandwich cultures (concentrations as indicated). BEI noted above bars unless unmeasurable. Closed and open bars indicate cultures with intact and disrupted canalicular networks, respectively. Data shown as mean±SD (n = 1 biological replicate, in triplicate). *p<0.05 Cells+BC and Cells-BC. Day 4 post-isolation.

2.3.3 Effects of EGF on [^{3}H]Digoxin Transport

Having observed that EGF may decrease the formation and integrity of canalicular networks in 2D sandwich cultures, the effect of 0.2ng/ml EGF on [^{3}H]digoxin transport, which is mainly transported into canalicular networks by Mdr1a/b[212], in 2D sandwich cultures on day 4 post-isolation was measured (Figure 2-4a). [^{3}H]-TCA transport, which is mainly transported into canalicular networks by Bsep[26], was also assessed in 2D sandwich cultures in the presence of this EGF concentration (Figure 2-4b). This EGF concentration was chosen because it is 10-fold lower than those assessed previously, and could aid in elucidating dose-dependent effects on canalicular network formation. A medium concentration of 0.1μM DEX was used in these cultures, and all subsequent studies. Transport was assessed by adding either 1μM [^{3}H]digoxin or 10μM [^{3}H]-TCA to the culture buffer and assessing total accumulation after 15min incubation in

matched pairs of cultures that had been pre-treated to exhibit either intact (Cells+BC) or disrupted (Cells-BC) bile canalicular networks during the 15 min accumulation period. BEI was calculated as previously described. Similar to the effect observed with [^{3}H]-TCA accumulation and CDF imaging, EGF significantly decreased canalicular [^{3}H]digoxin accumulation in these cultures. In the absence of EGF, the accumulation in Cells+BC cultures and Cells-BC cultures, as well as the BEI measured of 47±12%, were very similar to those previously published[212]. However, cultures in the presence of EGF had no significant difference in their accumulation between Cells+BC cultures and Cells-BC cultures. Interestingly, the concentration of EGF used in these studies was 10-fold lower than the lowest concentration used to study the effects of EGF and DEX on [^{3}H]-TCA transport (Figure 2-3). The effects of 0.2ng/ml EGF on [^{3}H]-TCA transport were similar, but not as prominent, to those measured for higher concentrations of EGF with BEIs of 83±39% and 67±7% in the absence and presence of EGF, respectively. Therefore, canalicular formation and integrity in 2D sandwich cultures is very sensitive to EGF-mediated effects.

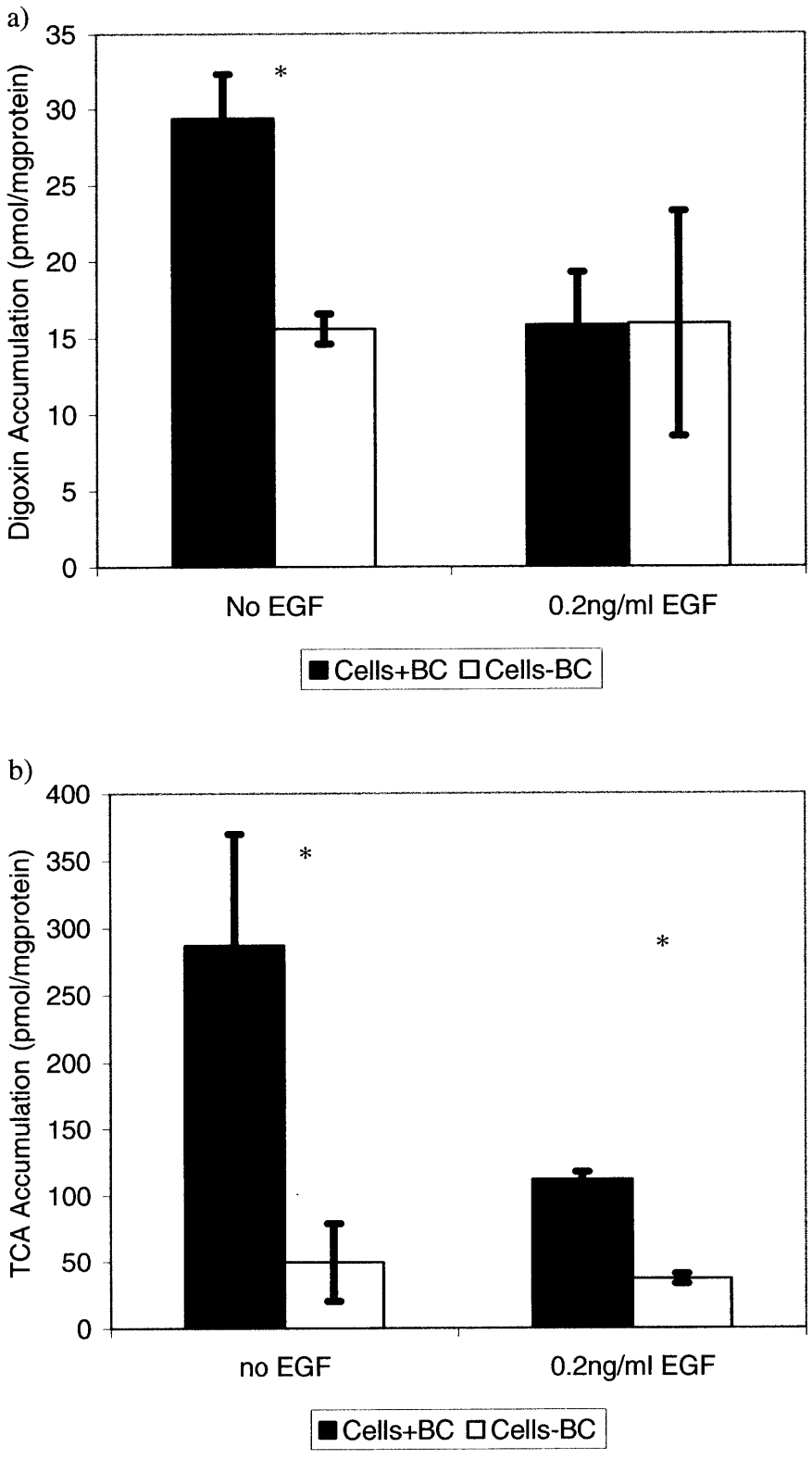

Figure 2-4: Effects of EGF on (a) [^{3}H]digoxin and (b) [^{3}H]-TCA transport in 2D sandwich culture. 15min accumulation of (a) 1μM [^{3}H]digoxin and (b) 10μM [^{3}H]-TCA in day 4 2D sandwich cultures in the presence and absence of 0.2ng/ml EGF. (a) BEI = 47±12% (No EGF), unmeasurable (+EGF). (b) BEI = 83±39% (No EGF), BEI = 67±7% (+EGF). Data shown as mean±SD (n = 1 biological replicate, in triplicate). *$p<0.05$ Cells+BC and Cells-BC.

2.3.4 Effects on Hepatobiliary Transport of Prolonged Exposure of CyA and TCA

CyA has been established to change the gene expression *in vivo* of transporters and other relevant transcripts[236]. High levels of TCA in the media or blood have also shown large effects in gene and protein expression of transporters *in vivo* as well[3, 9, 237]. Because the results in this chapter have shown that EGF and DEX both have significant effects on hepatobiliary transport, it was important to determine if transport in 2D sandwich cultures could also be affected by prolonged exposure to cholestatic agents. To assess the effects of 24hr exposure to CyA and TCA on [^{3}H]-TCA transport, 2D sandwich cultures were incubated for 24hr with CyA or TCA containing culture medium on day 3 post-isolation and [^{3}H]-TCA transport studies were conducted on day 4 post-isolation as described previously. 2D sandwich cultures were thoroughly washed to remove the compounds before the assay was performed so that transport would not be inhibited by the compounds themselves but by their effects on the phenotype of the cultures.

Supraphysiological levels of TCA did not affect the accumulation in the cell but did decrease the canalicular accumulation of [^{3}H]-TCA (Figure 2-5), which may indicate that the effect of these levels of bile acids elicited a response by the cell of increasing the permeability of the canalicular networks structures. Figure 2-5 also shows that CyA does decrease the cellular accumulation of these cultures, which would be consistent with CyA possibly leading to the cell decreasing uptake and increasing efflux of bile acids. High levels of CyA have been shown to have deleterious effects on the integrity of the cell membranes[236], and therefore results at over 1 μM CyA are complicated by these effects and probably are not reflecting the direct effects on transport.

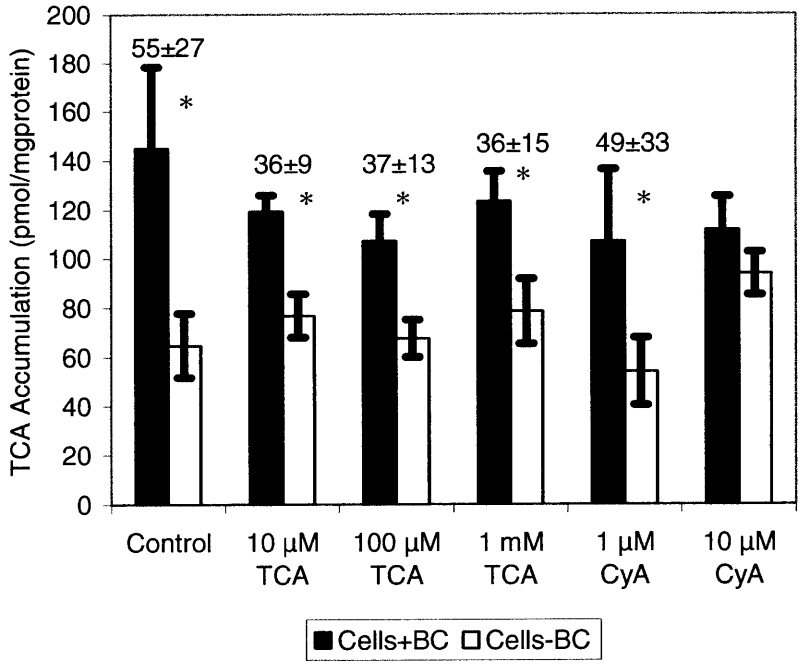

Figure 2-5: Effects of 24hr exposure to CyA and TCA (concentrations as noted) on [^{3}H]-TCA accumulation. BEI noted above bars unless unmeasurable. [^{3}H]-TCA accumulation after 15 minute incubation with 10μM [^{3}H]-TCA. Data shown as mean±SD (n = 3 biological replicates, in triplicate). *p<0.05 Cells+BC and Cells-BC.

2.4 Discussion and Conclusions

2D sandwich cultures have been widely used as an *in vitro* model for the study of hepatobiliary transport[147, 208-216]. However, the effect of media components such as DEX and EGF on hepatobiliary transport in 2D sandwich cultures has not been well studied. Determination of these effects is necessary in order to establish media composition conditions for other culture systems, such as perfused 3D cultures, which could be adapted to the study of hepatobiliary transport. However, the effects of these media components should be assessed in 3D cultures, as there may be mechanistic differences in the seeding, morphology, and physiology of 2D and 3D cultures.

As expected, DEX increased the formation and integrity of canalicular networks. It is especially interesting that lowering the concentration of DEX only to 30% of the standard concentration used throughout all other experiments was sufficient to

significantly diminish [^{3}H]-TCA canalicular retention. This emphasizes the need to have tight controls on the concentration of DEX in the culture medium. However, increasing the standard DEX concentration in culture medium may also have detrimental effects on [^{3}H]-TCA accumulation. High DEX concentrations (>1μM) have been shown to affect the expression of hepatic transporters, diminishing the expression of Ntcp and therefore decreasing bile acid uptake[213, 229].

EGF had a strong effect in decreasing canalicular [^{3}H]-TCA accumulation, which appears to be attributable to disruption of canalicular network formation. Previous studies, using transmission electron microscopy analysis, had shown that EGF could potentially disrupt the formation of canalicular networks in 2D sandwich cultures[207]. However, it was unexpected that even low concentrations of EGF caused an almost complete lack of canalicular [^{3}H]-TCA accumulation. The lack of canalicular accumulation of [^{3}H]digoxin and the decreased excretion of CDF into canalicular networks in the presence of EGF confirm that the diminished canalicular accumulation of [^{3}H]-TCA is due to EGF-mediated effects on canalicular network formation and not on diminished transport capabilities in these cultures. CDF, [^{3}H]digoxin, and [^{3}H]-TCA are excreted into the canaliculi mainly by Mrp2, Mdr1a/b, and Bsep, respectively, and thus are transported through independent pathways.

The effects of EGF on canalicular network formation were of interest because even though 2D sandwich studies had shown that EGF could potentially decrease canalicular network formation, it has been observed to increase tissue-formation and ECM in 3D hepatocyte cultures, such as spheroidal aggregates and organoid roller bottle cultures[188, 189, 223, 224, 238]. Canalicular networks have been imaged and

qualitatively determined to be functional in hepatocyte spheroidal aggregates with EGF present in the culture medium[224].

The effects of cholestatic agents on [^{3}H]-TCA transport have been previously published[219], as well as drug interactions on the transport of other compounds[216], however the long-term effects of such compounds has not been very well studied. In order to address this aspect, the effects of 24hr exposure to CyA and supraphysiological TCA levels on [^{3}H]-TCA transport were determined. It was observed that the only effect supraphysiologic TCA levels had on these studies was slight decrease in canalicular retention of [^{3}H]-TCA. This was unexpected as high levels of bile acids are known to induce increased Bsep expression, the main bile acid efflux transporter, through the FXR activation pathway[16, 46]. If Bsep expression would have been increased, an increase of canalicular [^{3}H]-TCA accumulation would have been observed. This indicates that these cultures may not be very sensitive to increase bile acid levels. The possible increase in canalicular porosity may be a morphological response by the hepatocyte cultures to reduce bile accumulation under these conditions.

CyA slightly decreased intracellular [^{3}H]-TCA accumulation which may indicate slightly diminished uptake or increased efflux of [^{3}H]-TCA. This may indicate that these cultures can be responsive to prolonged exposure to cholestatic agents. However, many other liver specific functions in 2D sandwich cultures decrease over time in culture[2, 4], and thus studies of the effects of longer time exposure to CyA and supraphysiological levels of TCA on [^{3}H]-TCA transport is not very feasible in this culture system. Therefore, adaptation of 2D sandwich culture protocols for transport studies to other

systems, such as perfused 3D cultures, is necessary to further understand the interactions between functions such as drug metabolism and hepatobiliary transport.

In the pursuit of this goal, it seems that based on the results in 2D sandwich cultures the studies to adapt these protocols to perfused 3D cultures should be performed with a standard concentration (0.1μM) of DEX in the culture medium and without EGF in the medium. However, because of the potential differences in effects of EGF on 2D sandwich hepatocyte culture morphology and perfused 3D hepatocyte culture morphology and tissue formation, it will also be necessary to explore the effects of EGF on these two platforms further.

Chapter 3

Adaptation of Hepatobiliary Transport Assays to Perfused 3D Hepatocyte Cultures

3.1 Introduction

Hepatobiliary transport of bile acids and other chemical compounds is one of the main functions of the liver[16, 46]. It has therefore been studied both *in vitro* and *in vivo* in order to determine the effects of various chemical compounds and conditions on this function[8, 147, 208-216, 237]. A widely used system for the study of hepatobiliary transport *in vitro* is the 2D sandwich culture[147, 208-216]. However, it has been shown that liver-specific functions, such as drug metabolism and albumin secretion, are not well maintained in these cultures over >7 days in culture[2, 4]. It is therefore of great interest to adapt protocols developed for the study of hepatobiliary transport in culture systems which can maintain these other functions as well, such as an *in vitro* physiological 3D perfused model of the liver[2, 225].

Bile acid transport studies are conducted in 2D sandwich cultures, which form extensive canalicular networks, by having paired cultures with intact and disrupted canalicular networks and measuring bile acid accumulation (e.g. [^{3}H]-TCA accumulation) after a specific incubation in bile acid containing buffer. The canalicular networks can be disrupted by the pre-incubation of cultures in a Ca^{2+}-free environment[147].

Most 2D rat hepatocyte sandwich culture transport studies are conducted on day 4 post-isolation cultures because that is the minimum amount of time necessary for cell re-polarization and canalicular network formation[147, 208-210]. However, tissue reorganization and formation may require a lengthier period of time for perfused 3D cultures[2, 225], and therefore an appropriate day of culture to perform bile acid transport assays must be determined.

In order to adapt transport study protocols developed for 2D sandwich cultures to a perfused 3D culture model, it is first necessary to establish whether the transport studies can be conducted without perfused culture media flow through the hepatocyte cultures. To determine whether perfused flow is necessary or a static media condition could be appropriate, it is important to calculate the first-order Thiele modulus, Φ^2, which is a dimensionless parameter that compares the time scale for reaction to the time scale for diffusion through the tissue.

$$\Phi^2 = \frac{V_{Vol} L^2}{K_M D}$$

The values to calculate the Thiele modulus, Φ^2, are either published values, extrapolations of published values, or measured values, such as the length scale, L. The value used for the length scale of the tissue, L, is 115μm in this case, half of the scaffold thickness. The value used for the diffusion coefficient, D, for TCA, the species of interest in this case, is $5.9X10^{-6}$ cm^2/s[239]. The Michaelis-Menten constant for TCA, K_M, used in this calculation is 28μM, which is the value that has been measured in 2D sandwich

cultures[147]. The volumetric uptake rate, V_{Vol}, used is an extrapolation calculated as follows:

$$V_{Vol} = V_M d_o d_P$$

The values used to extrapolate this value were also taken from published values. The maximum uptake rate for TCA, V_M, used is 1.19 nmol/mgprotein/min, which is the value that has been measured in 2D sandwich cultures[147]. The volumetric cell density for hepatocytes, d_o, and the amount of protein per cell in hepatocytes, d_P, used are $1.2X10^8$ cells/cm^3 and 1.1 ngprotein/cell, respectively[240]. Based on these values, the volumetric uptake rate is calculated to be 2.62μM/s.

Based on these numbers, the Thiele modulus is determined to be approximately 2, which would indicate that this process could be diffusion limited. Therefore, in order to obtain reliable measurements of [^{3}H]-TCA transport, it is necessary to conduct these studies with perfused buffer flow through the tissue cultures.

Having established that perfusion of tissue will be necessary in adapting these protocols, it is then also necessary to establish a time point of [^{3}H]-TCA accumulation measurement. It is of specific interest to determine a time point at which [^{3}H]-TCA accumulation is at steady state to diminish effects on [^{3}H]-TCA accumulation measurements due to experimental error in exact time point of measurement.

Canalicular network disruption in 2D sandwich cultures is achieved by Ca^{2+} modulation[147]. It will be necessary to determine whether perfused 3D cultures require longer periods of Ca^{2+} modulation in order for canalicular networks to be disrupted.

An important aspect in adapting and developing protocols for bile acid transport studies in perfused 3D cultures is to establish whether measured [^{3}H]-TCA accumulation

values are the result of actual transport activity, or whether it is the result of nonspecific effects or binding. It is therefore necessary to measure whether [^{3}H]-TCA transport activity can be inhibited by cholestatic agents, such as CyA[236]. Lack of an inhibitory effect on [^{3}H]-TCA transport would indicate that [^{3}H]-TCA accumulation values measured are not the result of transporter activity, but due to non-specific binding effects.

The studies presented in this chapter address all these considerations in order to develop transport studies protocols for perfused 3D cultures. Inhibitory studies were also conducted with CyA to confirm that accumulation measurements are due to hepatic transport activities and that these cultures can be affected by cholestatic agents and other chemicals.

3.2 Materials and Methods

3.2.1 Chemicals

[^{3}H] Taurocholic acid ([^{3}H]-TCA; 5 Ci/mmol, <95% purity) and UltimaGoldXR scintillation fluid (Perkin Elmer Life Sciences, Boston, MA, USA); Blendzyme® III and Complete® protease inhibitor cocktail (Roche Applied Science, Indianapolis, IN, USA); Dulbecco's modified Eagle's media (DMEM, w/sodium pyruvate, low glucose, pyridoxine HCl, w/o phenol red, glutamine), phosphate buffered saline (PBS), fetal bovine serum (FBS), and insulin (Invitrogen/Gibco, Carlsbad, CA, USA); RIPA buffer (Teknova, Hollister, CA, USA); EGTA, dexamethasone (DEX), gentamicin, essentially-fatty-acid-free bovine serum albumin (faf-BSA), bovine serum albumin (BSA), normal goat serum, Triton X-100, TCA, cyclosporin A (CyA), Hanks balanced salt solution (HBSS, w/$NaHCO_3$, w/o phenol red) (Sigma Chemical Co, Saint Louis, MO, USA);

ITS®, Matrigel® (w/o phenol red) and rat tail collagen type I (BD Biosciences, San Jose, CA, USA); all other chemicals and reagents were purchased at analytical grade from commercial sources.

3.2.2 Primary Liver Cell Isolation

Primary cells were isolated from male Fisher rats weighing 150-180 gm using a modification of the Seglen 2-step collagenase procedure as described previously [2, 230, 231]. Blendzyme III was used as the digestion enzyme instead of collagenase. Following isolation, the cell suspension DAG (DMEM w/2g/ml BSA, and 50mg/l gentamicin) was centrifuged two consecutive times at 50g (3min each) to obtain a hepatocyte rich fraction, and each time the supernatant was discarded, the cells were resuspended in 50ml of DAG. The final cell viability, as determined by trypan blue exclusion using a ViCell counter, was in the 90-95% range with cell density in the 8-13X10^6 cells/ml range.

3.2.3 Preparation of 2D Sandwich Cultures

Biocoat® Collagen Type I 24-well plates (BD Biosciences) were incubated with 350μL per well of plating hepatocyte growth media (pHGM; DMEM supplemented with 5% FBS, 4 mg/l insulin, 0.1 μM DEX, 0.03 g/l L-proline, 0.1 g/l L-ornithine, 0.305 g/l niacinamide, 2 g/l D-(+)-galactose, 1 mM L-glutamine, 50 mg/l gentamicin, 54.4 μg/l $ZnCl_2$, 75 μg/l $ZnSO_4 \cdot 7H_2O$, 20 μg/l $CuSO_4 \cdot 5H_2O$, 25 μg/L $MnSO_4$) overnight. Medium was aspirated off plates immediately before seeding. Primary hepatocytes from isolation were diluted in ice-cold seeding HGM (sHGM; pHGM w/1μM DEX) to a concentration of 10^6cells/mL, and 350μL of this dilution were added to each well. 2-3 hours post-

seeding, plates were gently shaken and wells were washed with 350μL of warm pHGM twice to remove non-adherent cells. 24 hours post-seeding, Matrigel® aliquots were thawed on ice and diluted to a protein concentration of 0.25 mg/mL in ice-cold modified hepatocyte growth medium (mHGM; pHGM supplemented w/ITS and 2g/l faf-BSA, w/o insulin and FBS). Cold pipette tips were always used when pipetting any Matrigel® dilution. Plates were very lightly shaken to remove any non-adherent cells, and 350μL of ice-cold Matrigel® dilution were added to each well. Plates were incubated at 37°C immediately. Medium was replaced with 350μL of warm mHGM every 24 hours for the duration of culture. Unless otherwise noted, all cultures were incubated in an environment at 37°C, 5% CO_2, and 95% humidity. Where noted, 20ng/ml EGF was added to all seeding and maintenance culture media.

3.2.4 Preparation of Perfused 3D Cultures

Perfused 3D cultures were prepared in multiwell reactor plates, as previously described[241]. After assembly of the multiwell reactor plates, 300μl of warm pHGM were added to each reservoir and multiwell plate was run at a flow rate of 0.2ml/min. The reactor pair was monitored to ensure proper priming and that air bubbles started to come out into the reactor pair within 90s±20% of priming being started. The reactor pairs were then filled to the fill line with warm pHGM (~ 4ml) and incubated overnight with a flow rate of 0.2ml/min. All reactor component parts were added to reactor pairs just before seeding, they were rinsed in PBS and all air bubbles were removed. 5 μm Millipore filters were incubated at RT for 30 minutes in PBS w/10g/ml BSA to passivate them and were rinsed briefly in PBS before placing them in each reactor pair. Polycarbonate scaffolds

were sonicated in 70% EtOH for 10 minutes to remove air bubbles from channels. Scaffolds were then rinsed 2X w/PBS, placed in a 30μg/mL type I collagen PBS solution and incubated at 37°C for >2 hours. Any air bubbles left in scaffolds were removed by pipetting collagen solution into channels. Scaffolds were removed from solution and left to dry for 2 hours at RT prior to seeding. Scaffolds were added to reactor wells <30min before seeding. Medium was aspirated off and reservoir/reactor pairs were filled to fill line with ice-cold pHGM. Medium was then aspirated slightly off reactor/reservoir pairs to ensure there was no liquid contact between reservoir and reactor. Flow was turned on at a flow rate of 0.2 ml/min in a downward direction through the channels and 800,000 cells were seeded per well, evenly distributing them throughout each scaffold. Cell suspension was not diluted before seeding. Each reactor/reservoir pair was filled to fill line with ice-cold pHGM immediately after seeding and multiwell reactor plate was incubated at 37°C, 5% CO_2, 95% humidity. Flow was maintained downward through the cells to promote attachment to scaffold and tissue-like structure development. Flow was reversed 0.2 ml/min upward through cells 8hrs post-seeding and maintained in this direction for the duration of culture to clear debris and non-adherent cells. On Day 1 post-isolation, culture medium was replaced with warm mHGM 3X to clear out pHGM completely from system. The reactor plate was allowed to flow for 1hr in between each media change to allow any left over pHGM in the system to completely mix with the fresh mHGM. Culture medium was replaced with mHGM (~2.5 ml) every 24 hrs for duration of culture.

3.2.5 Analysis of Bile Acid Transport in 2D Sandwich Cultures

Cultures were washed 3X with 500µl of either standard HBSS or Ca^{2+}-free HBSS (modified HBSS w/o Ca^{2+} or Mg^{2+}, w/1µM EGTA) and incubated for 10min in either buffer, unless otherwise noted. Cultures were then incubated in standard HBSS with 10µM [^{3}H]-TCA for 15min unless otherwise noted. Cultures were then rinsed vigorously 3X with ice-cold standard HBSS, 200µl of RIPA buffer was added to each well for cell lyses, and plate was put on a shaker for >20 min. 150µl of the cell lysate from [^{3}H]-TCA accumulation were then analyzed using liquid scintillation spectroscopy (LS 6500 scintillation counter, Beckman Coulter, Inc., Fullerton, CA, USA). Total protein concentration was determined using microplate method of the MicroBCA kit [232] (Pierce Biotechnology, Rockford, IL, USA) as described by the manufacturer. For experiments with CyA, 20µM CyA was added to buffer with [^{3}H]-TCA. As described in chapter 2, the bile excretion index (BEI) was calculated as the difference in accumulation in cultures with intact bile canaliculi-like structures and those with disrupted bile canaliculi-like normalized by the accumulation in cultures with intact canaliculi to give the percentage canalicular accumulation of the substrate[147]. The differences in accumulation between groups were analyzed with Student's t test and a p-value < 0.05 was considered statistically significant.

3.2.6 Analysis of Bile Acid Transport in Perfused 3D Cultures

Reservoir filters were removed from each reactor/reservoir pair and all media was aspirated. Each culture was washed 2X with 3ml of either standard HBSS or Ca^{2+}-free HBSS with a downward through cells flow rate of 0.2ml/min. Buffers were completely

aspirated off each reactor/reservoir pair and 800µl of either buffer was added on top of each reactor. The reactor/reservoir pairs were run for 5min at 0.2ml/min with 500µl added to the reactor portion after 2.5min and wash-through being constantly aspirated from reservoir portion to prevent liquid contact between reactor and reservoir. Reactor/reservoir pairs were then completely aspirated of any buffers and 800µl of either buffer was added to each reactor portion, the flow rate was changed to downward at 0.1ml/min for the duration of the study. Reactor/reservoir pairs were run for 10min with 500µl of buffer added to each reactor portion every 5min and constant reservoir buffer aspiration. Pairs were then thoroughly aspirated of any remaining buffers and 800µl of standard buffer with 10µM [^{3}H]-TCA was added to each reactor portion and reactor/reservoir pair was run for 15min, unless otherwise noted, following the same procedure as before. Scaffolds were removed from reactors, very gently washed 3X in 60mm Petri dishes with 10ml of ice-cold standard buffer, placed in 20ml scintillation vials with 700µl of RIPA buffer, and vortexed for ~30s. Vials were incubated at 4°C for >8 hours and scaffolds were inspected with light microscopy to ensure complete tissue removal and cell lyses. 500µl of cell lysate was analyzed using liquid scintillation spectroscopy. For experiments with CyA, 20µM CyA was added to buffer with [^{3}H]-TCA. Total protein was determined by MicroBCA assay [232] (Pierce Biotechnology), and BEI was determined as described.

3.3 Results

3.3.1 Time Course of Bile Acid Transport Studies

Canalicular network formation and re-polarization of hepatocytes in cultures following isolation typically requires a few days. In 2D collagen gel sandwich cultures, one the most widely-used *in vitro* culture systems for hepatic transport studies, require ~4 days for canalicular network formation and re-polarization of cells[210, 211]. The time required for cells to form canalicular networks and re-polarize so that transport studies can be conducted is unknown for perfused 3D rat hepatocyte cultures. In order to measure the functionality of canalicular networks in perfused 3D cultures, [^{3}H]-TCA transport studies were conducted on perfused 3D cultures on day 4 and day 7 of culture. These studies were also conducted on 2D primary rat hepatocyte sandwich cultures, a widely-used culture system for these studies[147, 208, 209]. [^{3}H]-TCA accumulation was measured after 15min incubation with 10μM [^{3}H]-TCA in paired cultures with intact (Cells+BC) and disrupted (Cells-BC) canalicular networks. Cultures were either exposed to a Ca^{2+}-rich or Ca^{2+}-free environment which is known to preserve or disrupt these networks, respectively[147], as described in chapter 2. Culture medium in these cultures contained 100nM DEX and no EGF, based on findings described in chapter 2.

Perfused 3D cultures demonstrated a slightly lower BEI and [^{3}H]-TCA accumulation than 2D sandwich cultures on day 4 post-isolation (Figure 3-1). However, Figure 3-1 shows that the accumulation and BEI levels in perfused 3D cultures do not seem to diminish at all on day 7 post-isolation from its day 4 levels whereas this is diminished severely in 2D sandwich cultures. The decrease in transport function of 2D sandwich cultures is consistent with an overall loss of phenotype and liver functions of

similarly plated cultures[2, 4]. Perfused 3D cultures may pose an advantage if long-term or multi-day studies are required, especially since perfused 3D cultures maintain other liver functions such as drug metabolism over these periods[2, 225]. Moreover, the slightly lower canalicular accumulation levels in perfused 3D cultures may be because the canalicular networks are more porous than in 2D sandwich cultures on day 4 of culture.

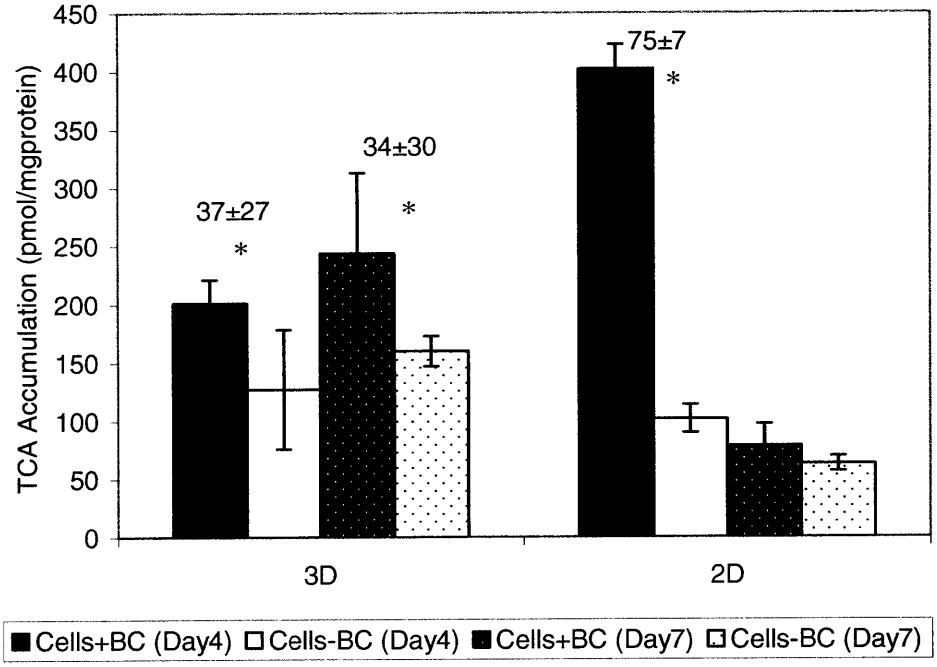

Figure 3-1: Time course of [^{3}H]-TCA transport. BEI noted above bars unless it was not measurable. Closed bars represent cultures with intact canalicular networks, open bars are cultures with disrupted canalicular networks. Solid bars, day 4 post-isolation; dotted bars, day 7 post-isolation. Data shown as mean±SD (n = 3 biological replicate, in triplicate). *p<0.05 Cells+BC and Cells-BC.

3.3.2 Effects of Pre-Incubation Time on [^{3}H]-TCA Accumulation

A concern in adapting the 2D sandwich [^{3}H]-TCA transport study protocols to perfused 3D cultures is that the pre-incubation times in a Ca^{2+}-free environment required for canalicular networks disruption may be longer in 3D cultures. Therefore, the effects of longer Ca^{2+}-free buffer pre-incubation time were systematically investigated in both 3D and 2D cultures. Specifically, [^{3}H]-TCA accumulation was measured in perfused 3D

cultures with 2min, 10min, and 20min pre-incubation time in either standard HBSS (Cells+BC) or Ca^{2+}-free HBSS (Cells-BC) on day 7 post-isolation. [^{3}H]-TCA accumulation was measured after 15min incubation with 10μM [^{3}H]-TCA. Culture medium in these cultures contained 100nM DEX and no EGF, based on findings described in chapter 2.

The difference in accumulation between cultures pre-incubated in a Ca^{2+}-rich environment and those in a Ca^{2+}-free environment was slightly lower for shorter pre-incubation periods in perfused 3D cultures (Figure 3-2). The BEI in these cultures was 18±16%, 34±30%, and 23±19% after 2min, 10min, and 20min pre-incubation time, respectively. These data are essential for validating TCA transport protocols in these cultures.

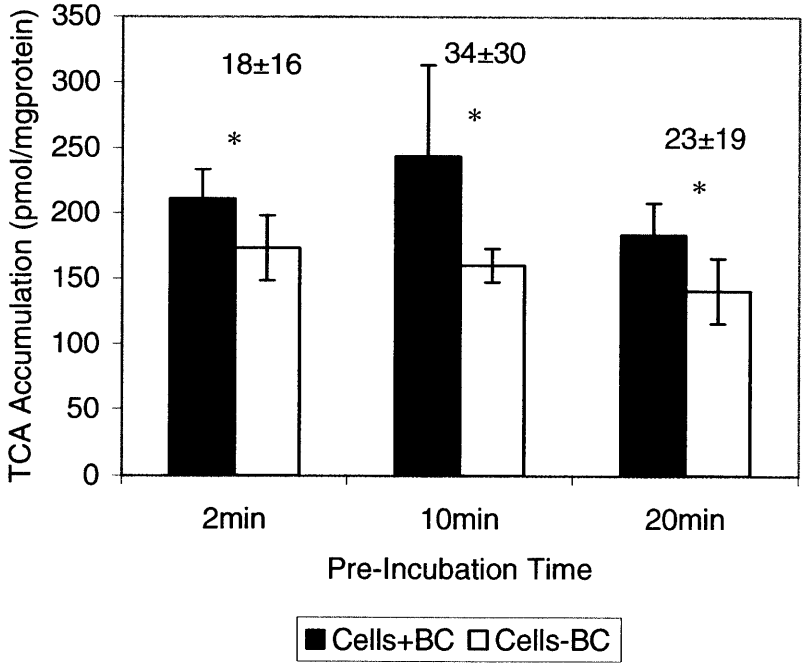

Figure 3-2: Effects of pre-incubation time on [^{3}H]-TCA accumulation in perfused 3D cultures on day 7 post-isolation. BEI noted above bars unless it was not measurable. Accumulation after 15min incubation with 10μM [^{3}H]-TCA. Data shown as mean±SD (n = 3 biological replicate, in triplicate). *$p<0.05$ Cells+BC and Cells-BC.

3.3.3 Time Course of [^{3}H]-TCA Accumulation

Having established that a 10min pre-incubation time was sufficient to open canalicular network in perfused 3D primary rat hepatocyte cultures, it was also necessary to establish a time point at which [^{3}H]-TCA accumulation is reliably at a steady-state level so that studies can be conducted to measure the effects on [^{3}H]-TCA transport by various culture conditions and compounds. Hepatic transport studies in 2D sandwich cultures have been shown that [^{3}H]-TCA accumulation levels reach a constant value after ~10-15min of incubation with [^{3}H]-TCA[147].

[^{3}H]-TCA accumulation value plateaus in perfused 3D cultures after 15min of incubation with 10μM [^{3}H]-TCA (Figure 3-3). Therefore, measurements made at this time point can inform effects on the kinetics of TCA transport without concerns of possible small variations in the actual measurement time.

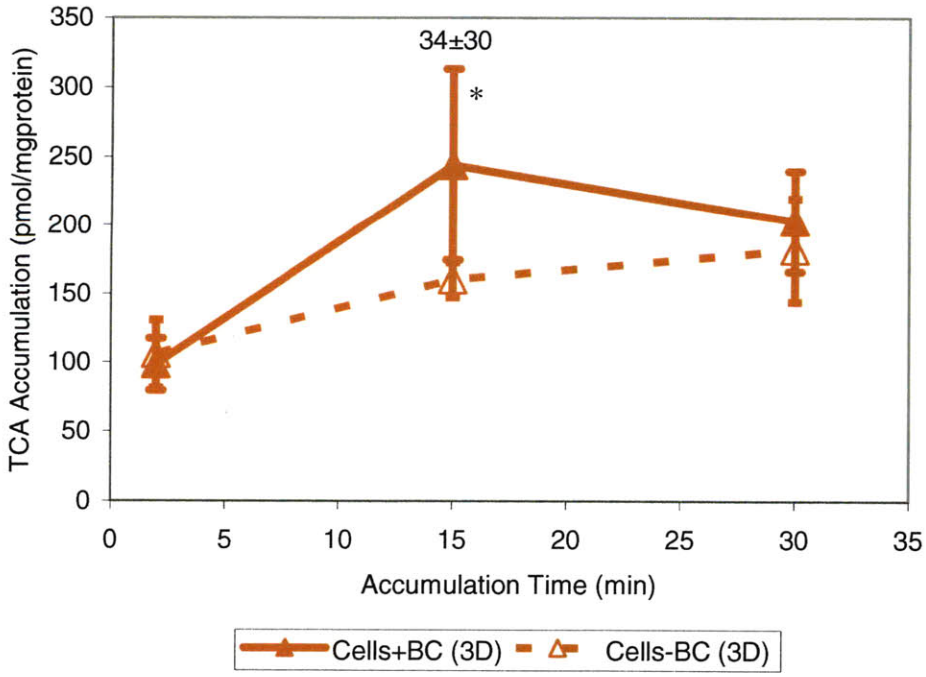

Figure 3-3: Time course of [^{3}H]-TCA accumulation in perfused 3D cultures. BEI noted above bars unless it was not measurable. Day 7 post-isolation. [^{3}H]-TCA buffer conc = 10μM. Data shown as mean±SD (n = 3 biological replicate, in triplicate). *$p<0.05$ Cells+BC and Cells-BC.

These findings are consistent with data obtained from 2D sandwich cultures obtained on day 4 post-isolation (Figure 3-4). Studies were conducted on day 4 post-isolation because most reported transport studies in these cultures have been conducted on day 4[147, 208-216]. Moreover, [^{3}H]-TCA accumulation in cultures in these 2D cultures on day 7 post-isolation is diminished thus a relevant time course could not be gathered under that condition (data not shown).

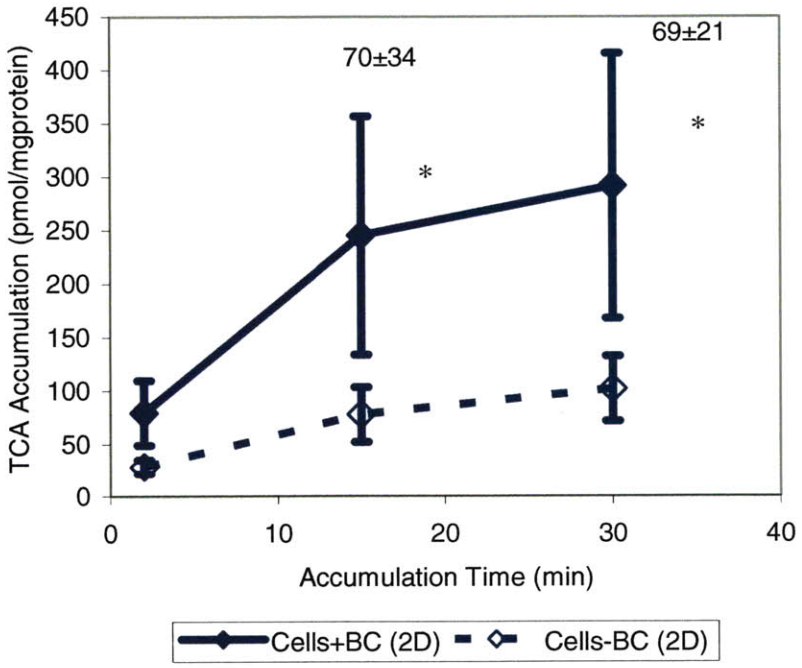

Figure 3-4: Time course of [^{3}H]-TCA accumulation in 2D sandwich cultures. BEI noted above bars unless it was not measurable. Day 4 post-isolation. [^{3}H]-TCA buffer conc = 10μM. Data shown as mean±SD (n = 3 biological replicate, in triplicate). *$p<0.05$ Cells+BC and Cells-BC.

3.3.4 Effects of Cyclosporin A on [^{3}H]-TCA Accumulation

In both 2D and 3D cultures, non-specific association of [^{3}H]-TCA with cells can influence the overall measurement of accumulation. The effects of non-specific association may be more pronounced in 3D cultures where fluid in the extracellular space

can trap molecules. The magnitude of these effects can be assessed by conducting the assay under conditions that inhibit [^{3}H]-TCA transport. CyA (cyclosporin A) has been shown to be a very effective broad spectrum inhibitor of bile acid transport, both uptake and efflux, and bile acid synthesis in both *in vivo* and *in vitro* systems[219, 236, 242, 243]. It has also been shown to have a very potent effect on the gene expression of transporters and other relevant transcripts *in vivo*[236]. It was therefore chosen as a [^{3}H]-TCA uptake and efflux inhibitor for the purposes of studying its effect on [^{3}H]-TCA accumulation in hepatocytes cultured under different conditions and different periods of time.

[^{3}H]-TCA transport studies were conducted by measuring [^{3}H]-TCA accumulation after 15min incubation with 10μM [^{3}H]-TCA and either no CyA or 20μM CyA in paired cultures with either intact (Cells+BC) or disrupted (Cells-BC) canalicular networks. The effect of CyA on [^{3}H]-TCA accumulation is complicated and demonstrates how the effects of a compound on bile acid transport can be inferred from accumulation data at one time point. In perfused 3D cultures on day 7 post-isolation, [^{3}H]-TCA accumulation in the Cells-BC condition increases slightly in the presence of CyA while BEI decreases from 34±30% to 21±15% in the absence and presence of CyA, respectively (Figure 3-5). This indicates that CyA is more potently inhibiting the excretion of [^{3}H]-TCA than it is its uptake. However, it does show that uptake is inhibited because the accumulation in Cells-BC does not increase significantly beyond the non-inhibited levels. If uptake was not inhibited, then the accumulation levels would have increased significantly. These results provide more evidence that steady-state accumulation data can supply very relevant information about the effects of compounds

on transport. Results for 2D sandwich cultures on day 7 post-isolation were difficult to interpret because of the diminished transport capabilities in these cultures (data not shown).

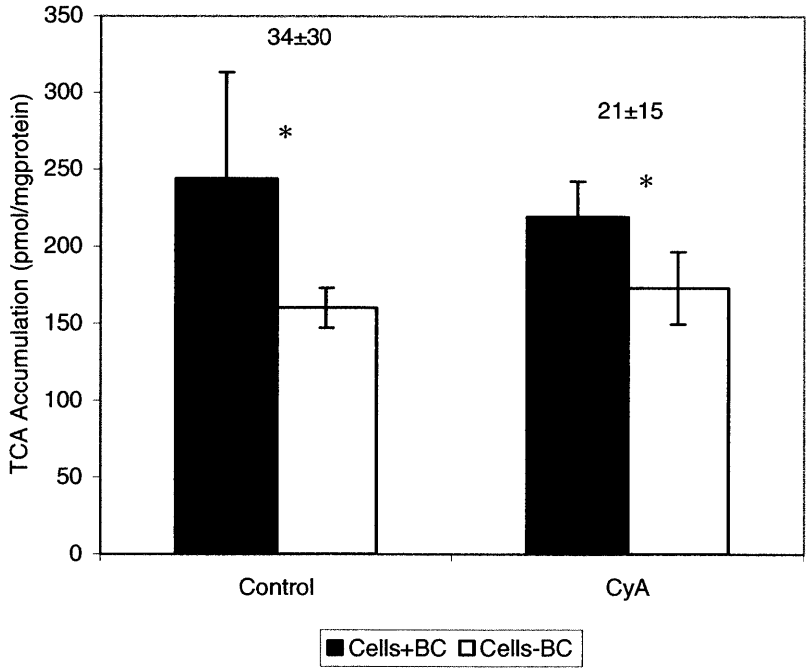

Figure 3-5: CyA inhibits [^{3}H]-TCA transport on day 7 post-isolation cultures. BEI noted above bars. Open and closed bars indicate cultures with disrupted and intact canalicular networks, respectively. 20μM CyA where noted. Day 7 post-isolation. Accumulation after 15min incubation with 10μM [^{3}H]-TCA. Data shown as mean±SD (n = 3 biological replicate, in triplicate). *$p<0.05$ Cells+BC and Cells-BC.

These accumulation patterns were also evident on day 4 data and were more striking in 2D sandwich cultures (Figure 3-6). The results are consistent with greater inhibition of efflux over uptake measured in perfused 3D cultures on day 7 post-isolation (Figure 3-5). However, 2D sandwich cultures demonstrated a greater decrease in [^{3}H]-TCA accumulation in the Cells+BC condition in the presence of CyA than perfused 3D cultures. This is consistent with the overall lower canalicular [^{3}H]-TCA accumulation in 3D cultures in comparison to 2D cultures.

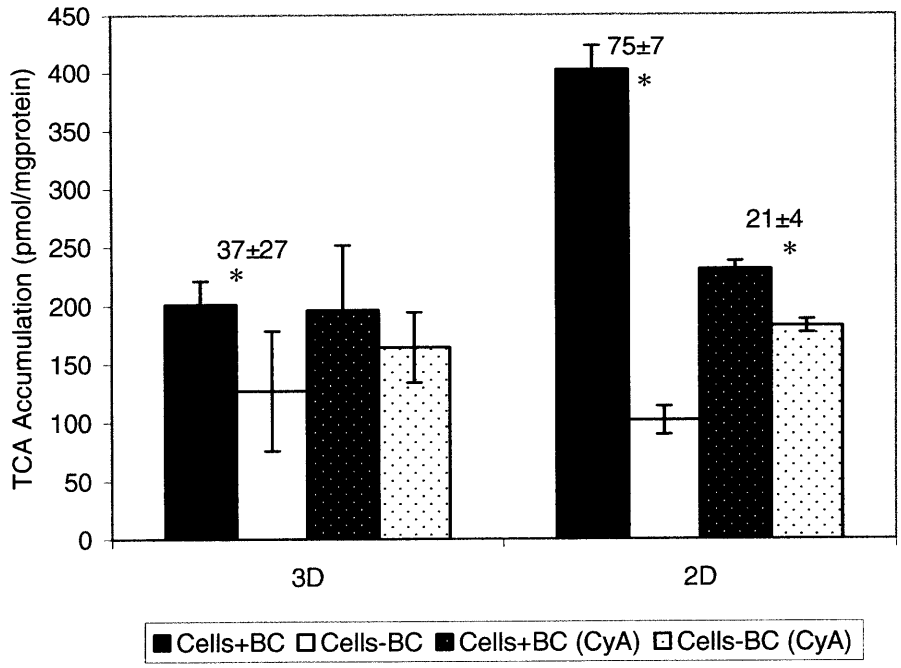

Figure 3-6: CyA inhibits [^{3}H]-TCA transport in day 4 post-isolation cultures. BEI noted above bars unless it was not measurable. Open and closed bars indicate cultures with disrupted and intact canalicular networks, respectively. Dotted bars denote presence of 20μM CyA. Day 4 post-isolation. Accumulation after 15min incubation with 10μM [^{3}H]-TCA. Data shown as mean±SD (n = 3 biological replicate, in triplicate). *$p<0.05$ Cells+BC and Cells-BC.

3.4 Discussion and Conclusions

Hepatobiliary circulation is one of the main functions of the liver, which can be affected and can affect other liver-specific functions such as drug metabolism[16, 46, 73]. It is thus necessary to develop an *in vitro* model for the concerted study of these functions over long-term in culture. Perfused 3D cultures maintained in a 3D physiological perfused model of liver have been shown to maintain liver-specific functions, such as drug metabolism and albumin secretion, for >7 days in culture[2, 225]. However, hepatic transport studies had not been performed with these cultures nor had protocols for transport studies been adapted.

One of the first steps in adapting these protocols to this system, was to determine whether it was necessary to maintain buffer perfusion through the tissue cultures during the transport studies. It was determined that the rate of diffusion of [^{3}H]-TCA and other small molecules into the tissue would be too slow in comparison to the rate of uptake, thus it would be necessary to have perfused tissues throughout the studies. Moreover, lack of media or buffer perfusion through the tissue cultures could result in oxygen depletion through the tissue and an altered phenotype[225].

Another important element was to determine whether transport studies could be conducted on long-term perfused 3D cultures. It was measured that there was essentially no difference in day 4 and day 7 [^{3}H]-TCA accumulation in perfused 3D cultures. Moreover, imaging of the cultures suggests that cell polarization may increase by day 7 in contrast to day 4 in perfused 3D cultures (data not shown). Thus, transport studies in these cultures should be conducted on day 7 post-isolation. Contrary to this result, [^{3}H]-TCA transport in 2D cultures is significantly diminished. As discussed previously, this is consistent with the overall loss of phenotype and liver-specific functions observed in 2D sandwich cultures in long-term culture[2, 4].

Perfused 3D cultures did exhibit lower canalicular [^{3}H]-TCA accumulation and BEI than 2D sandwich cultures on day 4 post-isolation. This may indicate that canalicular networks in perfused 3D cultures are more porous than in 2D sandwich cultures. This slightly higher porosity may also be a reason for the maintenance of transport accumulation over time in culture since there might be high concentrations of *de novo* synthesized bile acids trapped in the canalicular networks of 2D sandwich cultures, resulting in a cholestatic phenotype. However, this lack of canalicular accumulation may

be due to the lack of EGF in the culture medium. As discussed in the previous chapter, EGF has been observed to increase tissue formation and generation of ECM in other 3D hepatocyte cultures[188, 189, 223, 224, 238]. EGF may promote the formation of canalicular networks in these cultures as opposed to disrupting them as it does in 2D sandwich cultures.

The [^{3}H]-TCA accumulation time course demonstrated that [^{3}H]-TCA accumulation can reach a constant concentration in a time period shorter than what has been previously been published as necessary for recovery of canalicular network after Ca^{2+} repletion[147]. Therefore, accumulation measurements can be obtained without great effect from possible experimental time point of measurement variation. This is very similar to the results obtained with 2D sandwich cultures, indicating that the protocol can be adapted to perfused 3D cultures. However, there was a slight, not significant, drop in [^{3}H]-TCA accumulation at the 30min time point, which may indicate that lengthy protocols may have a detrimental effect on the cultures.

Lowering the pre-incubation time in either a Ca^{2+}-rich or Ca^{2+}-free environment resulted in slightly lower BEI in perfused 3D cultures. This is consistent with incomplete disruption of the canalicular networks. This indicates that the observed difference in [^{3}H]-TCA accumulation in cultures with intact and disrupted canalicular networks can be attributed to the disruption of these networks and not to nonspecific effects. This was confirmed by the effect that CyA had on canalicular accumulation of [^{3}H]-TCA. The decrease in canalicular [^{3}H]-TCA accumulation is consistent with inhibition of bile acid transport. The relatively low increase in intracellular [^{3}H]-TCA accumulation in the

presence of CyA indicates that CyA also inhibits [^{3}H]-TCA uptake, as has been previously observed[219, 236].

Overall, the results presented in this chapter show that 2D sandwich protocols for hepatic transport studies can be adapted for use in perfused 3D cultures. However, the relatively low levels of canalicular [^{3}H]-TCA accumulation may indicate diminished canalicular network formation in these cultures. As has been discussed previously, EGF may increase the formation of canalicular networks in perfused 3D hepatocyte cultures even though it has been shown to disrupt canalicular network formation in 2D sandwich cultures. Therefore, the effects of EGF on hepatic transport studies and bile acid synthesis need to be studied in these cultures.

Chapter 4

Effects of EGF on Hepatobiliary Transport and Bile Acid Synthesis

4.1 Introduction

Bile acid biosynthesis and transport is an essential function of the liver necessary for cholesterol homeostasis, and digestion of lipids and other lipophilic compounds[9]. Thus, hepatocytes have a highly polarized expression of bile acid uptake transporters on their basolateral surface and bile acid efflux transporters on their apical surface[26], along with polarized expression of other transporters involved in transport of organic compounds, such as drugs and other xenobiotics[46]. Along with cholesterol homeostasis, hepatobiliary disposition can also affect and be affected by glucose homeostasis, drug metabolism, and digestion[4, 9, 122], thus a concerted way of studying these functions is of great interest.

Previous studies have demonstrated that hepatocytes cultured in other 3D culture platforms can create extensive canalicular network[224]. Interestingly, epidermal growth factor (EGF) has been shown to promote tissue reorganization, cell attachment and greater formation of extracellular matrix (ECM) in other 3D culture platforms[188, 223, 224]. Moreover, activation of $p38^{MAPK}$ and the phosphatidylinositol 3-kinase (PI3K)/Akt pathway, which can be activated by an EGF-mediated pathway, can lead to greater expression of apically localized tight junction proteins occludin and claudin 2 *in vivo*[92, 99, 155]. In contrast, transmission electron microscopy studies provided some evidence

that EGF reduces canalicular network formation in 2D collagen sandwich cultured hepatocytes[207]. Therefore, it is possible tight junction regulation and canalicular network formation differs between hepatocytes cultured in 2D and 3D culture conditions and configurations.

EGF-mediated activation of kinase pathways through the activation of EGF-receptor (EGFR) can also have an effect on the expression of transporters and enzymes involved in the synthesis and transport of bile acids through the activation of liver-specific transporters. One possible pathway is the $p38^{MAPK}$-mediated phosphorylation and activation of hepatocyte nuclear factor 4 alpha (HNF4-alpha)[61]. HNF4-alpha which regulates the expression of many liver-specific enzyme including cholesterol 7 alpha-hydroxylase (cyp7a1), the rate-limiting enzyme in the classic pathway of cholesterol catabolism to bile acids, sterol 12 alpha-hydroxylase (cyp8b1), which catalyses the necessary step for cholic acid (CA) synthesis, and sterol 27-hydroxylase (cyp27a1), which is the rate limiting enzyme in the alternative bile acid synthesis pathway and also catalyses many other steps in bile acid synthesis[61-63, 66]. EGF can also affect bile acid synthesis and transport by mediating the activation of liver receptor homologue-1 (LRH-1), a transcription factor known to promote the expression of cyp7a1, cyp8b1, and the bile salt export pump (Bsep), the main canalicular bile acid efflux transporters[26, 69, 97, 244]. Therefore, although EGF may promote the formation of canalicular networks in 3D hepatocyte cultures and may be necessary to adapt 2D sandwich culture protocols to this culture platform, EGF may affect hepatobiliary transport in these cultures by the alteration of expression of these transporters and enzymes.

The studies detailed in this chapter focus on whether EGF increases canalicular network formation in perfused 3D primary rat hepatocyte cultures, and the effect it has on [^{3}H]-TCA uptake and canalicular efflux and retention, and gene and protein expression of key transporters. Effects of EGF and culture time on [^{3}H]-TCA transport and canalicular retention, and gene and protein expression of key transporters on 2D rat hepatocyte sandwich cultures were also evaluated. Finally, the effects of EGF on bile acid synthesis in perfused 3D cultures and 2D sandwich cultures were measured. The studies were conducted to analyze the potential differences in EGF-mediated effects on tissue structure organization and maintenance of some liver-specific functions between different hepatocyte culturing platforms and environments.

4.2 Materials and Methods

4.2.1 Chemicals

[^{3}H] Taurocholic acid ([^{3}H]-TCA; 5 Ci/mmol, <95% purity) and UltimaGoldXR scintillation fluid (Perkin Elmer Life Sciences, Boston, MA, USA); Blendzyme® III and Complete® protease inhibitor cocktail (Roche Applied Science, Indianapolis, IN, USA); Dulbecco's modified Eagle's media (DMEM, w/sodium pyruvate, low glucose, pyridoxine HCl, w/o phenol red, glutamine), phosphate buffered saline (PBS), fetal bovine serum (FBS), insulin, epidermal growth factor (EGF), Alexa Fluor 488 and Alexa Fluor 568 conjugated secondary antibodies, Draq5 stain, and Trizol® LS reagent (Invitrogen/Gibco, Carlsbad, CA, USA); anti-rat DPPIV antibody (Pharmingen, San Diego, CA, USA); anti-human/rat actin antibodies (Chemicon, San Diego, CA, USA); anti-mouse Bsep antibody with rat cross-reactivity (Kamiya Biomedical, Seattle, WA,

USA); anti-human/rat/mouse cyp7a1 antibody (Santa Cruz Biotechnology, Santa Cruz, CA, USA); anti-rat EGFR antibody (Abcam, Cambridge, MA, USA); anti-rat Ntcp antibody was a kind gift from Dr. Bruno Stieger (University Hospital, Department of Medicine, Zurich, Switzerland); RIPA buffer (Teknova, Hollister, CA, USA); HRP-conjugated anti-rabbit and anti-mouse secondary antibodies (Amersham, Piscataway, NJ, USA); EGTA, dexamethasone (DEX), gentamicin, essentially-fatty-acid-free bovine serum albumin (faf-BSA), bovine serum albumin (BSA), normal goat serum, Triton X-100, TCA, Hanks balanced salt solution (HBSS, w/$NaHCO_3$, w/o phenol red) (Sigma Chemical Co, Saint Louis, MO, USA); ITS®, Matrigel® (w/o phenol red) and rat tail collagen type I (BD Biosciences, San Jose, CA, USA); [^{2}H]-TCA and [^{2}H]-glycocholic acid internal standards were a kind gift from Prof. Steven R. Tannenbaum (Massachusetts Institute of Technology, Cambridge, MA, USA); all other chemicals and reagents were purchased at analytical grade from commercial sources.

4.2.2 Primary Liver Cell Isolation

Primary cells were isolated from male Fisher rats (Taconic, USA) weighing 150-180 gm using a modification of the Seglen 2-step collagenase procedure as described previously[2, 230, 231]. Blendzyme III was used as the digestion enzyme instead of collagenase. Following isolation, the cell suspension DAG (DMEM w/2g/ml BSA, and 50mg/l gentamicin) was centrifuged two consecutive times at 50g (3min each) to obtain a hepatocyte rich fraction, and each time the supernatant was discarded, the cells were resuspended in 50ml of DAG. The final cell viability, as determined by trypan blue

exclusion using a ViCell counter, was in the 90-95% range with cell density in the 8-13X10^6 cells/ml range.

4.2.3 Preparation of 2D Sandwich Cultures

Biocoat® Collagen Type I 24-well plates (BD Biosciences) were incubated with 350µL per well of plating hepatocyte growth media (pHGM; DMEM supplemented with 5% FBS, 4 mg/l insulin, 0.1 µM DEX, 0.03 g/l L-proline, 0.1 g/l L-ornithine, 0.305 g/l niacinamide, 2 g/l D-(+)-galactose, 1 mM L-glutamine, 50 mg/l gentamicin, 54.4 µg/l $ZnCl_2$, 75 µg/l $ZnSO_4$•$7H_2O$, 20 µg/l $CuSO_4$•$5H_2O$, 25 µg/L $MnSO_4$) overnight. Medium was aspirated off plates immediately before seeding. Primary hepatocytes from isolation were diluted in ice-cold seeding HGM (sHGM; pHGM w/1µM DEX) to a concentration of 10^6cells/mL, and 350µL of this dilution were added to each well. 2-3 hours post-seeding, plates were gently shaken and wells were washed with 350µL of warm pHGM twice to remove non-adherent cells. 24 hours post-seeding, Matrigel® aliquots were thawed on ice and diluted to a protein concentration of 0.25 mg/mL in ice-cold modified hepatocyte growth medium (mHGM; pHGM supplemented w/ITS and 2g/l faf-BSA, w/o insulin and FBS). Cold pipette tips were always used when pipetting any Matrigel® dilution. Plates were very lightly shaken to remove any non-adherent cells, and 350µL of ice-cold Matrigel® dilution were added to each well. Plates were incubated at 37°C immediately. Medium was replaced with 350µL of warm mHGM every 24 hours for the duration of culture. Unless otherwise noted, all cultures were incubated in an environment at 37°C, 5% CO_2, and 95% humidity. Where noted, 20ng/ml EGF was added to all seeding and maintenance culture media.

4.2.4 Preparation of Perfused 3D Cultures

Perfused 3D cultures were prepared in multiwell reactor plates, as previously described[226, 245]. After assembly of the multiwell reactor plates, 300µl of warm pHGM were added to each reservoir and multiwell plate was run at a flow rate of 0.2ml/min. The reactor pair was monitored to ensure proper priming and that air bubbles started to come out into the reactor pair within 90s±20% of priming being started. The reactor pairs were then filled to the fill line with warm pHGM (~ 4ml) and incubated overnight with a flow rate of 0.2ml/min. All reactor component parts were added to reactor pairs just before seeding, they were rinsed in PBS and all air bubbles were removed. 5 µm Millipore filters were incubated at RT for 30 minutes in PBS w/10g/ml BSA to passivate them and were rinsed briefly in PBS before placing them in each reactor pair. Polycarbonate scaffolds were sonicated in 70% EtOH for 10 minutes to remove air bubbles from channels. Scaffolds were then rinsed 2X w/PBS, placed in a 30µg/mL type I collagen PBS solution and incubated at 37°C for >2 hours. Any air bubbles left in scaffolds were removed by pipetting collagen solution into channels. Scaffolds were removed from solution and left to dry for 2 hours at RT prior to seeding. Scaffolds were added to reactor wells <30min before seeding. Medium was aspirated off and reservoir/reactor pairs were filled to fill line with ice-cold pHGM. Medium was then aspirated slightly off reactor/reservoir pairs to ensure there was no liquid contact between reservoir and reactor. Flow was turned on at a flow rate of 0.2 ml/min in a downward direction through the channels and 800,000 cells were seeded per well, evenly distributing them throughout each scaffold. Cell suspension was not diluted before

seeding. Each reactor/reservoir pair was filled to fill line with ice-cold pHGM immediately after seeding and multiwell reactor plate was incubated at 37°C, 5% CO_2, 95% humidity. Flow was maintained downward through the cells to promote attachment to scaffold and tissue-like structure development. Flow was reversed 0.2 ml/min upward through cells 8hrs post-seeding and maintained in this direction for the duration of culture to clear debris and non-adherent cells. On Day 1 post-isolation, culture medium was replaced with warm mHGM 3X to clear out pHGM completely from system. The reactor plate was allowed to flow for 1hr in between each media change to allow any left over pHGM in the system to completely mix with the fresh mHGM. Culture medium was replaced with mHGM (~2.5 ml) every 24 hrs for duration of culture.

4.2.5 Analysis of Bile Acid Transport in 2D Sandwich Cultures

Cultures were washed 3X with 500µl of either standard HBSS or Ca^{2+}-free HBSS (modified HBSS w/o Ca^{2+} or Mg^{2+}, w/1µM EGTA) and incubated for 10min in either buffer. Cultures were then incubated in standard HBSS with 10µM [^{3}H]-TCA for 15min unless otherwise noted. Cultures were then either imaged or rinsed vigorously 3X with ice-cold standard HBSS, 200µl of RIPA buffer was added to each well for cell lyses, and plate was put on a shaker for >20 min. 150µl of the cell lysate from [^{3}H]-TCA accumulation were then analyzed using liquid scintillation spectroscopy (LS 6500 scintillation counter, Beckman Coulter, Inc., Fullerton, CA, USA). Total protein concentration was determined using microplate method of the MicroBCA kit (Pierce Biotechnology, Rockford, IL, USA) as described by the manufacturer[232]. As described in chapter 2, the bile excretion index (BEI) was calculated as the difference in

accumulation in cultures with intact bile canaliculi-like structures and those with disrupted bile canaliculi-like normalized by the accumulation in cultures with intact canaliculi to give the percentage canalicular accumulation of the substrate[147]. The differences in accumulation between groups were analyzed with Student's t test and a p-value < 0.05 was considered statistically significant.

4.2.6 Analysis of Bile Acid Transport in Perfused 3D Cultures

As detailed in the previous chapter, this protocol was adapted from 2D sandwich culture transport protocols. Reservoir filters were removed from each reactor/reservoir pair and all media was aspirated. Each culture was washed 2X with 3ml of either standard HBSS or Ca^{2+}-free HBSS with a downward through cells flow rate of 0.2ml/min. Buffers were completely aspirated off each reactor/reservoir pair and 800µl of either buffer was added on top of each reactor. The reactor/reservoir pairs were run for 5min at 0.2ml/min with 500µl added to the reactor portion after 2.5min and wash-through being constantly aspirated from reservoir portion to prevent liquid contact between reactor and reservoir. Reactor/reservoir pairs were then completely aspirated of any buffers and 800µl of either buffer was added to each reactor portion, the flow rate was changed to downward at 0.1ml/min for the duration of the study. Reactor/reservoir pairs were run for 10min with 500µl of buffer added to each reactor portion every 5min and constant reservoir buffer aspiration. Pairs were then thoroughly aspirated of any remaining buffers and 800µl of standard buffer with 10µM [^{3}H]-TCA was added to each reactor portion and reactor/reservoir pair was run for 15min, unless otherwise noted, following the same procedure as before. Scaffolds were removed from reactors, very gently washed 3X in

60mm Petri dishes with 10ml of ice-cold standard buffer, placed in 20ml scintillation vials with 700µl of RIPA buffer, and vortexed for ~30s. Vials were incubated at 4°C for >8 hours and scaffolds were inspected with light microscopy to ensure complete tissue removal and cell lyses. 500µl of cell lysate was analyzed using liquid scintillation spectroscopy. Total protein was determined by MicroBCA assay (Pierce Biotechnology)[232], and BEI was determined as described.

4.2.7 Western Blotting

Cultures were lysed in ice-cold RIPA buffer w/Complete® protease inhibitor cocktail and kept at -80°C until analysis. Protein (~25µg) was loaded onto a NuPage® 4-12% Bis-Tris gel (Invitrogen, Carlsbad, CA, USA). Proteins were separated by electrophoresis and transferred to a PVDF membrane (BioRad Laboratories, Hercules, CA, USA). Membranes were blocked overnight at 4°C in 5%BSA (w/v) in PBS w/0.5% Tween-20 (PBST) and then incubated for 2hrs at RT with primary antibodies [anti-Ntcp (1:1000); anti-Bsep (1:1000); anti-cyp7a1 (1:1000); anti-EGFR (1:1000); anti-actin (1:10,000)] in 5%BSA in PBST. Membranes were washed 3X with PBST for 15min/wash. Membranes were incubated at RT with HRP-conjugated secondary antibodies (1:10,000) in 5% fat-free milk in PBST for 2hrs and washed 3X with PBST for 15 min/wash. Membranes were prepared for imaging of immuno-reactive proteins by chemiluminescence using Amersham ECL Advance Western Blotting Detection Kit (GE Healthcare Life Sciences, Piscataway, NJ, USA) and imaged on a Kodak Image Station 1000 (Eastman Kodak, USA).

4.2.8 Confocal Microscopy

Perfused 3D cultures for immunofluorescent imaging were prepared by removal of the scaffolds into a 12-well tissue culture treated plate with 500µl of ice-cold 2% paraformaldehyde. Cultures were placed on a plate shaker for 1hr. Wells were then washed 3X with PBS and cultures were permeabilized with 0.1% Triton X-100 for 30min at 37°C. Cultures were then washed 3X with 2%BSA (w/v) in PBS and blocked with 5% normal goat serum in 2%BSA in PBS for 45min at 37°C. Cultures were then washed 3X with 2%BSA in PBS and incubated with anti-DPPIV mouse anti-rat primary antibody (1:100) in 2%BSA in PBS at 4°C overnight. Cultures were washed 3X with 2% BSA in PBS and incubated for 1hr with Alexa Fluor 488 conjugated goat anti-mouse secondary antibody (1:1000) and Draq5 nuclear stain (1:1000) in 2%BSA in PBS at RT. Cultures were then washed 3X with 2% BSA in PBS and 3X with PBS. Scaffolds were then placed in a 35mm Petri dish with a 15mm glass imaging slide in the center (MaTek Corporation, Ashland, MA, USA) with 2ml PBS prior to imaging. DPPIV immunofluorescent imaging of perfused 3D cultures was done with spinning disc confocal microscopy. Spinning disc confocal images were acquired with a Nikon Eclipse TE2000-E inverted microscope (Nikon Instruments Inc, Melville, NY, USA) with a Visitech QLC 1000 Spinning disc head (Visitech International, Sunderland, UK) and an Innova 70C Spectrum laser (Coherent Inc, Santa Clara, CA, USA). Images were acquired in 0.647µm increments along the z-plane and the 20X objective was used for all acquisitions. Images were taken of the whole tissue of 3 channels of each polycarbonate scaffold. Three scaffolds from 3 biological replicates each were fixed per condition, representative images are shown.

4.2.9 RNA Isolation and cDNA Preparation

2D sandwich cultures were harvested with 500µl of ice-cold Trizol® reagent and stored at -80°C until analyzed. Perfused 3D cultures were harvested by removable of the scaffold from the reactor/reservoir pair, rinsing in PBS, and placing the scaffold in a 20ml glass scintillation vial with 1ml ice-cold Trizol® reagent. These were also stored at -80°C until analyzed. Trizol® was collected from each culture and 200µl of chloroform was added to each preparation per 1ml of Trizol®, samples were vigorously mixed and centrifuged at 12,000g for 15min at 4°C to separate aqueous and organic phases. The aqueous phase was separated and equal volumes of aqueous phase and 75% EtOH in DEPC-treated water (Qiagen, Valencia, CA, USA) were mixed to stabilize the RNA. The RNA was cleaned up using an RNeasy® kit (Qiagen), purity was determined as the ratio of the absorbance value of the sample at 260nm and 280nm, and only samples with purities above 1.8 were used for cDNA preparation. Any contaminating genomic DNA was removed using amplification grade DNAse I enzyme and 10X DNAse buffer (Invitrogen), incubating samples for 15min at RT, and denaturing the enzyme with 2.5mM EDTA and incubation at 65°C for 10min. cDNA was prepared using an Omniscript RT® kit (Qiagen) and RNAse inhibitor (Ambion, Austin, TX, USA). Once samples were prepared following the manufacturers instructions, they were incubated at 37°C for 1hr to allow conversion of RNA to cDNA. cDNA samples were then stored at -80°C until they were analyzed.

4.2.10 Semi-Quantitative RT-PCR Analysis

Primers for RT-PCR against specific gene transcripts were synthesized by Operon Biotechnologies, Inc., Huntsville, AL, USA. 1μl of cDNA sample was added to a mix of 25μl 2X SYBR® green master mix (Qiagen), 21μl of DEPC-treated water, 1.5μl of forward primer, and 1.5μl of reverse primer. Amplification was carried out in an Opticon Monitor 3 system with a Chromo4 Continuous Fluorescent Detector and a PTC-200 Thermal Cycler (MJ Research Inc, Waltham, MA, USA) using standard Qiagen SYBR Green RT-PCR annealing and melting protocols. Melting curves were generated after each amplification run to check for primer specificity. In addition, DNAsed RNA (without Omniscript RT added for cDNA formation) controls were run to look for presence of genomic DNA. The 18s gene was chosen to normalize the data because it had been previously shown[2] to be expressed in similar quantities per cell across many different culture platforms.

4.2.11 Primer Sequences

Oligonucleotide sequences for Ntcp (5- CACCACACTTACTGGCTACC-3 forward and 5- ACAGAGTTGAATGTTTTGGAA-3 reverse), Cyp27a1 (5- TAATGGCTTCCTCTTCCCTA-3 forward and 5- ATCGTCCTCTCTCTTCCTCA-3 reverse), and Shp (5- TGCCTGGAGTCTTTCTGGA-3 forward and 5- ATGTTCTTGAGGGTGGAAGC-3 reverse) were designed using the Primer3 open source software (website link: http://frodo.wi.mit.edu/cgi-bin/primer3/primer3_www.

cgi) using the gene sequences published on the NCBI database accessible at http://www.ncbi.nlm.nih.gov/entrez/query.fcgi?db=Nucleotide. All other primer sequences used were previously designed and optimized[2, 225].

4.2.12 Bile and Plasma Collection

Portal blood and bile were collected from male Fisher rats (Taconic, USA) weighing 150-180 gm. Portal blood was collected with a heparin-coated syringe from the portal vein, blood was centrifuged at >10,000g for 10min to separate plasma and cell fraction. Supernatant was collected and stored at -80°C. Bile was collected by bile duct cannulation, cannula was inserted in the main bile duct, and bile was collected for 15min. Bile was diluted 1 in 30 in EtOH before storage at -80°C.

4.2.13 Quantitative Analysis of Bile Acid Synthesis

Analysis of bile acid synthesis from cultures was conducted by collection of spent culture medium from each culture before media change each day and stored at -20°C until analyzed. *In vivo* samples were collected from plasma and bile. Protein in samples was denatured using acetonitrile and samples were centrifuged for 10min at $16.1X10^3$g. Internal standards were then added to each sample. 500μL of supernatant was put through an activated Bond Elut solid phase extraction (SPE) column (Varian, Palo Alto, CA, USA). SPE column was activated by flowing 3mL of 100% MeOH, and 3mL of deionized water (DW) through the column prior to experiment. After sample was flowed through SPE column, column was washed with 2mL of DW and then 2mL of 20% MeOH. Bile acids were eluted from column with 5mL of 0.1% formic acid in MeOH.

Elution was evaporated and remaining solid fraction was dissolved in 60μL of mobile phase (10 mM ammonium acetate; 0.1% formic acid; 0.1% acetonitrile;20% MeOH). Mobile phase was then directed into an LC-MSD-TRAP-XCT Mass Spectrometer with a ZORBAX XDB-C18 1.0*50mm, 3.5μm particle size column for mass spectrum analysis (Agilent Technologies, Santa Clara, CA, USA). Detection limit of current protocol is ~5 nM with a resolution of 0.1 nM. Recovery studies were conducted by dissolving bile acid standards (Sigma Aldrich, USA) in fresh HGM or Ca^{2+}-free buffer. 500 nM concentrations of each bile acid were used for recovery studies. LC/MS analysis was conducted by Dr. Jungnyun Kim, Dr. Ju Liu and Dr. Yu Zeng, under the supervision of Prof. Steven Tannenbaum, Principal Investigator.

4.3 Results

4.3.1 Immunolocalization of Canalicular Marker DPPIV Demonstrates Formation of Bile Canaliculi in Perfused 3D Cultures

In normal liver, dipeptidyl peptidase IV (DPPIV; CD26) is localized to bile canalicular membranes, hence, DPPIV serves as a canonical marker of bile canalicular polarization in culture[210]. To assess the influence of EGF on formation of canalicular networks in culture, perfused 3D cultures were fixed on day 7 of culture, immunostained with anti-DPPIV antibody, and imaged with confocal microscopy. Cultures maintained in the presence of 20ng/ml EGF exhibited polarized localization of DPPIV to canalicular-like structures (Figure 4-1a, green). Analysis of individual planes from the confocal z-stack (presented as reconstructed 3D images in Figure 4-1 a & b) showed that in the

presence of EGF, >90% of hepatocytes exhibited a cuboidal shape, indicating a tissue-like architecture, and were in contact well-formed canalicular networks. In the absence of EGF, there were fewer canalicular networks formed as assessed by DPPIV localization (Figure 4-1b, green). Moreover, in the absence of EGF, most (~80%) cells exhibited a rounded shape and did not appear to be organized in a tissue-like architecture. Therefore, EGF is necessary for either formation of or localization of DPPIV to canalicular networks in 3D perfused cultures. Consistent with confocal imaging of DPPIV, phase contrast images of 3D perfused cultures show what appear to be slightly less compact tissue formation in the absence of EGF (Figure 4-1c), as compared to cultures in the presence of 20ng/ml EGF (Figure 4-1d). Furthermore, total protein content on day 7 in 3D cultures is ~35% greater in the presence of EGF (Figure 4-1e), indicating that EGF may be increasing cell attachment, survival, proliferation, and/or ECM formation in these cultures.

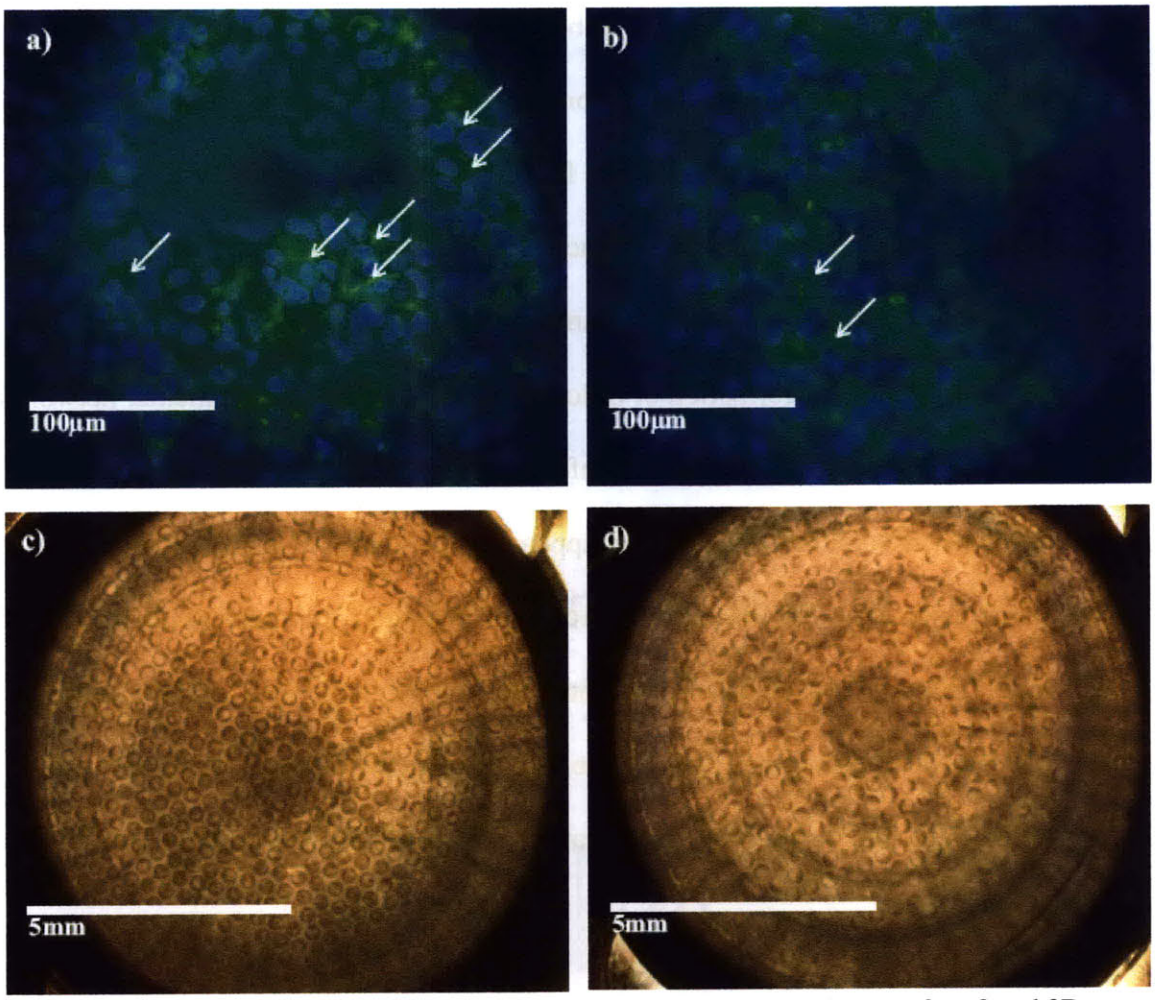

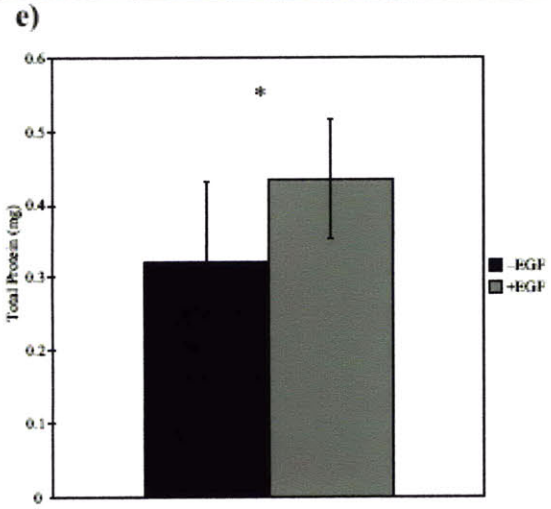

Figure 4-1: Confocal image of perfused 3D cultures, fixed day 7 post-isolation, DPPIV (green) and draq5 nuclear staining (blue). In the presence of 20 ng/ml EGF (a), DPPIV staining localized primarily between hepatocytes in canalicular networks (arrows). In the absence of EGF (b), DPPIV localization is more diffuse and fewer canalicular networks are seen; hepatocytes exhibit a rounded shape and less tissue-like organization. Phase constrast images of perfused 3D cultures, day 7 post-isolation, in the absence of EGF (-EGF) (c) exhibit what appear to have less compact tissues than in the presence of 20ng/ml EGF (+EGF) (d). Total protein content (e) in 3D perfused cultures, day 7 post-isolation. Data shown as mean±SD (n = 3 biological replicates, in sextuplet). *$p<0.05$ –EGF and +EGF.

4.3.2 Effects of EGF on [^{3}H]-TCA Transport in Perfused 3D Cultures and 2D Sandwich Cultures

Having established that EGF influenced cell morphology and DPPIV distribution, and possibly altered hepatocyte polarization, the effect of EGF on [^{3}H]-TCA transport and canalicular integrity was assessed in 2D and 3D cultures maintained for 7 days in the presence (+EGF) or absence (-EGF) of 20ng/mL EGF. Transport was assessed by adding 10μM [^{3}H]-TCA to the culture buffer and assessing total accumulation after 15min incubation in matched pairs of cultures that had been pre-treated to exhibit either intact (Cells+BC) or disrupted (Cells-BC) bile canalicular networks during the 15 min accumulation period. As discussed in previous chapters, a standard 2D assay was adapted to the 3D format for transport studies. The values of [^{3}H]-TCA accumulation in the Cells-BC case represent the balance between rates of uptake and rates of efflux. The difference between accumulation in the Cells+BC condition compared to the Cells-BC condition allows estimation of the amount of [^{3}H]-TCA accumulated in the canaliculi as a normalized biliary excretion index [BEI = (Cells+BC – Cells-BC)/Cells+BC].

[^{3}H]-TCA accumulation in canaliculi on day 7 post-isolation was significant in 3D+EGF cultures (BEI 52±19%) while it was not measurable in the absence of EGF in 3D cultures (Figure 4-2a). No [^{3}H]-TCA accumulation in canaliculi was detectable in 2D cultures in either +EGF or -EGF conditions on day 7. Taken together with immunostaining of the canalicular structures, it can be inferred that the lack of accumulation in the canalicular space in 2D cultures and in 3D-EGF cultures arises from poorly organized or non-patent canalicular networks, rather than defects in either uptake or efflux, as the values of [^{3}H]-TCA accumulation in the Cells-BC condition are

comparable for the +EGF and -EGF conditions within each culture format. The degree of [^{3}H]-TCA accumulation in canalicular networks in 2D cultures is lower than that in 3D cultures and is independent of EGF, which may indicate a loss of transporter expression or activity.

2D sandwich cultures (2D) of primary rat hepatocytes have been widely-used to measure bile acid transport function; however most of these studies are conducted on day 4 of culture because it is the minimum amount of culture time required to form functional canalicular networks[147, 210, 214] and the differentiated functions of hepatocytes in 2D culture typically decline significantly by day 7[2]. It was confirmed that these 2D cultures exhibited [^{3}H]-TCA transport properties comparable to those previously reported in the literature on day 4 post-seeding (Figure 4-2b)[214]. In the absence of EGF, a condition comparable to those used by others analyzing bile transport in 2D[214], and a BEI of 77±22% was observed. Addition of EGF significantly reduced the level of [^{3}H]-TCA accumulation in the bile canaliculi, leading to a BEI of 31±18% in 2D–EGF cultures. These results suggest that there is EGF-dependent decrease in canalicular integrity in 2D cultures. Interestingly, [^{3}H]-TCA accumulation in Cells-BC was decreased by ~40% in 2D+EGF as compared with 2D–EGF, indicating a disturbed uptake to efflux activity in 2D+EGF cultures.

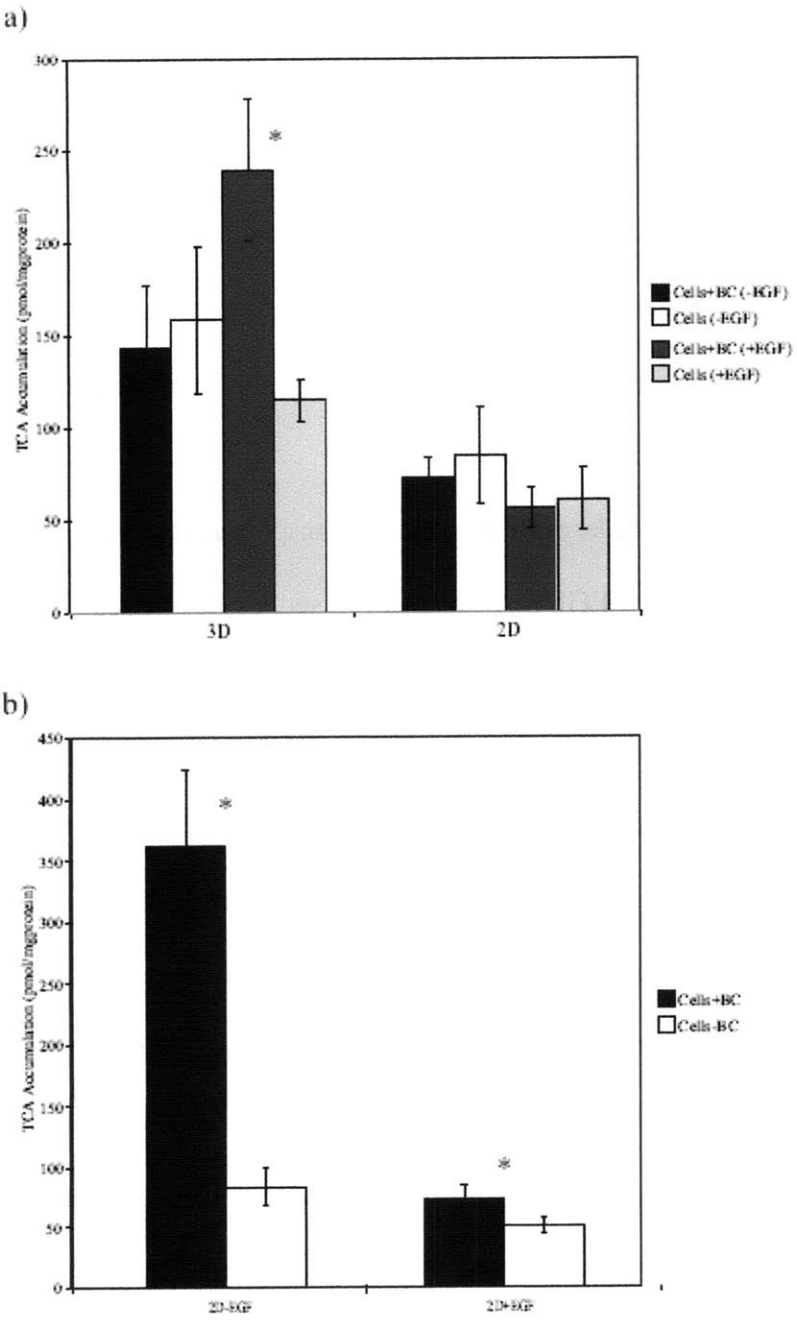

Figure 4-2: [^{3}H]-TCA accumulation (a) in perfused 3D cultures and 2D sandwich cultures on day 7 of culture in the presence (+EGF) and absence (-EGF) of 20ng/ml EGF with intact (Cells+BC) or disrupted (Cells-BC) canaliculi. EGF appears to be essential to obtain measureable accumulation of [^{3}H]-TCA in canalicular networks in 3D. BEI in 3D+EGF was measured to be 52±19%, and not measurable in any other condition. Data shown as mean±SD (n = 3 biological replicates, in triplicate). *p<0.05 Cells+BC and Cells-BC. [^{3}H]-TCA accumulation (b) in 2D sandwich cultures (2D) on day 4 of culture. EGF highly decreases [^{3}H]-TCA accumulation in canalicular networks in contrast with results in 3D cultures. BEI were 77±22% and 31±18% in the absence and presence of EGF, respectively. Data shown as mean±SD (n = 3 biological replicates, in triplicate). *p<0.05 Cells+BC and Cells-BC.

4.3.3 Effects of EGF on Expression of Bile Acid Transporters and Transcription Factors in Perfused 3D Cultures and 2D Sandwich Cultures

To investigate whether the EGF-induced reduction in canalicular [^{3}H]-TCA accumulation in 3D perfused cultures was due to EGF-dependent modulation of canalicular integrity or due to influences on transporter expression, the expression of the key uptake and efflux transporters was assessed using whole cell lysates to probe levels of protein and mRNA present at specific culture times.

Immunoblot analysis for Bsep, the key bile acid efflux transporter, showed that 3D cultures maintained in the presence of EGF for 7 days expressed levels of Bsep comparable to freshly-isolated hepatocytes (Figure 4-3). Interestingly, omission of EGF resulted in an almost two-fold increase in expression of this efflux transporter relative to freshly-isolated cells (Figure 4-3a). Although Bsep protein expression levels were maintained or elevated, Bsep mRNA expression on day 7 in 3D culture was reduced by 20-50 fold compared freshly isolated cells (Figure 4-3b). Still, gene expression level in the –EGF case was about 2-fold higher than in the +EGF case, mirroring the trend of higher protein expression in the –EGF case. The half-life of Bsep *in vivo* is 4-6 days[26], hence the discordance between mRNA and protein suggests degradation is substantially slowed in these culture conditions. In contrast to Bsep, which showed an EGF-dependent expression, the presence of EGF in culture medium had no significant effect on expression of the bile acid uptake transporter protein, Ntcp, at day 7 in 3D culture (Figure 4-3 a & b). Expression of Ntcp at day 7 was moderately decreased (70% of the value in freshly-isolated cells) at the protein level in both conditions, and significantly depressed at the mRNA level (12-fold lower than in freshly-isolated cells). Taken together, the net

effect of EGF on expression levels of uptake and efflux reporters does not seem to account for the dramatic difference in efflux into canalicular space for these two different culture conditions, as reflected in undetectable BEI in the –EGF case, where Bsep expression is elevated above both the *in vivo* values and above the +EGF case. Failure to detect canalicular accumulation of [^{3}H]-TCA for the –EGF case may thus arise from failure to localize Bsep to the cell surface, failure to form patent canaliculi, or a combination of these and other factors.

In contrast to 3D culture, where both Bsep and Ntcp protein expression levels are at most moderately changed from the freshly-isolated levels and a pronounced effect of EGF is observed in day 7 cultures for Bsep expression, EGF did not change expression of Bsep or Ntcp protein at day 7 in 2D cultures, and the overall expression levels of both Bsep and Ntcp are significantly below levels in 3D culture for the same time points and conditions (Figure 4-3a), and moderately (for Bsep) to greatly (for Ntcp) below those for freshly-isolated hepatocytes (Figure 4-3a). Expression of both Bsep and Ntcp mRNA was also significantly decreased at day 7 (Figure 4-3b), independent of EGF treatment. The depressed levels of both transporter proteins compared to 3D culture is consistent with the relatively lower overall accumulation of [^{3}H]-TCA in cells in 2D compared to 3D at this day 7 time point (Figure 4-2a).

Because a pronounced inhibitory effect of EGF on canalicular [^{3}H]-TCA accumulation in 2D cultures on day 4 was observed (Figure 4-2b), a time point which is typically used for transport studies in 2D culture, expression of Bsep and Ntcp at this time point was examined for 2D cultures. Omission of EGF from the culture medium increased the expression of Bsep in 2D cultures at day 4 to a value over twice that of

freshly-isolated cells (Figure 4-3a) while the presence of EGF resulted in a modest (1.3-fold) increase in Bsep protein expression at this time point. These trends in relative Bsep protein expression in the –EGF and +EGF conditions thus mirror those for effects of EGF on Bsep protein expression in 3D day 7 cultures, where the –EGF condition similarly had greater Bsep expression. The presence of EGF in culture medium significantly decreased Bsep mRNA expression (7 fold lower in the +EGF condition), which was similar to the effect of EGF on Bsep protein expression. Expression of Ntcp protein was reduced to ~50% of that observed in freshly-isolated cells in both the –EGF and +EGF conditions at day 4 in 2-D culture, and EGF decreased values slightly relative to the –EGF condition (levels were 0.5 and 0.4 relative to freshly isolated cells for the –EGF and +EGF cases respectively; Figure 4-3a). Ntcp mRNA expression was reduced 10-20 fold compared to freshly-isolated hepatocytes (Figure 4-3b). In the presence of EGF, there was a slight (<2-fold) decrease in Ntcp mRNA expression in these cultures, consistent with the slight decrease in protein expression observed in the +EGF condition.

Having observed that presence of EGF decreases the expression of Bsep, the canalicular transporter of bile acids, the effects of EGF on the mRNA expression of canalicular transporters involved in excretion of two other main bile components were examined: phospholipids, which reduce the detergent-like activity of bile, and organic anions, which are excreted as waste products through the biliary and digestive tract. In cultures maintained in the absence of EGF, the gene expression of the canalicular phospholipid transporter Mdr2 was reduced 6-7 fold on day 7 of culture as compared to in freshly-isolated hepatocytes independent of culture format (Figure 4-3b). Moreover, EGF reduced these mRNA levels 2.5 fold as compared to the –EGF case in both 2D and

3D cultures. EGF reduced Mdr2 mRNA levels 8-fold in day 4 2D cultures (where mRNA levels in the absence of EGF were not significantly different from freshly-isolated hepatocytes; Figure 4-3b). This effect of EGF is consistent with the EGF-related decrease in Bsep mRNA, another canalicular transporter, measured across culture platforms and culturing time. However, this effect of EGF on canalicular transporter mRNA expression was not detected with the canalicular efflux transporter of organic anions, Mrp2. Mrp2 mRNA levels were all measured to be within 2-fold of freshly-isolated hepatocyte levels in all culture systems independent of EGF or day of culture. This is consistent with reports of Mrp2 maintenance in primary hepatocyte cultures in both the presence and absence of EGF[2, 210].

Because EGF was shown to decrease the mRNA levels of some canalicular transporters, it was important to determine whether EGF was mediating this effect by reducing the expression of transcription factors important in the regulation of Bsep expression. A transcription factor directly involved in promoting regulation of Bsep is FXR, which dimerizes with RXR when activated and directly promotes SHP, another transcription factor which inhibits Ntcp transcription[46]. The mRNA levels of these transcription factors was within 4-fold of freshly-isolated hepatocyte levels (Figure 4-3c), with the exception of RXR in 2D cultures which was 5-fold decreased independent of EGF presence on day 7 of culture and 2D+EGF cultures on day 4. Compared with 3D-EGF, FXR and SHP levels were slightly increased by (<2-fold) in 3D+EGF, respectively, while RXR was not significantly affected by EGF. The increase in SHP levels correspond with the increase in levels of FXR, which is directly involved in its regulation and this indicates that FXR activity may be saturated as an increase in its expression corresponded

to a direct increase in the expression of a gene it is known to directly regulate. However, the effects of EGF on Bsep and Ntcp expression is probably FXR- and SHP-independent because an increase in FXR and SHP should correspond to an increase in Bsep and decrease in Ntcp expression. Interestingly, EGF mediated a 2-4 fold decrease mRNA levels of FXR and RXR in 2D cultures on day 4 of culture. However, this decrease did not correspond to a significant decrease in SHP expression.

EGFR is internalized and degraded following stimulation by EGF[93]. Expression of EGFR in 2D primary hepatocyte cultures has previously been shown to decline rapidly to <20% of that in freshly-isolated cells when hepatocytes are maintained in medium with insulin, and the decline is further enhanced in the presence of EGF[246]. Hence, it can be hypothesized that EGFR expression would decline in all cultures, and more so in +EGF conditions. Immunoblot analysis of cell lysates support this hypothesis: EGFR protein expression decreased significantly (40-80%) in all culture conditions, with greater declines in +EGF compared to –EGF conditions (Figure 4-3 c & d). EGFR gene expression levels, as compared to day 0 levels, were decreased 5.3- and 4.1-fold in 3D-EGF and 3D+EGF, respectively, and ~2.8-fold in 2D, independent of EGF presence. The loss of EGFR protein expression in the presence of EGF is consistent with EGF-mediated increased internalization and subsequent degradation of activated EGFR[246]. Increased EGFR gene expression in 3D+EGF as compared to 3D-EGF culture may be the result of greater EGFR transcript in response to greater EGFR degradation.

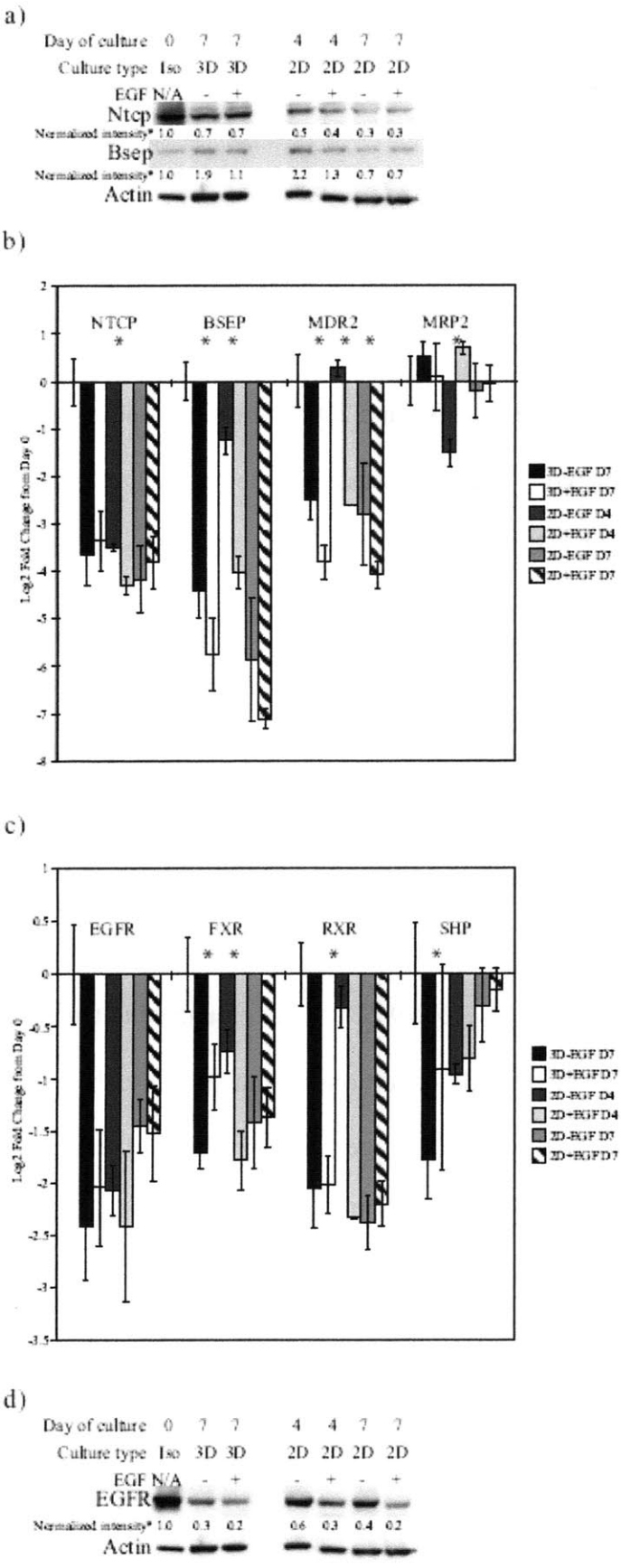

Figure 4-3: Expression (a) of Ntcp and Bsep proteins as evaluated by immunoblot in perfused 3D cultures (3D) and 2D sandwich cultures (2D), day of culture noted. Bsep expression was observed to be lower in EGF cultures while Ntcp expression levels are unaffected. *Optical density expressed as a ratio normalized to actin. Expression ratio on Day 0 isolated hepatocytes (Iso) was set to 1.0. Expression (b) of gene transcripts for Ntcp, Bsep, Mdr2 and Mrp2 as measured by semi-quantitative RT-PCR, day of culture as noted. EGF lowered expression of canalicular transporters (Bsep, Mdr2, and Mrp2) slightly while not having an effect on the uptake transporters Ntcp, consistent with protein expression results. Error bars for day 0 shown, data shown as log2 fold change from day 0, mean±SD (n = 3 biological replicates, in triplicate). *$p<0.05$ -EGF and +EGF. Expression (c) of gene transcripts for relevant transcription factors as measured by semi-quantitative RT-PCR exhibits less than a 4-fold decrease in signal from day 0 indicating that transcription regulation is not greatly affected by EGF presence. Day of culture as noted. Error bars for day 0 shown, data shown as log2 fold change from day 0, mean±SD (n = 3 biological replicates, in triplicate). *$p<0.05$ - EGF and +EGF. EGFR protein expression (d) as evaluated by immunoblot is lower in EGF cultures consistent with higher degradation of EGFR by persistent activation with EGF. Day of culture as noted. *Optical density expressed as a ratio normalized to actin. Expression ratio on Day 0 was set to 1.0.

4.3.4 Effects of EGF on Bile Acid Synthesis in Perfused 3D Cultures and 2D Sandwich Cultures

Expression of bile acid transporters and functional integrity of canaliculi as assessed by [^{3}H]-TCA transport may be affected by cellular production of bile acids, which in turn may be regulated by EGF. Therefore, analysis of bile acid concentration and composition in culture medium collected from 3D and 2D cultures in the absence (-EGF) and presence (+EGF) of EGF on day 7 of culture was conducted using liquid chromatography/mass spectrometry (LC/MS) analysis (Figure 4-4a). The presence of EGF greatly suppressed bile acid production in 3D culture, as bile acid production in 3D-EGF was over 7-fold higher than in 3D+EGF. Although in both conditions, the cholic acid (CA) conjugates represented over 95% of the total bile acids present (similar to that measured in male Fisher rats; Figure 4-5). Glycine conjugates dominated over taurine conjugates (81% and 17%, respectively) for the 3D-EGF condition and taurine conjugates dominated (32% glycine and in the 61% taurine) in the +EGF condition. Taurine conjugates are in highest abundance *in vivo* (>90% of CA conjugated to taurine; Figure 4-5). The average synthesis rate in 3D–EGF conditions is comparable to the *in vivo* bile acid synthesis rates of ~2nmol/mgprotein (averaged over the sinusoid) and EGF depressed the rate to sub-physiological average values in 3D[29]. Compared to 3D, bile acid production was very significantly diminished in 2D culture in the absence of EGF and also showed further depression in the presence of EGF (about 15- and 3-fold lower than 3D-EGF and 3D+EGF, respectively).

To assess whether the effects of EGF on bile acid synthesis are mediated by a decrease in bile acid synthesis enzymes, cyp7a1 protein expression was assessed by immunoblot analysis (Figure 4-4b). Cyp7a1 protein expression was maintained at similar levels to freshly isolated hepatocytes in 3D-EGF cultures, but decreased ~50% in 3D +EGF cultures, a result that corresponds well with the trends in the observed EGF-mediated decrease in bile acid synthesis in 3D+EGF conditions. Interestingly, in 2D culture, cyp7a1 expression increased slightly (10%) compared to the value in freshly isolated cells in the –EGF case, an unexpected finding given the depressed value of bile acid synthesis rate observed compared to the 3D–EGF condition, which had comparable cyp7a1 expression. Maintenance of 2D cultures in the presence of EGF resulted in a decrease in cyp7a1 expression, which is consistent with EGF-mediated decrease in bile acid synthesis rate. However, the bile acid synthesis rate in 2D cultures was much lower than in 3D cultures independent of EGF, which is not consistent with observed cyp7a1 levels. This may indicate that cyp7a1 activity in 2D cultures is not the rate-limiting step for decreased bile acid synthesis in these cultures and suggests that synthesis of a bile acid precursor, such as cholesterol, might be significantly diminished. Interestingly, cyp7a1 mRNA levels were measured to be 40-65 fold diminished in all 3D and 2D cultures as compared to freshly-isolated hepatocyte levels (Figure 4-4c). The only effect of EGF on cyp7a1 mRNA levels measured was a slight (<2-fold) decrease measured in 3D cultures.

To further investigate the potential mechanisms by which EGF affects bile acid synthesis rates in 3D and 2D cultures, mRNA levels of cyp27a1, the rate-limiting enzyme in the alternative bile acid synthesis pathway and mediates many steps downstream of

cyp7a1 in the classical pathway[9], and cyp8b1, which catalyses the necessary synthesis step to produce CA, were determined (Figure 4-4c). Cyp27a1 gene expression was maintained within 3-fold of day 0 levels independent of culture system and EGF presence, which is consistent with other reports of cyp27a1 expression being well maintained in primary hepatocyte cultures[67]. Figure 4-4c also shows that cyp8b1 gene expression is decreased by approximately 80-fold in 3D-EGF, 3D+EGF and 2D-EGF cultures, but is decreased over 6,500-fold in 2D+EGF cultures. 2D+EGF cyp8b1 gene expression contrasts the complete lack of detection of chenodeoxycholic acid products in 2D+EGF culture medium or in any other culture condition, which suggests that enough cyp8b1 activity is conserved in 2D+EGF cultures to produce the low levels of CA measured in these cultures.

a)

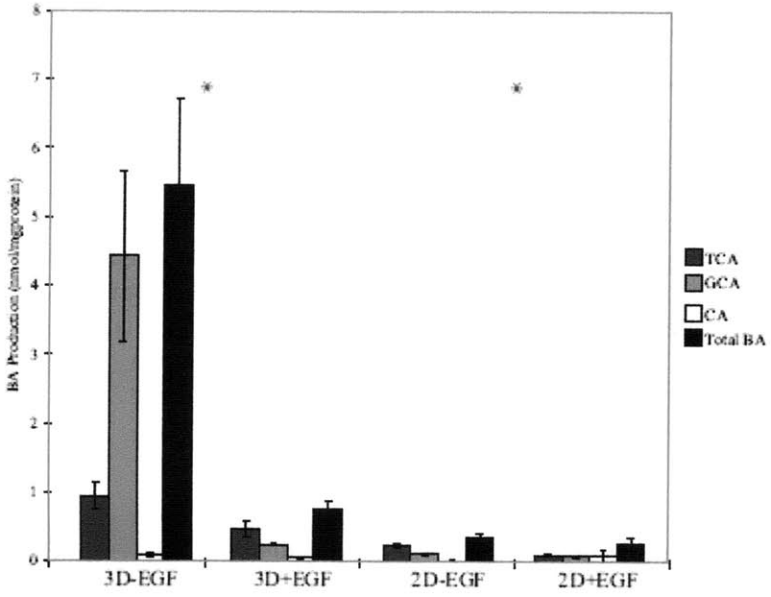
BA Production (nmol/mg protein)
8
7
6
5
4
3
2
1
0
*
*
3D-EGF
3D+EGF
2D-EGF
2D+EGF
TCA
GCA
CA
Total BA

b)

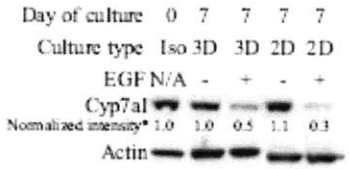
Day of culture 0 7 7 7 7
Culture type Iso 3D 3D 2D 2D
EGF N/A - + - +
Cyp7a1
Normalized intensity* 1.0 1.0 0.5 1.1 0.3
Actin

c)

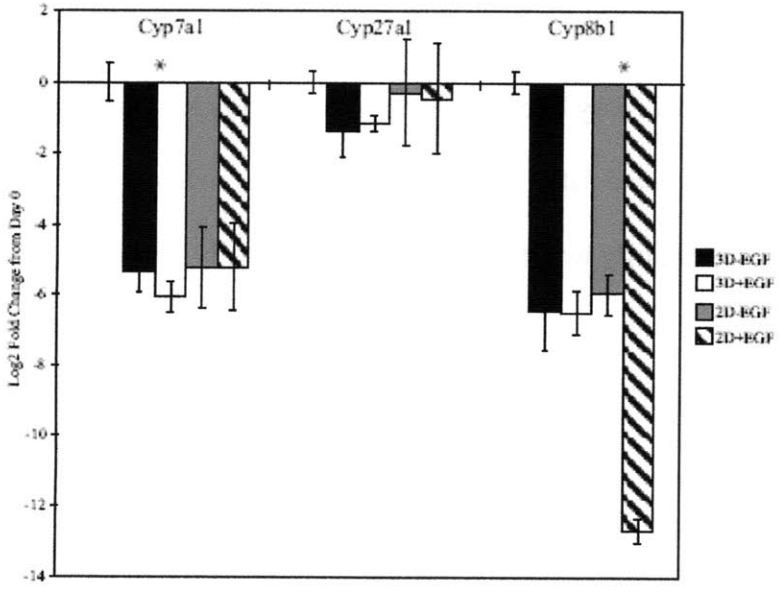
Cyp7a1
Cyp27a1
Cyp8b1
*
*
Log2 Fold Change from Day 0
2
0
-2
-4
-6
-8
-10
-12
-14
3D-EGF
3D+EGF
2D-EGF
2D+EGF

Figure 4-4: Bile acid production (a) in perfused 3D cultures (3D) and 2D sandwich cultures (2D) on day 7 of culture as measured from LC/MS analysis of media in the absence (-EGF) and presence (+EGF) of 20 ng/ml EGF. EGF highly decreases bile acid synthesis in 3D while the effect is more attenuated in 2D, which has diminished bile acid synthesis overall. Bile acid composition is mostly CA conjugates consistent with in vivo bile composition (data not shown). Data shown as mean±SD (n = 3 biological replicates, in triplicate). *p<0.05 -EGF and +EGF. Cyp7a1 protein expression (b) as evaluated by immunoblot is conserved in both 3D and 2D cultures in the absence of EGF but is significantly decreased in the presence of 20 ng/ml EGF, consistent with bile acid synthesis data.*Optical density expressed as a ratio normalized to actin. Expression ratio of Day 0 isolated hepatocytes (Iso) was set to 1.0. Expression (c) of gene transcripts for relevant enzymes in the bile acid synthesis pathway as measured by semi-quantitative RT-PCR exhibits similar levels for both 3D and 2D cultures on day 7 independent of EGF presence, except of cyp8b1 which is significantly more decreased in the 2D+EGF cultures. Error bars for day 0 shown, data shown as log2 fold change from day 0, mean±SD (n = 3 biological replicates, in triplicate). *p<0.05 -EGF and +EGF.

In order to compare the composition of the bile acids produced by these cultures to *in vivo* rat bile composition, analysis of bile acid concentration and composition in plasma and bile collected from adult male Fisher rats was conducted using liquid chromatography/mass spectrometry (LC/MS) analysis (Figure 4-5). TCA was the predominant bile acid synthesized *in vivo*, consistent with other published studies[39-41], and the concentration of bile acids was 1000-fold higher in bile than in plasma. Concentrations of unconjugated and tertiary bile acids were significantly low, which is consistent with healthy enterohepatic circulation[9]. Certain bile acids, including lithocholic acid, are synthesized primarily by intestinal flora, so relatively small concentrations indicate a healthy amount of this flora. The relatively small concentrations of unconjugated primary bile acids are indicative of normal bile acid synthesis and regulation.

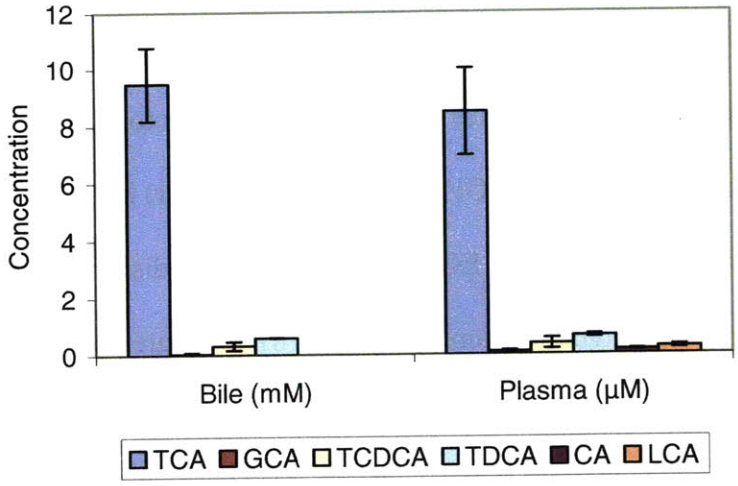

Figure 4-5: Bile acid composition of *in vivo* bile and plasma. N = 2 (3 technical replicates). Bile data in mM, plasma data in μM. Abbreviations: TCA, taurocholic acid; GCA, glycocholic acid; TCDCA, taurochenodeoxycholic acid; TDCA, taurodeoxycholic acid; CA, cholic acid; LCA, lithocholic acid

4.4 Discussion and Conclusions

The liver regulates a myriad of vital functions, including drug metabolism, albumin and urea secretion, cholesterol homeostasis, bile acid synthesis and hepatobiliary transport, some of which have been shown to be preserved *in vitro* in long-term culture in reactor systems similar to that used in these studies[2], however bile acid synthesis and transport had not been assessed in these systems. EGF has been shown to aid in plating and survival of hepatocytes *in vitro* and is associated with long-term maintenance of some liver functions, while detrimentally affecting others. The results detailed in this chapter show that EGF increases tissue and canalicular network formation, together with bile acid canalicular retention, in primary rat hepatocytes cultured in a micro-scale *in vitro* perfused 3D physiological model thus allowing bile acid transport protocols to be adapted to this system.

EGF was necessary for the extensive formation of canalicular networks in perfused 3D cultures as shown by DPPIV localization to these structures, which is consistent with its effect on other 3-dimensional culturing systems such as spheroid

cultures[224, 238]. Tobe et al, showed that EGF was not just essential for the formation of three-dimensional hepatocyte spheroid structures, but that the degree of formation was dependent on EGF concentration[188]. Hepatocytes have also been shown to form more connective tissue when cultured with EGF and HGF (hepatic growth factor) in other three dimensional culturing systems[223]. Conversely, EGF has been shown to disrupt formation of canalicular networks and tight junctions in 2D sandwich cultured primary hepatocytes[207]. It may be reasonable to hypothesize that canalicular networks are disrupted in these cultures because of other stimulatory effects, such as EGF stimulation of proliferative response[199]. However, EGF also stimulates the recycling of E-cadherin, an essential transmembrane protein in the formation of anchoring junctions and tight junctions, and also phosphorylates beta-catenin, which is a cytosolic member of anchoring junctions, decreasing its interaction with E-cadherin[174, 177]. Although this may explain the decrease of canalicular networks in 2D hepatocyte cultures when cultured with EGF, recent studies have shown that hepatocytes lacking E-cadherin can still form bile canaliculi, although to a lesser extent[235]. Therefore, cultures with a greater formation of ECM and greater number of cell-cell interactions can potentially form canaliculi even with a reduction of E-cadherin.

The effect of EGF on canalicular network formation in perfused 3D cultures may also be responsible for the much higher retention of TCA in the canalicular space in these cultures. In the absence of EGF, a complete lack of difference was observed in TCA accumulation in perfused 3D cultures with intact and disrupted canalicular networks. However, the TCA accumulation inside the cellular space was similar to that measured for 2D sandwich cultures, 3D cultures in the presence of EGF, and accumulation levels

reported in 2D cultures in other studies[214]. Moreover, Bsep protein expression levels in these cultures were greater than levels in freshly isolated rat hepatocytes, and Ntcp levels were similar in the presence and absence of EGF. Therefore, it is not likely that TCA uptake and efflux function was significantly inhibited, rather canalicular network formation is compromised. The BEI and TCA accumulation levels measured in the absence of EGF in perfused 3D cultures in the studies presented in this chapter are different from those presented in chapter 3. This indicates that there is great variability in the hepatic transport function of 3D cultures cultured in the complete absence of EGF, possibly due to idiosyncratic differences between experiments. This finding highlights the necessity of EGF in the culture media of these cultures to establish consistent cell re-polarization and canalicular network formation between biological replicates.

EGF has the inverse effect on 2D sandwich cultures on day 4 of culture. Decreased TCA canalicular accumulation in the presence of EGF is caused by disruption of canalicular network formation and not an inhibition of transport, since accumulation in the canalicular space of digoxin and CDF were also significantly diminished, as discussed in chapter 2. However, TCA accumulation is significantly diminished in 2D sandwich cultures on day 7 of culture independent of the presence of EGF, which corresponds well with the highly decreased expression of Ntcp and a decreased Bsep expression as well. Moreover, there may also be an EGF-independent disruption of canalicular networks on day 7 of culture, as seen by diminished retention of CDF in these networks, as discussed in chapter 2.

The measured transporter expression and transcriptional activity provided some evidence that the effects of EGF on cultured hepatocytes was similar between culture

systems, as opposed to the effect on canalicular formation, as summarized in Table 4-1. EGF decreased the mRNA expression of canalicular transporters Bsep and Mdr2, and the expression of Bsep. Overall, mRNA expression of Bsep was decreased as compared to freshly isolated hepatocytes, however the half-life of Bsep *in vivo* is 4-6 days[26], hence the discordance between mRNA and protein suggests degradation is substantially slowed in these culture conditions. EGF may affect Bsep expression by increasing its expression on the canalicular membrane and thus reducing Bsep ubiquitination and degradation[101, 247]. This potential reduction in Bsep degradation and increase of canalicular expression may make greater Bsep transcription unnecessary. A potentially greater degradation due to a possible reduction of canalicular Bsep expression may explain the higher overall Bsep protein expression observed in cultures not exposed to EGF.

EGF also has a significant effect on bile acid production in both perfused 3D cultures and 2D sandwich cultures. In the absence of EGF, total bile acid production in 3D cultures was measured to be 5.5±1.3 nmol/mgprotein/day. This is approximately 3-fold *in vivo* bile acid rates, which are ~2 nmol/mgprotein/day[29], and is consistent with *in vivo* increases in bile acid production after partial ileal bypass[9, 248]. This level of bile acid production activity on day 7 of culture is consistent with maintenance of other liver functions observed in hepatocytes cultured long-term in a single-unit perfused 3D culture system as previously reported[2, 225], such as phase I and phase II drug metabolism activity, albumin secretion, and urea production. Bile acid formation in 2D cultures was significantly lower and is also consistent with an overall decrease in liver-specific functions over time in culture observed in hepatocytes cultured under similar conditions[2, 4]. However, cyp7a1 protein expression was comparable in 3D and 2D

cultures, suggesting that 2D cultures may have significantly diminished synthesis of a bile acid precursor, such as cholesterol.

The EGF-mediated decrease of bile acid production is consistent with the decrease in cyp7a1 expression in the presence of EGF. The possible pathways by which EGF could affect bile acid production and cyp7a1 protein and gene expression and cyp8b1 gene expression are complicated and not well understood. The pathway appears to be FXR- and SHP-independent since the gene expression of these transcription factors involved in the inhibition of cyp7a1 and cyp8b1 transcription is within 4-fold of day 0 levels and the levels of bile acids in the culture medium are not high enough to illicit the FXR regulatory pathway[32, 35, 36, 57, 59, 62, 70]. It has been observed that EGF signaling can mediate the phosphorylation and activation of many different transcription factors involved in the regulation of bile acid synthesis enzymes and bile acid transporters, including LRH-1[57, 61-63, 66, 69, 97]. Short-term EGF exposure has been reported to increase the activation of LRH-1 through an ERK1/2 mediated pathway, however prolonged EGF exposure has been seen to reduce the activation of ERK1/2 in cultured hepatocytes[97, 99]. LRH-1 is involved in the regulation of cyp7a1, cyp8b1, and Bsep, which were all measured to have decreased expression in the presence of EGF[59, 62, 65, 69]. Therefore, it is possible that long-term exposure to EGF decreases the activation or expression of LRH-1.

Decreased EGFR protein expression in the presence of EGF was measured in both 3D and 2D cultures, and this is consistent with EGF-mediated increased internalization and subsequent degradation of activated EGFR[246]. Therefore, activation of the pathways described previously is possible in both culture systems and indicates that EGF

may have similar effects on signaling pathways and transcription in cultured hepatocytes independent of culture platform.

The bile acid composition in all systems was very similar to *in vivo*, which were mostly cholic acid conjugates[42]. However, the high bile acid production of perfused 3D cultures in the absence of EGF may point to an important discovery. Conjugation of primary bile acids to either taurine or glycine is catalyzed by bile acid CoA:amino acid *N*-acyltransferase, with the Km for taurine being much lower in human, and especially in rat[42]. Hardison and Proffitt demonstrated that the amount of taurine conjugation is a function of the intrahepatic taurine pool size without an effect from the intrahepatic glycine pool size[42]. Therefore, the large production of glycocholic acid in perfused 3D cultures in the absence of EGF may indicate a reduced taurine pool in these cultures. This may have some implications for glycogen storage capabilities and other factors in these cultures[249, 250].

The effects of EGF on hepatocytes and on the liver are numerous. The results detailed in this chapter have shown that the influence of EGF on primary rat hepatocyte culture can also depend on the *in vitro* culturing system itself, with widely different outcomes. Though EGF enhanced some liver functions, it also had very deleterious effects on others. Therefore, further investigation into the causes of these effects, the differences observed between culturing systems, and a dose- and time-dependent response is warranted. It is also warranted to develop an experimental setup of measurements to obtain quantitative pharmacokinetic parameters of [^{3}H]-TCA transport so that the effects of different culture conditions on transport can be quantitatively assessed.

Table 4-1: Effects of EGF of on 3D and 2D cultures

	Culture Platform			
	3D		2D	
EGF	+	–	+	–
Canalicular network formation	++	–	–	++
Canalicular bile acid retention	++	–	–	++
Transporter expression				
Canalicular	±	++	–	–
Basolateral	±	±	–	–
Bile acid synthesis	–	++	– –	–
Bile acid synthesis enzyme expression	±	–	±	–

Chapter 5

Numerical Modeling for Optimization of *In Vitro* Hepatobiliary Transport Studies

5.1 Introduction

Hepatobiliary transport of bile acids, cholesterol, phospholipids, xenobiotics and other compounds is one of the main functions of the liver[46]. Hepatic uptake of compounds is commonly an initial and necessary step for the biotransformation of cholesterol, bile acids, xenobiotics and other compounds, and the excretion of these compounds into the bile canaliculi is one the main pathways of excretion of compounds[3, 16, 46]. It is thus of great importance to be able to study the effects of different compounds and other conditions on hepatobiliary transport in a quantitative manner for comparison of effects.

As has been described in previous chapters, a multi-unit *in vitro* 3D physiological perfused model has been developed for the culturing of primary rat hepatocytes. These perfused 3D primary rat hepatocyte cultures, along with 2D sandwich cultures, have been used to study the effects of different media components and hepatobiliary transport inhibitors on [^{3}H]-TCA transport and accumulation, bile acid synthesis, canalicular network formation and retention, and protein and gene expression of liver-specific transporters and enzymes. However, even though it was possible to measure differences in [^{3}H]-TCA accumulation, it was not possible to make quantitative assessments on the

effects of different conditions on uptake, efflux, and canalicular integrity. One of the main reasons this could not be measured was that measuring [^{3}H]-TCA accumulation at one time point and one [^{3}H]-TCA buffer concentration allow only for qualitative assessments of these three different parameters, which can then be partially corroborated with transporter protein expression data.

It is thus necessary to conduct [^{3}H]-TCA accumulation measurements at various time points and [^{3}H]-TCA buffer concentrations. Unfortunately, [^{3}H]-TCA uptake and efflux occur over short (10-15min) time spans[147], and precise measurements at early accumulation time points is necessary. Moreover, perfused 3D cultures require more resources and effort to set up, seed and maintain, and the multiwell reactor platform used in the preparation of perfused 3D cultures is not commercially or readily available. It is therefore necessary to reduce the number of [^{3}H]-TCA accumulation measurements needed in order to determine quantitative uptake, efflux and canalicular retention kinetic parameters in perfused 3D cultures under different conditions.

In this chapter, a numerical model for the reduction of measurements necessary for the determination of hepatobiliary transport kinetic parameters will be detailed. The model also aided in determining whether kinetic parameters can be obtained measuring [^{3}H]-TCA accumulation at steady state accumulation levels only, exclusively varying the [^{3}H]-TCA buffer concentration. Finally, this chapter also details sensitivity analysis conducted on this model to determine which change in parameter would diminish the accuracy of the kinetic parameter measurements.

5.2 Description of Numerical Model

In developing the approach to this numerical model, a pharmacokinetic model of [^{3}H]-TCA transport in 2D sandwich cultures published by Liu et al, 1999, was used as a platform (Figure 5-1) [147]. Liu et al, 1999, determined that hepatocyte uptake and efflux of [^{3}H]-TCA in 2D sandwich cultures could be modeled as having Michaelis-Menten kinetics[147], which is consistent with kinetics determined *in vivo* and using microsomes[8, 25, 44, 237, 251]. It was also determined that canalicular retention could be modeled as first-order kinetics[147], which would be consistent with both passive diffusion and active contraction of canalicular networks to excrete contents.

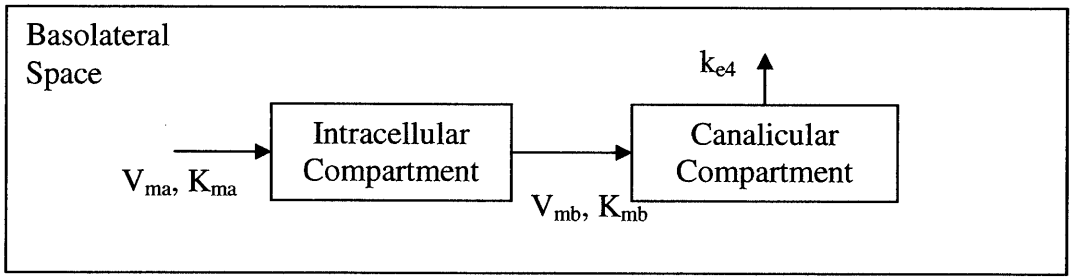

Figure 5-1: Pharmacokinetic model for the enterohepatic circulation of bile acids. The arrow heads point in the direction of biliary flow. Basolateral space constitutes the medium or buffer; intracellular compartment includes uptake and excretion of bile acids; canalicular compartment constitutes bile accumulation in canaliculi-like structures. Michaelis-Menten kinetics are assumed for uptake and excretion as described by Liu et al., 1999

In the studies conducted by Liu et al, 1999, measurements of [^{3}H]-TCA accumulation were taken in paired 2D sandwich cultures with either disrupted (Cells-BC) or intact (Cells+BC) canalicular networks at the time points and [^{3}H]-TCA buffer concentrations outlined on Table 5-1. The pharmacokinetic parameters measured in those studies are listed on Table 5-2, and are used as a basis for the numerical model described

in this chapter. The numerical model described in this section attempts to decrease the number of time points and concentrations required to determine [^{3}H]-TCA hepatic transport pharmacokinetic parameters.

Table 5-1: Time points and Concentrations to Measure [^{3}H]-TCA Transport Kinetics

Time points (min)	[^{3}H]-TCA Buffer Concentrations (μM)
0.5, 1, 1.5, 2, 5, and 10	1, 10, 20, 50, and 100

[^{3}H]-TCA accumulation time points with various [^{3}H]-TCA buffer concentrations measured by Liu et al, 1999, to determine [^{3}H]-TCA transport kinetics in 2D sandwich cultures.

The numerical model entails the following algorithm:

1. Each kinetic parameter as listed on Table 5-2 is multiplied by a randomly generated number in the range of 50%-150%. This simulates the possible differences in kinetic parameters that will be measured under different culture conditions.
2. The pharmacokinetic model as described by Liu et al, 1999[147], is used to determine the [^{3}H]-TCA accumulation measurement expected at the time points and buffer concentrations being considered, for the parameters created in step 1.
3. The [^{3}H]-TCA accumulation measurements are multiplied by randomly generated numbers with a normal distribution with the mean of 100% and a decreasing standard deviation at greater time point. This incorporates potential experimental error in collection of [^{3}H]-TCA accumulation measurements. The standard deviation decreases with increasing time points to account for greater potential variability in experimental measurements at shorter time points.

4. The corrected [^{3}H]-TCA accumulation measurements created in step 3 are then used to solve for kinetic parameters as it would be done if the accumulation measurements were experimentally determined.
5. The kinetic parameters determined in step 4 are compared to the original parameters created in step 1 (% parameter error) and the largest % parameter error per simulation is noted.
6. Each algorithm is repeated 1000 times and the mean % parameter error is used as a metric to compare different time point and buffer concentration considerations.

Table 5-2: [^{3}H]-TCA Pharmacokinetic Parameters in 2D Sandwich Cultures

Parameter	Value
K_{ma}	28 μM
V_{ma}	1.19 nmol/mgprotein/min
K_{e4}	0.849 1/min
K_{mb}	1.03 nmol/mgprotein
V_{mb}	1.82 nmol/mgprotein

[^{3}H]-TCA pharmacokinetic parameters determined by Liu et al, 1999[147].

The %parameter error was calculated as follows:

$$\%ParameterError = \frac{abs(P_{EXP} - P_{Real})}{P_{Real}} * 100\%$$

where:

%ParameterError = %Parameter Error to be calculated

P_{EXP} = parameter value obtained in step 4 of the algorithm

P_{Real} = parameter value obtained in step 1 of the algorithm and used to obtain the simulated measurements in step 2

Mean % parameter errors were determined for the time points and buffer concentrations listed on Table 5-1. Each time point and buffer concentration were then removed in each subsequent simulation and mean % parameter errors were compared. Steady state conditions were also determined and varying buffer concentrations were used to determine the fewest possible measurements necessary to obtain kinetic parameters. The algorithm detailed above was also used to determine mean % parameter errors for steady state conditions.

All simulations were performed using Matlab 7.6.0.324 (R2008a) software for WindowsXP with a time determined seed for the random number generator.

5.2.1 Description of Sensitivity Analysis

Sensitivity analysis was performed on this model by measuring the mean % parameter error and varying one parameter from 10^{-2} to 10^{2} of the value listed on Table 5-2, while maintaining all other parameters at the value listed on Table 5-2. The algorithm outlined previously was used to obtain mean % parameter errors. This was performed to assess whether decreasing the number of measurements taken will decrease the reliability of parameters obtained.

5.3 Results

5.3.1 Reduction of Experimental Conditions

The effects of reducing [^{3}H]-TCA accumulation measurements on the reliability of pharmacokinetic parameters were assessed by comparing mean % parameter errors (Table 5-3). The mean % parameter error for the full experimental setup of measurements outlined in Table 5-1 was 42%. It was found that removing certain time points and buffer concentrations from the experimental setups actually reduced the mean % parameter. The greatest reduction was obtained when the time points at 1 and 1.5 or 2 min were removed, in conjunction with the 1μM buffer concentration condition. However, in order to reduce the number of conditions as much as possible, the 1, 1.5 and 5 min time points can be removed from the experimental set up as well as the 1μM buffer concentration condition. The mean % parameter error in this condition is 40%, which is still below the mean % error for the full experimental measurement setup detailed in Table 5-1. This would result in a reduction of 30 conditions to 12 conditions. However, this could still require a considerable number of perfused 3D cultures to be setup in parallel in order to obtain these parameters. Moreover, because of the physical constraints of the multiwell reactor platform in which perfused 3D cultures are prepared, it is difficult to reliably measure [^{3}H]-TCA accumulation at early incubation time points such as 0.5min. Therefore, it is necessary to explore whether it is possible to obtain a mean % parameter error comparable to that obtained with the full experimental measurement setup.

The mean % parameter errors for steady state condition experimental setups were mostly higher than those with discrete time point measurements. However, it was observed that experimental setups with low [^{3}H]-TCA buffer concentrations had mean %

parameter errors within 10% of the full experimental measurement setup (48%). It should be noted that a steady state experimental measurement setup would result in a 10-fold decrease in necessary measurements from 30 conditions to 3 conditions. If this setup was experimentally determined to robustly determine pharmacokinetic parameters, it would allow for the quantitative assessment of [^{3}H]-TCA transport in a great number of culture conditions in parallel.

Table 5-3: Mean % Parameter Errors for Different Sets of Experimental Measurements

Proposed Experimental Measurement Set Up		
Buffer Concentrations (μM)	Time Points (min)	Mean % Parameter Error
1, 10, 20, 50, 100	0.5, 1, 1.5, 2, 5, 10	42%
10, 20, 50, 100	0.5, 1, 1.5, 2, 5, 10	43%
1, 20, 50, 100	0.5, 1, 1.5, 2, 5, 10	48%
1, 10, 50, 100	0.5, 1, 1.5, 2, 5, 10	45%
1, 10, 20, 100	0.5, 1, 1.5, 2, 5, 10	43%
1, 10, 20, 50	0.5, 1, 1.5, 2, 5, 10	47%
20, 50, 100	0.5, 1, 1.5, 2, 5, 10	63%
10, 50, 100	0.5, 1, 1.5, 2, 5, 10	61%
10, 20, 100	0.5, 1, 1.5, 2, 5, 10	55%
10, 20, 50	0.5, 1, 1.5, 2, 5, 10	61%
1, 50, 100	0.5, 1, 1.5, 2, 5, 10	78%
1, 20, 100	0.5, 1, 1.5, 2, 5, 10	62%
1, 20, 50	0.5, 1, 1.5, 2, 5, 10	69%
1, 10, 100	0.5, 1, 1.5, 2, 5, 10	61%
1, 10, 50	0.5, 1, 1.5, 2, 5, 10	61%
1, 10, 20	0.5, 1, 1.5, 2, 5, 10	74%
1, 10, 20, 50, 100	1, 1.5, 2, 5, 10	57%
1, 10, 20, 50, 100	0.5, 1.5, 2, 5, 10	42%
1, 10, 20, 50, 100	0.5, 1, 1.5, 5, 10	41%
1, 10, 20, 50, 100	0.5, 1, 1.5, 2, 10	46%

Table 5-3 (Contd')

Proposed Experimental Measurement Set Up		
Buffer Concentrations (μM)	Time Points (min)	Mean % Parameter Error
1, 10, 20, 50, 100	0.5, 1, 1.5, 2, 5	50%
1, 10, 20, 50, 100	1.5, 2, 5, 10	68%
1, 10, 20, 50, 100	1, 2, 5, 10	53%
1, 10, 20, 50, 100	1, 1.5, 5, 10	55%
1, 10, 20, 50, 100	1, 1.5, 2, 10	61%
1, 10, 20, 50, 100	1, 1.5, 2, 5	67%
1, 10, 20, 50, 100	0.5, 2, 5, 10	37%
1, 10, 20, 50, 100	0.5, 1.5, 5, 10	37%
1, 10, 20, 50, 100	0.5, 1.5, 2, 10	46%
1, 10, 20, 50, 100	0.5, 1.5, 2, 5	49%
1, 10, 20, 50, 100	0.5, 1, 5, 10	39%
1, 10, 20, 50, 100	0.5, 1, 2, 10	45%
1, 10, 20, 50, 100	0.5, 1, 2, 5	48%
1, 10, 20, 50, 100	0.5, 1, 1.5, 10	48%
1, 10, 20, 50, 100	0.5, 1, 1.5, 5	52%
1, 10, 20, 50, 100	0.5, 1, 1.5, 2	77%
1, 10, 20, 50, 100	2, 5, 10	71%
1, 10, 20, 50, 100	1.5, 5, 10	65%
1, 10, 20, 50, 100	1.5, 2, 10	70%
1, 10, 20, 50, 100	1.5, 2, 5	77%

Table 5-3 (contd')

Proposed Experimental Measurement Set Up		
Buffer Concentrations (μM)	Time Points (min)	Mean % Parameter Error
1, 10, 20, 50, 100	1, 5, 10	57%
1, 10, 20, 50, 100	1, 2, 10	54%
1, 10, 20, 50, 100	1, 2, 5	62%
1, 10, 20, 50, 100	1, 1.5, 10	56%
1, 10, 20, 50, 100	1, 1.5, 5	64%
1, 10, 20, 50, 100	1, 1.5, 2	93%
1, 10, 20, 50, 100	0.5, 5, 10	44%
1, 10, 20, 50, 100	0.5, 2, 10	40%
1, 10, 20, 50, 100	0.5, 2, 5	45%
1, 10, 20, 50, 100	0.5, 1.5, 10	40%
1, 10, 20, 50, 100	0.5, 1.5, 5	46%
1, 10, 20, 50, 100	0.5, 1.5, 2	81%
1, 10, 20, 50, 100	0.5, 1, 10	44%
1, 10, 20, 50, 100	0.5, 1, 5	49%
1, 10, 20, 50, 100	0.5, 1, 2	71%
1, 10, 20, 50, 100	0.5, 1, 1.5	87%
10, 20, 50, 100	0.5, 1.5, 2, 5, 10	42%
10, 20, 50, 100	0.5, 1, 2, 5, 10	40%
10, 20, 50, 100	0.5, 1, 1.5, 5, 10	44%
10, 20, 50, 100	0.5, 2, 5, 10	37%

Table 5-3 (contd')

Proposed Experimental Measurement Set Up		
Buffer Concentrations (μM)	Time Points (min)	Mean % Parameter Error
10, 20, 50, 100	0.5, 1.5, 5, 10	37%
10, 20, 50, 100	0.5, 5, 10	38%
10, 20, 50, 100	0.5, 1.5, 10	41%
10, 20, 50, 100	0.5, 2, 10	40%
10, 20, 100	0.5, 2, 5, 10	42%
10, 20, 100	0.5, 1.5, 5, 10	43%
1, 10, 20, 50, 100	Steady state	125%
10, 20, 50, 100	Steady state	126%
1, 20, 50, 100	Steady state	125%
1, 10, 50, 100	Steady state	124%
1, 10, 20, 100	Steady state	116%
1, 10, 20, 50	Steady state	123%
0.01, 0.1, 1	Steady state	47%
0.1, 0.5, 1	Steady state	105%
0.05, 0.1, 1	Steady state	48%

Highlighted results indicate no increase or reduction of mean % parameter error from first experimental setup

5.3.2 Sensitivity Analysis

In order to determine whether the various experimental measurements setups could robustly determine pharmacokinetic parameter values for [^{3}H]-TCA hepatic transport, it was necessary to determine mean % parameter errors with varying pharmacokinetic parameters. For this analysis, one pharmacokinetic parameter was maintained constant at values ranging from 10^{-2} to 10^2 times the parameters determined by Liu et al, 1999 (Table 5-2)[147], while the other parameters were varied as described in the numerical model description. When the analysis was conducted on the full experimental setup, it was observed that the greatest increases in mean % parameter error were observed when V_{ma}, the maximum velocity of uptake into the cell, and K_{e4}, the canalicular retention constant, increased significantly (Figure 5-2). Therefore, the reliability of parameters measure decreases when uptake of [^{3}H]-TCA increases or when canalicular retention decreases significantly.

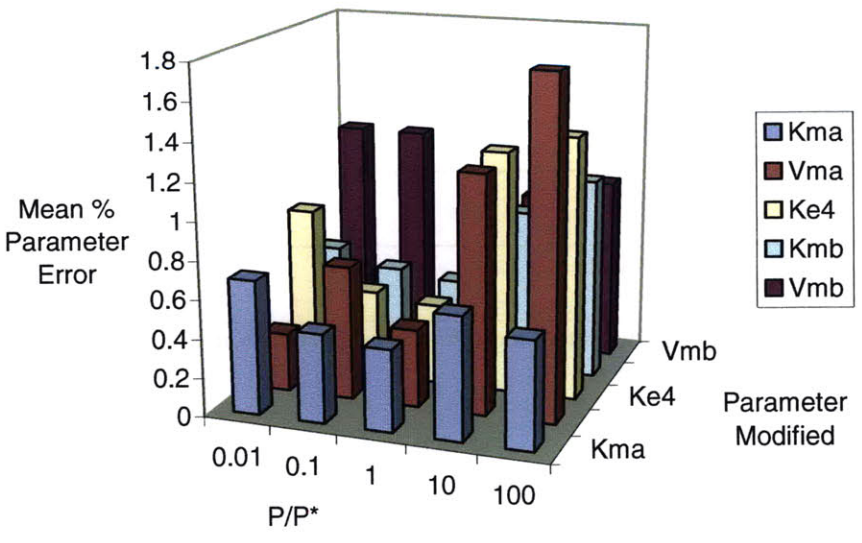

Figure 5-2: Sensitivity analysis for full experimental measurement setup. Parameter (P) is fixed at proportional value of original parameter value (P^*). Mean % parameter error increases significantly at high Vma and Ke4 values.

When the analysis was conducted on the experimental measurement setup with time point measurements of 0.5, 2 and 10min and buffer concentrations of 10, 20, 50 and 100μM, the experimental setup with the lowest number of measurement conditions with a low mean % parameter error, the increase in mean % parameter error followed a similar pattern of sensitivity (Figure 5-3). The greatest increases occur when V_{ma} and K_{e4} increase significantly.

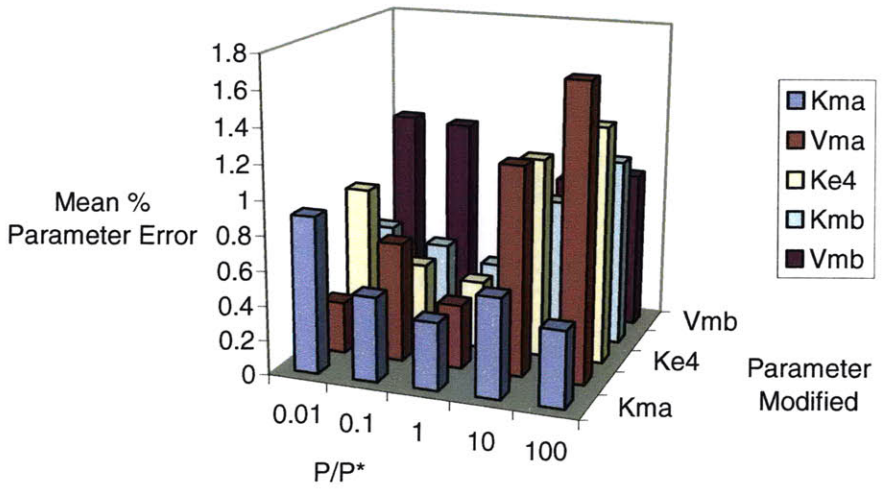

Figure 5-3: Sensitivity analysis for reduced experimental measurement setup. Parameter (P) is fixed at proportional value of original parameter value (P^*). Mean % parameter error increases significantly at high Vma and Ke4 values.

When the analysis was performed on an experimental measurement setup where measurements are conducted at steady state accumulation conditions with buffer concentrations of 0.05, 0.1 and 1μM [^{3}H]-TCA, there appeared to be a lower sensitivity to changing parameter values (Figure 5-4). However, this experimental setup seems to also be sensitive to decreasing bile acid efflux as this resulted in a comparable increase in mean % parameter error to a high increase in hepatic uptake. Therefore, it is possible that

while this set of experimental measurements may provide higher baseline error in pharmacokinetic parameter measurements, it may provide more robust parameter measurements.

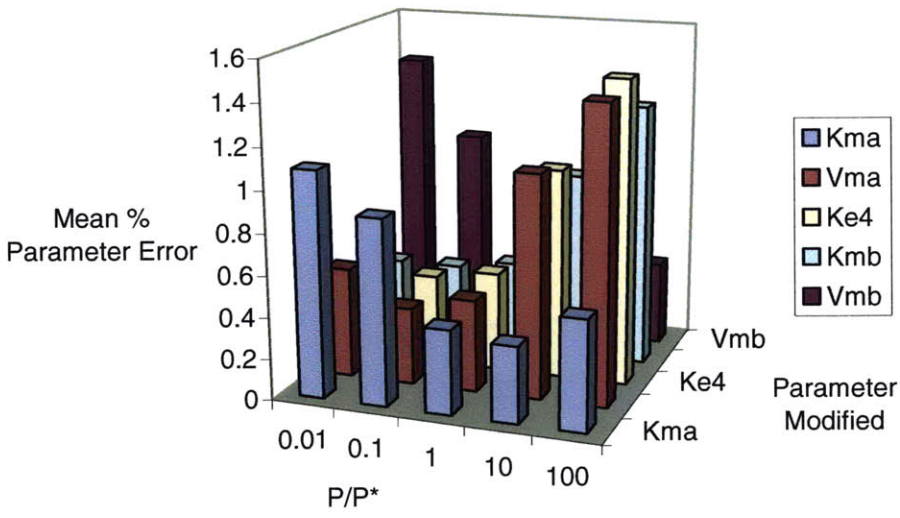

Figure 5-4: Sensitivity analysis for steady state experimental measurement setup. Parameter (P) is fixed at proportional value of original parameter value (P^*). Mean % parameter error increases significantly at high Vma and Ke4 values.

5.4 Discussion and Conclusions

The study of hepatic transport of compounds is of great importance in understanding of liver function, the disposition of drugs and other compounds, and liver metabolism of these species. It is thus necessary to have an experimental framework for the quantitative determination of uptake and efflux transport kinetics of these compounds. It is also necessary to reduce the amount of measurements necessary to determine kinetic parameters and in so doing allowing for a greater number of experimental conditions to be compared in parallel.

The numerical model described in this chapter attempts to use a stochastic method to account for random error and noise in the measurement of hepatic transport. It also

uses a stochastic method to determine potential kinetic parameters that could be measured, and thus reducing a bias to a particular kinetic parameter result. Having accounted for these considerations, it is thus possible to simulate the potential effects on the reliability of pharmacokinetic parameter measurements when the number of measurements of transport activity is reduced.

It was determined that elimination of certain time point measurements resulted in a vast decrease in the reliability of parameter measurement. This effect was greatest for the earliest time point considered, 0.5min. This was to be expected as the earlier time points establish the initial phase of the accumulation profile while intermediate time points may not supply very much information. In fact, elimination of some time points increased parameter measurement reliability. This is probably due to the effect that slight errors in the collection of these time points may have on the accurate determination of the kinetic profile. This added information is thus detrimental in reliable parameter measurement and should be eliminated.

The elimination of buffer concentrations was determined to overall decrease the reliability of parameter measurement, with the exception of the lowest concentration, C = 1μM. This result was unexpected as this concentration was the only one that was an order of magnitude lower than the K_{ma} used in these simulations[147]. Thus it was the only condition that supplied information about the linear uptake kinetics. However, it seems that because under this condition, V_{ma} and K_{ma} become a ratio of each other, as do V_{mb} and K_{mb}, the information this condition provides in determining parameters is not very useful and can thus also be eliminated.

Contrary to the above result, low buffer concentrations increase reliability of parameter measurement when steady state conditions were simulated. Interestingly, this effect is probably attributable to the same circumstance that makes low concentration kinetic data superfluous for determination of kinetic parameters when time course data is available. The fact that the uptake and efflux rates become ratios of the parameters at low buffer concentration supplies information about these parameters and thus they can be determined much more reliably.

The simulations of exclusively steady state measurements did not provide as great reliability of parameter measurement as conditions where time course measurements were included. However, these conditions allow for the greatest reduction in measurements necessary to obtain pharmacokinetic parameters of hepatic transport. Moreover, the sensitivity analysis performed showed that even though these conditions had a baseline lower reliability, the reliability did not decrease as much over a wide range of potential parameter values as it did for conditions with time course measurements. Thus, this could be a viable set of experimental measurements to perform in order to determine pharmacokinetic parameters of hepatic transport under different culture conditions.

The sensitivity analysis also revealed one weakness of the protocol for transport studies as used throughout experiments reported in this thesis. The reliability of parameters measured decreases greatly when either the uptake capabilities increase (V_{ma}) or canalicular porosity increase (Ke_4). The reason for this is most probably that under both of these conditions, the intracellular-canalicular concentration measured and the intracellular+canalicular concentration measured are basically equal. Without a large

significant difference between those two concentrations, it is very difficult to make any quantitative or even qualitative assessment of uptake and efflux kinetics of compounds.

Having determined by numerical modeling possible sets of experimental measurements to perform in order to obtain a quantitative assessment of transport kinetics, it is now possible, after experimental confirmation, to use systems like perfused 3D hepatocyte cultures, which are very constrained in the amount of conditions that can be studied in parallel, to study the effects of various chemical compounds or culture conditions on hepatic transport in a quantitative way. Therefore, that could provide greater understanding as to the underlying mechanisms that are causing the observed effects on hepatic transport.

Chapter 6

Conclusions and Recommendations

This thesis has focused on the use of hepatocyte cultures in an *in vitro* 3D physiological perfused model of *in vivo* liver in the study of hepatobiliary transport and bile acid synthesis. In order to achieve this, appropriate culture conditions had to be determined, protocols for hepatic transport studies had to be developed for this system, and the effects of media components on tissue morphology and function had to be determined.

In order to determine appropriate culture conditions so that perfused 3D cultures could be used to study hepatic transport, the effects of media components on a system widely used for *in vitro* hepatic transport, 2D sandwich cultures, were determined. Dexamethasone (DEX) was determined to be essential in the formation of canalicular networks and this effect was determined to be dose-dependent. Epidermal growth factor (EGF) was shown to disrupt canalicular network formation in 2D sandwich cultures. This effect was observed even at very low concentrations of EGF. The effect of EGF on hepatic transport studies was determined to be as a result of canalicular formation inhibition or disruption and not due to effects on transport activity. This was achieved by measuring the same EGF-mediated effect on hepatic transport using [^{3}H]-TCA, [^{3}H]digoxin, and CDF, which are excreted into canalicular networks by three different transporters. These cultures were also used to determine the effects of prolonged exposure to the cholestatic agent cyclosporin A (CyA) and supraphysiologic levels of

TCA on hepatic transport of [^{3}H]-TCA. The effect of both compounds was not significant and may indicate a loss of phenotype which would result in a lack of response to the stimuli of these compounds. This finding underscores the necessity of developing protocols to perform hepatic transport studies in cultures that have been shown to maintain liver-specific functions over long-term in culture, such as perfused 3D cultures[2, 225].

Having determined the effects of DEX and EGF on hepatic transport studies in 2D sandwich cultures, baseline hepatic transport studies performed in perfused 3D cultures would be executed with DEX and without EGF in the culture medium. In developing protocols for hepatic transport studies in perfused 3D cultures, it was estimated that the studies had to be conducted under continued perfused flow through the tissue cultures. It was estimated that the rate of uptake in the tissue would be greater than the rate of diffusion through the tissue. The protocol developed was an adaptation of the transport studies performed in 2D sandwich cultures and consisted of comparing [^{3}H]-TCA accumulation in paired cultures with intact and disrupted canalicular networks. The canalicular networks were disrupted by incubation in a Ca^{2+}-free environment. A time point for [^{3}H]-TCA accumulation measurement was determined by conducting a time course of accumulation. It was shown that [^{3}H]-TCA accumulation could reach a semi-steady state before canalicular networks were regenerated after Ca^{2+} repletion. It was also shown that [^{3}H]-TCA accumulation could be affected by CyA inhibition, and thus confirming that the accumulation measurements obtained reflected transport activity. However, in all these experiments, the canalicular [^{3}H]-TCA accumulation in perfused 3D cultures was much lower than in day 4 2D sandwich cultures.

Using confocal microscopy and DPPIV immunostaining, it was determined that EGF increased the re-polarization hepatocytes and the formation of canalicular networks in perfused 3D cultures in contrast to EGF-mediated effects on canalicular network formation in 2D sandwich cultures. Further evidence for this effect was provided by greater canalicular [^{3}H]-TCA accumulation in perfused 3D cultures with EGF in the culture medium. However, the effect of EGF on protein and mRNA expression of transporters was similar between perfused 3D cultures and 2D sandwich cultures. This indicates that the opposing effects of EGF on canalicular formation between these two types of hepatocyte culture are due to EGF effects on tight junction regulation and recycling of tight junction proteins. The effect of EGF on transporter and enzyme transcription seems to be similar between the two types of culture.

EGF was observed to significantly decrease bile acid synthesis in both culture types, which indicates this effect on hepatocytes is inherit to EGF and does not vary by culture platform. EGF also decreased the protein expression of cyp7a1, the rate-limiting enzyme in the classical bile acid synthesis pathway, by ~50%, indicating a pathway by which bile acid synthesis was inhibited. Of note, even though EGF decreased bile acid synthesis in 2D sandwich cultures, bile acid synthesis levels in these cultures were overall much lower than in perfused 3D cultures. However, cyp7a1 protein expression was very similar in 2D and 3D cultures. Therefore, this indicates that 2D cultures may not be synthesizing important bile acid precursors, such as cholesterol.

EGF was determined to be essential in formation of canalicular networks in perfused 3D cultures, however it decreased both bile acid synthesis and the expression of some canalicular liver transporters. Therefore, future studies should focus on determining

whether EGF is only necessary to establish canalicular networks during the first few days of culture but is not necessary for the maintenance of these networks. If so, EGF could be removed at an experimentally determined day in culture and its inhibitory effects could be ameliorated. Moreover, the different pathways by which EGF seems to increase cell-cell interactions and tissue formation in 3D and reduces tight junction formation in 2D cultures should be examined. A time course of the effect of EGF on the expression and localization of adherens and tight junction proteins would help elucidate the possible mechanistic differences.

One of the main motivations for this thesis work was the development of a culture system that would allow not just for long-term studies of hepatic transport, but the study of how different liver functions, such as drug metabolism, affect and are affected by hepatobiliary transport. Therefore, a numerical model was developed to reduce the number of measurements required to quantitatively determine pharmacokinetic parameters of different compounds under varying culture conditions. Experimental studies must be conducted to validate the results of this model. Sensitivity analysis of this numerical model also revealed an inherit weakness in the hepatic transport protocol. Lack of significant canalicular accumulation of the compound of interest makes the calculation of kinetic parameters very unreliable.

Having developed protocols for the study of hepatobiliary transport in perfused 3D cultures, it should be possible to conduct studies where drug metabolism of a compound and its hepatic transport can be measured in a concerted way. It will also allow for the study of long term effect of drug metabolism enzyme inducers and their effect on liver transporter expression. Many liver transporters and drug metabolism enzymes have

similar transcriptional pathways. Furthermore, the effects of a novel compound on drug metabolism and liver transport can be studied and more potential drug-drug interactions can be determined. Moreover, potential pathways for hepatotoxicity involving inhibition of transport can be readily studied as well.

References

1. Desmet, V., *Organizational Principles*, in *The liver: Biology and pathobiology*, I. Arias, et al., Editors. 2001, Lippincott: New York. p. 3-15.
2. Sivaraman, A., et al., *A Microscale In Vitro Physiological Model of the Liver: Predictive Screens for Drug Metabolism and Enzyme Induction.* Current Drug Metabolism, 2005. **6**: p. 569-591.
3. Chandra, P. and K. Brouwer, *The Complexities of Hepatic Drug Transport: Current Knowledge and Emerging Concepts.* Pharmaceutical Research, 2004. **21**(5): p. 719-735.
4. LeCluyse, E.L., P.L. Bullock, and A. Parkinson, *Strategies for restoration and maintenance of normal hepatic structure and function in long-term cultures of rat hepatocytes.* Advanced Drug Delivery Reviews, 1996. **22**(1-2): p. 133-186.
5. Vinken, M., et al., *Involvement of Cell Junctions in Hepatocyte Culture Functionality.* Critical Reviews in Toxicology, 2006. **36**(4): p. 299 - 318.
6. Gebhardt, R., *METABOLIC ZONATION OF THE LIVER - REGULATION AND IMPLICATIONS FOR LIVER-FUNCTION.* Pharmacology & Therapeutics, 1992. **53**(3): p. 275-354.
7. Arias, I., et al., *The liver : biology and pathobiology.* 4th ed. 2001, New York: Lippincott.
8. Leevy, C.M. and T. Kiernan, *HEPATIC CIRCULATION AND PORTAL-HYPERTENSION.* Clinics in Gastroenterology, 1975. **4**(2): p. 381-394.
9. Russell, D.W., *THE ENZYMES, REGULATION, AND GENETICS OF BILE ACID SYNTHESIS.* Annual Review of Biochemistry, 2003. **72**(1): p. 137-174.
10. Junqueira, L.C. and J. Carneiro, *Basic Histology.* 1999, Stamford, CT: Appleton and Lange.
11. McCuskey, R., *The Hepatic Microenvironment*, in *The Liver: Biology and Pathobiology*, I. Arias, et al., Editors. 2001, Lippincott, Williams & Wilkins: New York. p. 1089-1106.
12. Klassen, C.D., *Casarett and Doul's Toxicology: The Basic Science of Poisons.* 2001, New York: McGraw-Hill Medical Publishing Division.
13. Lodish, H., et al., *Molecular Cell Biology.* 5th ed. 2004, New York: W. H. Freeman & Co.
14. Stieger, B., B. Oneill, and P.J. Meier, *ATP-DEPENDENT BILE-SALT TRANSPORT IN CANALICULAR RAT-LIVER PLASMA-MEMBRANE VESICLES.* Biochemical Journal, 1992. **284**: p. 67-74.
15. Noe, B., et al., *Isolation of a multispecific organic anion and cardiac glycoside transporter from rat brain.* Proceedings of the National Academy of Sciences of the United States of America, 1997. **94**(19): p. 10346-10350.
16. Kullak-Ublick, G.A., U. Beuers, and G. Paumgartner, *Hepatobiliary transport.* Journal of Hepatology, 2000. **32**: p. 3-18.
17. Hagenbuch, B. and P.J. Meier, *MOLECULAR-CLONING, CHROMOSOMAL LOCALIZATION, AND FUNCTIONAL-CHARACTERIZATION OF A HUMAN LIVER NA+ BILE-ACID COTRANSPORTER.* Journal of Clinical Investigation, 1994. **93**(3): p. 1326-1331.

18. Eckhardt, U., et al., *Polyspecific substrate uptake by the hepatic organic anion transporter Oatp1 in stably transfected CHO cells.* American Journal of Physiology-Gastrointestinal and Liver Physiology, 1999. **276**(4): p. G1037-G1042.
19. Kullak-Ublick, G.A., et al., *FUNCTIONAL-CHARACTERIZATION OF THE BASOLATERAL RAT-LIVER ORGANIC ANION TRANSPORTING POLYPEPTIDE.* Hepatology, 1994. **20**(2): p. 411-416.
20. Reichel, C., et al., *Localization and function of the organic anion-transporting polypeptide Oatp2 in rat liver.* Gastroenterology, 1999. **117**(3): p. 688-695.
21. Satlin, L.M., V. Amin, and A.W. Wolkoff, *Organic anion transporting polypeptide mediates organic anion/HCO3- exchange.* Journal of Biological Chemistry, 1997. **272**(42): p. 26340-26345.
22. Kakyo, M., et al., *Molecular characterization and functional regulation of a novel rat liver-specific organic anion transporter rlst-1.* Gastroenterology, 1999. **117**(4): p. 770-775.
23. Cattori, V., et al., *Identification of organic anion transporting polypeptide 4 (Oatp4) as a major full-length isoform of the liver-specific transporter-1 (rlst-1) in rat liver.* Febs Letters, 2000. **474**(2-3): p. 242-245.
24. Geier, A., et al., *Extrahepatic cholestasis downregulates Oatp1 by TNF-alpha signalling without affecting Oatp2 and Oatp4 expression and sodium-independent bile salt uptake in rat liver.* Liver International, 2007. **27**(8): p. 1056-1065.
25. Gerloff, T., et al., *The sister of P-glycoprotein represents the canalicular bile salt export pump of mammalian liver.* Journal of Biological Chemistry, 1998. **273**(16): p. 10046-10050.
26. Meier, P.J. and B. Stieger, *Bile salt transporters.* Annual Review of Physiology, 2002. **64**: p. 635-661.
27. Hirohashi, T., et al., *ATP-dependent transport of bile salts by rat multidrug resistance-associated protein 3 (Mrp3).* Journal of Biological Chemistry, 2000. **275**(4): p. 2905-2910.
28. Soroka, C.J., et al., *Cellular localization and up-regulation of multidrug resistance-associated protein 3 in hepatocytes and cholangiocytes during obstructive cholestasis in rat liver.* Hepatology, 2001. **33**(4): p. 783-791.
29. Javitt, N.B., *Bile acid synthesis from cholesterol: regulatory and auxiliary pathways.* FASEB J., 1994. **8**(15): p. 1308-1311.
30. Pandak, W.M., et al., *REGULATION OF CHOLESTEROL 7-ALPHA-HYDROXYLASE MESSENGER-RNA AND TRANSCRIPTIONAL ACTIVITY BY TAUROCHOLATE AND CHOLESTEROL IN THE CHRONIC BILIARY DIVERTED RAT.* Journal of Biological Chemistry, 1991. **266**(6): p. 3416-3421.
31. Chiang, J.Y., *Regulation of bile acid synthesis.* Front Biosci, 1998. **3**: p. d176-93.
32. Repa, J.J. and D.J. Mangelsdorf, *The role of orphan nuclear receptors in the regulation of cholesterol homeostasis.* Annual Review of Cell and Developmental Biology, 2000. **16**: p. 459-481.
33. Axelson, M. and J. Sjovall, *POTENTIAL BILE-ACID PRECURSORS IN PLASMA - POSSIBLE INDICATORS OF BIOSYNTHETIC PATHWAYS TO CHOLIC AND CHENODEOXYCHOLIC ACIDS IN MAN.* Journal of Steroid Biochemistry and Molecular Biology, 1990. **36**(6): p. 631-640.

34. Ishibashi, S., et al., *Disruption of cholesterol 7 alpha-hydroxylase gene in mice .1. Postnatal lethality reversed by bile acid and vitamin supplementation.* Journal of Biological Chemistry, 1996. **271**(30): p. 18017-18023.
35. Twisk, J., E.C.M. Dewit, and H.M.G. Princen, *SUPPRESSION OF STEROL 27-HYDROXYLASE MESSENGER-RNA AND TRANSCRIPTIONAL ACTIVITY BY BILE-ACIDS IN CULTURED RAT HEPATOCYTES.* Biochemical Journal, 1995. **305**: p. 505-511.
36. Twisk, J., et al., *STRUCTURAL ASPECTS OF BILE-ACIDS INVOLVED IN THE REGULATION OF CHOLESTEROL 7-ALPHA-HYDROXYLASE AND STEROL 27-HYDROXYLASE.* European Journal of Biochemistry, 1995. **228**(3): p. 596-604.
37. Twisk, J., E.M. Lehmann, and H.M.G. Princen, *DIFFERENTIAL FEEDBACK-REGULATION OF CHOLESTEROL 7-ALPHA-HYDROXYLASE MESSENGER-RNA AND TRANSCRIPTIONAL ACTIVITY BY RAT BILE-ACIDS IN PRIMARY MONOLAYER-CULTURES OF RAT HEPATOCYTES.* Biochemical Journal, 1993. **290**: p. 685-691.
38. Vlahcevic, Z.R., et al., *Transcriptional regulation of hepatic sterol 27-hydroxylase by bile acids.* American Journal of Physiology-Gastrointestinal and Liver Physiology, 1996. **33**(4): p. G646-G652.
39. Falany, C.N., et al., *Cloning, expression, and chromosomal localization of mouse liver bile acid CoA:amino acid N-acyltransferase.* J. Lipid Res., 1997. **38**(6): p. 1139-1148.
40. Falany, C.N., et al., *Glycine and taurine conjugation of bile acids by a single enzyme. Molecular cloning and expression of human liver bile acid CoA:amino acid N-acyltransferase.* J. Biol. Chem., 1994. **269**(30): p. 19375-19379.
41. Killenberg, P.G. and J.T. Jordan, *Purification and characterization of bile acid-CoA:amino acid N-acyltransferase from rat liver.* J. Biol. Chem., 1978. **253**(4): p. 1005-1010.
42. Hardison, W.G.M. and J.H. Proffitt, *INFLUENCE OF HEPATIC TAURINE CONCENTRATION ON BILE-ACID CONJUGATION WITH TAURINE.* American Journal of Physiology, 1977. **232**(1): p. E75-E79.
43. Kullak-Ublick, G.A., et al. *Stable expression and functional characterization of a Na+-taurocholate cotransporting green fluorescent protein in human hepatoblastoma HepG2 cells.* 2000: Kluwer Academic Publ.
44. Meier, P.J., et al., *Substrate specificity of sinusoidal bile acid and organic anion uptake systems in rat and human liver.* Hepatology, 1997. **26**(6): p. 1667-1677.
45. Meyer-Wentrup, F., et al., *Membrane localization of the electrogenic cation transporter rOCT1 in rat liver.* Biochemical and Biophysical Research Communications, 1998. **248**(3): p. 673-678.
46. Kullak-Ublick, G.A. and M.B. Becker. *Regulation of drug and bile salt transporters in liver and intestine.* 2003: Marcel Dekker Inc.
47. Konig, J., et al., *Conjugate export pumps of the multidrug resistance protein (MRP) family: localization, substrate specificity, and MRP2-mediated drug resistance.* Biochimica Et Biophysica Acta-Biomembranes, 1999. **1461**(2): p. 377-394.

48. Pastan, I., et al., *MULTIPLE-DRUG RESISTANCE IN HUMAN CANCER.* New England Journal of Medicine, 1987. **316**(22): p. 1388-1393.
49. Smit, J.J.M., et al., *HOMOZYGOUS DISRUPTION OF THE MURINE MDR2 P-GLYCOPROTEIN GENE LEADS TO A COMPLETE ABSENCE OF PHOSPHOLIPID FROM BILE AND TO LIVER-DISEASE.* Cell, 1993. **75**(3): p. 451-462.
50. Faber, K.N., M. Muller, and P.L.M. Jansen, *Drug transport proteins in the liver.* Advanced Drug Delivery Reviews, 2003. **55**(1): p. 107-124.
51. Graf, G.A., et al., *ABCG5 and ABCG8 are obligate heterodimers for protein trafficking and biliary cholesterol excretion.* Journal of Biological Chemistry, 2003. **278**(48): p. 48275-48282.
52. Suzuki, M., et al. *ABCG2 transports sulfated conjugates of steroids and xenobiotics.* 2003: Amer Soc Biochemistry Molecular Biology Inc.
53. Stroup, D., *Kinase/phosphatase regulation of CYP7A1.* Front Biosci, 2005. **10**: p. 1678-1692.
54. Hofmann, A.F. and L.R. Hagey, *Bile acids: Chemistry, pathochemistry, biology, pathobiology, and therapeutics.* Cellular and Molecular Life Sciences, 2008. **65**(16): p. 2461-2483.
55. Kuipers, F., et al., *The Farnesoid X Receptor (FXR) as Modulator of Bile Acid Metabolism.* Reviews in Endocrine & Metabolic Disorders, 2004. **5**(4): p. 319-326.
56. Makishima, M., et al., *Identification of a nuclear receptor for bile acids.* Science, 1999. **284**(5418): p. 1362-1365.
57. Goodwin, B., et al., *A Regulatory Cascade of the Nuclear Receptors FXR, SHP-1, and LRH-1 Represses Bile Acid Biosynthesis.* 2000. **6**(3): p. 517-526.
58. Galarneau, L., et al., *The alpha(1)-fetoprotein locus is activated by a nuclear receptor of the Drosophila FTZ-F1 family.* Molecular and Cellular Biology, 1996. **16**(7): p. 3853-3865.
59. Lu, T.T., et al., *Molecular Basis for Feedback Regulation of Bile Acid Synthesis by Nuclear Receptors.* 2000. **6**(3): p. 507-515.
60. Xu, G.R., et al., *Dietary cholesterol stimulates CYP7A1 in rats because farnesoid X receptor is not activated.* American Journal of Physiology-Gastrointestinal and Liver Physiology, 2004. **286**(5): p. G730-G735.
61. Xu, Z.M., et al., *Activation of bile acid biosynthesis by the p38 mitogen-activated protein kinase (MAPK) - Hepatocyte nuclear factor-4 alpha phosphorylation by the p38 MAPK is required for cholesterol 7 alpha-hydroxylase expression.* Journal of Biological Chemistry, 2007. **282**(34): p. 24607-24614.
62. Yang, Y.Z., et al., *On the mechanism of bile acid inhibition of rat sterol 12 alpha-hydroxylase gene (CYP8B1) transcription: roles of alpha-fetoprotein transcription factor and hepatocyte nuclear factor 4 alpha.* Biochimica Et Biophysica Acta-Molecular and Cell Biology of Lipids, 2002. **1583**(1): p. 63-73.
63. Crestani, M., et al., *Transcriptional activation of the cholesterol 7 alpha-hydroxylase gene (CYP7A) by nuclear hormone receptors.* Journal of Lipid Research, 1998. **39**(11): p. 2192-2200.
64. Zhang, M. and J.Y.L. Chiang, *Transcriptional regulation of the human sterol 12 alpha-hydroxylase gene (CYP8B1) - Roles of hepatocyte nuclear factor 4 alpha in*

mediating bile acid repression. Journal of Biological Chemistry, 2001. **276**(45): p. 41690-41699.
65. del Castillo-Olivares, A. and G. Gil, *alpha(1)-fetoprotein transcription factor is required for the expression of sterol 12 alpha-hydroxylase, the specific enzyme for cholic acid synthesis - Potential role in the bile acid-mediated regulation of gene transcription.* Journal of Biological Chemistry, 2000. **275**(23): p. 17793-17799.
66. Chen, W.L. and J.Y.L. Chiang, *Regulation of human sterol 27-hydroxylase gene (CYP27A1) by bile acids and hepatocyte nuclear factor 4 alpha (HNF4 alpha).* Gene, 2003. **313**: p. 71-82.
67. Stravitz, R.T., et al., *Regulation of sterol 27-hydroxylase and an alternative pathway of bile acid biosynthesis in primary cultures of rat hepatocytes.* Journal of Steroid Biochemistry and Molecular Biology, 1996. **57**(5-6): p. 337-347.
68. Ananthanarayanan, M., et al., *Human bile salt export pump promoter is transactivated by the farnesoid X receptor/bile acid receptor.* Journal of Biological Chemistry, 2001. **276**(31): p. 28857-28865.
69. Song, X.L., et al., *Liver receptor homolog 1 transcriptionally regulates human bile salt export pump expression.* Journal of Lipid Research, 2008. **49**(5): p. 973-984.
70. Denson, L.A., et al. *The orphan nuclear receptor, shp, mediates bile acid-induced inhibition of the rat bile acid transporter, ntcp.* 2001: W B Saunders Co.
71. Denson, L.A., et al., *Interleukin-1 beta suppresses retinoid transactivation of two hepatic transporter genes involved in bile formation.* Journal of Biological Chemistry, 2000. **275**(12): p. 8835-8843.
72. Kast, H.R., et al., *Regulation of multidrug resistance-associated protein 2 (ABCC2) by nuclear receptors pregnane X receptor, farnesoid X-activated receptor, and constitutive androstane receptor.* Journal of Biological Chemistry, 2002. **277**(4): p. 2908-2915.
73. Kullak-Ublick, G.A., *ABC transporter regulation by bile acids: where PXR meets FXR.* Journal of Hepatology, 2003. **39**(4): p. 628-630.
74. Staudinger, J.L., et al., *Regulation of drug transporter gene expression by nuclear receptors.* Drug Metabolism and Disposition, 2003. **31**(5): p. 523-527.
75. Donner, M.G. and D. Keppler, *Up-regulation of basolateral multidrug resistance protein 3 (Mrp3) in cholestatic rat liver.* Hepatology, 2001. **34**(2): p. 351-359.
76. Cherrington, N.J., et al., *Organ distribution of multidrug resistance proteins 1, 2, and 3 (Mrp1, 2, and 3) rnRNA and hepatic induction of mrp3 by constitutive androstane receptor activators in rats.* Journal of Pharmacology and Experimental Therapeutics, 2002. **300**(1): p. 97-104.
77. Schuetz, E.G., et al., *Disrupted Bile Acid Homeostasis Reveals an Unexpected Interaction among Nuclear Hormone Receptors, Transporters, and Cytochrome P450.* J. Biol. Chem., 2001. **276**(42): p. 39411-39418.
78. Hagenbuch, N., et al. *Effect of phenobarbital on the expression of bile salt and organic anion transporters of rat liver.* 2001: Elsevier Science Bv.
79. Donner, M.G., et al., *Obstructive cholestasis induces TNF-alpha- and IL-1 beta-mediated periportal downregulation of Bsep and zonal regulation of Ntcp, Oatp1a4, and Oatp1b2.* American Journal of Physiology-Gastrointestinal and Liver Physiology, 2007. **293**(6): p. G1134-G1146.

80. Geick, A., M. Eichelbaum, and O. Burk, *Nuclear receptor response elements mediate induction of intestinal MDR1 by rifampin.* Journal of Biological Chemistry, 2001. **276**(18): p. 14581-14587.
81. Synold, T.W., I. Dussault, and B.M. Forman, *The orphan nuclear receptor SXR coordinately regulates drug metabolism and efflux.* Nature Medicine, 2001. **7**(5): p. 584-590.
82. Fitzgerald, M.L., K.J. Moore, and M.W. Freeman, *Nuclear hormone receptors and cholesterol trafficking: the orphans find a new home.* Journal of Molecular Medicine-Jmm, 2002. **80**(5): p. 271-281.
83. Miranda, S., et al., *Overexpression of mdr2 gene by peroxisome proliferators in the mouse liver.* Journal of Hepatology, 1997. **26**(6): p. 1331-1339.
84. Kok, T., et al. *Peroxisome proliferator-activated receptor alpha (PPAR alpha)-mediated regulation of multidrug resistance 2 (Mdr2) expression and function in mice*. 2003: Portland Press.
85. Grandal, M.V. and I.H. Madshus, *Epidermal growth factor receptor and cancer: control of oncogenic signalling by endocytosis.* Journal of Cellular and Molecular Medicine, 2008. **12**(5A): p. 1527-1534.
86. Hayashi, H., et al., *Down-regulation of the PI3-kinase/Akt pathway by ERK MAP kinase in growth factor signaling.* Genes to Cells, 2008. **13**(9): p. 941-947.
87. Ramos, J.W., *The regulation of extracellular signal-regulated kinase (ERK) in mammalian cells.* International Journal of Biochemistry & Cell Biology, 2008. **40**(12): p. 2707-2719.
88. Henson, E.S. and S.B. Gibson, *Surviving cell death through epidermal growth factor (EGF) signal transduction pathways: Implications for cancer therapy.* Cellular Signalling, 2006. **18**(12): p. 2089-2097.
89. Lo, H.W., S.C. Hsu, and M.C. Hung, *EGFR signaling pathway in breast cancers: from traditional signal transduction to direct nuclear translocalization.* Breast Cancer Research and Treatment, 2006. **95**(3): p. 211-218.
90. Lee, M.Y., et al., *EGF-induced inhibition of glucose transport is mediated by PKC and MAPK signal pathways in primary cultured chicken hepatocytes.* Am J Physiol Gastrointest Liver Physiol, 2006. **291**(4): p. G744-750.
91. Vergarajauregui, S., A. San Miguel, and R. Puertollano, *Activation of p38 Mitogen-Activated Protein Kinase Promotes Epidermal Growth Factor Receptor Internalization.* Traffic, 2006. **7**(6): p. 686-698.
92. Thoresen, G.H., T.K. Guren, and T. Christoffersen, *Role of ERK, p38 and Pl3-kinase in EGF receptorMediated mitogenic signalling in cultured rat hepatocytes: Requirement for sustained ERK activation.* Cellular Physiology and Biochemistry, 2003. **13**(4): p. 229-238.
93. Carpenter, G., *The EGF receptor: a nexus for trafficking and signaling.* Bioessays, 2000. **22**(8): p. 697-707.
94. Gupta, S., et al., *Deoxycholic Acid Activates the c-Jun N-terminal Kinase Pathway via FAS Receptor Activation in Primary Hepatocytes: ROLE OF ACIDIC SPHINGOMYELINASE-MEDIATED CERAMIDE GENERATION IN FAS RECEPTOR ACTIVATION.* J. Biol. Chem., 2004. **279**(7): p. 5821-5828.

95. Gupta, S., et al., *Down-regulation of Cholesterol 7alpha -Hydroxylase (CYP7A1) Gene Expression by Bile Acids in Primary Rat Hepatocytes Is Mediated by the c-Jun N-terminal Kinase Pathway.* J. Biol. Chem., 2001. **276**(19): p. 15816-15822.
96. Reinehr, R., D. Graf, and D. Haussinger, *Bile salt-induced hepatocyte apoptosis involves epidermal growth factor receptor-dependent CD95 tyrosine phosphorylation.* Gastroenterology, 2003. **125**(3): p. 839-853.
97. Lee, Y.-K., et al., *Phosphorylation of the Hinge Domain of the Nuclear Hormone Receptor LRH-1 Stimulates Transactivation.* J. Biol. Chem., 2006. **281**(12): p. 7850-7855.
98. Crestani, M., D. Stroup, and J.Y. Chiang, *Hormonal regulation of the cholesterol 7 alpha-hydroxylase gene (CYP7).* J. Lipid Res., 1995. **36**(11): p. 2419-2432.
99. Dajani, O.F., et al., *Prostaglandin E-2 upregulates EGF-stimulated signaling in mitogenic pathways involving Akt and ERK in hepatocytes.* Journal of Cellular Physiology, 2008. **214**(2): p. 371-380.
100. Michalopoulos, G.K., et al., *HGF-, EGF-, and Dexamethasone-Induced Gene Expression Patterns During Formation of Tissue in Hepatic Organoid Cultures.* Gene Expression, 2003. **11**: p. 55-75.
101. Kubitz, R., et al., *Trafficking of the bile salt export pump from the Golgi to the canalicular membrane is regulated by the p38 MAP kinase.* Gastroenterology, 2004. **126**(2): p. 541-553.
102. McConkey, M., et al., *Cross-talk between protein kinases C zeta and B in cyclic AMP-mediated sodium taurocholate co-transporting polypeptide translocation in hepatocytes.* Journal of Biological Chemistry, 2004. **279**(20): p. 20882-20888.
103. Kubitz, R., et al., *Ca2+-dependent Protein Kinase C Isoforms Induce Cholestasis in Rat Liver.* J. Biol. Chem., 2004. **279**(11): p. 10323-10330.
104. Bouscarel, B., et al., *Ursodeoxycholic acid inhibits glucagon-induced cAMP formation in hamster hepatocytes: a role for PKC.* Am J Physiol Gastrointest Liver Physiol, 1995. **268**(2): p. G300-310.
105. Kubitz, R., et al., *Protein kinase C-dependent distribution of the multidrug resistance protein 2 from the canalicular to the basolateral membrane in human HepG2 cells.* Hepatology, 2001. **34**(2): p. 340-350.
106. Kurz, A.K., et al., *Tauroursodesoxycholate-induced choleresis involves p38(MAPK) activation and translocation of the bile salt export pump in rats.* Gastroenterology, 2001. **121**(2): p. 407-419.
107. Schliess, F., et al., *Mitogen-activated protein kinases mediate the stimulation of bile acid secretion by tauroursodeoxycholate in rat liver.* Gastroenterology, 1997. **113**(4): p. 1306-1314.
108. Thomas, C., et al., *Targeting bile-acid signalling for metabolic diseases.* Nature Reviews Drug Discovery, 2008. **7**(8): p. 678-693.
109. Fukushima, K., et al., *REGULATION OF BILE-ACID SYNTHESIS IN THE RAT - RELATIONSHIP BETWEEN HEPATIC CHOLESTEROL 7-ALPHA-HYDROXYLASE ACTIVITY AND PORTAL BILE-ACIDS.* Journal of Lipid Research, 1995. **36**(2): p. 315-321.
110. Schwarz, M., et al., *Alternate pathways of bile acid synthesis in the cholesterol 7{alpha}-hydroxylase knockout mouse are not upregulated by either cholesterol or cholestyramine feeding.* J. Lipid Res., 2001. **42**(10): p. 1594-1603.

111. Yasuda, H., et al., *Involvement of membrane-type bile acid receptor M-BAR/TGR5 in bile acid-induced activation of epidermal growth factor receptor and mitogen-activated protein kinases in gastric carcinoma cells.* Biochemical and Biophysical Research Communications, 2007. **354**(1): p. 154-159.
112. Voronina, S., et al., *Bile acids induce calcium signals in mouse pancreatic acinar cells: implications for bile-induced pancreatic pathology.* J Physiol, 2002. **540**(1): p. 49-55.
113. Voronina, S.G., et al., *Bile Acids Induce a Cationic Current, Depolarizing Pancreatic Acinar Cells and Increasing the Intracellular Na+ Concentration.* J. Biol. Chem., 2005. **280**(3): p. 1764-1770.
114. Kim, J.Y., et al., *Transporter-mediated bile acid uptake causes Ca2+-dependent cell death in rat pancreatic acinar cells.* Gastroenterology, 2002. **122**(7): p. 1941-1953.
115. Keitel, V., et al., *The G-protein coupled bile salt receptor TGR5 is expressed in liver sinusoidal endothelial cells.* Hepatology, 2007. **45**(3): p. 695-704.
116. Fischer, L., et al., *Phosphatidylinositol 3-kinase facilitates bile acid-induced Ca2+ responses in pancreatic acinar cells.* Am J Physiol Gastrointest Liver Physiol, 2007. **292**(3): p. G875-886.
117. Bernstein, H., et al., *Bile acids as carcinogens in human gastrointestinal cancers.* Mutation Research/Reviews in Mutation Research, 2005. **589**(1): p. 47-65.
118. Houten, S.M., M. Watanabe, and J. Auwerx, *Endocrine functions of bile acids.* Embo Journal, 2006. **25**(7): p. 1419-1425.
119. Duane, W.C., W. Xiong, and J. Wolvers, *Effects of bile acids on expression of the human apical sodium dependent bile acid transporter gene.* Biochimica Et Biophysica Acta-Molecular and Cell Biology of Lipids, 2007. **1771**(11): p. 1380-1388.
120. Debruyne, P.R., et al., *The role of bile acids in carcinogenesis.* Mutation Research/Fundamental and Molecular Mechanisms of Mutagenesis, 2001. **480-481**: p. 359-369.
121. Dent, P., et al., *Conjugated bile acids promote ERK1/2 and AKT activation via a pertussis toxin-sensitive mechanism in murine and human hepatocytes.* Hepatology, 2005. **42**(6): p. 1291-1299.
122. Nguyen, A. and B. Bouscarel, *Bile acids and signal transduction: Role in glucose homeostasis.* Cellular Signalling, 2008. **20**(12): p. 2180-97.
123. Qiao, L., et al., *Deoxycholic acid (DCA) causes ligand-independent activation of epidermal growth factor receptor (EGFR) and FAS receptor in primary hepatocytes: Inhibition of EGFR/mitogen-activated protein kinase-signaling module enhances DCA-induced apoptosis.* Molecular Biology of the Cell, 2001. **12**(9): p. 2629-2645.
124. Qiao, L., et al., *Inhibition of the MAPK and PI3K pathways enhances UDCA-induced apoptosis in primary rodent hepatocytes.* Hepatology, 2002. **35**(4): p. 779-789.
125. Ikegami, T., et al., *Decreased Glucagon Responsiveness by Bile Acids: A Role for Protein Kinase C{alpha} and Glucagon Receptor Phosphorylation.* Endocrinology, 2006. **147**(11): p. 5294-5302.

126. Rao, Y.P., et al., *Activation of the Raf-1/MEK/ERK cascade by bile acids occurs via the epidermal growth factor receptor in primary rat hepatocytes.* Hepatology, 2002. **35**(2): p. 307-314.
127. Barone, M., et al., *Modulation of rat hepatocyte proliferation by bile salts: In vitro and in vivo studies.* Hepatology, 1996. **23**(5): p. 1159-1166.
128. Bouscarel, B., S.D. Kroll, and H. Fromm, *Signal transduction and hepatocellular bile acid transport: Cross talk between bile acids and second messengers.* Gastroenterology, 1999. **117**(2): p. 433-452.
129. Bouscarel, B., et al. *Regulation of taurocholate and ursodeoxycholate uptake in hamster hepatocytes by Ca2+-mobilizing agents.* 1996: Amer Physiological Soc.
130. Bouscarel, B., et al., *Changes in G protein expression account for impaired modulation of hepatic cAMP formation after BDL.* Am J Physiol Gastrointest Liver Physiol, 1998. **274**(6): p. G1151-1159.
131. Angst, B.D., C. Marcozzi, and A.I. Magee, *The cadherin superfamily: diversity in form and function.* Journal of Cell Science, 2001. **114**(4): p. 629-641.
132. Blaschuk, O.W. and T.M. Rowlands, *Plasma membrane components of adherens junctions (Review).* Molecular Membrane Biology, 2002. **19**(2): p. 75-80.
133. Geiger, B. and O. Ayalon, *CADHERINS.* Annual Review of Cell Biology, 1992. **8**: p. 307-332.
134. Getsios, S., A.C. Huen, and K.J. Green, *Working out the strength and flexibility of desmosomes.* Nature Reviews Molecular Cell Biology, 2004. **5**(4): p. 271-281.
135. Gooding, J.M., K.L. Yap, and M. Ikura, *The cadherin-catenin complex as a focal point of cell adhesion and signalling: new insights from three-dimensional structures.* Bioessays, 2004. **26**(5): p. 497-511.
136. Green, K.J. and C.A. Gaudry, *Are desmosomes more than tethers for intermediate filaments?* Nature Reviews Molecular Cell Biology, 2000. **1**(3): p. 208-216.
137. Huber, O., *Structure and function of desmosomal proteins and their role in development and disease.* Cellular and Molecular Life Sciences, 2003. **60**(9): p. 1872-1890.
138. Ihara, A., et al., *Expression of epithelial cadherin and alpha- and beta-catenins in nontumoral livers and hepatocellular carcinomas.* Hepatology, 1996. **23**(6): p. 1441-1447.
139. Ikeda, T., et al., *Induction of tyrosine aminotransferase of primary cultured rat hepatocytes depends on the organization of microtubules.* Journal of Cellular Physiology, 1998. **175**(1): p. 41-49.
140. Linnemann, D., et al., *CHARACTERIZATION OF N-CADHERIN MESSENGER-RNA AND POLYPEPTIDE EXPRESSION IN RAT.* International Journal of Developmental Neuroscience, 1994. **12**(5): p. 441-450.
141. Matsui, T., et al., *K-Ras mediates cytokine-induced formation of E-cadherin-based adherens junctions during liver development.* Embo Journal, 2002. **21**(5): p. 1021-1030.
142. Monga, S.P.S., et al., *beta-catenin antisense studies in embryonic liver cultures: Role in proliferation, apoptosis, and lineage specification.* Gastroenterology, 2003. **124**(1): p. 202-216.
143. Nagafuchi, A., *Molecular architecture of adherens junctions.* Current Opinion in Cell Biology, 2001. **13**(5): p. 600-603.

144. Schmelz, M., V.J. Schmid, and A.R. Parrish, *Selective disruption of cadherin/catenin complexes by oxidative stress in precision-cut mouse liver slices.* Toxicological Sciences, 2001. **61**(2): p. 389-394.
145. Wheelock, M.J. and K.R. Johnson, *Cadherins as modulators of cellular phenotype.* Annual Review of Cell and Developmental Biology, 2003. **19**: p. 207-235.
146. Yap, A.S., W.M. Brieher, and B.M. Gumbiner, *Molecular and functional analysis of cadherin-based adherens junctions.* Annual Review of Cell and Developmental Biology, 1997. **13**: p. 119-146.
147. Liu, X., et al., *Use of Ca2+ Modulation to Evaluate Biliary Excretion in Sandwich-Cultured Rat Hepatocytes.* J Pharmacol Exp Ther, 1999. **289**(3): p. 1592-1599.
148. Garrod, D.R., A.J. Merritt, and Z.X. Nie, *Desmosomal adhesion: structural basis, molecular mechanism and regulation (Review).* Molecular Membrane Biology, 2002. **19**(2): p. 81-94.
149. Kojima, T., et al., *Cx32 but not Cx26 is associated with tight junctions in primary cultures of rat hepatocytes.* Experimental Cell Research, 2001. **263**(2): p. 193-201.
150. Sakaguchi, T., et al., *Cloning of the human claudin-2 5 '-flanking region revealed a TATA-less promoter with conserved binding sites in mouse and human for caudal-related homeodomain proteins and hepatocyte nuclear factor-1 alpha.* Journal of Biological Chemistry, 2002. **277**(24): p. 21361-21370.
151. Rahner, C., L.L. Mitic, and J.M. Anderson, *Heterogeneity in expression and subcellular localization of claudins 2, 3, 4, and 5 in the rat liver, pancreas, and gut.* Gastroenterology, 2001. **120**(2): p. 411-422.
152. Furuse, M., et al., *Claudin-1 and -2: Novel integral membrane proteins localizing at tight junctions with no sequence similarity to occludin.* Journal of Cell Biology, 1998. **141**(7): p. 1539-1550.
153. Furuse, M., et al., *OCCLUDIN - A NOVEL INTEGRAL MEMBRANE-PROTEIN LOCALIZING AT TIGHT JUNCTIONS.* Journal of Cell Biology, 1993. **123**(6): p. 1777-1788.
154. Morita, K., et al., *Claudin multigene family encoding four-transmembrane domain protein components of tight junction strands.* Proceedings of the National Academy of Sciences of the United States of America, 1999. **96**(2): p. 511-516.
155. Yamamoto, T., et al., *IL-1 beta regulates expression of Cx32, occludin, and claudin-2 of rat hepatocytes via distinct signal transduction pathways.* Experimental Cell Research, 2004. **299**(2): p. 427-441.
156. Martin-Padura, I., et al., *Junctional adhesion molecule, a novel member of the immunoglobulin superfamily that distributes at intercellular junctions and modulates monocyte transmigration.* Journal of Cell Biology, 1998. **142**(1): p. 117-127.
157. Tomko, R.P., et al., *Expression of the adenovirus receptor and its interaction with the fiber knob.* Experimental Cell Research, 2000. **255**(1): p. 47-55.
158. Fallon, M.B., A. Mennone, and J.M. Anderson, *ALTERED EXPRESSION AND LOCALIZATION OF THE TIGHT JUNCTION PROTEIN ZO-1 AFTER*

COMMON BILE-DUCT LIGATION. American Journal of Physiology, 1993. **264**(6): p. C1439-C1447.
159. Stevenson, B.R., et al., *IDENTIFICATION OF ZO-1 - A HIGH-MOLECULAR-WEIGHT POLYPEPTIDE ASSOCIATED WITH THE TIGHT JUNCTION (ZONULA OCCLUDENS) IN A VARIETY OF EPITHELIA.* Journal of Cell Biology, 1986. **103**(3): p. 755-766.
160. Willott, E., et al., *LOCALIZATION AND DIFFERENTIAL EXPRESSION OF 2 ISOFORMS OF THE TIGHT JUNCTION PROTEIN ZO-1.* American Journal of Physiology, 1992. **262**(5): p. C1119-C1124.
161. Balda, M.S. and J.M. Anderson, *2 CLASSES OF TIGHT JUNCTIONS ARE REVEALED BY ZO-1 ISOFORMS.* American Journal of Physiology, 1993. **264**(4): p. C918-C923.
162. Jesaitis, L.A. and D.A. Goodenough, *MOLECULAR CHARACTERIZATION AND TISSUE DISTRIBUTION OF ZO-2, A TIGHT JUNCTION PROTEIN HOMOLOGOUS TO ZO-1 AND THE DROSOPHILA DISKS-LARGE TUMOR-SUPPRESSOR PROTEIN.* Journal of Cell Biology, 1994. **124**(6): p. 949-961.
163. Lora, L., et al., *Hepatocyte tight-junctional permeability is increased in rat experimental colitis.* Gastroenterology, 1997. **113**(4): p. 1347-1354.
164. Zhong, Y., et al., *MONOCLONAL-ANTIBODY 7H6 REACTS WITH A NOVEL TIGHT JUNCTION-ASSOCIATED PROTEIN DISTINCT FROM ZO-1, CINGULIN AND ZO-2.* Journal of Cell Biology, 1993. **120**(2): p. 477-483.
165. Sakisaka, S., et al., *Alterations in tight junctions differ between primary biliary cirrhosis and primary sclerosing cholangitis.* Hepatology, 2001. **33**(6): p. 1460-1468.
166. Martin, P.E.M. and W.H. Evans, *Incorporation of connexins into plasma membranes and gap junctions.* Cardiovascular Research, 2004. **62**(2): p. 378-387.
167. Musil, L.S., et al., *Regulation of connexin degradation as a mechanism to increase gap junction assembly and function.* Journal of Biological Chemistry, 2000. **275**(33): p. 25207-25215.
168. Fischer, R., et al., *Intercellular communication via gap junctions in activated rat hepatic stellate cells.* Gastroenterology, 2005. **128**(2): p. 433-448.
169. Paul, D.L., *MOLECULAR-CLONING OF CDNA FOR RAT-LIVER GAP JUNCTION PROTEIN.* Journal of Cell Biology, 1986. **103**(1): p. 123-134.
170. Kumar, N.M. and N.B. Gilula, *CLONING AND CHARACTERIZATION OF HUMAN AND RAT-LIVER CDNAS CODING FOR A GAP JUNCTION PROTEIN.* Journal of Cell Biology, 1986. **103**(3): p. 767-776.
171. Nicholson, B., et al., *2 HOMOLOGOUS PROTEIN-COMPONENTS OF HEPATIC GAP-JUNCTIONS.* Nature, 1987. **329**(6141): p. 732-734.
172. Zhang, J.T. and B.J. Nicholson, *SEQUENCE AND TISSUE DISTRIBUTION OF A 2ND PROTEIN OF HEPATIC GAP-JUNCTIONS, CX26, AS DEDUCED FROM ITS CDNA.* Journal of Cell Biology, 1989. **109**(6): p. 3391-3401.
173. Alexander, D.B. and G.S. Goldberg, *Transfer of biologically important molecules between cells through gap junction channels.* Current Medicinal Chemistry, 2003. **10**(19): p. 2045-2058.
174. Hoschuetzky, H., H. Aberle, and R. Kemler, *BETA-CATENIN MEDIATES THE INTERACTION OF THE CADHERIN CATENIN COMPLEX WITH EPIDERMAL*

GROWTH-FACTOR RECEPTOR. Journal of Cell Biology, 1994. **127**(5): p. 1375-1380.
175. Matter, K. and M.S. Balda, *Signalling to and from tight junctions.* Nature Reviews Molecular Cell Biology, 2003. **4**(3): p. 225-236.
176. Nelson, W.J., *Regulation of cell-cell adhesion by the cadherin-catenin complex.* Biochemical Society Transactions, 2008. **36**: p. 149-155.
177. Bryant, D.M., et al., *EGF induces macropinocytosis and SNX1-modulated recycling of E-cadherin.* Journal of Cell Science, 2007. **120**(10): p. 1818-1828.
178. Behrens, J., et al., *DISSOCIATION OF MADIN-DARBY CANINE KIDNEY EPITHELIAL-CELLS BY THE MONOCLONAL-ANTIBODY ANTI-ARC-1 - MECHANISTIC ASPECTS AND IDENTIFICATION OF THE ANTIGEN AS A COMPONENT RELATED TO UVOMORULIN.* Journal of Cell Biology, 1985. **101**(4): p. 1307-1315.
179. Gonzalezmariscal, L., B.C. Deramirez, and M. Cereijido, *TIGHT JUNCTION FORMATION IN CULTURED EPITHELIAL-CELLS (MDCK).* Journal of Membrane Biology, 1985. **86**(2): p. 113-125.
180. Gumbiner, B. and K. Simons, *A FUNCTIONAL ASSAY FOR PROTEINS INVOLVED IN ESTABLISHING AN EPITHELIAL OCCLUDING BARRIER - IDENTIFICATION OF A UVOMORULIN-LIKE POLYPEPTIDE.* Journal of Cell Biology, 1986. **102**(2): p. 457-468.
181. Balda, M.S., et al., *ASSEMBLY AND SEALING OF TIGHT JUNCTIONS - POSSIBLE PARTICIPATION OF G-PROTEINS, PHOSPHOLIPASE-C, PROTEIN-KINASE-C AND CALMODULIN.* Journal of Membrane Biology, 1991. **122**(3): p. 193-202.
182. Dealmeida, J.B., et al., *TARGETING OF CHIMERIC G-ALPHA(I) PROTEINS TO SPECIFIC MEMBRANE DOMAINS.* Journal of Cell Science, 1994. **107**: p. 507-515.
183. Dodane, V. and B. Kachar, *Identification of isoforms of G proteins and PKC that colocalize with tight junctions.* Journal of Membrane Biology, 1996. **149**(3): p. 199-209.
184. Denker, B.M., et al., *Involvement of a heterotrimeric G protein alpha subunit in tight junction biogenesis.* Journal of Biological Chemistry, 1996. **271**(42): p. 25750-25753.
185. Meyer, T.N., C. Schwesinger, and B.M. Denker, *Zonula occludens-1 is a scaffolding protein for signaling molecules - G alpha(12) directly binds to the Src homology 3 domain and regulates paracellular permeability in epithelial cells.* Journal of Biological Chemistry, 2002. **277**(28): p. 24855-24858.
186. Durer, U., et al., *TFF3 and EGF induce different migration patterns of intestinal epithelial cells in vitro and trigger increased internalization of E-cadherin.* Cellular Physiology and Biochemistry, 2007. **20**(5): p. 329-346.
187. Kim, S.H. and T. Akaike, *Epidermal growth factor signaling for matrix-dependent cell proliferation and differentiation in primary cultured hepatocytes.* Tissue Engineering, 2007. **13**(3): p. 601-609.
188. Tobe, S., et al., *Tissue Reconstruction in Primary Cultured Rat Hepatocytes on Asialoglycoprotein Model Polymer.* Artificial Organs, 1992. **16**(5): p. 526-532.

189. Tobe, S., et al., *Receptor-mediated formation of multilayer aggregates of primary cultured adult rat hepatocytes on lactose-substituted polystyrene.* Biochemical and Biophysical Research Communications, 1992. **184**(1): p. 225-230.
190. Kojima, T., et al., *Inhibition of MAP kinase activity moderates changes in expression and function of Cx32 but not claudin-1 during DNA synthesis in primary cultures of rat hepatocytes.* Medical Electron Microscopy, 2004. **37**(2): p. 101-113.
191. Kojima, T., et al. *Role of the p38 MAP-kinase signaling pathway for Cx32 and claudin-1 in the rat liver.* 2003: Taylor & Francis Ltd.
192. Yamamoto, T., et al., *p38 MAP-kinase regulates function of gap and tight junctions during regeneration of rat hepatocytes.* Journal of Hepatology, 2005. **42**(5): p. 707-718.
193. Kojima, T.L., et al., *Different changes in expression and function of connexin 26 and connexin 32 during DNA synthesis and redifferentiation in primary rat hepatocytes using a DMSO culture system.* Hepatology, 1997. **26**(3): p. 585-597.
194. Takaki, Y., et al., *Dynamic changes in protein components of the tight junction during liver regeneration.* Cell and Tissue Research, 2001. **305**(3): p. 399-409.
195. Michalopoulos, G.K., *Liver regeneration.* Journal of Cellular Physiology, 2007. **213**(2): p. 286-300.
196. Diez, J.A., M. Elvira, and A. Villalobo, *The epidermal growth factor receptor tyrosine kinase phosphorylates connexin32.* Molecular and Cellular Biochemistry, 1998. **187**(1-2): p. 201-210.
197. Imamura, M., et al., *Oncostatin M induces upregulation of claudin-2 in rodent hepatocytes coinciding with changes in morphology and function of tight junctions.* Experimental Cell Research, 2007. **313**(9): p. 1951-1962.
198. Perez, L.M., et al. *Oxidative stress induces actin-cyto skeletal and tight-junctional alterations in hepatocytes by a Ca2+-dependent, PKC-mediated mechanism: Protective effect of PKA.* 2006: Elsevier Science Inc.
199. Fassett, J., D. Tobolt, and L.K. Hansen, *Type I collagen structure regulates cell morphology and EGF signaling in primary rat hepatocytes through cAMP-dependent protein kinase A.* Molecular Biology of the Cell, 2006. **17**(1): p. 345-356.
200. Raimondi, F., et al., *Bile acids modulate tight junction structure and barrier function of Caco-2 monolayers via EGFR activation.* American Journal of Physiology-Gastrointestinal and Liver Physiology, 2008. **294**(4): p. G906-G913.
201. Suzuki, T., A. Seth, and R. Rao, *Role of phospholipase C gamma-induced activation of protein kinase C epsilon (PKC epsilon) and PKC beta I in epidermal growth factor-mediated protection of tight junctions from acetaldehyde in caco-2 cell monolayers.* Journal of Biological Chemistry, 2008. **283**(6): p. 3574-3583.
202. Flores-Benitez, D., et al., *Control of tight junctional sealing: role of epidermal growth factor.* American Journal of Physiology-Renal Physiology, 2007. **292**(2): p. F828-F836.
203. Basuroy, S., et al., *Acetaldehyde disrupts tight junctions and adherens junctions in human colonic mucosa: protection by EGF and L-glutamine.* American Journal of Physiology-Gastrointestinal and Liver Physiology, 2005. **289**(2): p. G367-G375.

204. Bi, Y.A., D. Kazolias, and D.B. Duignan, *Use of cryopreserved human hepatocytes in sandwich culture to measure hepatobiliary transport.* Drug Metabolism and Disposition, 2006. **34**(9): p. 1658-1665.
205. Lengyel, G., et al., *Canalicular and sinusoidal disposition of bilirubin mono- and diglucuronides in sandwich-cultured human and rat primary hepatocytes.* Drug Metabolism and Disposition, 2005. **33**(9): p. 1355-1360.
206. Lecluyse, E.L., K.L. Audus, and J.H. Hochman, *FORMATION OF EXTENSIVE CANALICULAR NETWORKS BY RAT HEPATOCYTES CULTURED IN COLLAGEN-SANDWICH CONFIGURATION.* American Journal of Physiology, 1994. **266**(6): p. C1764-C1774.
207. Michalopoulos, G.K., et al., *Comparative analysis of mitogenic and morphogenic effects of HGF and EGF on rat and human hepatocytes maintained in collagen gels.* Journal of Cellular Physiology, 1993. **156**(3): p. 443-452.
208. Liu, X.R., et al., *Correlation of biliary excretion in sandwich-cultured rat hepatocytes and in vivo in rats.* Drug Metabolism and Disposition, 1999. **27**(6): p. 637-644.
209. Liu, X.R., et al. *Biliary excretion in primary rat hepatocytes cultured in a collagen-sandwich configuration.* 1999: Amer Physiological Soc.
210. Hoffmaster, K., et al., *P-glycoprotein Expression, Localization, and Function in Sandwich-Cultured Primary Rat and Human Hepatocytes: Relevance to the Hepatobiliary Disposition of a Model Opioid Peptide.* Pharmaceutical Research, 2004. **21**(7): p. 1294-1302.
211. Hoffmaster, K.A., et al., *Hepatobiliary Disposition of the Metabolically Stable Opioid Peptide [D-Pen2, D-Pen5]-Enkephalin (DPDPE): Pharmacokinetic Consequences of the Interplay between Multiple Transport Systems.* J Pharmacol Exp Ther, 2004. **311**(3): p. 1203-1210.
212. Annaert, P.P., et al., *P-glycoprotein-mediated in vitro biliary excretion in sandwich-cultured rat hepatocytes.* Drug Metabolism and Disposition, 2001. **29**(10): p. 1277-1283.
213. Turncliff, R.Z., P.J. Meier, and K.L.R. Brouwer, *EFFECT OF DEXAMETHASONE TREATMENT ON THE EXPRESSION AND FUNCTION OF TRANSPORT PROTEINS IN SANDWICH-CULTURED RAT HEPATOCYTES.* Drug Metab Dispos, 2004. **32**(8): p. 834-839.
214. Turncliff, R.Z., X. Tian, and K.L.R. Brouwer, *Effect of culture conditions on the expression and function of Bsep, Mrp2, and Mdr1a/b in sandwich-cultured rat hepatocytes.* Biochemical Pharmacology, 2006. **71**(10): p. 1520-1529.
215. Zamek-Gliszczynski, M.J., et al., *Pharmacokinetics of 5 (and 6)-carboxy-2 ',7 '-dichlorofluorescein and its diacetate promoiety in the liver.* Journal of Pharmacology and Experimental Therapeutics, 2003. **304**(2): p. 801-809.
216. Annaert, P.P. and K.L.R. Brouwer, *Assessment of drug interactions in hepatobiliary transport using rhodamine 123 in sandwich-cultured rat hepatocytes.* Drug Metabolism and Disposition, 2005. **33**(3): p. 388-394.
217. Berthiaume, F., et al., *Effect of extracellular matrix topology on cell structure, function, and physiological responsiveness: Hepatocytes cultured in a sandwich configuration.* Faseb Journal, 1996. **10**(13): p. 1471-1484.

218. Moghe, P.V., et al., *Culture matrix configuration and composition in the maintenance of hepatocyte polarity and function.* Biomaterials, 1996. **17**(3): p. 373-385.
219. Kostrubsky, V.E., et al., *Evaluation of hepatotoxic potential of drugs by inhibition of bile-acid transport in cultured primary human hepatocytes and intact rats.* Toxicological Sciences, 2003. **76**(1): p. 220-228.
220. Musat, A.I., et al., *REESTABLISHMENT OF CELL POLARITY OF RAT HEPATOCYTES IN PRIMARY CULTURE.* Hepatology, 1993. **18**(1): p. 198-205.
221. Dunn, J.C., et al., *Hepatocyte function and extracellular matrix geometry: long-term culture in a sandwich configuration [published erratum appears in FASEB J 1989 May;3(7):1873].* FASEB J., 1989. **3**(2): p. 174-177.
222. Michalopoulos, G.K., et al., *Hepatocytes undergo phenotypic transformation to biliary epithelium in organoid cultures.* Hepatology, 2002. **36**(2): p. 278-283.
223. Michalopoulos, G.K., et al., *Histological organization in hepatocyte organoid cultures.* American Journal of Pathology, 2001. **159**(5): p. 1877-1887.
224. Abu-Absi, S.F., et al., *Structural polarity and functional bile canaliculi in rat hepatocyte spheroids.* Experimental Cell Research, 2002. **274**(1): p. 56-67.
225. Sivaraman, A., *A microfabricated 3D tissue engineered "Liver on a Chip" : High information content assays for in vitro drug metabolism studies*, in *Chemical Engineering*. 2004, Massachusetts Institute of Technology: Cambridge. p. 228.
226. Inman, S.W., *Development of a high throughput 3D perfused liver tissue bioreactor*, in *Mechanical Engineering*. 2006, Massachusetts Institute of Technology: Cambridge. p. 178.
227. De Smet, K., et al., *Effects of epidermal growth factor on CYP inducibility by xenobiotics, DNA replication, and caspase activations in collagen I gel sandwich cultures of rat hepatocytes.* Biochemical Pharmacology, 2001. **61**(10): p. 1293-1303.
228. LeCluyse, E., et al., *Expression and regulation of cytochrome P450 enzymes in primary cultures of human hepatocytes.* Journal of Biochemical and Molecular Toxicology, 2000. **14**(4): p. 177-188.
229. Luttringer, O., et al., *Influence of isolation procedure, extracellular matrix and dexamethasone on the regulation of membrane transporters gene expression in rat hepatocytes.* Biochemical Pharmacology, 2002. **64**(11): p. 1637-1650.
230. Powers, M.J., et al., *Functional Behavior of Primary Rat Liver Cells in a Three-Dimensional Perfused Microarray Bioreactor.* Tissue Engineering, 2002. **8**(3): p. 499-513.
231. Powers, M.J., et al., *A microfabricated array bioreactor for perfused 3D liver culture.* Biotechnology and Bioengineering, 2002. **78**(3): p. 257-269.
232. Smith, P.K., et al., *Measurement of protein using bicinchoninic acid.* Analytical Biochemistry, 1985. **150**(1): p. 76-85.
233. Ren, P., et al., *ENHANCEMENT OF LIVER-CELL GAP JUNCTION PROTEIN EXPRESSION BY GLUCOCORTICOIDS.* Carcinogenesis, 1994. **15**(9): p. 1807-1813.
234. Wanson, J.C., et al., *ADULT RAT HEPATOCYTES IN PRIMARY MONOLAYER-CULTURE - ULTRASTRUCTURAL CHARACTERISTICS OF INTERCELLULAR*

CONTACTS AND CELL-MEMBRANE DIFFERENTIATIONS. Journal of Cell Biology, 1977. **74**(3): p. 858-877.
235. Theard, D., et al., *Cell polarity development and protein trafficking in hepatocytes lacking E-cadherin/beta-catenin-based adherens junctions.* Molecular Biology of the Cell, 2007. **18**(6): p. 2313-2321.
236. Bramow, S., et al., *Cholestasis and regulation of genes related to drug metabolism and biliary transport in rat liver following treatment with cyclosporine A and sirolimus (Rapamycin).* Pharmacology & Toxicology, 2001. **89**(3): p. 133-139.
237. Hung, D.Y., et al., *Hepatic pharmacokinetics of taurocholate in the normal and cholestatic rat liver.* Br J Pharmacol, 2005. **145**(1): p. 57-65.
238. Torok, E., et al. *Morphological and functional analysis of rat hepatocyte spheroids generated on poly(L-lactic acid) polymer in a pulsatile flow bioreactor.* 2006: Mary Ann Liebert Inc.
239. Woodford, F.P., *Enlargement of taurocholate micelles by added cholesterol and monoolein: self-diffusion measurements.* J. Lipid Res., 1969. **10**(5): p. 539-545.
240. Dickins, M. and R.E. Peterson, *EFFECTS OF A HORMONE-SUPPLEMENTED MEDIUM ON CYTOCHROME-P-450 CONTENT AND MONO-OXYGENASE ACTIVITIES OF RAT HEPATOCYTES IN PRIMARY CULTURE.* Biochemical Pharmacology, 1980. **29**(9): p. 1231-1238.
241. Domansky K, I.W., Serdy J, Griffith L, *Perfused microreactors for liver tissue engineering.* Conf Proc IEEE Eng Med Biol Soc, 2005. **7**: p. 7490-2.
242. Princen, H.M.G., et al., *CYCLOSPORINE-A BLOCKS BILE-ACID SYNTHESIS IN CULTURED-HEPATOCYTES BY SPECIFIC-INHIBITION OF CHENODEOXYCHOLIC ACID SYNTHESIS.* Biochemical Journal, 1991. **275**: p. 501-505.
243. Wolf, A., et al., *Cyclosporine A-induced oxidative stress in rat hepatocytes.* Journal of Pharmacology and Experimental Therapeutics, 1997. **280**(3): p. 1328-1334.
244. Nitta, M., et al., *CPF: An orphan nuclear receptor that regulates liver-specific expression of the human cholesterol 7 alpha-hydroxylase gene.* Proceedings of the National Academy of Sciences of the United States of America, 1999. **96**(12): p. 6660-6665.
245. Domansky, K., et al., *Perfused microreactors for liver tissue engineering.* Conf Proc IEEE Eng Med Biol Soc, 2005. **7**: p. 7490-2.
246. Scheving, L.A., et al., *The emergence of ErbB2 expression in cultured rat hepatocytes correlates with enhanced and diversified EGF-mediated signaling.* American Journal of Physiology-Gastrointestinal and Liver Physiology, 2006. **291**(1): p. G16-G25.
247. Hayashi, H. and Y. Sugiyama, *Short-Chain Ubiquitination Is Associated with the Degradation Rate of a Cell-Surface-Resident Bile Salt Export Pump (BSEP/ABCB11).* Mol Pharmacol, 2009. **75**(1): p. 143-150.
248. Uchida, K., et al., *Effect of partial ileal bypass on cholesterol and bile acid metabolism in rats.* Yonago Acta Medica, 2001. **44**(1): p. 69-77.

249. Kulakowski, E.C. and J. Maturo, *HYPOGLYCEMIC PROPERTIES OF TAURINE - NOT MEDIATED BY ENHANCED INSULIN RELEASE.* Biochemical Pharmacology, 1984. **33**(18): p. 2835-2838.
250. You, J.S. and K.J. Chang. *Taurine protects the liver against lipid peroxidation and membrane disintegration during rat hepatocarcinogenesis.* 1998: Plenum Press Div Plenum Publishing Corp.
251. Kouzuki, H., et al., *Contribution of sodium taurocholate co-transporting polypeptide to the uptake of its possible substrates into rat hepatocytes.* Journal of Pharmacology and Experimental Therapeutics, 1998. **286**(2): p. 1043-1050.

Appendices: Protocols and Detailed Experimental Methods

Appendix 1 – Isolation and Viability Assessment of Primary Rat Hepatocytes

I Preparation

(Prepare these items at LEAST a day in advance of the perfusion)

Perfusion Kit

Materials

- Tray and Cover
- Scalpel Holder
- 1 pair of Tissue Forceps
- 2 pairs of Small Tooth Curved Forceps (VWR 25601-010)
- Hemostat (Henry Schein 100-2376)
- Small Scissors
- Q-Tips (Puritan)
- Nu Gauze 2x2in, 4 ply (Johnson&Johnson via VWR #7632)
- Ethicon™ Silk – 4 Strands of 4-0 Silk (VWR 25942-249)
- Blue Paper
- 100μm Nytex Filter
- Funnel

Method:

1. Place 100μm Filter on Funnel, tape edges of filter to funnel with autoclave tape, and Wrap in Blue Paper. Seal with autoclave tape.
2. Assemble and Wrap Kit in Blue Paper.
3. AUTOCLAVE DRY Cycle 45 : 15

Ca^{2+} Free Buffer (1L)

Materials	Qty	Notes
Milli-Q Water	1L	
NaCl	8.3g	Sterile Perfusion Stock
KCl	0.5g	Sterile Perfusion Stock
Hepes	2.383g	Sterile Perfusion Stock
NaOH	2 Tabs	

Method:

1. Mix together in a Sterile, Autoclaved Bottle. Use a stir bar.
2. Ensure that the NaOH Tabs have fully dissolved
3. Adjust pH to 7.45 – 7.5 with 1N NaOH or HCl

Notes:

1. Use chemicals on Perfusion Bench

2. Keep these chemicals Sterile! Do not put excess chemicals back into the original container, use a new scooper for each chemical

10X $CaCl_2(H_2O)_2$ Solution

Materials	Qty	Notes
Milli-Q Water		
$CaCl_2(H_2O)_2$	6.36g/L	

DAG

Materials	Qty	Notes
DMEM	500mL (one bottle)	
BSA	1g	
Gentamicin	500µL (one aliquot)	
500mL Sterile filter unit		0.2µm pore size, Nalgene

Method:

1. Measure 1g BSA
2. Pour BSA into DMEM bottle and gently swirl until suspended – wait until BSA is completely dissolved
3. Put DMEM + BSA, filter unit, and gentamicin into TC room hood.
4. Vacuum filter
5. Add gentamicin and swirl solution.
6. Aliquot into 50mL centrifuge tubes (one 30mL aliquot for every four 40mL aliquots)

II Perfusion Apparatus Setup

Peristaltic Pump

Materials

- Pump
- Masterflex™ Tubing
  - Small (96410-14)
  - Slightly Larger (96410-16)

- 2 - 500mL Orange Cap Bottles filled with ~350mL 70% Ethanol
- 2 - 500mL Orange Cap Bottles
- Milli-Q Water

Method:

1. Prime the Pump by recirculating the attached 70% Ethanol for ~5min in each bottle at the highest flow rate (86mL/min). Ensure that the bubble trap fills and empties.
2. Remove lines from Ethanol and allow each line to air dry for ~5min or longer. Save and Recap the Ethanol bottles.
3. Run 200-400mL of Milli-Q water through each line using a clean 500mL "Rinse"

Bottle and a 500mL "Waste" Bottle. Ensure that the bubble trap fills.

4. Remove lines and allow the lines to air dry until the perfusion time (86mL/min).

Notes:

- The 70% Ethanol should be changed once every 3 weeks. Make a note of when it is changed on the Rat Logbook Sheet.
- You can reuse the "Rinse" and "Waste" bottles. Just rinse and shake them with ~100mL Milli-Q water a few times, and recap them for next time.

Rat and Animal House

Notes:

- Call the DCM office (x3-3050) and request 1-2mL of Pentobarbitol, or leave a message.
- Bring Key Card and the rat room key.
- Update and Initial the Green Rat Inventory Sheet outside the Rat Room
- Note Rat Weight (160-230 g)
- Get Pentobarbitol

Water Bath

Materials

- Milli-Q Water (ddH_2O)
- Celsius Thermometer
- 1 Sterile 500mL Orange Cap Bottle
- 250mL Graduated Cylinder
- 50mL Graduated Cylinder
- 375mL Ca^{2+} Free Solution
- 2 Red Water Bath Weights
- Filter Flask, 0.2μm Nalgene

Methods

1. Set bath Temperature to 43^{0} C

2. Sterile Filter 250mL of Ca^{2+}-Free Buffer through a 0.2μM filter and place in bath.

Connect the filter solution to the pump and fill up the bubble trap.

3. Prepare Blendzyme 3 Solution. The aliquot of Blendzyme 3 should thaw and be kept on ice until it's ready to be added to its solution.

Notes:

- The 43^{O} C provides for a 37^{O} C liquid temperature through the catheter.

Liberase Blendzyme 3 Preparation

Reconstitution:

70mg bottle

1. Add 10mL HPLC quality H_2O
2. On ice, let powder rehydrate for 30min. Mix occasionally by swirling.
3. Aliquot into 1mL centrifuge tubes [715uL each = 5mg]
4. Makes approximately 13-14 aliquots
5. Save extra little bit in a separate tube
6. Label with info: Name, 5mg, date of aliquot, lot#, volume

Materials:
- 28mL 10X $CaCl_2(H_20)_2$ Solution
- 222mL Ca^{2+} Free Buffer
- Filter Flask, 0.2μm (Nalgene)

Materials	Qty	Notes
Ca^{2+} Free Buffer	222mL	
10X $CaCl_2(H_20)_2$	28mL	
Roche Liberase Blendzyme 3	5mg	Cat# 1814184

Method:
1. Combine Ca^{2+} Free Buffer and 10X $CaCl_2$ Solution in a sterile 500mL Orange top bottle.
2. Place in water bath until needed
3. AT THE APPROPRIATE TIME (mentioned later)
   Add Blendzyme 3 to the 250mL of solution
4. Sterile Filter (0.2μm) and place in bath. Attach to the pump.

III Perfusion

Animal Preparation

Materials
- Male Fisher Rat (160-230g)
- 1.25" 20 Gauge Polyethylene Catheter-JELCO, Johnson and Johnson
- 2 1mL Syringes (Becton Dickinson-VWR #309602)
- 1 "Blue" 25G Needle (Becton Dickinson-VWR #305122)
- Sodium Pentobarbitol
- Phosphate Buffered Saline (PBS)
- DecapiCone™
- Procedure Board, Covered with Blue Paper
- Autoclave Tape
- Hair Clippers
- Dust Buster™
- Gauze
- 70% Ethanol
- Betadine

Method:

1. Using a "Blue" 25G Needle anaesthetize rat with Na-Pentobarbitol according to animal weight, diluted with an equal volume of 1x PBS. Inject into the intraperitoneal (IP), just to the left of the midline. Pull back on the plunger and make sure there is a visible bubble to ensure that you are in the body cavity and not in the bladder, intestine, etc.
2. *As soon as the rat shows no reflexes to quick blows of air*, check the drug effect through tail pinches. Do not continue until the rat does not respond to the pinches. Pinching in between the toes is also a good indicator.
3. *Working Quickly*, shave the rat over the entire incision area.
4. Apply Betadine using gauze (Optional).
5. Secure the animal to the procedure board with autoclave tape.
   Fully extend the lower legs and tape them down
   Raise the upper legs and *gently* tape each arm separately.
8. Open the lid of the Surgical Kit *without* touching the inside of the kit or lid.
9. Carefully open the Catheter and 1mL Syringes onto the Surgical Kit without touching the instruments.

Notes:

- Refer back to the Rat Perfusion Logbook to check how much Pentobarbitol to inject given the weight of the rat.
- The most prominent Tail Pinch response is flexing of the abdominal muscles just above the lower legs. It's almost like a shiver.

The Perfusion

Materials:

- Surgical Gloves (Allegiance #2D7254)
- Sterile Gauze (Johnson&Johnson Nu-Gauze™)
  Silk (Ethicon)
  Q-Tips (Puritan)
- 2 Forceps (VWR)
- Tissue Forceps (Henry Schein)
- Scissors (Henry Schein)
- Additional Materials listed above

Method:

1. *From this point move as quickly as possible to maintain adequate blood pressure and to minimize the effects of other unforeseen events.*

2. Don surgical gloves. Keep these sterile to avoid contamination. Only touch the instruments within the Kit and the rat body. Do not touch anything else.

3. Make an "I" incision on the ventral side using the Tissue Forceps and Scissors. The incision should run from the lower abdominal area around the bladder to the Zyphoid

process and Rib area. Avoid nicking the liver. As you cut towards the ribs, you may have to gently massage liver through the skin to loosen it from the skin.
4. Gently displace the guts to the right with a fresh Q-Tip, exposing the Inferior Vena Cava (IVC) and Portal Vein (PV).

5. Using fresh, dry Q-Tips further expose the IVC inferior to the liver from the bladder region up to the liver. To do this, apply pressure to the connective tissue in opposite directions until the IVC is completely visible. Be sure not to hinder blood flow while you clear away the excess tissue.

6. Using the forceps, make openings in the connective tissue to the left and right of the IVC just above the branch to the kidney.

7. Pull a silk suture through the opening and tie a loose ligature around the IVC. To do this: grasp the right end of the silk with the left forceps and wrap it twice around the tip of the right forceps. Keeping hold of the right end, grasp the left end of the silk with the right forceps and pull it through the loops.

8. Insert Catheter into the IVC 0.5-1cm away from loose ligature. Remove metal piece and maneuver the catheter past the knot. If there is no blood flowing freely from the catheter, you may have to gently palpate the chest area to draw the blood down, or use a syringe to gently pull blood to the end of the catheter. Tightly tie off the loose ligature around the catheter.

9. Begin perfusing with Ca^{2+} Free Buffer at 25mL/min (15 mL/min to retrieve a greater fraction of NPCs). Immediately cut the Portal Vein (PV) to allow for drainage and prevent over-inflation of the liver. Cut the IVC below the Catheter.

10. Puncture the diaphragm to expose the IVC superior to the liver and tie a ligature around it using the same technique as before.

11. Check to make sure that fluid is freely flowing from the PV. If there is a clot, gently massage the PV until the flow resumes.

12. At this point prepare the Blendzyme 3 Solution. See **Blendzyme Preparation.**

13. Perfuse for 6 to 7 minutes. The liver should clear of blood. Gently roll the liver between two moist cotton swabs to help. The liver should be a light caramel color.

14. After the allotted time for the Calcium free buffer, switch over the Blendzyme solution and perfuse the entire 250mL volume. It should take about 10 minutes at 25mL/min.

15. Throughout the perfusion keep the liver moist by wetting a fresh Q-Tip with run-off buffer and gently dabbing the liver.

16. Remove the liver from the rat and place it in a 50mL Centrifuge Tube filled with 30mL DAG. Avoid cutting or poking other organs to prevent contamination.

V Hepatocyte Isolation

Materials:

- Ice Bucket
- DAG
- Pre-Autoclaved Funnel with 300μm mesh
- Trypan Blue
- Hemostat and tissue forceps

Methods:

1. Prepare an ice bucket with 4- 50mL centrifuge tubes filled with 40ml DAG.
2. Obtain the liver from the perfusionist. Also take with you a flat ice pack, an autoclaved funnel with 100-μm mesh, and a hemostat and tissue forceps with tips wrapped in sterile gauze.
3. In the hood, gently pour the liver with 30ml DAG into a 100mm Petri dish. Use the hemostat and forceps to peel back the capsule on each lobe.
4. Use the hemostat to clamp down on the connective tissue of the liver, and gently agitate the liver by knocking the hinge part of the hemostat on the sidewall of the Petri dish. Your other hand should hold the Petri dish to prevent it from sliding off the ice pack which may become slippery due to condensation. Try to keep most of the liver submerged under liquid and pay attention not to squeeze the liver between the bottom of the dish and the tip of the hemostat. The tip of the hemostat should not touch the bottom of the dish.
5. Break more areas of the capsules if the liver is not breaking up well. Otherwise, when the solution looks like the color of caramel, the shaking should be enough.
6. Prepare a clean 50ml tube and place the funnel into it. Place the remains of the liver on the mesh with the hemostat. Use a pipette to transfer all liquid into the tube through the mesh.
7. Replace the liver in the Petri dish and wash again with 40mL DAG to isolate all the cells you can. Filter this as before into another 50mL tube.
8. Dispose of the mesh and the liver remains. Equilibrate the two tubes by pouring the liquid back and forth between the two tubes. Pour down the walls of the tube to minimize stress to cells.
9. Spin the two cone tubes of cell solution at 50g for 3 minutes at 4°C.
10. Remove supernatant (save it if NPC's are needed). Re-suspend the cell pellets with fresh DAG, 40mL per tube. Carefully pour each tube of DAG into the tubes with the cell pellet. Be careful not to let liquid directly land on top of the pellets. Tilt both tubes so that the liquid is flowing slowly on the tube wall. After both 40ml tubes of DAG are transferred, cap the tube with cells and start re-suspending cells by rocking both tubes gently. Do this until the pellet is completely in suspension.
11. Spin again at 50g for 3 minutes at 4°C.

12. During this spin, prepare the Trypan blue: 700uL DAG, 200ul Trypan blue. Or, if using Vi-Cell Coulter Counter make a 1:10 dilution of the cells suspension by pipetting 900uL of DAG, and 100uL of the final cell solution.
13. Remove supernatant (save it if NPC's are needed). Re-suspend each cell pellet with 20mL of fresh DAG. Make sure that when pipetting in the liquid, the liquid flows slowly on the wall instead of hitting the pellets directly. Pour one tube of solution into the other to consolidate down to one tube (about 45mL total).
14. Take 100μm from the tube and place it into the Trypan blue tube. Use the hemacytometer to count the cell viability and cell concentration as the first final count. Count all 8 squares.
15. Record on the Hepatocyte count document and save under the date.

VI Troubleshooting

Working Quickly

- Working quickly during the preparation of the rat, and the surgery up to the time of perfusion will help minimize the effects of, for example, the rat dying. It will also help with issues related to blood pressure, and the length of time the liver is exposed to air.
- After the Perfusion has started, quickly cut the Portal Vein to prevent over-inflation of the liver, which can cause cell damage.

Rat Dies

1. Working quickly should minimize the effects of premature rat death. Try to perfuse as soon as possible.
2. Gently palpate the upper abdominal region, near the ribs, to help resuscitate the rat.
3. Be aware that the perfusion with Ca^{2+} Free Buffer may take longer to fully clear out the Red Blood Cells and to become a caramel color.
4. Try to keep the liver moist on the outside by wetting Q-Tips with run-off buffer and gently dabbing the liver.

IVC Catheter Insertion and Placement

- **Insertion**: Keep the catheter parallel to the IVC. Keep the bevel up, and the catheter as horizontal as possible, as to not poke all the way through the vein. Once inserted, **gently** push the catheter further into the vein until the plastic portion of the catheter is just in the vein. Avoid twisting the catheter because you may accidentally create new hole in the IVC. Try to create opposing tension by pulling the IVC downward with a Q-tip. Position the Q-tip on the muscle to the left or right of the IVC and apply gently pressure. This will anchor the IVC a little and make it less apt to stretch as you try to cannulate. Once you remove the metal part, you should feel no resistance at all, and the catheter should readily slip into the vein when you apply even the slightest pressure. Do not push the metal needle of the catheter into the vein more than you need to; once the white plastic is visible inside the vein, remove the needle while inserting the catheter farther up the IVC. Follow the IVC past the loose ligature.

Remember this is easier to do if you flex the catheter so you can see the tip through the top of the vein. The vein changes direction as it meet the liver, navigate the catheter accordingly. Note that the degree to which the IVC direction varies from rat to rat.

Portal Vein (PV) Perfusion

1. Expose the Portal Vein.

2. Tie a loose ligature around the Portal Vein, making sure it is located above any branches.

3. Make a small cut approximately 1/2 way through the portal vein. Be careful not to cut through the entire vein.

4. Insert Catheter into portal vein, while using gauze to control blood loss.

5. Remove Metal Portion of catheter and then slide catheter past ligature and tie it off. Connect the pump and start flow of **Ca^{2+} Free Solution** at **8mL/min.**

6. Immediately cut the IVC inferior to the liver to prevent over inflation.

7. Puncture the diaphragm to expose the IVC superior to the liver, then tie a ligature around it.

8. Inflate the liver occasionally by placing a Q-tip on the IVC. Do not over inflate.

9. Perfuse until the liver is cleared of blood.

10. Throughout the perfusion keep the liver moist by wetting a fresh Q-Tip with run-off buffer and gently dabbing he liver. Otherwise, there should be no need to touch the liver.

11. Perfusion with Blendzyme 3 Solution.

Isolation Information

- **Qualitative, Cell Count, and Viability information can be used in conjunction with one another to assess the effectiveness of the perfusion with Blendzyme 3.**
- **Qualitative information about how the liver "breaks up" during the isolation** can clue you into how effective the digestion with Blendzyme 3 was. It is generally good when the liver completely disintegrates, and there is little intact liver. If the liver does not readily disintegrate, the collagenase may not have run long enough to allow for proper separation of the cells.
- **Cell Counts:** High cell counts indicate good separation of the cells. This is usually accompanied by nearly complete disintegration of the liver during isolation. Low cell counts indicate that the perfusion may not have run long enough.

• **Viability:** Low viability may indicate that the cells were exposed to Pentobarbital for too long, the surgery took too long, that the Blendzyme was at a too high/low concentration, etc....

Appendix 2 – Culture Media Formulations for Primary Rat Hepatocytes

Seeding Hepatocyte Growth Medium (sHGM; first 2-3 hours of 2D sandwich culture)

Base Medium: Dulbecco's Modified Eagles Medium, low glucose, pyridoxine HCl, sodium pyruvate, no glutamine, no phenol red (GIBCO 11054-020)

Supplements and Modifications:

- 0.03 g/L L-Proline (SIGMA P-4655)
- 0.1 g/L L-Ornithine (SIGMA P-4655)
- 0.305 g/L Niacinamide (SIGMA P-4655)
- 2 g/L D-(+)-Glucose (2 g/L is added, 1 g/L is already present from supplier; SIGMA G-7021)
- 2 g/L D-(+)-Galactose (SIGMA G-5388)
- 54.4 μg/L $ZnCl_2$
- 75 μg/L $ZnSO_4 \cdot 7H_2O$
- 20 μg/L $CuSO_4 \cdot 5H_2O$
- 25 μg/L $MnSO_4$

Filter the above solution with Nalgene PES 0.2μm filter unit, before addition of following substances:

- 5% Fetal Bovine Serum (GIBCO 26140-111)
- 4 mg/L Insulin (SIGMA I1882)
- 1 μM Dexamethasone (10X amount in plating and modified hepatocyte growth medium; SIGMA D-8893)
- 1 mM L-Glutamine (GIBCO 25030-081)
- 50 mg/L Gentamicin (SIGMA G-1397)

Plating Hepatocyte Growth Medium (pHGM; from 2-3 hours post-seeding to 24 hours post-isolation)

- Seeding hepatocyte growth medium w/0.1 μM dexamethasone (all other supplements and additives are the same as sHGM)

Modified Hepatocyte Growth Medium (mHGM; from Day 1 until duration of culture)

Base Medium: Dulbecco's Modified Eagles Medium, low glucose, pyridoxine HCl, sodium pyruvate, no glutamine, no phenol red (GIBCO 11054-020)

Supplements and Modifications:

- 0.03 g/L L-Proline (SIGMA P-4655)
- 0.1 g/L L-Ornithine (SIGMA P-4655)

- 0.305 g/L Niacinamide (SIGMA P-4655)
- 2 g/L D-(+)-Glucose (2 g/L is added, 1 g/L is already present from supplier; SIGMA G-7021)
- 2 g/L D-(+)-Galactose (SIGMA G-5388)
- 2 g/L Essentially fatty acid free Bovine Serum Albumin (SIGMA A6003)
- 54.4 µg/L $ZnCl_2$
- 75 µg/L $ZnSO_4 \cdot 7H_2O$
- 20 µg/L $CuSO_4 \cdot 5H_2O$
- 25 µg/L $MnSO_4$

Filter the above solution with Nalgene PES 0.2µm filter unit, before addition of following substances:

- 5 mg/L Insulin/5 mg/L Transferrin/5 µg/L Sodium Selenite (ITS Cocktail; ROCHE 1074 547)
- 0.1 µM Dexamethasone (SIGMA D-8893)
- 1 mM L-Glutamine (GIBCO 25030-081)
- 50 mg/L Gentamicin (SIGMA G-1397)

Gentamicin and L-glutamine were aliquoted sterile and stored at -20°C and 4°C, respectively. ITS and dexamethasone had to be reconstituted, aliquoted, and stored at -20°C before addition to media in the following manner:

- **500µl Insulin-Transferrin-Sodium Selenite** (sterile); ROCHE 1074 547 5mg/l-5mg/l-5µg/l in medium; ROCHE 1074 547 (50mg); 1213 849 (250mg); dissolve 50mg or 250mg powder in 5ml or 25ml sterile milliQ water, dispense into 520µl aliquots, store at –20°C.
- **400µl Dexamethasone** (sterile); 0.1µM in medium; SIGMA D-8893, dissolve 1mg in 1ml EtOH using sterile syringe and needle, after powder is dissolved add 19ml sterile PBS, mix thoroughly, dispense into 420µl aliquots, store at –20°C, expires 3 months from date of reconstitution.

NOTE: Some culture media used contained 20ng/mL epidermal growth factor (or concentration as noted). Epidermal growth factor was reconstituted, aliquoted, and stored at -20°C before addition to media in the following manner:

- **200µl Epidermal Growth Factor (EGF)** (sterile); BD Biosciences 354001 20ng/ml in medium; dissolve 100ug powder in 2 ml sterile milliQ water, dispense into 220µl aliquots, store at –20°C, expires 3 months from date of reconstitution.

Appendix 3 – 2D Primary Rat Hepatocyte Sandwich Culture Protocols

Preparation of BD Biocoat™ Collagen Type I 24-well Plates

- Incubate BD Biocoat™ Collagen Type I 24-well plates with 350 µL per well of plating hepatocyte growth medium (pHGM) overnight in a 37°C, 5% CO_2, 95% humidity environment. Aspirate medium off plates immediately before seeding.
- Dilute primary rat hepatocytes from isolation in ice-cold seeding hepatocyte growth medium (sHGM) to a concentration of 10^6cells/mL, and add 350µL of this dilution to each well. Incubate plates at 37°C, 5% CO_2, 95% humidity immediately after seeding.
- 2-3 hours post-seeding, shake plates gently to remove non-adherent cells. Wash wells with 350µL of warm pHGM twice to remove non-adherent cells and incubate at 37°C, 5% CO_2, 95% humidity.

Preparation of Matrigel™ Overlay

- On Day 1 post-seeding, thaw Matrigel™ aliquots on ice and dilute to a protein concentration of 0.25 mg/mL in ice-cold modified hepatocyte growth medium (mHGM). Always use ice-cold pipette tips when pipetting Matrigel™. Store ice-cold pipette tips at -20°C.
- Shake plates very lightly to remove any non-adherent cells, and pipette 350µL of ice-cold Matrigel™ dilution to each well. Incubate plates at 37°C, 5% CO_2, 95% humidity immediately after adding ice-cold dilution to warm cells and recover them from thermal shock.
- Change medium with 350µL of warm mHGM every 24 hours for the duration of culture.

NOTE: Matrigel™ aliquots should be thawed on ice to avoid spontaneous gelling. To aliquot, Matrigel™ stock should put on ice and incubated at 4°C overnight to thaw. Matrigel™ should be aliquoted into eppendorf tubes stored at -20°C.

Materials

Product Description	Cat#	Supplier	Notes
2D BioCoat Collagen Type I 24-well plate	354408 (5/pack) 356408 (50/case)	BD Biosciences	
Matrigel Basement Membrane Matrix, Phenol-Red Free	356237	BD Biosciences	Usually on backorder; order with anticipation; use ice-cold tips and keep on ice always

Appendix 4 – Detailed Multiwell Reactor Assembly, Seeding, and Maintenance of Perfused 3D Cultures

Materials Required

- Reactor plate (1)
- Pneumatic plate (1)
- Peristaltic membrane (1)
- ¼" hex screws (29)
- Washers (29)
- 1/8" hex screws (4)
- Cover plate (2)
- Red membrane (2)
- Reactor lid (1)
- Retaining rings (24)
- Polycarbonate scaffold with 300μmX230μm (DIAXD) channels (12)
- 5μm Millipore filter, polycarbonate scaffold sized, punched out (24)
- Filter support (12)
- O-ring (12)
- Tweezers (1 pair sufficient, 2 pairs recommended)
- Plunger (1)
- Autoclaved blue paper (2 packs of 3 sheets minimum, packs of 5 sheets recommended)
- Single-unit docking station
- Reactor controller

Preparation of Multiwell Reactor

- Incubate polycarbonate scaffolds, o-rings, filter supports, retaining rings, reactor plate, pneumatic plate, screws, washers, tweezers, plunger and cover plates in 5% 7X solution for >1hr. **NOTE:** Incubate and sonicate plastic parts and metallic pieces separately.
- Sonicate parts for 10min in 5% 7X solution.
- Rinse 5X or more times with deionized water, sonicate 10min in deionized water.
- Rinse 3X with milliQ H_2O and sonicate 10min.
- Set down ~5 Kimwipes and lay down pneumatic plate to air dry. Sonicate all other parts in 70% EtOH for 10min. **NOTE:** Submersion of pneumatic plate in EtOH can cause the plate to crack.
- Using tweezers, place all parts and plates down on the Kimwipes to air dry.
- After all pieces air dry, autoclave o-rings, filter supports, retaining rings, screws, washers, tweezers, plungers, and blue autoclave paper. **NOTE:** DO NOT autoclave polycarbonate scaffolds, cover plates or pneumatic plate.
    - Punch out Millipore filters and autoclave them also.
    - Using pressurized air, make sure to dry the reactor plate completely, especially the pumping chambers and channels. Inspect plate under microscope to ensure all fluidic channels are clean. Autoclave plate.

- Using pressurized air, make sure to dry the pneumatic plate completely, especially all the fluidic channels. Do this many times until no more water all comes out from channels.

Assembly of Multiwell Reactor

- It is recommended to assemble the reactor the day prior to seeding to ensure the assembly is not leaking, however it is possible to assemble this plate on the seeding day.
- In a sterile cabinet, set autoclaved blue paper down on enough of its surface to allow for comfortable assembly of reactor. This surface should be considered sterile and should not be touched with glove.
- Soak a Kimwipe with 70% EtOH and use to wipe down pneumatic plate before putting plate in sterile cabinet. DO NOT spray pneumatic plate with EtOH as it may enter fluidic channels.
- Place reactor plate in sterile cabinet along with EtO sterilized peristaltic membrane and sterile reactor lid. Do not place reactor plate down on sterile paper. Grab plate by its sides, place reactor lid on reactor plate, and place plate down on lid. NEVER place bottom of plate (pumping chamber side) down on sterile paper.
- Place peristaltic membrane properly on reactor plate using guide pins, ensure no screw holes are covered by membrane and that the membrane is not folded. Place pneumatic plate over it. Screw plates together with ¼" hex screws and washers with a maximum torque of 16 lb-in on each screw. Inspect pumping chambers and ensure that every set of chambers is sealed from the other sets so that each reservoir/reactor pair will be fluidically isolated from each other and to reduce leaks. If a loose seal is apparent, tighter screws around chamber slightly until membrane becomes clear and seal is apparent.
- Place red membranes and cover plates over pneumatic indicators and screw them in with 1/8" hex screws. Dock multiwell reactor assembly in single-unit docking station.
- Add 300μL of warm seeding hepatocyte growth medium (sHGM) to each reservoir and run multiwell plate at a flow rate of 0.2 mL/min. Monitor reactor pair to ensure proper priming and check that air bubbles start to come out into the reactor pair within 90s±20% of priming being started.
- Add another 300μL of warm sHGM to each reservoir, run multiwell plate at a flow rate of 0.2 mL/min, and monitor reactor pair to make sure no air bubbles come through within 5 seconds of running media.
- Fill each reactor/reservoir pair up to the fill line with warm sHGM and incubate at 37°C, 5% CO_2, 95% humidity overnight. Look for leaks or lowering medium levels in reactor/reservoir pairs.

Preparation of Polycarbonate Scaffolds

- Sonicate scaffolds in 70% EtOH for 10 minutes to remove air bubbles from channels.
- Rinse scaffolds with 1X sterile PBS and place in a 30μg/mL rat tail collagen type I solution in 1X PBS (BD Biosciences, Cat# 354236). Remove any air bubbles

left in scaffolds by pipetting collagen solution into channels. Incubate scaffolds at 37°C, 5% CO_2, 95% humidity overnight (or at least 2 hours).

- Remove scaffolds from solution and let them air dry for 2 hours prior to seeding. Place scaffolds in sterile cabinet and put on 45° angle against the side and bottom of a 100mm Petri dish to air dry.

NOTE: ALWAYS use tweezers to handle scaffolds and all other reactor components.

Multiwell Reactor Seeding

- Incubate Millipore filters at RT for 30 minutes in a 1% BSA solution in 1X PBS.
- Stop flow on the multiwell reactor plate and place o-rings in each reactor well, and aspirate off air bubbles. Inspect reactor surface for trapped air bubble and use tweezers to try to coax them out. NOTE: Rinse all components in sterile PBS before placing in reactor.
- Place filter support in a 50mL Falcon tube and fill completely with sterile PBS, seal, remove from sterile cabinet and tap tube on table surface to remove all air bubbles from filter supports. Place filter supports in each reactor well, tamp down with tweezers, and aspirate air bubbles off.
- Place filters in each reactor and reservoir well ensuring that no air bubbles are trapped below it. Tamp down filters, and aspirate air bubbles off.
- Place retaining rings in each reservoir well and secured down until completely flat and against bottom of well with plunger. Make sure filters do not get crimped.
- Place scaffolds in each reactor well, tamped down, and aspirate off air bubbles. If scaffold is slightly concave, place scaffold concave down so that retaining ring will force scaffolds surface down.
- Place retaining rings in each reservoir well and secure down until completely flat and against bottom of well with plunger.
- Aspirated off medium and fill reservoir/reactor pairs to fill line with ice-cold sHGM.
- Aspirate medium completely off reservoir wells. Aspirate medium slightly off reactor wells to ensure there is no liquid bridge to reservoir pair.
- Turn on flow at a flow rate of 0.2 ml/min in a downward direction and seed 800,000 cells from isolation, evenly distributed, onto each scaffold. Do not dilute cell suspension before seeding. Fill each reactor/reservoir pair to fill line with ice-cold sHGM immediately after seeding and incubate multiwell reactor plate at 37°C, 5% CO_2, 95% humidity.
- Set reactor control so that flow will reverse into the upward direction 8 hours post-seeding.
- On Day 1 post-isolation, replace culture medium with warm mHGM. To do this, aspirate all medium from reservoir (careful not to aspirate medium from below filter), aspirate medium off from reactor well but do not allow level to fall below retaining ring level, aspirate all medium off sides and from reactor/reservoir bridge before filling reactor/reservoir pair with fresh warm mHGM to fill line. Replace culture medium every 1hr (do this 3X total on day 1) with warm HGM to minimize amount of FBS from sHGM left in culture. Replace culture medium with mHGM every 24 hours for duration of culture.

Appendix 5 – 2D Sandwich Culture Hepatobiliary Transport Studies Protocols

Materials Required

Product Description	Cat#	Supplier	Notes
Hanks' Balanced Salt Solution (HBSS); with $NaHCO_3$; without phenol red, $CaCl_2$, $MgSO_4$	H6648	Sigma	Order in 500 mL bottles and Ca-containing in 1 L bottles
HBSS; with $NaHCO_3$; without phenol red	H8264	Sigma	Order this buffer in 1L bottles
Ethylene glycol-bis(2-aminoethylether)-*N,N,N',N'*-tetraacetic acid (EGTA)	E0396	Sigma	
Taurocholic acid (TCA)	T4009	Sigma	
Digoxin	D6003	Sigma	
[^{3}H]-Taurocholic acid	NET322250UC	Perkin Elmer	Contact Radiation Protection Program to notify them of delivery
[^{3}H]-Digoxin	NET222250UC	Perkin Elmer	Contact Radiation Protection Program to notify them of delivery
5-(and-6)-carboxy-2',7'-dichlorofluorescein diacetate (CDFDA)	C-369	Molecular Probes (Invitrogen)	
RIPA buffer	R3792	Teknova	
Ultima Gold XR	6013111	Perkin Elmer	
MicroBCA protein assay kit	23235	Pierce Biotechnology	

Preparation of Buffers

- Ca^{2+}-free buffer
  - HBSS w/o $CaCl_2$, $MgSO_4$
  - 1μM EGTA
- Standard buffer
  - HBSS w/ $CaCl_2$, $MgSO_4$
- TCA solution
  - 1mM TCA in standard buffer
- [^{3}H]-TCA buffer
  - 0.1μM [^{3}H]-TCA
  - 9.9μM TCA (dilute from TCA solution)
  - Standard buffer

- [^{3}H]-digoxin buffer
    - 0.1μM [^{3}H]-digoxin
    - 0.9μM digoxin
    - Standard buffer
- CDFDA buffer
    - 2μM CDFDA
    - 1:1000 dilution Hoescht stain
    - Standard buffer

Hepatic Transport Study Assay

- Prepare and warm buffers before beginning. Put 45mL of standard buffer per 24-well plate assayed on ice before beginning.
- Wash each well 3X with 500μL of either warm standard or warm Ca^{2+}-free buffer. Incubate at 37°C, 5% CO_2, 95% humidity for 10min (or for desired pre-incubation time). Ca^{2+}-free buffer will disrupt canalicular networks in cultures while standard buffer will not.
- Wash each well 3X with 500μL warm standard buffer, add 500μL of either [^{3}H]-TCA buffer, [^{3}H]-digoxin buffer, or CDFDA buffer depending on species of interest. Incubate at 37°C, 5% CO_2, 95% humidity for 15min (or for desired accumulation time).
- For CDFDA studies: Image plates after incubation.
- For all other studies: wash each well 3X with 500μL ice-cold standard buffer. Completely aspirate off all buffer and add 200μL RIPA buffer to each well. Place on rocker for >20min to ensure cell lyses. If scintillation device is not available, or more studies will be conducted, seal plate with a strip of parafilm around edges of plate and store at 4°C.

Scintillation Counting

- Pipette 150μL of sample into a 4mL scintillation tube. Add 350μL RIPA buffer.
- Add 3.5mL of UltimaGold XR scintillation fluid to each tube. Cap and vortex for 5-10sec.
- Allow tubes to rest for ~10min, load tubes into scintillation racks and into a Beckman Coulter LS 6500 Multipurpose Scintillation Counter. Make sure automation labels are properly placed for the user number desired.
- Make sure user program is set to 2 min counting and set to detect ^{3}H scintillation.
- Conversion factor from counts per minute to pico Curies is 1.38pCi/cpm as experimentally determined from standard curve.

NOTE: Scintillation signal significantly diminishes after ~3-4hr of addition of scintillation fluid so do not do run more than ~80 samples at one time.

Total Protein Assay

- Dilute all samples 1:50 in MilliQ water (make 350μL of each dilution).
- Using the MicroBCA protein assay kit (Pierce Biotechnology), prepare protein standards using the 2mg/mL BSA stock ampoules. Prepare a 1:50 dilution of

RIPA buffer in MilliQ as diluent to prepare standards. Prepare dilutions of standards per 96-well plate to be assayed (23 samples) as follows:

Vial	Volume of diluent	Volume and source of BSA	Final BSA Concentration
A	450 µL	50 µL of stock	200 µg/mL
B	1.26 mL	315 µL of vial A dilution	40 µg/mL
C	175 µL	1.225 mL of vial B dilution	35 µg/mL
D	175 µL	1.05 mL of vial C dilution	30 µg/mL
E	175 µL	875 µL of vial D dilution	25 µg/mL
F	175 µL	700 µL of vial E dilution	20 µg/mL
G	175 µL	525 µL of vial F dilution	15 µg/mL
H	175 µL	350 µL of vial G dilution	10 µg/mL
I	175 µL	175 µL of vial H dilution	5 µg/mL
J	350 µL	0	0 µg/mL (blank)

- Prepare 12mL of MicroBCA working reagent per 96-well plate to be assayed. Keep reagent protected from light with aluminum foil. Prepare reagent as follows:
    - 6mL MicroBCA reagent MA
    - 5.76mL MicroBCA reagent MB
    - 240µL MicroBCA reagent MC
- Pipette 100µL of standards (except vial A and stock) and samples into each well of a 96-well clear non-tissue culture treated plate (do triplicates of each sample and standard).
- Using a multi-channel pipettor, pipette 100µL of working reagent into each well, mix with samples by pipetting up and down 2X. Wrap plate in aluminum foil and incubate at 37°C, 95% humidity for 90-120 min.
- Using a Molecular Devices Spectramax 250 plate reader, read the absorbance in each well at 562nm wavelength. Use standards to create a standard curve and correlate absorbance to protein concentration in samples.

Appendix 6 – Perfused 3D Culture Hepatobiliary Transport Studies Protocols

Materials Required

Product Description	Cat#	Supplier	Notes
Hanks' Balanced Salt Solution (HBSS); with $NaHCO_3$; without phenol red, $CaCl_2$, $MgSO_4$	H6648	Sigma	Order in 500 mL bottles and Ca-containing in 1 L bottles
HBSS; with $NaHCO_3$; without phenol red	H8264	Sigma	Order this buffer in 1L bottles
Ethylene glycol-bis(2-aminoethylether)-*N,N,N',N'*-tetraacetic acid (EGTA)	E0396	Sigma	
Taurocholic acid (TCA)	T4009	Sigma	
[^{3}H]-Taurocholic acid	NET322250UC	Perkin Elmer	Contact Radiation Protection Program to notify them of delivery
RIPA buffer	R3792	Teknova	
Ultima Gold XR	6013111	Perkin Elmer	
MicroBCA protein assay kit	23235	Pierce Biotechnology	

Preparation of Buffers

- Ca^{2+}-free buffer
  - HBSS w/o $CaCl_2$, $MgSO_4$
  - 1μM EGTA
- Standard buffer
  - HBSS w/ $CaCl_2$, $MgSO_4$
- TCA solution
  - 1mM TCA in standard buffer
- [^{3}H]-TCA buffer
  - 0.1μM [^{3}H]-TCA
  - 9.9μM TCA (dilute from TCA solution)
  - Standard buffer

Hepatic Transport Study Assay

- Prepare and warm buffers before beginning. Put 120mL of standard buffer per full multiwell reactor plate assayed on ice before beginning.
- Remove retaining rings and filters from reservoir.
- Stop flow and remove as much medium as possible from reservoir and reactor/reservoir bridge. Aspirate medium from reactor down to retaining ring level.

- Fill each reactor/reservoir pair to fill line with either warm standard buffer or warm Ca^{2+}-free buffer. Turn on flow at 0.2ml/min in downward direction, swirl plates gently, stop flow and aspirate buffers off as before. **Repeat these wash steps a total of 3X**. Ca^{2+}-free buffer will disrupt canalicular networks in cultures while standard buffer will not.
- Pipette 800µL of either warm standard buffer or warm Ca^{2+}-free buffer into reactor well. Turn downward flow on at 0.2ml/min. Return reactor to 37°C, 5% CO_2, 95% humidity incubator.
- After 2.5min, without stopping flow aspirate buffer off from reservoir and reactor/reservoir bridge. Add 500µL of either warm standard buffer or warm Ca^{2+}-free buffer into reactor well.
- After a total of 5min (2.5min after previous step), stop flow, and aspirate buffers off as much as possible from reservoir surfaces and reactor/reservoir bridge. Aspirate buffer in reactor down to retaining ring level.
- Add 800µL of either warm standard buffer or warm Ca^{2+}-free buffer into reactor well. Turn on downward flow at 0.1ml/min and incubate at 37°C, 5% CO_2, 95% humidity with either of these two buffers for 10min (or for desired pre-incubation time). Every 5min, aspirate buffer from reservoir and add 500µL of buffer into reactor, do not stop flow.
- After pre-incubation, aspirate buffers from all surfaces. Add 800µL of [^{3}H]-TCA buffer to each reactor. Turn on downward flow at 0.1ml/min and incubate at 37°C, 5% CO_2, 95% humidity for 15min (or for desired accumulation time). Every 5min, aspirate buffer from reservoir and add 500µL of buffer into reactor, do not stop flow.
- During the accumulation step, set three 60-mm Petrie dishes per condition assayed (six for intact and disrupted conditions). Put 10mL ice-cold standard buffer into each Petrie dish.
- Without stopping flow, remove retaining ring from reactors, remove scaffold gently and put scaffold in the first ice-cold 60-mm Petrie dish. This step must be done very gently and smoothly to not disrupt culture tissue. When putting scaffold into ice-cold buffer, put it in at a 45° angle when breaking surface tension of buffer. Place all scaffolds of the same condition in the same dish.
- With tweezers, swirl each scaffold in the ice cold buffer, take scaffold out of buffer gently at a 45° angle, gently introduce scaffold into next ice-cold buffer full Petrie dish, swirl again, take scaffold out again and put into the third Petrie dish, swirl again.
- Pipette 700µL RIPA buffer into a 20mL scintillation vial and place thoroughly washed scaffold into the vial. Vortex vials for ~30sec. Incubate at 4°C overnight. Inspect each scaffold under a microscope to ensure all tissue has been removed.

Scintillation Counting

- Pipette 500µL of sample into a 4mL scintillation tube.
- Add 3.5mL of UltimaGold XR scintillation fluid to each tube. Cap and vortex for 5-10sec.

- Allow tubes to rest for ~10min, load tubes into scintillation racks and into a Beckman Coulter LS 6500 Multipurpose Scintillation Counter. Make sure automation labels are properly placed for the user number desired.
- Make sure user program is set to 2 min counting and set to detect ^{3}H scintillation.
- Conversion factor from counts per minute to pico Curies is 1.38pCi/cpm as experimentally determined from standard curve.

NOTE: Scintillation signal significantly diminishes after ~3-4hr of addition of scintillation fluid so do not do run more than ~80 samples at one time.

Total Protein Assay

- Dilute all samples 1:50 in MilliQ water (make 350µL of each dilution).
- Using the MicroBCA protein assay kit (Pierce Biotechnology), prepare protein standards using the 2mg/mL BSA stock ampoules. Prepare a 1:50 dilution of RIPA buffer in MilliQ as diluent to prepare standards. Prepare dilutions of standards per 96-well plate to be assayed (23 samples) as follows:

Vial	Volume of diluent	Volume and source of BSA	Final BSA Concentration
A	450 µL	50 µL of stock	200 µg/mL
B	1.26 mL	315 µL of vial A dilution	40 µg/mL
C	175 µL	1.225 mL of vial B dilution	35 µg/mL
D	175 µL	1.05 mL of vial C dilution	30 µg/mL
E	175 µL	875 µL of vial D dilution	25 µg/mL
F	175 µL	700 µL of vial E dilution	20 µg/mL
G	175 µL	525 µL of vial F dilution	15 µg/mL
H	175 µL	350 µL of vial G dilution	10 µg/mL
I	175 µL	175 µL of vial H dilution	5 µg/mL
J	350 µL	0	0 µg/mL (blank)

- Prepare 12mL of MicroBCA working reagent per 96-well plate to be assayed. Keep reagent protected from light with aluminum foil. Prepare reagent as follows:
  - 6mL MicroBCA reagent MA
  - 5.76mL MicroBCA reagent MB
  - 240µL MicroBCA reagent MC
- Pipette 100µL of standards (except vial A and stock) and samples into each well of a 96-well clear non-tissue culture treated plate (do triplicates of each sample and standard).
- Using a multi-channel pipettor, pipette 100µL of working reagent into each well, mix with samples by pipetting up and down 2X. Wrap plate in aluminum foil and incubate at 37°C, 95% humidity for 90-120 min.
- Using a Molecular Devices Spectramax 250 plate reader, read the absorbance in each well at 562nm wavelength. Use standards to create a standard curve and correlate absorbance to protein concentration in samples.

Appendix 7 – Cell Lyses, SDS-PAGE and Western Blotting Protocols

Lyses Buffer

- RIPA buffer
- Complete® protease inhibitor cocktail mini tablet (ROCHE Cat#11836153001). Use 1 tablet per 10mL buffer.

Cell Lyses Protocols

- Freshly isolated hepatocytes
  - Pipette 10^6 cells into a 1.5mL eppendorf tube, centrifuge at 50g for 3min.
  - Aspirate off supernatant, add 500µL ice-cold lyses buffer. Pipette up and down to disrupt pellet and for more efficient lyses.
  - Incubate 30min on ice to allow for cell lyses. Store at -80°C.
- 2D sandwich cultures
  - Wash cells 3X with ice-cold PBS, pipette 150µL of lyses buffer into each well, seal plate sides with parafilm, and put on shaker for 30min in a 4°C cold room.
  - Put cell lyses samples into a 1.5mL eppendorf tube and store at -80°C.
- Perfused 3D cultures
  - Wash reactor/reservoir plates with 3X PBS, remove retaining rings and scaffolds, and place scaffolds in 20mL scintillation vials with 500µL of ice-cold buffer.
  - Vortex samples ~1min.
  - Drill a 1/8" hole in the center of one 20mL scintillation vial cap, place this cap tightly on a vial with perfused 3D culture sample. Wedge a pipette tip into hole and with the pipettor cylinder depressed, release pipettor cylinder to cause a slight vacuum inside the vial. This will cause all bubbles in lyses buffer to burst. Repeat this procedure until all bubbles are gone. Do this procedure on ice.
  - Allow cells to lyse over 30min on ice before storing samples in 1.5mL eppendorf tubes at -80°C.

Sample Preparation for SDS-PAGE Electrophoresis

- Thaw cell lysates on ice and centrifuge samples at in a mini-centrifuge at 10,000 rpm for 5min at 4°C to separate insoluble fraction.
- Make sample preparations so that a dilution of 1:6 of 6X reducing buffer is achieved with 1µg/µL total protein concentration of sample. Dilute with RIPA buffer. Make 30µL per lane, however only 25µg will be loaded on gel.
- Make molecular weight (MW) marker
  - 17.5µL Kaleidoscope marker (BioRad Laboratories Cat# 161-0375)
  - 3.5µL 6X reducing buffer
- Vortex samples to mix.
- Incubate samples on a 70°C heating block for 10min.
- Spin down samples (3-5 sec quick spin on a mini-centrifuge).

NuPage Gel Electrophoresis (SDS-PAGE)

- Solution preparations:
    - 1X Running Buffer (RB)
        - 40mL 20X MOPS RB (Invitrogen Cat# NP0001)
        - 760mL MilliQ water
    - 1X Running Buffer + Antioxidant
        - 200mL of 1X RB (above)
        - 500µL NuPage antioxidant (Invitrogen Cat# NP0005)
- Remove precast gels from package, rinse gently with MilliQ water, and remove white strip from bottom.
    - Use NuPage 4-12% Bis-Tris gels (Invitrogen Cat# NP0321BOX)
- Rinse buffer core, NuPage cell, and tension wedge with MilliQ water.
- Lower buffer core into cell and insert gel cassettes on both sides (make sure the shorter well side faces inward). Insert tension wedge and lock in place. If only one gel is to be run, insert gel blank cassette into one side of buffer core.
- Fill the buffer core with 200mL 1X RB + antioxidant. Make sure this section DOES NOT leak before adding liquid to the outside. Carefully remove the comb from top of gel cassette and pipette out air bubble with 1X RB + antioxidant. Fill outer part of case with 600mL of RB.
- Fill the wells with samples:
    - Add 15µL MW markers to first well
    - Fill all other channels with 25µL of prepared samples. Fill each well slowly to avoid air bubbles and spill over.
    - Label outside of NuPage cell with a taped label to identify gels and channels.
- Match the + and – electrode ends and set the voltage apparatus to run for 50min at 200V.

Transferring Proteins to Immunoblots

- Solution preparations:
    - 1X Transfer buffer (TB) + antioxidant
        - 50mL 20X NuPage Transfer Buffer (Invitrogen Cat# NP0006)
        - 1mL NuPage antioxidant (Invitrogen Cat# NP0005)
        - 200mL MeOH
        - 749mL MilliQ water
- Make tray of MeOH, tray of MilliQ water, and tray of TB for preparation of immunoblot PVDF membrane (7X8.4cm; BioRad Laboratories Cat# 162-0174).
- Dip membrane in MeOH, then in MilliQ water and finally leave to soak in TB.
- Rinse blotting pads, NuPage transfer core, and NuPage cell with MilliQ water.
- Place transfer core in a small container (only slightly larger then core).
- Soak blotting pads thoroughly in TB and place 2 pads on cathode (–) side of transfer core.
- Soak one sheet of filter paper in TB thoroughly and place on top of blotting pads. Add TB to transfer core to maintain pads and paper soaked.
- Unlock wedge from gel rig to release gel cassettes, crack open gel plates with a gel knife. With gel knife, remove gel well dividers and excess gel from bottom.

- Use gel knives to place gel on filter paper. Dip knives in TB so gel will not stick to gel.
- Add membrane on top of gel and a thoroughly soaked filter paper on top.
- Thoroughly soak another blotting pad in TB and place on top of filter paper.
- Thoroughly soak another piece of filter paper in TB and place on top of blotting pad.
- Add the second gel on top of this filter paper, and second membrane of top of this gel, following the preparation steps outlined above.
- Place a soaked filter paper on top of membrane and two soaked blotting pads on top of this.
- Squeeze blot module closed with anode top and place in NuPage cell. Add tension wedge to cell and lock it.
- Fill inside of transfer core with TB above the level of the blotting pads and filter paper but do not overflow. Make sure the transfer core has no leaks.
- Fill the outside of the cell with MilliQ water to ~2cm from top.
- Match the + and – electrode ends and set the voltage apparatus to run for 1hr at 30V.

In summary, the gel membrane sandwich should be set up as follows:

- Starting from cathode end:
    - Blotting pad
    - Blotting pad
    - Filter paper
    - First gel
    - Transfer membrane
    - Filter paper
    - Blotting pad
    - Filter paper
    - Second gel
    - Transfer membrane
    - Filter paper
    - Blotting pad
    - Blotting pad

Western Blotting Protocol

- Solution preparations:
    - Wash buffer (PBS-T)
        - 1L 10X PBS (VWR Cat# EM-6505)
        - 8.95L MilliQ water
        - 50mL Tween-20 (BioRad Laboratories Cat#170-6531)
    - BSA blocking solution (prepare >500mL)
        - 5g BSA
        - 100mL PBS-T
    - Milk blocking solution
        - 0.5g dry fat-free milk

        - 10mL PBS-T
    - Detection Reagents
        - ECL Advance Western Blotting Detection Kit (GE Healthcare Cat# RPN 2135)
            - 3mL reagent A
            - 3mL reagent B
- Remove membrane paper from transfer core apparatus, cut as necessary, and use a marker to indicate which side was in contact with the gel (keep this side of the membrane up throughout the rest of the procedure).
- Place membrane in a small container (just slightly larger than membrane) and add >20mL of BSA blocking solution. Incubate at RT for 2hr with constant agitation on a rocker.
- Place membrane in 10mL primary antibody solution (1:1000 dilution in BSA blocking solution for most antibodies, 1:10,000 dilution for actin antibody). Incubate at 4°C overnight with constant agitation or, alternatively, incubate for 2hr at RT with constant agitation.
- Wash membrane 3X with wash buffer. Incubate 10min at RT with constant agitation for each wash step.
- Place membrane in 10mL secondary antibody solution (1:10,000 dilution in milk blocking solution; HRP-conjugated donkey anti-rabbit secondary antibody, GE Healthcare Cat# NA934; HRP-conjugated sheep anti-mouse secondary antibody, GE Healthcare Cat#NA931). Incubate at RT for 2hr with constant agitation on a rocker.
- Wash membrane 3X with wash buffer. Incubate 10min at RT with constant agitation for each wash step.

Developing Immunoblot on Kodak Image Station 1000

- Set camera dial to 2 to image blot.
- Ideal temperature is -20°C, track temperature in Capture window with Ctrl+T.
- Place immunoblot membrane in detection reagents for 1min (light sensitive).
- Place blot protein side down on glass window in Image Station.
- Click on the Predict button in the Capture window to set exposure time, click on Capture to get immunoblot image.
- If needed for later use, store blot in SaranWrap with PBS-T at 4°C for <1 month.

Stripping and Reprobing

- Solution preparations:
    - Stripping buffer:
        - 3mL 20% SDS
        - 0.75mL 2.5M Tris, pH 6.8 (62.5mM)
        - 0.21mL 14.3M BME
        - 26.04mL dH_2O
- Place blot in 25mL stripping buffer for 30min at 50°C in a water bath in a sealed container. Agitate every 10min.
- Rinse 3X with dH_2O into a toxic waste container.

- Wash blot 3X in dH_2O, incubate at RT for 5min with constant agitation for each wash step.
- Wash blot 3X with PBS-T, incubate at RT for 5min with constant agitation for each wash step.
- Repeat immunoblot steps starting with blocking in BSA blocking buffer.

NOTE: Electrophoresis and transfer were conducted in an Invitrogen NuPage XCell SureLock Electrophoresis Cell and an Invitrogen NuPage XCell Blot Module.

Appendix 8 – RNA Purification Protocol

Cell Sample Collection

- Freshly isolated hepatocytes
  - Pipette 10^6 cells from cell suspension into a 1.5mL eppendorf tube, centrifuge at 50g for 3min, and aspirate off supernatant.
  - Add 1mL of ice-cold Trizol LS reagent (Invitrogen Cat#10296010) and pipette up and down to break up pellet.
  - Vortex to mix thoroughly and store at -80°C for up to 2 months.
- 2D sandwich cultures
  - Wash wells 3X with ice-cold PBS, pipette 500µL of ice-cold Trizol into each well.
  - Place plate on rocker for 20min at 4°C. Transfer sample into eppendorf and store at -80°C for up to 2 months.
- Perfused 3D cultures
  - Wash reactor wells 3X with PBS, remove retaining ring, and place scaffold in a 20mL scintillation vial.
  - Add 1mL ice-cold Trizol to scintillation vial and vortex 30sec.
  - Store at -80°C overnight.
  - Thaw sample on ice and transfer to eppendorf tube. Store at -80°C for up to 2 months.

NOTE: RNA can degrade very quickly. During all the following isolation procedures, do not do more than 8 samples at a time. Try to keep samples on ice or on a cold pack as much as possible to reduce degradation.

- Thaw sample on ice.
- Homogenize sample by passing through a 26g needle/syringe (1 mL) 12-15 times.
- Add 200µL Chloroform per 1mL of Trizol in each sample.
- Invert a few times by hand and then vortex for 5 seconds.
- Incubate RT for 2-3 mins; sample will start to settle (clear w/ RNA on the top; pink w/ DNA and Protein on the bottom).
- Centrifuge samples for 15 min @ 12,000 RPM in a mini-centrifuge.
- Set a heating block to 65°C. Put 80µL/sample of RNAse-free water on heating block.
- After spin, carefully remove top layer of supernatant (clear, aqueous phase; contains the RNA) and place in 1.5mL Eppendorf tube. To do this, set pipette to 200µL and leave some behind if necessary so that there is no contamination with the pink layer (contains DNA and other cellular components).
  - Keep track of how much material was removed (should yield about 550-600µL).
  - Store remaining sample (DNA/Protein) in –80°C.

From here onward, keep all samples on ice! The following steps use a Qiagen Mini RNEasy kit (Qiagen Cat# 74106). Follow RNEasy Mini Handbook (Qiagen) from step 4 of protocol *(with a few modifications)*:

- Add equal volume (or more) of 75% EtOH to sample: mix by tipping and pipetting (do not vortex).
- Remove up to 700µL solution and place in an RNEasy column with collection tube.
    - Centrifuge for 15 sec @ ≥ 8000g (10,000 RPM) .
    - Repeat spin by returning eluent to top of filter (15 seconds).
    - Discard waste (solution in the bottom of filter unit) after the 2 centrifugation steps.
    - Add remaining and repeat centrifugation steps.
- Add 700µl of Buffer RW1 to the RNEasy column. Centrifuge for 15 sec @ ≥ 8000g (10,000 RPM) and discard flow-through and collection tube.
- Transfer column to a new collection tube and add 500µL of RPE Wash Buffer to filter. Centrifuge for 15 sec @ ≥ 8000g (10,000 RPM) and discard waste.
- Add another 500µL of RPE Wash Buffer to System and centrifuge for 2 min (15 sec @ ≥ 8000g) to dry membrane.
    - RECOMMENDED: Place column in new collection tube and centrifuge at full speed for 1 minute to ensure that all ethanol is removed.
- Add 30µL DEPC treated water (heated to 65 ^{o}C) to filter; incubate RT for 2-3 minutes.
    - Centrifuge for 2 minutes in a clean Eppendorf tube to elute.
    - Repeat with another 30µL DEPC water (if desired, this is a requisite if there are one million cells or more, but is recommended for >250,000 cells).

To measure quantity and purity of RNA:

- Using a NanoDrop 100 machine:
    - Open ND-100 v3.1.2 software.
    - Select "Nucleic Acid" tab.
    - Clean the sample pedestal with RNAse free water and a Kimwipe.
    - To initialize, add 2 µL of RNAse free water, put top arm down and click OK.
    - Select RNA-40 in the sample type window in the upper right corner.
    - Wipe off the sample pedestal and blank the device with 2 µL of the buffer that the sample is in, which for these RNA samples is RNAse-free water.
    - Wipe off the sample pedestal and pipette 2 µL of your sample, put the arm down and click on measure.

NOTES: Only read a volume of sample once, you can read another 2 µL and so on if you want replicates. The reading will change on subsequent reads of the same sample. The sample pedestal only needs to be wiped clean with a Kimwipe between multiple samples. Keep RNA samples on ice at all times during measurement. Store at -80°C immediately for up to 2 months.

Appendix 9 – cDNA Generation Protocol

This cDNA protocol is based on synthesis from 200 ng of total RNA and will yield 20μL of cDNA. This is enough to run real-time PCR on 5-6 genes. If more genes need to be measured, or if greater amounts of cDNA are wanted for long term storage since it degrades less rapidly than the RNA samples, all volumes listed can be doubled or tripled to get 40 or 60 μL of cDNA from 400 or 600 ng of RNA, respectively.

- Add the following to a 0.5 mL Eppendorf tube:
    - Calculate the volume of the RNA sample to make 200 ng total RNA from nanodrop reading. Make sure to re-read your RNA sample if it's been stored for a while.
    - Calculate the remaining volume of DEPC water so the total volume (RNA+H_20) is 8μL.
    - Add DEPC water, and then RNA and keep all samples on ice.
    - Add 1μL of 10x DNAse Buffer to each sample. Mix buffer well with a pipette before adding.
    - Add 1μL of DNAse I enzyme (Invitrogen Cat# 18068-015) to each sample. Take DNAse out just before adding (don't need to thaw it) and mix with a pipette before adding.
- Let the sample sit at room temperature for 15 minutes. Put the remaining RNA back in the -80°C freezer. Turn on the heating block and set to 65°C.
- Add 1μL of EDTA to each sample (25mM, Invitrogen) to each sample and return the samples on ice. When EDTA has been added to all samples, centrifuge them at 2000 RPM for ~5 seconds. Incubate samples at 65°C for 10 minutes.
- Thaw Random Hexamer Primers (Qiagen Cat# 79236), RT Buffer (Qiagen, from Omniscript kit Cat# 205113), RNAse Inhibitor (Ambion Cat# 2682) on ice
- Make dilutions of 10x RT buffer, Random Hexamers, and RNAse Inhibitor:
    - RT Buffer: 1:10 dilution of the 10x RT buffer necessary for RNAse inhibitors. Add 9μL of DEPC water for every 1μL of 10x RT buffer. Make a little extra so volumes will be correct.
    - Primer dilution: 1:10 (e.g. 9μL of DEPC water and 1μL of Primer working stock). Again, plan to make 1-2 rxns worth extra so volumes will be accurate. Make the dilution fresh every time.
    - RNAse Inhibitor: 1:4 Dilution with 3μL of 1x RT buffer from above for every 1μL of RNAse inhibitor. Make fresh each time, and again make 1-2 rxns additional dilution so volume will be accurate for stock solution.
- Make the Stock Solution containing for each sample (make one to two extras):

    - 1μL DEPC water
    - 2μL dNTP (Qiagen, Omniscript kit)
    - 2μL Primer dilution (from previous step)
    - 1μL RNAse inhibitor dilution (from previous step)
    - 2μL 10x RT buffer (Qiagen, Omniscript kit)
    - 1μL Omniscript Reverse Transcriptase (RT O, Qiagen)

- Remove samples from heat at the end of 10 minutes. Centrifuge for ~5 seconds at 2000 RPM. Return samples to ice.
- Add 9μL of the Stock Solution to each sample to make the total volume 20 μL.
- Spin down samples for ~5 seconds at 2000 RPM.
- Incubate samples at 37°C in the water bath. Make sure bottom of tube is in the water but that tube tops aren't submerged.
- Remove samples from the water bath, centrifuge ~5 seconds at 2000 RPM, and store samples at -80°C.

Appendix 10 – Real-time, Reverse Transcriptase SYBR Green PCR Protocol

This is a general protocol for any primer set of interest to measure mRNA expression using the Chromo4 Real-time PCR set-up and Opticon Monitor 3 software.

- Make "Master Mix" containing (or 20X):
  - 25uL SYBR Green (500μL; Qiagen Cat# 204145)
  - 21uL DEPC water (420μL)
  - 1.5uL forward primer (30μL; custom-made, Operon Biotechnologies)
  - 1.5uL reverse primer (30μL; custom-made, Operon Biotechnologies)
- Vortex sample and spin down. Vortex master mix and spin down.
- Get BioRad 96-well plate (white plastic) and place in a black plate tray.
- Add 49μL master mix to each well.
- Add 1uL cDNA to each sample. Use triplicates. Leave one triplicate for no RT spaces.
- Cover each well with a sample in it with a clear plastic cap.
- Return cDNA samples to -80°C freezer.
- Insert sample into RT-PCR machine. Gently close the top and secure the latch.
- Open "Opticon Monitor 3" software.
- Open your user profile. Open Master file (top set) and make changes to plate and protocol setup.
- Change the plate setup so each grid spot where there is a sample has a red circle. Make sure that the proper plate type (MJ White) and dye types (SYBR Green, in this case) are selected – these cannot be changed later.
- Change the protocol to have the optimal primer annealing temperature and number of cycles. Make sure that the proper reaction volume is typed in (50 μL here) – this cannot be changed later.
- Save the protocol file, then the plate setup file, then the master file.
- Click Run: the computer will prompt you for a file name for the data file. The computer automatically saves this file at the end of the run protocol.
- You can click on 'quantification' during the run to check the status of your sample.
- When the run is complete, set the threshold magnitude by looking in both the log view and regular view to make sure it is in the early linear range of the amplification. Keep this value consistent between runs for accurate comparison of C_Ts between samples.

Appendix 11 – Primer Design Procedures and Guidelines

Identify Gene Sequence

- Use NCBI Nucleotide Search (http://www.ncbi.nlm.nih.gov/) to find the target genes' mRNA sequence, as far as possible use complete cds or the mRNA sequence.
- Include species (e.g. *Rattus norvegicus* for Norwegian rat strains) and RNA type (e.g. mRNA, rRNA, etc.) in your search.

Design Initial Primer

- Input the resulting gene sequence into MIT's Primer3 software (Whitehead Institute; http://frodo.wi.mit.edu/)
- Specify the following conditions
    - 100-200 basepair target sequence
    - 18-30 nucleotides in length
    - 45-55% GC content

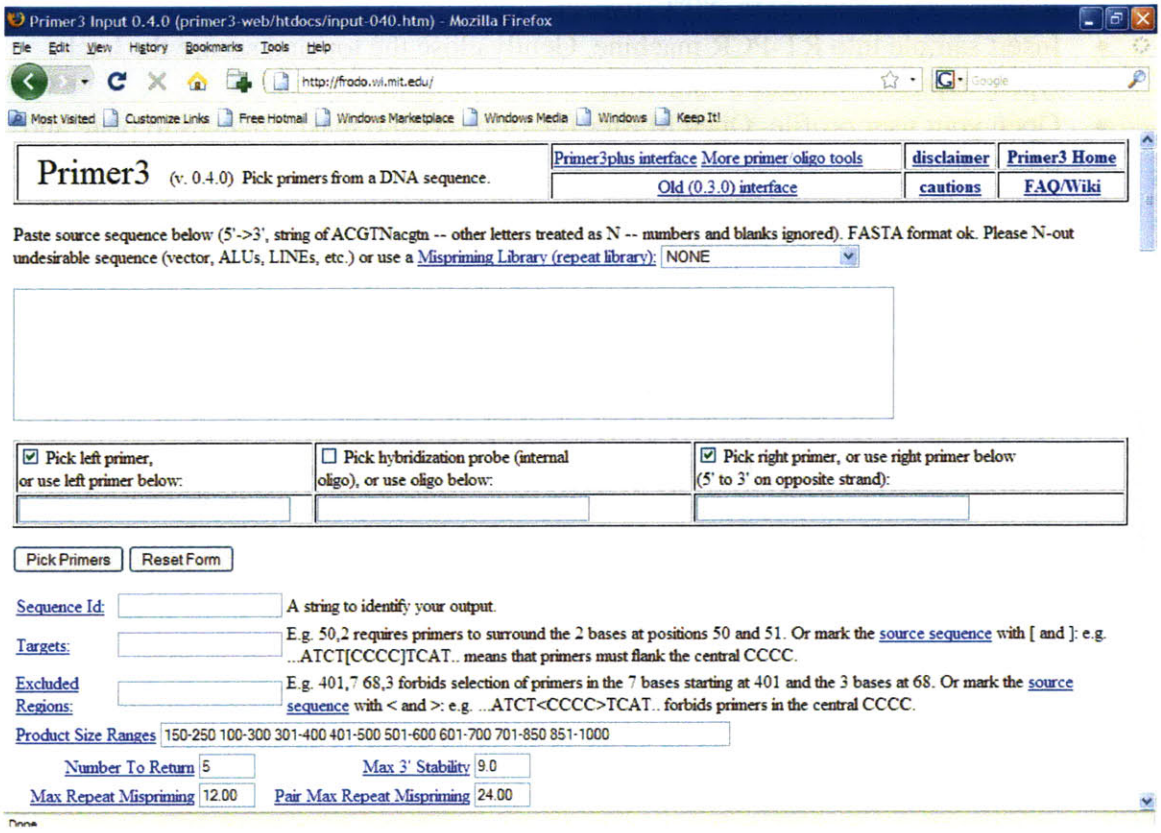

- Try to keep the product melting temperature as high as possible, so that it is much greater than the melting temperature of the primer-dimers and genomic DNA products.
- Keep the primer melting temperatures of the forward and reverse primers as close to each other as possible (±1°C).

- Software will give a list of candidate primers in ranked order as determined by their algorithm.
- Select primers from the generated options that:
    - Avoid runs of 3 or more G/C at the 3' end.
    - Avoid complementarities within the primer sequences and between the primer.
    - Avoid complementarities and mismatches of 2 or more bases at the 3' ends of the primer and the target-template sequences.
    - Avoid a 3' end T pair.
    - Use primers that give a product with a high melting temperature.
    - As far as possible, make sure to select a primer set that binds to a sequence on the gene that lies in the intron-exon boundary (this can be known by looking at where the primer binds to the mRNA sequence and then comparing the sequence where the primer binds to the complete cds sequence). If this is not possible, make sure that the gene product spans this intron-exon boundary.

Verify Targets of Primer Design

- Go to NCBI Blast (http://www.ncbi.nlm.nih.gov/BLAST/). Click on the 'short, nearly exact matches link' and input the determined primer sequence into the input box. Click on the BLAST tab and look up the set of genes that are listed each of which can be an RT-PCR product for the chose primer set.
- The primer sequence should yield the target gene with considerably greater significance than the next closest match for the same animal species (e.g. *Rattus norvegicus*). Similarities between the gene specificity of different species are not important.

Appendix 12 – Plasma and Bile Collection from *In Vivo* Liver

Materials

- Tray and Cover
- Scalpel Holder
- 1 pair of Tissue Forceps
- 2 pairs of Small Tooth Curved Forceps (VWR 25601-010)
- Hemostat (Henry Schein 100-2376)
- Small Scissors
- Microscissors
- Q-Tips (Puritan)
- Nu Gauze 2x2in, 4 ply (Johnson&Johnson via VWR #7632)
- Ethicon™ Silk – 4 Strands of 4-0 Silk (VWR 25942-249)
- Blue Paper

Autoclave all materials prior to surgery.

- Using a "Blue" 25G Needle anaesthetize rat with Na-Pentobarbitol according to animal weight, diluted with an equal volume of 1x PBS. Inject into the intraperitoneal (IP), just to the left of the midline. Pull back on the plunger and make sure there is a visible bubble to ensure that you are in the body cavity and not in the bladder, intestine, etc.
- As soon as the rat shows no reflexes to quick blows of air, check the drug effect through tail pinches. Do not continue until the rat does not respond to the pinches. Pinching in between the toes is also a good indicator.
- Working quickly, shave the rat over the entire incision area.
- Apply Betadine using gauze (Optional).
- Secure the animal to the procedure board with autoclave tape.
    - Fully extend the lower legs and tape them down
    - Raise the upper legs and *gently* tape each arm separately.
- Open the lid of the Surgical Kit *without* touching the inside of the kit or lid.
- Don surgical gloves. Keep these sterile to avoid contamination. Only touch the instruments within the Kit and the rat body. Do not touch anything else.
- Make an "I" incision on the ventral side using the Tissue Forceps and Scissors. The incision should run from the lower abdominal area around the bladder to the Zyphoid process and Rib area. Avoid nicking the liver. As you cut towards the ribs, you may have to gently massage liver through the skin to loosen it from the skin.
- Gently displace the guts to the right with a fresh Q-Tip, exposing the Inferior Vena Cava (IVC) and Portal Vein (PV).
- Locate the bile duct by gently lifting the liver.
- Separate the bile duct from the intestinal wall using tweezers.
- Tie a silk suture loosely above point where perforation will occur.

- Nick the bile duct with the use of microscissors and insert a small piece of PE10 tubing into the duct. DO NOT cut all the way through the duct, this will cause the duct to collapse.
- Once tubing is secure, tighten suture to stabilize tubing. Do not tighten too much as this may collapse the bile duct.
- Collect bile into an eppendorf tube for 15 minutes.
- During the bile duct cannulation and bile collection, keep the internal organs moist by draping gauze soaked in sterile 1X PBS over the organs.
- Using a heparin-coated syringe, draw 1 mL of blood from the portal vein and collected it in an eppendorf tube. Coat the syringe by drawing a solution of 1000IU heparin in and out of syringe 3X.
- Centrifuge blood at 10,000g for 10min to separate plasma.
- Collect plasma (supernatant), and store at -80°C.
- Dilute bile 1:30 in 100% EtOH and store at -80°C.
- Once both plasma and bile are collected, the rat, still under anesthesia, should be euthanized by piercing the diaphragm inducing hypoxia.

Appendix 13 – Immunohistochemical Staining of Perfused 3D Cultures and Confocal Imaging

Immunohistochemical Staining

- Wash reactor wells 3X with sterile PBS. Remove retaining ring and transfer scaffolds to a 12-well non-culture treated plate with 800μL PBS in each well.
- Aspirate off PBS, and fix tissue by pipetting 800μL of 2% paraformaldehyde into each well and placing plate on a Nutator at RT for 1hr.
- Aspirate off paraformaldehyde and wash scaffolds 3X with 800μL PBS. If staining will not be performed immediately, seal plate with parafilm and store at 4°C for up to 1 month.
- Permeabilize the tissue by incubating in 800μL 0.1% Triton X-100 for 30min on a Nutator at 37°C, 5%CO2, 95% humidity (inside an incubator).
- Wash 3X with 800μL of 2%BSA in PBS.
- Incubate with 800μL normal goat serum (1:20 dilution in 2%BSA in PBS for CD26, BD Biosciences Pharmingen, Cat# 559639) for 45 minutes on a Nutator at 37°C, 5%CO2, 95% humidity (inside an incubator).
- Wash 3X with 800μL of 2% BSA in PBS.
- Incubate with primary antibody (use 800μL of a 1:100 dilution in 2% BSA in PBS) on a Nutator at 4°C overnight. The long duration of incubation is ESSENTIAL for the antibody to penetrate the depth of the tissue.
- Wash 3X with 800μL of 2%BSA in PBS at RT.
- Incubate with dye-conjugated secondary antibody (use 800μL of a 1:1,000 dilution of secondary and a 1:1,000 dilution draq5 nuclear stain in 2% BSA in PBS) for 1hr at RT.
- Wash 3X with 800μL of 2%BSA in PBS.
- Wash 3X with PBS. Store at 4°C.

NOTE: Secondary antibody recommended is Alexa Fluor 488 goat anti-mouse IgG, highly cross-absorbed (Invitrogen Cat# A11029). Draq5 nuclear staining (Axxora Cat# BOS-889-001-R050).

Confocal Imaging

This protocol details confocal imaging of tissue cultures using a spinning disc confocal microscope at the MIT Cancer Research Center. The microscope is a Nikon Eclipse TE2000-E with a Visitech QLC 1000 spinning head and an Innova 70C Spectrum Laser.

- Turn on microscope and laser as follows:
    - Turn on water source for chiller pump to cool the laser.
    - Turn on chiller water pump.
    - Turn laser key to on.
    - Bring laser intensity to 15Amps.
    - Turn laser on.
    - Turn on all peripherals including spinning head and mechanical stage.
- Open Metamorph Software and select appropriate camera.
- If not already on microscope, screw in 20X objective.

- Place scaffold to be imaged in the center of a MatTek 35mm glass bottom Petrie dish with a 20mm diameter glass bottom and No. 0 glass thickness (MatTek Corporation Cat# P35G-0-20-C). Fill dish with PBS.
- Place dish on mechanical stage.
- Select the "Phase Eyes" setting on Metamorph to use phase microscopy.
- Looking into the microscope eye piece, use the mechanical stage controller to center on a tissue channel of interest. Turn off phase contrast as soon as possible.
- Set aperture to 3 and laser intensity to ~30Amps.
- Using the Acquire function, specify acquire multiple wavelengths and set wavelengths to AOTF 488 Confocal and AOTF 648 Confocal. Select the Z-stack option with defined top and bottom.
- Set Metamorph to AOTF 488 Confocal, set exposure time to 500ms and click on "Live" button.
- Use live camera capture to set upper and lower limits for Z-stack capture.
- Set Metamorph to AOTF 648 Confocal, click of "Live" button to make sure nuclear stain can also be captured.
- Set step size of Z-stack to 0.647μm.
- Click on Acquire. Save stacks at the end.

Appendix 14 – Matlab Numerical Models and Code

```
% Jose Ricardo Llamas Vidales
% Code to run numerical model to reduce experimental conditions in
Hepatic
% transport studies

clear all;
close all;

recycler_counter = 5;

% Variables

% Parameters from Liu et al, 1999.
Kmareal = 28;
Vmareal = 1.19;
Ke4real = 0.849;
Kmbreal = 1.03;
Vmbreal = 1.82;

tspan = 45; %min

C = [1 10 20 50 100];%uM, buffer concentration
numcells = 2.*(10.^5); %cell, number of cells in culture
protpcell = 1.5.*(10.^(-6)); %mgprotein/cell, protein per cell
Vol_conc = 0.001; %L
t = [0 0.5 1 1.5 2 5 10];%min, time points of interest

IC = [0 0 0]; %Initial condition of intracellular levels of
accumulation

b01 = [Kmareal Vmareal Ke4real Kmbreal Vmbreal]; %Initial "guess" for
nonlinear regression calculation

Kma = 28.*(0.5.*ones(1,1000));

% Set of matrices to collect all data generated by model
howoff = zeros(size(Kma,2),5,recycler_counter);
maxoff = zeros(size(Kma,2),recycler_counter);
propoff = zeros(size(Kma,2),5,recycler_counter);
maxpropoff = zeros(size(Kma,2),recycler_counter);
whichoff = zeros(size(Kma,2),5,recycler_counter);
whichoffsum = zeros(recycler_counter,5);
howoffrand = zeros(size(Kma,2),5,recycler_counter);
maxoffrand = zeros(size(Kma,2),recycler_counter);
propoffrand = zeros(size(Kma,2),5,recycler_counter);
maxpropoffrand = zeros(size(Kma,2),recycler_counter);
whichoffrand = zeros(size(Kma,2),5,recycler_counter);
whichoffsumrand = zeros(recycler_counter,5);
probmore20 = zeros(1,recycler_counter);
probmore40 = zeros(1,recycler_counter);
probmore20rand = zeros(1,recycler_counter);
probmore40rand = zeros(1,recycler_counter);
```

```
% Matrices to capture accumulation data generated by ODE model
x1Kma =
zeros(size(t,2),size(IC,2),size(Kma,2),size(C,2),recycler_counter);
x1rand =
zeros(size(t,2),size(IC,2),size(Kma,2),size(C,2),recycler_counter);

% Matrices to capture accumulation data as concentration
ConcKma =
zeros(size(t,2),size(IC,2),size(Kma,2),size(C,2),recycler_counter);
Concrand =
zeros(size(t,2),size(IC,2),size(Kma,2),size(C,2),recycler_counter);

% Matrices to capture maximum concentrations
CmaxKma = zeros(1,size(Kma,2),2,size(C,2),recycler_counter);
Cmaxrand = zeros(1,size(Kma,2),2,size(C,2),recycler_counter);

tconstKma = zeros(1,size(Kma,2),2,size(C,2),recycler_counter);

topen = 3; %min, time for tight junctions to open
Vol_buff = 0.001; %L, amount of buffer volume
tpre = 15; %min


for r = 1:recycler_counter

    rand('twister',sum(100*clock));
    randn('state',sum(100*clock));

% Matrices of randomly generated parameter values
Kma = 28.*(0.5.*ones(1,1000) + rand(1,1000));%uM
Vma = 1.19.*(0.5.*ones(1,1000) + rand(1,1000));%nmol/min/mgprotein
Ke4 = 0.849.*(0.5.*ones(1,1000) + rand(1,1000));%1/min
Kmb = 1.03.*(0.5.*ones(1,1000) + rand(1,1000));%nmol/mgprotein
Vmb = 1.82.*(0.5.*ones(1,1000) + rand(1,1000));%nmol/min/mgprotein


% Loop using ODE solver to produce accumulation data
for i = 1:size(Kma,2)

                    for n = 1:size(C,2)

                        IC(1,3) = C(1,n);

                        [t,x] =
ode23s(@TCA_efflux_eq_liu_thesis,t,IC,optimset('Display','off'),Kma(1,i
),Vma(1,i),Ke4(1,i),Kmb(1,i),Vmb(1,i),C(1,n),topen,Vol_buff,tpre,numcel
ls,protpcell);

                        x1Kma(:,:,i,n,r) = x;

                        x(:,3) =
x1Kma(:,3,i,n,r).*Vol_conc./(numcells.*protpcell);
```

```
                        x1rand(:,:,i,n,r) =
x1Kma(:,:,i,n,r).*(ones(size(x1Kma,1),size(x1Kma,2)) +
0.1.*(randn(size(x1Kma,1),size(x1Kma,2)))); %This step adds
"experimental" error to accumulation measurements

                        ConcKma(:,:,i,n,r) =
numcells.*x.*protpcell./Vol_conc; %nM

                        Concrand(:,1:2,i,n,r) =
numcells.*x1rand(:,1:2,i,n,r).*protpcell./Vol_conc;

                        Concrand(:,3,i,n,r) = x1rand(:,3,i,n,r);

                        CmaxKma(1,i,1,n,r) =
ConcKma(size(ConcKma,1),1,i,n,r);

                        CmaxKma(1,i,2,n,r) =
ConcKma(size(ConcKma,1),2,i,n,r);

                        Cmaxrand(1,i,1,n,r) =
Concrand(size(Concrand,1),1,i,n,r);

                        Cmaxrand(1,i,2,n,r) =
Concrand(size(Concrand,1),2,i,n,r);

                        p = find(ConcKma(:,1,i,n,r) >= (1 - exp(-
1)).*CmaxKma(1,i,1,n,r),1);

                        tconstKma(1,i,1,n,r) = ((1 - exp(-
1)).*CmaxKma(1,i,1,n,r) - ConcKma((p - 1),1,i,n,r)).*(t(p,1) - t((p -
1),1))./(ConcKma(p,1,i,n,r) - ConcKma((p - 1),1,i,n,r)) + t((p - 1),1);

                        q = find(ConcKma(:,2,i,n,r) >= (1 - exp(-
1)).*CmaxKma(1,i,2,n,r),1);

                        tconstKma(1,i,2,n,r) = ((1 - exp(-
1)).*CmaxKma(1,i,2,n,r) - ConcKma((q - 1),2,i,n,r)).*(t(q,1) - t((q -
1),1))./(ConcKma(q,2,i,n,r) - ConcKma((q - 1),2,i,n,r)) + t((q - 1),1);

                    end

end

% This loop uses accumulation loop results to produce new parameters
% determined by nonlinear regression analysis

for k = 1:size(Kma,2)

    dxdt1 = zeros(size(x1Kma,1),2,size(C,2));

    dxdtreal1 = zeros(size(x1Kma,1),3,size(C,2));
```

```
    xlin1 = zeros(size(x1Kma,1),3,size(C,2));

    for i = 1:size(C,2)

        for j = 2:(size(t,1) - 1)

            dxdt1(j,1,i) = (x1Kma(j + 1,1,k,i,r).*(t(j,1) - t(j - 1,1))
- x1Kma(j,1,k,i,r).*(2.*t(j,1) - t(j + 1,1) - t(j - 1,1)) - x1Kma(j -
1,1,k,i,r).*(t(j + 1,1) - t(j,1))./(2.*(t(j + 1,1) - t(j,1)).*(t(j,1)
- t(j - 1,1)));

            dxdt1(j,2,i) = (x1Kma(j + 1,2,k,i,r).*(t(j,1) - t(j - 1,1))
- x1Kma(j,2,k,i,r).*(2.*t(j,1) - t(j + 1,1) - t(j - 1,1)) - x1Kma(j -
1,2,k,i,r).*(t(j + 1,1) - t(j,1))./(2.*(t(j + 1,1) - t(j,1)).*(t(j,1)
- t(j - 1,1)));

        end

        dxdt1(size(dxdt1,1),:,i) = (x1Kma(size(x1Kma,1),1:2,k,i,r) -
x1Kma(size(x1Kma,1) - 1,1:2,k,i,r))./(t(size(t,1),1) - t(size(t,1) -
1,1));

        dxdt1(1,:,i) = 2.*dxdt1(2,:,i) - dxdt1(3,:,i);

        xlin1(:,3,i) = C(1,i).*ones(size(xlin1,1),1);

        xlin1(:,2,i) = x1Kma(:,2,k,i,r);

        xlin1(:,1,i) = x1Kma(:,1,k,i,r);

        dxdtreal1(:,1,i) = (Vma(1,k).*x1Kma(:,3,k,i,r)./(Kma(1,k) +
x1Kma(:,3,k,i,r))) - Ke4(1,k).*(x1Kma(:,1,k,i,r) - x1Kma(:,2,k,i,r));
        dxdtreal1(:,2,i) = (Vma(1,k).*x1Kma(:,3,k,i,r)./(Kma(1,k) +
x1Kma(:,3,k,i,r))) - (Vmb(1,k).*x1Kma(:,2,k,i,r)./(Kmb(1,k) +
x1Kma(:,2,k,i,r)));

    end

    Beta1 = lsqnonlin(@TCA_efflux_model_liu_nlin_thesis,b01,[0 0 0 0
0],2.*b01,optimset('Display','off'),xlin1,dxdt1);

    howoff(k,:,r) = abs(Beta1 - [Kma(1,k) Vma(1,k) Ke4(1,k) Kmb(1,k)
Vmb(1,k)]);
    propoff(k,:,r) = howoff(k,:,r)./[Kma(1,k) Vma(1,k) Ke4(1,k)
Kmb(1,k) Vmb(1,k)];

    maxoff(k,r) = max(howoff(k,:,r),[],2);
    maxpropoff(k,r) = max(propoff(k,:,r),[],2);

    dxdt1 = zeros(size(x1Kma,1),2,size(C,2));

    xlin1 = zeros(size(x1Kma,1),3,size(C,2));
```

```
    for i = 1:size(C,2)

        for j = 2:(size(t,1) - 1)

            dxdt1(j,1,i) = (x1rand(j + 1,1,k,i,r).*(t(j,1) - t(j -
1,1)) - x1rand(j,1,k,i,r).*(2.*t(j,1) - t(j + 1,1) - t(j - 1,1)) -
x1rand(j - 1,1,k,i,r).*(t(j + 1,1) - t(j,1))./(2.*(t(j + 1,1) -
t(j,1)).*(t(j,1) - t(j - 1,1)));

            dxdt1(j,2,i) = (x1rand(j + 1,2,k,i,r).*(t(j,1) - t(j -
1,1)) - x1rand(j,2,k,i,r).*(2.*t(j,1) - t(j + 1,1) - t(j - 1,1)) -
x1rand(j - 1,2,k,i,r).*(t(j + 1,1) - t(j,1))./(2.*(t(j + 1,1) -
t(j,1)).*(t(j,1) - t(j - 1,1)));

        end

        dxdt1(size(dxdt1,1),:,i) = (x1rand(size(x1rand,1),1:2,k,i,r) -
x1rand(size(x1rand,1) - 1,1:2,k,i,r))./(t(size(t,1),1) - t(size(t,1) -
1,1));

        dxdt1(1,:,i) = 2.*dxdt1(2,:,i) - dxdt1(3,:,i);

        xlin1(:,3,i) = C(1,i).*ones(size(xlin1,1),1);

        xlin1(:,2,i) = x1rand(:,2,k,i,r);

        xlin1(:,1,i) = x1rand(:,1,k,i,r);

    end

    Beta1 = lsqnonlin(@TCA_efflux_model_liu_nlin_thesis,b01,[0 0 0 0
0],2.*b01,optimset('Display','off'),xlin1,dxdt1);

    howoffrand(k,:,r) = abs(Beta1 - [Kma(1,k) Vma(1,k) Ke4(1,k)
Kmb(1,k) Vmb(1,k)]);
    propoffrand(k,:,r) = howoffrand(k,:,r)./[Kma(1,k) Vma(1,k) Ke4(1,k)
Kmb(1,k) Vmb(1,k)];

    maxoffrand(k,r) = max(howoffrand(k,:,r),[],2);
    maxpropoffrand(k,r) = max(propoffrand(k,:,r),[],2);

    % Conditional statements to assess which regression-determined
    % parameter is farther from initial parameter
    if propoff(k,1,r) == maxpropoff(k,r)

        whichoff(k,1,r) = 1;

    elseif propoff(k,2,r) == maxpropoff(k,r)

        whichoff(k,2,r) = 1;

    elseif propoff(k,3,r) == maxpropoff(k,r)
```

```
        whichoff(k,3,r) = 1;

    elseif propoff(k,4,r) == maxpropoff(k,r)

        whichoff(k,4,r) = 1;

    else

        whichoff(k,5,r) = 1;

    end
    if propoffrand(k,1,r) == maxpropoffrand(k,r)

        whichoffrand(k,1,r) = 1;

    elseif propoffrand(k,2,r) == maxpropoffrand(k,r)

        whichoffrand(k,2,r) = 1;

    elseif propoffrand(k,3,r) == maxpropoffrand(k,r)

        whichoffrand(k,3,r) = 1;

    elseif propoffrand(k,4,r) == maxpropoffrand(k,r)

        whichoffrand(k,4,r) = 1;

    else

        whichoffrand(k,5,r) = 1;

    end

end

whichoffsum(r,:) = sum(whichoff(:,:,r),1);
whichoffsumrand(r,:) = sum(whichoffrand(:,:,r),1);

probmore20(1,r) = (size(find(maxpropoff(:,r) >
0.2),1))./(size(maxpropoff(:,r),1));
probmore20rand(1,r) = (size(find(maxpropoffrand(:,r) >
0.2),1))./(size(maxpropoffrand(:,r),1));
probmore40(1,r) = (size(find(maxpropoff(:,r) >
0.4),1))./(size(maxpropoff(:,r),1));
probmore40rand(1,r) = (size(find(maxpropoffrand(:,r) >
0.4),1))./(size(maxpropoffrand(:,r),1));

end

% Matrices to store mean %parameter error and std dev of %parameter
error
meanmaxpropoff = mean(maxpropoff);
meanmaxpropoffrand = mean(maxpropoffrand);
```

```
totmean = mean(meanmaxpropoff,2);
totmeanrand = mean(meanmaxpropoffrand,2);
stdmaxpropoff = std(maxpropoff);
stdmaxpropoffrand = std(maxpropoffrand);
allpropoff = zeros(size(maxpropoff,2).*size(maxpropoff,1),1);
allpropoffrand = zeros(size(maxpropoff,2).*size(maxpropoffrand,1),1);

for r = 1:size(maxpropoff,2)

    allpropoff(((r - 1).*(size(maxpropoff,1)) +
1):(r.*(size(maxpropoff,1))),1) = maxpropoff(:,r);
    allpropoffrand(((r - 1).*(size(maxpropoffrand,1)) +
1):(r.*(size(maxpropoffrand,1))),1) = maxpropoffrand(:,r);

end

totstd = std(allpropoff);
totstdrand = std(allpropoffrand);
```

```
% Jose Ricardo Llamas Vidales
% ODE model following Liu et al, 1999, published model

function dxdt =
TCA_efflux_eq_liu_thesis(t,x,Kma,Vma,Ke4,Kmb,Vmb,C,topen,Vol_buff,tpre,
numcells,protpcell)

dxdt = [(Vma.*x(3)./(Kma + x(3))) - Ke4.*(x(1) - x(2));
        Vma.*x(3)./(Kma + x(3)) - (Vmb.*x(2)./(Kmb + x(2)));
        ((Ke4.*(x(1) - x(2))) - (Vma.*x(3)./(Kma +
x(3)))).*numcells.*protpcell.*(10.^(-3))./Vol_buff];
```

```
% Jose Ricardo Llamas Vidales
% Nonlinear regression function to calculate parameter values

function F = TCA_efflux_solver_nlin(beta,x,dxdt)

F = zeros(size(dxdt,2),size(dxdt,1));

for i = 1:size(dxdt,2)

F(i,:) = [(beta(2).*x(:,1,i)'./(beta(1) + x(:,1,i)')) -
beta(3).*x(:,2,i)' - dxdt(:,i)'];

end
```

```
% Jose Ricardo Llamas Vidales
% Code to run numerical model to reduce experimental conditions in
Hepatic
% transport studies at steady state conditions

clear all;
close all;

recycler_counter = 5;
num_parameters = 5;

% Variables

% Parameters from Liu et al, 1999.
Kmareal = 28;%uM
Vmareal = 1.19;%nmol/min/mgprotein
Ke4real = 0.849;%1/min
Kmbreal = 1.03;%nmol/mgprotein
Vmbreal = 1.82;%nmol/min/mgprotein

C = [0.05 0.1 1]; %uM, buffer concentration
numcells = 2.*(10.^5); %cell, number of cells in culture
protpcell = 1.5.*(10.^(-6)); %mgprotein/cell, protein per cell
Vol_conc = 0.001; %L
Vol_buff = 0.001; %L, amount of buffer values

IC = [0 0 0];

Kma = 28.*(0.5.*ones(1,1000));%uM

% Set of matrices to collect all data generated by model
howoff = zeros(size(Kma,2),num_parameters,recycler_counter);
maxoff = zeros(size(Kma,2),recycler_counter);
propoff = zeros(size(Kma,2),num_parameters,recycler_counter);
maxpropoff = zeros(size(Kma,2),recycler_counter);
whichoff = zeros(size(Kma,2),num_parameters,recycler_counter);
whichoffsum = zeros(recycler_counter,num_parameters);
howoffrand = zeros(size(Kma,2),num_parameters,recycler_counter);
maxoffrand = zeros(size(Kma,2),recycler_counter);
propoffrand = zeros(size(Kma,2),num_parameters,recycler_counter);
maxpropoffrand = zeros(size(Kma,2),recycler_counter);
whichoffrand = zeros(size(Kma,2),num_parameters,recycler_counter);
whichoffsumrand = zeros(recycler_counter,num_parameters);
probmore20 = zeros(1,recycler_counter);
probmore40 = zeros(1,recycler_counter);
probmorerand20 = zeros(1,recycler_counter);
probmorerand40 = zeros(1,recycler_counter);

b01 = [Kmareal Vmareal Ke4real Kmbreal Vmbreal]; %Initial "guess" for
nonlinear regression calculation

% Matrices to store steaty state accumulations
Cmax = zeros(size(C,2),size(IC,2),size(Kma,2),recycler_counter);
Cmaxrand = zeros(size(C,2),size(IC,2),size(Kma,2),recycler_counter);
```

```
for r = 1:recycler_counter

    rand('twister',sum(100*clock));
    randn('state',sum(100*clock));

    % Matrices of randomly generated parameter values
    Kma = 28.*(0.5.*ones(1,1000) + rand(1,1000));%uM
    Vma = 1.19.*(0.5.*ones(1,1000) + rand(1,1000));%nmol/min/mgprotein
    Ke4 = 0.849.*(0.5.*ones(1,1000) + rand(1,1000));%1/min
    Kmb = 1.03.*(0.5.*ones(1,1000) + rand(1,1000));%nmol/mgprotein
    Vmb = 1.82.*(0.5.*ones(1,1000) + rand(1,1000));%nmol/min/mgprotein

% Loop to create steady state accumulation data
for i = 1:size(Vma,2)

        for n = 1:size(C,2)

            uptakerate = Vma(1,i).*C(1,n)./(Kma(1,i) + C(1,n));

            Cmax(n,2,i,r) = (uptakerate.*Kmb(1,i))./(Vmb(1,i) -
uptakerate);

            Cmax(n,1,i,r) = Cmax(n,2,i,r) + uptakerate./Ke4(1,i);

            Cmax(n,3,i,r) = C(1,n);

            Cmaxrand(n,3,i,r) = C(1,n);

        end

    Cmaxrand(:,:,i,r) = Cmax(:,:,i,r).*(ones(size(C,2),size(IC,2)) +
0.1.*randn(size(C,2),size(IC,2))); %This step adds "experimental" error
to accumulation measurements

end


% This loop uses accumulation loop results to produce new parameters
% determined by nonlinear regression analysis
for k = 1:size(Kma,2)

    Beta1 = lsqnonlin(@TCA_efflux_model_liu_nlin_thesis,b01,[0 0 0 0
0],2.*b01,optimset('Display','off'),Cmax(:,:,k,r));

    howoff(k,:,r) = abs(Beta1 - [Kma(1,k) Vma(1,k) Ke4(1,k) Kmb(1,k)
Vmb(1,k)]);
    propoff(k,:,r) = howoff(k,:,r)./[Kma(1,k) Vma(1,k) Ke4(1,k)
Kmb(1,k) Vmb(1,k)];

    maxoff(k,r) = max(howoff(k,:,r),[],2);
    maxpropoff(k,r) = max(propoff(k,:,r),[],2);
```

```
    % Conditional statements to assess which regression-determined
    % parameter is farther from initial parameter
    if propoff(k,1,r) == maxpropoff(k,r)

        whichoff(k,1,r) = 1;

    elseif propoff(k,2,r) == maxpropoff(k,r)

        whichoff(k,2,r) = 1;

    elseif propoff(k,3,r) == maxpropoff(k,r)

        whichoff(k,3,r) = 1;

    elseif propoff(k,4,r) == maxpropoff(k,r)

        whichoff(k,4,r) = 1;

    else

        whichoff(k,5,r) = 1;

    end

    Beta1 = lsqnonlin(@TCA_efflux_model_liu_nlin_thesis,b01,[0 0 0 0
0],2.*b01,optimset('Display','off'),Cmaxrand(:,:,k,r));

    howoffrand(k,:,r) = abs(Beta1 - [Kma(1,k) Vma(1,k) Ke4(1,k)
Kmb(1,k) Vmb(1,k)]);
    propoffrand(k,:,r) = howoffrand(k,:,r)./[Kma(1,k) Vma(1,k) Ke4(1,k)
Kmb(1,k) Vmb(1,k)];

    maxoffrand(k,r) = max(howoffrand(k,:,r),[],2);
    maxpropoffrand(k,r) = max(propoffrand(k,:,r),[],2);

    % Conditional statements to assess which regression-determined
    % parameter is farther from initial parameter
    if propoffrand(k,1,r) == maxpropoffrand(k,r)

        whichoffrand(k,1,r) = 1;

    elseif propoffrand(k,2,r) == maxpropoffrand(k,r)

        whichoffrand(k,2,r) = 1;

    elseif propoffrand(k,3,r) == maxpropoffrand(k,r)

        whichoffrand(k,3,r) = 1;

    elseif propoffrand(k,4,r) == maxpropoffrand(k,r)

        whichoffrand(k,4,r) = 1;
```

```
    else

        whichoffrand(k,5,r) = 1;

    end
end


whichoffsum(r,:) = sum(whichoff(:,:,r),1);
whichoffsumrand(r,:) = sum(whichoffrand(:,:,r),1);

probmore20(1,r) = (size(find(maxpropoff(:,r) >
0.2),1))./(size(maxpropoff(:,r),1));
probmorerand20(1,r) = (size(find(maxpropoffrand(:,r) >
0.2),1))./(size(maxpropoffrand(:,r),1));
probmore40(1,r) = (size(find(maxpropoff(:,r) >
0.4),1))./(size(maxpropoff(:,r),1));
probmorerand40(1,r) = (size(find(maxpropoffrand(:,r) >
0.4),1))./(size(maxpropoffrand(:,r),1));

end

% Matrices to store mean %parameter error and std dev of %parameter
error
meanmaxpropoff = mean(maxpropoff);
meanmaxpropoffrand = mean(maxpropoffrand);
totmean = mean(meanmaxpropoff,2);
totmeanrand = mean(meanmaxpropoffrand,2);
stdmaxpropoff = std(maxpropoff);
stdmaxpropoffrand = std(maxpropoffrand);
allpropoff = zeros(size(maxpropoff,2).*size(maxpropoff,1),1);
allpropoffrand = zeros(size(maxpropoff,2).*size(maxpropoffrand,1),1);

for r = 1:size(maxpropoff,2)

    allpropoff(((r - 1).*(size(maxpropoff,1)) +
1):(r.*(size(maxpropoff,1))),1) = maxpropoff(:,r);
    allpropoffrand(((r - 1).*(size(maxpropoffrand,1)) +
1):(r.*(size(maxpropoffrand,1))),1) = maxpropoffrand(:,r);

end

totstd = std(allpropoff);
totstdrand = std(allpropoffrand);
```

```
% Jose Ricardo Llamas Vidales
% Nonlinear regression function to calculate parameter values
% Steady State condition

function F = TCA_efflux_model_liu_nlin_thesis(beta,x)

F = zeros(2,size(x,1));

F(1,:) = beta(2).*x(:,3)./(beta(1) + x(:,3)) - beta(3).*(x(:,1) -
x(:,2));
F(2,:) = beta(2).*x(:,3)./(beta(1) + x(:,3)) -
beta(5).*x(:,2)./(beta(4) + x(:,2));
```

```
% Jose Ricardo Llamas Vidales
% Code to run sensitivity analysis for numerical model to reduce
% experimental conditions in Hepatic transport studies

clear all;
close all;

recycler_counter = 5;
num_parameters = 5;


% Variables

% Parameters from Liu et al, 1999 multiplied by a range from 0.01 to
100
Kmareal = 28.*logspace(-2,2,5); %uM
Vmareal = 1.19.*logspace(-2,2,5); %nmol/min/mgprotein
Ke4real = 0.849.*logspace(-2,2,5); %1/min
Kmbreal = 1.03.*logspace(-2,2,5); %nmol/mgprotein
Vmbreal = 1.82.*logspace(-2,2,5); %nmol/min/mgprotein

tspan = 45; %min

C = [1 10 20 50 100];%uM, buffer concentration
numcells = 2.*(10.^5); %cell, number of cells in culture
protpcell = 1.5.*(10.^(-6)); %mgprotein/cell, protein per cell
Vol_conc = 0.001; %L
t = [0 0.5 1 1.5 2 5 10];%min, time points of interest

IC = [0 0 0];%Initial condition of intracellular levels of accumulation

Kma = 28.*(0.5.*ones(1,1000));%uM

% Set of matrices to collect all data generated by model
howoff =
zeros(size(Kma,2),num_parameters,recycler_counter,size(Kmareal,2),num_p
arameters);
maxoff =
zeros(size(Kma,2),recycler_counter.*size(Kmareal,2).*num_parameters);
propoff =
zeros(size(Kma,2),num_parameters,recycler_counter,size(Kmareal,2),num_p
arameters);
maxpropoff =
zeros(size(Kma,2),recycler_counter.*size(Kmareal,2).*num_parameters);
whichoff =
zeros(size(Kma,2),num_parameters,recycler_counter,size(Kmareal,2),num_p
arameters);
whichoffsum =
zeros(recycler_counter.*size(Kmareal,2).*num_parameters,num_parameters)
;
howoffrand =
zeros(size(Kma,2),num_parameters,recycler_counter,size(Kmareal,2),num_p
arameters);
maxoffrand =
zeros(size(Kma,2),recycler_counter.*size(Kmareal,2).*num_parameters);
```

```
propoffrand =
zeros(size(Kma,2),num_parameters,recycler_counter,size(Kmareal,2),num_p
arameters);
maxpropoffrand =
zeros(size(Kma,2),recycler_counter.*size(Kmareal,2).*num_parameters);
whichoffrand =
zeros(size(Kma,2),num_parameters,recycler_counter,size(Kmareal,2),num_p
arameters);
whichoffsumrand =
zeros(recycler_counter.*size(Kmareal,2).*num_parameters,num_parameters)
;
probmore20 = zeros(size(Kmareal,2).*num_parameters,recycler_counter);
probmore40 = zeros(size(Kmareal,2).*num_parameters,recycler_counter);
probmore20rand =
zeros(size(Kmareal,2).*num_parameters,recycler_counter);
probmore40rand =
zeros(size(Kmareal,2).*num_parameters,recycler_counter);
meanmaxpropoff = zeros(size(Kmareal,2).*num_parameters,
recycler_counter);
meanmaxpropoffrand = zeros(size(Kmareal,2).*num_parameters,
recycler_counter);
stdmaxpropoff = zeros(size(Kmareal,2).*num_parameters,
recycler_counter);
stdmaxpropoffrand = zeros(size(Kmareal,2).*num_parameters,
recycler_counter);
totmean = zeros(size(Kmareal,2),num_parameters);
totmeanrand = zeros(size(Kmareal,2),num_parameters);
totstd = zeros(size(Kmareal,2),num_parameters);
totstdrand = zeros(size(Kmareal,2),num_parameters);

% Matrices to capture accumulation data generated by ODE model
x1Kma =
zeros(size(t,2),size(IC,2),size(Kma,2),size(C,2),recycler_counter,size(
Kmareal,2),num_parameters);
x1rand =
zeros(size(t,2),size(IC,2),size(Kma,2),size(C,2),recycler_counter,size(
Kmareal,2),num_parameters);

% Matrices to capture accumulation data as concentration
ConcKma =
zeros(size(t,2),size(IC,2),size(Kma,2),size(C,2),recycler_counter,size(
Kmareal,2),num_parameters);
Concrand =
zeros(size(t,2),size(IC,2),size(Kma,2),size(C,2),recycler_counter,size(
Kmareal,2),num_parameters);

% Matrices to capture maximum concentrations
CmaxKma =
zeros(1,size(Kma,2),2,size(C,2),recycler_counter,size(Kmareal,2),num_pa
rameters);
Cmaxrand =
zeros(1,size(Kma,2),2,size(C,2),recycler_counter,size(Kmareal,2),num_pa
rameters);
```

```
tconstKma =
zeros(1,size(Kma,2),2,size(C,2),recycler_counter,size(Kmareal,2),num_pa
rameters);

topen = 3; %min, time for tight junctions to open
Vol_buff = 0.001; %L, amount of buffer volume
tpre = 15; %min

for u = 1:num_parameters

    for v = 1:size(Kmareal,2)

for r = 1:recycler_counter

    rand('twister',sum(100*clock));
    randn('state',sum(100*clock));

    %Conditional statements to set fix one parameter at a specific
value
    %and randomly generate the rest
    if u == 1

        Kma = Kmareal(1,v).*ones(1,1000);%.*logspace(-2,2,5); %uM
        Vma = Vmareal(1,3).*(0.5.*ones(1,1000) +
rand(1,1000));%.*logspace(-2,2,5); %nmol/min/mgprotein
        Ke4 = Ke4real(1,3).*(0.5.*ones(1,1000) +
rand(1,1000));%.*logspace(-2,2,5); %1/min
        Kmb = Kmbreal(1,3).*(0.5.*ones(1,1000) +
rand(1,1000));%.*logspace(-2,2,5); %nmol/mgprotein
        Vmb = Vmbreal(1,3).*(0.5.*ones(1,1000) +
rand(1,1000));%.*logspace(-2,2,5); %nmol/min/mgprotein
        b01 = [Kmareal(1,v) Vmareal(1,3) Ke4real(1,3) Kmbreal(1,3)
Vmbreal(1,3)];

    elseif u == 2

        Kma = Kmareal(1,3).*(0.5.*ones(1,1000) +
rand(1,1000));%.*logspace(-2,2,5); %uM
        Vma = Vmareal(1,v).*ones(1,1000);%.*logspace(-2,2,5);
%nmol/min/mgprotein
        Ke4 = Ke4real(1,3).*(0.5.*ones(1,1000) +
rand(1,1000));%.*logspace(-2,2,5); %1/min
        Kmb = Kmbreal(1,3).*(0.5.*ones(1,1000) +
rand(1,1000));%.*logspace(-2,2,5); %nmol/mgprotein
        Vmb = Vmbreal(1,3).*(0.5.*ones(1,1000) +
rand(1,1000));%.*logspace(-2,2,5); %nmol/min/mgprotein
        b01 = [Kmareal(1,3) Vmareal(1,v) Ke4real(1,3) Kmbreal(1,3)
Vmbreal(1,3)];

    elseif u == 3

        Kma = Kmareal(1,3).*(0.5.*ones(1,1000) +
rand(1,1000));%.*logspace(-2,2,5); %uM
        Vma = Vmareal(1,3).*(0.5.*ones(1,1000) +
rand(1,1000));%.*logspace(-2,2,5); %nmol/min/mgprotein
```

```
        Ke4 = Ke4real(1,v).*ones(1,1000);%.*logspace(-2,2,5); %1/min
        Kmb = Kmbreal(1,3).*(0.5.*ones(1,1000) +
rand(1,1000));%.*logspace(-2,2,5); %nmol/mgprotein
        Vmb = Vmbreal(1,3).*(0.5.*ones(1,1000) +
rand(1,1000));%.*logspace(-2,2,5); %nmol/min/mgprotein
        b01 = [Kmareal(1,3) Vmareal(1,3) Ke4real(1,v) Kmbreal(1,3)
Vmbreal(1,3)];

    elseif u == 4

        Kma = Kmareal(1,3).*(0.5.*ones(1,1000) +
rand(1,1000));%.*logspace(-2,2,5); %uM
        Vma = Vmareal(1,3).*(0.5.*ones(1,1000) +
rand(1,1000));%.*logspace(-2,2,5); %nmol/min/mgprotein
        Ke4 = Ke4real(1,3).*(0.5.*ones(1,1000) +
rand(1,1000));%.*logspace(-2,2,5); %1/min
        Kmb = Kmbreal(1,v).*ones(1,1000);%.*logspace(-2,2,5);
%nmol/mgprotein
        Vmb = Vmbreal(1,3).*(0.5.*ones(1,1000) +
rand(1,1000));%.*logspace(-2,2,5); %nmol/min/mgprotein
        b01 = [Kmareal(1,3) Vmareal(1,3) Ke4real(1,3) Kmbreal(1,v)
Vmbreal(1,3)];

    elseif u == 5

        Kma = Kmareal(1,3).*(0.5.*ones(1,1000) +
rand(1,1000));%.*logspace(-2,2,5); %uM
        Vma = Vmareal(1,3).*(0.5.*ones(1,1000) +
rand(1,1000));%.*logspace(-2,2,5); %nmol/min/mgprotein
        Ke4 = Ke4real(1,3).*(0.5.*ones(1,1000) +
rand(1,1000));%.*logspace(-2,2,5); %1/min
        Kmb = Kmbreal(1,3).*(0.5.*ones(1,1000) +
rand(1,1000));%.*logspace(-2,2,5); %nmol/mgprotein
        Vmb = Vmbreal(1,v).*ones(1,1000);%.*logspace(-2,2,5);
%nmol/min/mgprotein
        b01 = [Kmareal(1,3) Vmareal(1,3) Ke4real(1,3) Kmbreal(1,3)
Vmbreal(1,v)];

    end

% Loop using ODE solver to produce accumulation data
for i = 1:size(Kma,2)

                    for n = 1:size(C,2)

                        IC(1,3) = C(1,n);

                        [t,x] =
ode23s(@TCA_efflux_eq_liu_thesis,t,IC,optimset('Display','off'),Kma(1,i
),Vma(1,i),Ke4(1,i),Kmb(1,i),Vmb(1,i),C(1,n),topen,Vol_buff,tpre,numcel
ls,protpcell);

                        x1Kma(:,:,i,n,r,v,u) = x;
```

```
                        x(:,3) =
x1Kma(:,3,i,n,r,v,u).*Vol_conc./(numcells.*protpcell);

                        x1rand(:,:,i,n,r,v,u) =
x1Kma(:,:,i,n,r,v,u).*(ones(size(x1Kma,1),size(x1Kma,2)) +
0.1.*(randn(size(x1Kma,1),size(x1Kma,2))));%This step adds
"experimental" error to accumulation measurements

                        ConcKma(:,:,i,n,r,v,u) =
numcells.*x.*protpcell./Vol_conc; %nM

                        Concrand(:,1:2,i,n,r,v,u) =
numcells.*x1rand(:,1:2,i,n,r,v,u).*protpcell./Vol_conc;

                        Concrand(:,3,i,n,r,v,u) =
x1rand(:,3,i,n,r,v,u);

                        CmaxKma(1,i,1,n,r,v,u) =
ConcKma(size(ConcKma,1),1,i,n,r,v,u);

                        CmaxKma(1,i,2,n,r,v,u) =
ConcKma(size(ConcKma,1),2,i,n,r,v,u);

                        Cmaxrand(1,i,1,n,r,v,u) =
Concrand(size(Concrand,1),1,i,n,r,v,u);

                        Cmaxrand(1,i,2,n,r,v,u) =
Concrand(size(Concrand,1),2,i,n,r,v,u);

                        p = find(ConcKma(:,1,i,n,r,v,u) >= (1 - exp(-
1)).*CmaxKma(1,i,1,n,r,v,u),1);

                        tconstKma(1,i,1,n,r,v,u) = ((1 - exp(-
1)).*CmaxKma(1,i,1,n,r,v,u) - ConcKma((p - 1),1,i,n,r,v,u)).*(t(p,1) -
t((p - 1),1))./(ConcKma(p,1,i,n,r,v,u) - ConcKma((p - 1),1,i,n,r,v,u))
+ t((p - 1),1);

                        q = find(ConcKma(:,2,i,n,r,v,u) >= (1 - exp(-
1)).*CmaxKma(1,i,2,n,r,v,u),1);

                        tconstKma(1,i,2,n,r,v,u) = ((1 - exp(-
1)).*CmaxKma(1,i,2,n,r,v,u) - ConcKma((q - 1),2,i,n,r,v,u)).*(t(q,1) -
t((q - 1),1))./(ConcKma(q,2,i,n,r,v,u) - ConcKma((q - 1),2,i,n,r,v,u))
+ t((q - 1),1);

                    end

end


% This loop uses accumulation loop results to produce new parameters
% determined by nonlinear regression analysis
for k = 1:size(Kma,2)
```

```
    dxdt1 = zeros(size(x1Kma,1),2,size(C,2));

    dxdtreal1 = zeros(size(x1Kma,1),3,size(C,2));

    xlin1 = zeros(size(x1Kma,1),3,size(C,2));

    for i = 1:size(C,2)

        for j = 2:(size(t,1) - 1)

            dxdt1(j,1,i) = (x1Kma(j + 1,1,k,i,r,v,u).*(t(j,1) - t(j -
1,1)) - x1Kma(j,1,k,i,r,v,u).*(2.*t(j,1) - t(j + 1,1) - t(j - 1,1)) -
x1Kma(j - 1,1,k,i,r,v,u).*(t(j + 1,1) - t(j,1))./(2.*(t(j + 1,1) -
t(j,1)).*(t(j,1) - t(j - 1,1)));

            dxdt1(j,2,i) = (x1Kma(j + 1,2,k,i,r,v,u).*(t(j,1) - t(j -
1,1)) - x1Kma(j,2,k,i,r,v,u).*(2.*t(j,1) - t(j + 1,1) - t(j - 1,1)) -
x1Kma(j - 1,2,k,i,r,v,u).*(t(j + 1,1) - t(j,1))./(2.*(t(j + 1,1) -
t(j,1)).*(t(j,1) - t(j - 1,1)));

        end

        dxdt1(size(dxdt1,1),:,i) = (x1Kma(size(x1Kma,1),1:2,k,i,r,v,u)
- x1Kma(size(x1Kma,1) - 1,1:2,k,i,r,v,u))./(t(size(t,1),1) -
t(size(t,1) - 1,1));

        dxdt1(1,:,i) = 2.*dxdt1(2,:,i) - dxdt1(3,:,i);

        xlin1(:,3,i) = C(1,i).*ones(size(xlin1,1),1);

        xlin1(:,2,i) = x1Kma(:,2,k,i,r,v,u);

        xlin1(:,1,i) = x1Kma(:,1,k,i,r,v,u);

        dxdtreal1(:,1,i) = (Vma(1,k).*x1Kma(:,3,k,i,r,v,u)./(Kma(1,k) +
x1Kma(:,3,k,i,r,v,u))) - Ke4(1,k).*(x1Kma(:,1,k,i,r,v,u) -
x1Kma(:,2,k,i,r,v,u));
        dxdtreal1(:,2,i) = (Vma(1,k).*x1Kma(:,3,k,i,r,v,u)./(Kma(1,k) +
x1Kma(:,3,k,i,r,v,u))) - (Vmb(1,k).*x1Kma(:,2,k,i,r,v,u)./(Kmb(1,k) +
x1Kma(:,2,k,i,r,v,u)));

    end

    Beta1 = lsqnonlin(@TCA_efflux_model_liu_nlin_thesis,b01,[0 0 0 0
0],2.*b01,optimset('Display','off'),xlin1,dxdt1);

    howoff(k,:,r,v,u) = abs(Beta1 - [Kma(1,k) Vma(1,k) Ke4(1,k)
Kmb(1,k) Vmb(1,k)]);
    propoff(k,:,r,v,u) = howoff(k,:,r,v,u)./[Kma(1,k) Vma(1,k) Ke4(1,k)
Kmb(1,k) Vmb(1,k)];
```

```
    maxoff(k,r + recycler_counter.*(v - 1) +
recycler_counter.*size(Kmareal,2).*(u - 1)) =
max(howoff(k,:,r,v,u),[],2);
    maxpropoff(k,r + recycler_counter.*(v - 1) +
recycler_counter.*size(Kmareal,2).*(u - 1)) =
max(propoff(k,:,r,v,u),[],2);

    dxdt1 = zeros(size(x1Kma,1),2,size(C,2));

    xlin1 = zeros(size(x1Kma,1),3,size(C,2));

    for i = 1:size(C,2)

        for j = 2:(size(t,1) - 1)

            dxdt1(j,1,i) = (x1rand(j + 1,1,k,i,r,v,u).*(t(j,1) - t(j -
1,1)) - x1rand(j,1,k,i,r,v,u).*(2.*t(j,1) - t(j + 1,1) - t(j - 1,1)) -
x1rand(j - 1,1,k,i,r,v,u).*(t(j + 1,1) - t(j,1))./(2.*(t(j + 1,1) -
t(j,1)).*(t(j,1) - t(j - 1,1)));

            dxdt1(j,2,i) = (x1rand(j + 1,2,k,i,r,v,u).*(t(j,1) - t(j -
1,1)) - x1rand(j,2,k,i,r,v,u).*(2.*t(j,1) - t(j + 1,1) - t(j - 1,1)) -
x1rand(j - 1,2,k,i,r,v,u).*(t(j + 1,1) - t(j,1))./(2.*(t(j + 1,1) -
t(j,1)).*(t(j,1) - t(j - 1,1)));

        end

        dxdt1(size(dxdt1,1),:,i) =
(x1rand(size(x1rand,1),1:2,k,i,r,v,u) - x1rand(size(x1rand,1) -
1,1:2,k,i,r,v,u))./(t(size(t,1),1) - t(size(t,1) - 1,1));

        dxdt1(1,:,i) = 2.*dxdt1(2,:,i) - dxdt1(3,:,i);

        xlin1(:,3,i) = C(1,i).*ones(size(xlin1,1),1);

        xlin1(:,2,i) = x1rand(:,2,k,i,r,v,u);

        xlin1(:,1,i) = x1rand(:,1,k,i,r,v,u);

    end

    Beta1 = lsqnonlin(@TCA_efflux_model_liu_nlin_thesis,b01,[0 0 0 0
0],2.*b01,optimset('Display','off'),xlin1,dxdt1);

    howoffrand(k,:,r,v,u) = abs(Beta1 - [Kma(1,k) Vma(1,k) Ke4(1,k)
Kmb(1,k) Vmb(1,k)]);
    propoffrand(k,:,r,v,u) = howoffrand(k,:,r,v,u)./[Kma(1,k) Vma(1,k)
Ke4(1,k) Kmb(1,k) Vmb(1,k)];

    maxoffrand(k,r + recycler_counter.*(v - 1) +
recycler_counter.*size(Kmareal,2).*(u - 1)) =
max(howoffrand(k,:,r,v,u),[],2);
```

```
    maxpropoffrand(k,r + recycler_counter.*(v - 1) +
recycler_counter.*size(Kmareal,2).*(u - 1)) =
max(propoffrand(k,:,r,v,u),[],2);

    % Conditional statements to assess which regression-determined
    % parameter is farther from initial parameter
    if propoff(k,1,r,v,u) == maxpropoff(k,r + recycler_counter.*(v - 1)
+ recycler_counter.*size(Kmareal,2).*(u - 1))

        whichoff(k,1,r,v,u) = 1;

    elseif propoff(k,2,r,v,u) == maxpropoff(k,r + recycler_counter.*(v
- 1) + recycler_counter.*size(Kmareal,2).*(u - 1))

        whichoff(k,2,r,v,u) = 1;

    elseif propoff(k,3,r,v,u) == maxpropoff(k,r + recycler_counter.*(v
- 1) + recycler_counter.*size(Kmareal,2).*(u - 1))

        whichoff(k,3,r,v,u) = 1;

    elseif propoff(k,4,r,v,u) == maxpropoff(k,r + recycler_counter.*(v
- 1) + recycler_coúnter.*size(Kmareal,2).*(u - 1))

        whichoff(k,4,r,v,u) = 1;

    else

        whichoff(k,5,r,v,u) = 1;

    end
    if propoffrand(k,1,r,v,u) == maxpropoffrand(k,r +
recycler_counter.*(v - 1) + recycler_counter.*size(Kmareal,2).*(u - 1))

        whichoffrand(k,1,r,v,u) = 1;

    elseif propoffrand(k,2,r,v,u) == maxpropoffrand(k,r +
recycler_counter.*(v - 1) + recycler_counter.*size(Kmareal,2).*(u - 1))

        whichoffrand(k,2,r,v,u) = 1;

    elseif propoffrand(k,3,r,v,u) == maxpropoffrand(k,r +
recycler_counter.*(v - 1) + recycler_counter.*size(Kmareal,2).*(u - 1))

        whichoffrand(k,3,r,v,u) = 1;

    elseif propoffrand(k,4,r,v,u) == maxpropoffrand(k,r +
recycler_counter.*(v - 1) + recycler_counter.*size(Kmareal,2).*(u - 1))

        whichoffrand(k,4,r,v,u) = 1;

    else
```

```
        whichoffrand(k,5,r,v,u) = 1;

    end

end

whichoffsum(r + recycler_counter.*(v - 1) +
recycler_counter.*size(Kmareal,2).*(u - 1),:) =
sum(whichoff(:,:,r,v,u),1);
whichoffsumrand(r + recycler_counter.*(v - 1) +
recycler_counter.*size(Kmareal,2).*(u - 1),:) =
sum(whichoffrand(:,:,r,v,u),1);

probmore20(v + size(Kmareal,2).*(u - 1),r) = (size(find(maxpropoff(:,r
+ recycler_counter.*(v - 1) + recycler_counter.*size(Kmareal,2).*(u -
1)) > 0.2),1))./(size(maxpropoff(:,r + recycler_counter.*(v - 1) +
recycler_counter.*size(Kmareal,2).*(u - 1)),1));
probmore20rand(v + size(Kmareal,2).*(u - 1),r) =
(size(find(maxpropoffrand(:,r + recycler_counter.*(v - 1) +
recycler_counter.*size(Kmareal,2).*(u - 1)) >
0.2),1))./(size(maxpropoffrand(:,r + recycler_counter.*(v - 1) +
recycler_counter.*size(Kmareal,2).*(u - 1)),1));
probmore40(v + size(Kmareal,2).*(u - 1),r) = (size(find(maxpropoff(:,r
+ recycler_counter.*(v - 1) + recycler_counter.*size(Kmareal,2).*(u -
1)) > 0.4),1))./(size(maxpropoff(:,r + recycler_counter.*(v - 1) +
recycler_counter.*size(Kmareal,2).*(u - 1)),1));
probmore40rand(v + size(Kmareal,2).*(u - 1),r) =
(size(find(maxpropoffrand(:,r + recycler_counter.*(v - 1) +
recycler_counter.*size(Kmareal,2).*(u - 1)) >
0.4),1))./(size(maxpropoffrand(:,r + recycler_counter.*(v - 1) +
recycler_counter.*size(Kmareal,2).*(u - 1)),1));

end

% Matrices to store mean %parameter error and std dev of %parameter
error
meanmaxpropoff((v + size(Kmareal,2).*(u - 1)),:) =
mean(maxpropoff(:,((v - 1).*recycler_counter + (u -
1).*size(Kmareal,2).*recycler_counter + 1):((u - 1).*size(Kmareal,2) +
v).*recycler_counter));
meanmaxpropoffrand((v + size(Kmareal,2).*(u - 1)),:) =
mean(maxpropoffrand(:,((v - 1).*recycler_counter + (u -
1).*size(Kmareal,2).*recycler_counter + 1):((u - 1).*size(Kmareal,2) +
v).*recycler_counter));
totmean(v,u) = mean(meanmaxpropoff((v + size(Kmareal,2).*(u -
1)),:),2);
totmeanrand(v,u) = mean(meanmaxpropoffrand((v + size(Kmareal,2).*(u -
1)),:),2);
stdmaxpropoff((v + size(Kmareal,2).*(u - 1)),:) = std(maxpropoff(:,((v
- 1).*recycler_counter + (u - 1).*size(Kmareal,2).*recycler_counter +
1):((u - 1).*size(Kmareal,2) + v).*recycler_counter));
stdmaxpropoffrand((v + size(Kmareal,2).*(u - 1)),:) =
std(maxpropoffrand(:,((v - 1).*recycler_counter + (u -
1).*size(Kmareal,2).*recycler_counter + 1):((u - 1).*size(Kmareal,2) +
v).*recycler_counter));
allpropoff = zeros(recycler_counter.*size(maxpropoff,1),1);
```

```
allpropoffrand = zeros(recycler_counter.*size(maxpropoffrand,1),1);

for r = 1:recycler_counter

    allpropoff(((r - 1).*size(maxpropoff,1) +
1):(size(maxpropoff,1).*r),1) = maxpropoff(:,r + (v -
1).*recycler_counter + (u - 1).*size(Kmareal,2).*recycler_counter);
    allpropoffrand(((r - 1).*size(maxpropoff,1) +
1):(size(maxpropoff,1).*r),1) = maxpropoffrand(:,r + (v -
1).*recycler_counter + (u - 1).*size(Kmareal,2).*recycler_counter);

end

totstd(v,u) = std(allpropoff);
totstdrand(v,u) = std(allpropoffrand);

    end
end
```

```
% Jose Ricardo Llamas Vidales
% Code to run sensitivity analysis for numerical model to reduce
% experimental conditions in Hepatic transport studies, steady state
% condition

clear all;
close all;

num_parameters = 5;
recycler_counter = 5;

% Variables

% Parameters from Liu et al, 1999 multiplied by a range from 0.01 to
100
Kmareal = 28.*logspace(-2,2,5); %uM
Vmareal = 1.19.*logspace(-2,2,5); %nmol/min/mgprotein
Ke4real = 0.849.*logspace(-2,2,5); %1/min
Kmbreal = 1.03.*logspace(-2,2,5); %nmol/mgprotein
Vmbreal = 1.82.*logspace(-2,2,5); %nmol/min/mgprotein
C = [0.05 0.1 1]; %uM, buffer concentration
numcells = 2.*(10.^5); %cell, number of cells in culture
protpcell = 1.5.*(10.^(-6)); %mgprotein/cell, protein per cell
Vol_conc = 0.001; %L
Vol_buff = 0.001; %L, amount of buffer volume

IC = [0 0 0];

Kma = 28.*(0.5.*ones(1,1000));%uM

% Set of matrices to collect all data generated by model
howoff =
zeros(size(Kma,2),num_parameters,recycler_counter,size(Kmareal,2),num_p
arameters);
maxoff =
zeros(size(Kma,2),recycler_counter.*size(Kmareal,2).*num_parameters);
propoff =
zeros(size(Kma,2),num_parameters,recycler_counter,size(Kmareal,2),num_p
arameters);
maxpropoff =
zeros(size(Kma,2),recycler_counter.*size(Kmareal,2).*num_parameters);
whichoff =
zeros(size(Kma,2),num_parameters,recycler_counter,size(Kmareal,2),num_p
arameters);
whichoffsum =
zeros(recycler_counter.*size(Kmareal,2).*num_parameters,num_parameters)
;
howoffrand =
zeros(size(Kma,2),num_parameters,recycler_counter,size(Kmareal,2),num_p
arameters);
maxoffrand =
zeros(size(Kma,2),recycler_counter.*size(Kmareal,2).*num_parameters);
propoffrand =
zeros(size(Kma,2),num_parameters,recycler_counter,size(Kmareal,2),num_p
arameters);
```

```
    elseif propoffrand(k,2,r,v,u) == maxpropoffrand(k,r +
recycler_counter.*(v - 1) + recycler_counter.*size(Kmareal,2).*(u - 1))

        whichoffrand(k,2,r,v,u) = 1;

    elseif propoffrand(k,3,r,v,u) == maxpropoffrand(k,r +
recycler_counter.*(v - 1) + recycler_counter.*size(Kmareal,2).*(u - 1))

        whichoffrand(k,3,r,v,u) = 1;

    elseif propoffrand(k,4,r,v,u) == maxpropoffrand(k,r +
recycler_counter.*(v - 1) + recycler_counter.*size(Kmareal,2).*(u - 1))

        whichoffrand(k,4,r,v,u) = 1;

    else

        whichoffrand(k,5,r,v,u) = 1;

    end



end

whichoffsum(r + recycler_counter.*(v - 1) +
recycler_counter.*size(Kmareal,2).*(u - 1),:) =
sum(whichoff(:,:,r,v,u),1);
whichoffsumrand(r + recycler_counter.*(v - 1) +
recycler_counter.*size(Kmareal,2).*(u - 1),:) =
sum(whichoffrand(:,:,r,v,u),1);

probmore20(v + size(Kmareal,2).*(u - 1),r) = (size(find(maxpropoff(:,r
+ recycler_counter.*(v - 1) + recycler_counter.*size(Kmareal,2).*(u -
1)) > 0.2),1))./(size(maxpropoff(:,r + recycler_counter.*(v - 1) +
recycler_counter.*size(Kmareal,2).*(u - 1)),1));
probmorerand20(v + size(Kmareal,2).*(u - 1),r) =
(size(find(maxpropoffrand(:,r + recycler_counter.*(v - 1) +
recycler_counter.*size(Kmareal,2).*(u - 1)) >
0.2),1))./(size(maxpropoffrand(:,r + recycler_counter.*(v - 1) +
recycler_counter.*size(Kmareal,2).*(u - 1)),1));
probmore40(v + size(Kmareal,2).*(u - 1),r) = (size(find(maxpropoff(:,r
+ recycler_counter.*(v - 1) + recycler_counter.*size(Kmareal,2).*(u -
1)) > 0.4),1))./(size(maxpropoff(:,r + recycler_counter.*(v - 1) +
recycler_counter.*size(Kmareal,2).*(u - 1)),1));
probmorerand40(v + size(Kmareal,2).*(u - 1),r) =
(size(find(maxpropoffrand(:,r + recycler_counter.*(v - 1) +
recycler_counter.*size(Kmareal,2).*(u - 1)) >
0.4),1))./(size(maxpropoffrand(:,r + recycler_counter.*(v - 1) +
recycler_counter.*size(Kmareal,2).*(u - 1)),1));


end
```

```
maxpropoffrand =
zeros(size(Kma,2),recycler_counter.*size(Kmareal,2).*num_parameters);
whichoffrand =
zeros(size(Kma,2),num_parameters,recycler_counter,size(Kmareal,2),num_p
arameters);
whichoffsumrand =
zeros(recycler_counter.*size(Kmareal,2).*num_parameters,num_parameters)
;
probmore20 = zeros(size(Kmareal,2).*num_parameters,recycler_counter);
probmore40 = zeros(size(Kmareal,2).*num_parameters,recycler_counter);
probmorerand20 =
zeros(size(Kmareal,2).*num_parameters,recycler_counter);
probmorerand40 =
zeros(size(Kmareal,2).*num_parameters,recycler_counter);
meanmaxpropoff = zeros(size(Kmareal,2).*num_parameters,
recycler_counter);
meanmaxpropoffrand = zeros(size(Kmareal,2).*num_parameters,
recycler_counter);
stdmaxpropoff = zeros(size(Kmareal,2).*num_parameters,
recycler_counter);
stdmaxpropoffrand = zeros(size(Kmareal,2).*num_parameters,
recycler_counter);
totmean = zeros(size(Kmareal,2),num_parameters);
totmeanrand = zeros(size(Kmareal,2),num_parameters);
totstd = zeros(size(Kmareal,2),num_parameters);
totstdrand = zeros(size(Kmareal,2),num_parameters);

% Matrices to store steaty state accumulations
Cmax =
zeros(size(C,2),size(IC,2),size(Kma,2),recycler_counter,size(Kmareal,2)
,num_parameters);
Cmaxrand =
zeros(size(C,2),size(IC,2),size(Kma,2),recycler_counter,size(Kmareal,2)
,num_parameters);


for u = 1:num_parameters

    for v = 1:size(Kmareal,2)

for r = 1:recycler_counter

    rand('twister',sum(100*clock));
    randn('state',sum(100*clock));

    %Conditional statements to set fix one parameter at a specific
value
    %and randomly generate the rest
    if u == 1

        Kma = Kmareal(1,v).*ones(1,1000);%uM
        Vma = Vmareal(1,3).*(0.5.*ones(1,1000) +
rand(1,1000));%nmol/min/mgprotein
        Ke4 = Ke4real(1,3).*(0.5.*ones(1,1000) + rand(1,1000));%1/min
```

```
        Kmb = Kmbreal(1,3).*(0.5.*ones(1,1000) +
rand(1,1000));%nmol/mgprotein
        Vmb = Vmbreal(1,3).*(0.5.*ones(1,1000) +
rand(1,1000));%nmol/min/mgprotein
        b01 = [Kmareal(1,v) Vmareal(1,3) Ke4real(1,3) Kmbreal(1,3)
Vmbreal(1,3)];

    elseif u == 2

        Kma = Kmareal(1,3).*(0.5.*ones(1,1000) +
rand(1,1000));%.*logspace(-2,2,5); %uM
        Vma = Vmareal(1,v).*ones(1,1000);%.*logspace(-2,2,5);
%nmol/min/mgprotein
        Ke4 = Ke4real(1,3).*(0.5.*ones(1,1000) +
rand(1,1000));%.*logspace(-2,2,5); %1/min
        Kmb = Kmbreal(1,3).*(0.5.*ones(1,1000) +
rand(1,1000));%.*logspace(-2,2,5); %nmol/mgprotein
        Vmb = Vmbreal(1,3).*(0.5.*ones(1,1000) +
rand(1,1000));%.*logspace(-2,2,5); %nmol/min/mgprotein
        b01 = [Kmareal(1,3) Vmareal(1,v) Ke4real(1,3) Kmbreal(1,3)
Vmbreal(1,3)];

    elseif u == 3

        Kma = Kmareal(1,3).*(0.5.*ones(1,1000) +
rand(1,1000));%.*logspace(-2,2,5); %uM
        Vma = Vmareal(1,3).*(0.5.*ones(1,1000) +
rand(1,1000));%.*logspace(-2,2,5); %nmol/min/mgprotein
        Ke4 = Ke4real(1,v).*ones(1,1000);%.*logspace(-2,2,5); %1/min
        Kmb = Kmbreal(1,3).*(0.5.*ones(1,1000) +
rand(1,1000));%.*logspace(-2,2,5); %nmol/mgprotein
        Vmb = Vmbreal(1,3).*(0.5.*ones(1,1000) +
rand(1,1000));%.*logspace(-2,2,5); %nmol/min/mgprotein
        b01 = [Kmareal(1,3) Vmareal(1,3) Ke4real(1,v) Kmbreal(1,3)
Vmbreal(1,3)];

    elseif u == 4

        Kma = Kmareal(1,3).*(0.5.*ones(1,1000) +
rand(1,1000));%.*logspace(-2,2,5); %uM
        Vma = Vmareal(1,3).*(0.5.*ones(1,1000) +
rand(1,1000));%.*logspace(-2,2,5); %nmol/min/mgprotein
        Ke4 = Ke4real(1,3).*(0.5.*ones(1,1000) +
rand(1,1000));%.*logspace(-2,2,5); %1/min
        Kmb = Kmbreal(1,v).*ones(1,1000);%.*logspace(-2,2,5);
%nmol/mgprotein
        Vmb = Vmbreal(1,3).*(0.5.*ones(1,1000) +
rand(1,1000));%.*logspace(-2,2,5); %nmol/min/mgprotein
        b01 = [Kmareal(1,3) Vmareal(1,3) Ke4real(1,3) Kmbreal(1,v)
Vmbreal(1,3)];

    elseif u == 5

        Kma = Kmareal(1,3).*(0.5.*ones(1,1000) +
rand(1,1000));%.*logspace(-2,2,5); %uM
```

```
        Vma = Vmareal(1,3).*(0.5.*ones(1,1000) +
rand(1,1000));%.*logspace(-2,2,5); %nmol/min/mgprotein
        Ke4 = Ke4real(1,3).*(0.5.*ones(1,1000) +
rand(1,1000));%.*logspace(-2,2,5); %1/min
        Kmb = Kmbreal(1,3).*(0.5.*ones(1,1000) +
rand(1,1000));%.*logspace(-2,2,5); %nmol/mgprotein
        Vmb = Vmbreal(1,v).*ones(1,1000);%.*logspace(-2,2,5);
%nmol/min/mgprotein
        b01 = [Kmareal(1,3) Vmareal(1,3) Ke4real(1,3) Kmbreal(1,3)
Vmbreal(1,v)];

    end


% Loop to create steady state accumulation data
for i = 1:size(Vma,2)

        for n = 1:size(C,2)

            uptakerate = Vma(1,i).*C(1,n)./(Kma(1,i) + C(1,n));

            Cmax(n,2,i,r,v,u) = (uptakerate.*Kmb(1,i))./(Vmb(1,i) -
uptakerate);

            Cmax(n,1,i,r,v,u) = Cmax(n,2,i,r,v,u) +
uptakerate./Ke4(1,i);

            Cmax(n,3,i,r,v,u) = C(1,n);

            Cmaxrand(n,3,i,r,v,u) = C(1,n);

            Cmaxrand(:,:,i,r,v,u) =
Cmax(:,:,i,r,v,u).*(ones(size(C,2),size(IC,2)) +
0.1.*randn(size(C,2),size(IC,2)));%This step adds "experimental" error
to accumulation measurements

end


% This loop uses accumulation loop results to produce new parameters
% determined by nonlinear regression analysis
for k = 1:size(Kma,2)

    Beta1 = lsqnonlin(@TCA_efflux_model_liu_nlin_thesis,b01,[0 0 0 0
0],2.*b01,optimset('Display','off'),Cmax(:,:,k,r,v,u));

    howoff(k,:,r,v,u) = abs(Beta1 - [Kma(1,k) Vma(1,k) Ke4(1,k)
Kmb(1,k) Vmb(1,k)]);
    propoff(k,:,r,v,u) = howoff(k,:,r,v,u)./[Kma(1,k) Vma(1,k) Ke4(1,k)
Kmb(1,k) Vmb(1,k)];

    maxoff(k,r + recycler_counter.*(v - 1) +
recycler_counter.*size(Kmareal,2).*(u - 1)) =
max(howoff(k,:,r,v,u),[],2);
```

```
    maxpropoff(k,r + recycler_counter.*(v - 1) +
recycler_counter.*size(Kmareal,2).*(u - 1)) =
max(propoff(k,:,r,v,u),[],2);

    % Conditional statements to assess which regression-determined
    % parameter is farther from initial parameter
    if propoff(k,1,r,v,u) == maxpropoff(k,r + recycler_counter.*(v - 1)
+ recycler_counter.*size(Kmareal,2).*(u - 1))

        whichoff(k,1,r,v,u) = 1;

    elseif propoff(k,2,r,v,u) == maxpropoff(k,r + recycler_counter.*(v
- 1) + recycler_counter.*size(Kmareal,2).*(u - 1))

        whichoff(k,2,r,v,u) = 1;

    elseif propoff(k,3,r,v,u) == maxpropoff(k,r + recycler_counter.*(v
- 1) + recycler_counter.*size(Kmareal,2).*(u - 1))

        whichoff(k,3,r,v,u) = 1;

    elseif propoff(k,4,r,v,u) == maxpropoff(k,r + recycler_counter.*(v
- 1) + recycler_counter.*size(Kmareal,2).*(u - 1))

        whichoff(k,4,r,v,u) = 1;

    else

        whichoff(k,5,r,v,u) = 1;

    end

    Beta1 = lsqnonlin(@TCA_efflux_model_liu_nlin_thesis,b01,[0 0 0 0
0],2.*b01,optimset('Display','off'),Cmaxrand(:,:,k,r,v,u));

    howoffrand(k,:,r,v,u) = abs(Beta1 - [Kma(1,k) Vma(1,k) Ke4(1,k)
Kmb(1,k) Vmb(1,k)]);
    propoffrand(k,:,r,v,u) = howoffrand(k,:,r,v,u)./[Kma(1,k) Vma(1,k)
Ke4(1,k) Kmb(1,k) Vmb(1,k)];

    maxoffrand(k,r + recycler_counter.*(v - 1) +
recycler_counter.*size(Kmareal,2).*(u - 1)) =
max(howoffrand(k,:,r,v,u),[],2);
    maxpropoffrand(k,r + recycler_counter.*(v - 1) +
recycler_counter.*size(Kmareal,2).*(u - 1)) =
max(propoffrand(k,:,r,v,u),[],2);

    % Conditional statements to assess which regression-determined
    % parameter is farther from initial parameter
    if propoffrand(k,1,r,v,u) == maxpropoffrand(k,r +
recycler_counter.*(v - 1) + recycler_counter.*size(Kmareal,2).*(u - 1))

        whichoffrand(k,1,r,v,u) = 1;
```

```
% Matrices to store mean %parameter error and std dev of %parameter
error
meanmaxpropoff((v + size(Kmareal,2).*(u - 1)),:) =
mean(maxpropoff(:,((v - 1).*recycler_counter + (u -
1).*size(Kmareal,2).*recycler_counter + 1):((u - 1).*size(Kmareal,2) +
v).*recycler_counter));
meanmaxpropoffrand((v + size(Kmareal,2).*(u - 1)),:) =
mean(maxpropoffrand(:,((v - 1).*recycler_counter + (u -
1).*size(Kmareal,2).*recycler_counter + 1):((u - 1).*size(Kmareal,2) +
v).*recycler_counter));
totmean(v,u) = mean(meanmaxpropoff((v + size(Kmareal,2).*(u -
1)),:),2);
totmeanrand(v,u) = mean(meanmaxpropoffrand((v + size(Kmareal,2).*(u -
1)),:),2);
stdmaxpropoff((v + size(Kmareal,2).*(u - 1)),:) = std(maxpropoff(:,((v
- 1).*recycler_counter + (u - 1).*size(Kmareal,2).*recycler_counter +
1):((u - 1).*size(Kmareal,2) + v).*recycler_counter));
stdmaxpropoffrand((v + size(Kmareal,2).*(u - 1)),:) =
std(maxpropoffrand(:,((v - 1).*recycler_counter + (u -
1).*size(Kmareal,2).*recycler_counter + 1):((u - 1).*size(Kmareal,2) +
v).*recycler_counter));
allpropoff = zeros(recycler_counter.*size(maxpropoff,1),1);
allpropoffrand = zeros(recycler_counter.*size(maxpropoffrand,1),1);

for r = 1:recycler_counter

    allpropoff(((r - 1).*size(maxpropoff,1) +
1):(size(maxpropoff,1).*r),1) = maxpropoff(:,r + (v -
1).*recycler_counter + (u - 1).*size(Kmareal,2).*recycler_counter);
    allpropoffrand(((r - 1).*size(maxpropoff,1) +
1):(size(maxpropoff,1).*r),1) = maxpropoffrand(:,r + (v -
1).*recycler_counter + (u - 1).*size(Kmareal,2).*recycler_counter);

end

totstd(v,u) = std(allpropoff);
totstdrand(v,u) = std(allpropoffrand);

    end

end
```